TECHNICAL REPORT STANDARD TITLE PAGE

1. Report No.	2. Government Accession No.	3. Recipient's Catalog No.
FHWA/TX-87/39+436-1		

4. Title and Subtitle	5. Report Date
FACTORS AFFECTING THE LONG TERM STRENGTH OF COMPACTED BEAUMONT CLAY	October 1986
	6. Performing Organization Code
7. Author(s)	8. Performing Organization Report No.
Roger Green and Stephen G. Wright	Research Report 436-1
9. Performing Organization Name and Address	10. Work Unit No.
Center for Transportation Research The University of Texas at Austin Austin, Texas 78712-1075	11. Contract or Grant No. Research Study 3-8-85-436
	13. Type of Report and Period Covered
12. Sponsoring Agency Name and Address Texas State Department of Highways and Public Transportation; Transportation Planning Division P. O. Box 5051 Austin, Texas 78763-5051	Interim
	14. Sponsoring Agency Code

15. Supplementary Notes

Study conducted in cooperation with the U. S. Department of Transportation, Federal Highway Administration. Research Study Title: "Development of Design Practice and Procedures for Determining Embankment Slope Stability"

16. Abstract

This report describes results of an ongoing study of the stability of embankments constructed of highly plastic clays in Texas. Previous studies showed that such embankments failed by sliding many (10-30) years after construction and that the apparent shear strengths were substantially lower than the long-term shear strengths determined on the basis of laboratory tests on compacted specimens. This report presents the finding of several series of tests performed to understand better the reasons for the discrepancies between field and laboratory shear strengths. Triaxial shear tests were performed to measure the effective stress shear strength parameters on (a) undisturbed specimens taken from actual slopes which had failed, (b) specimens prepared by consolidating soil from a slurry in the laboratory, and (c) specimens prepared by packing (remolding) soil into a special mold in the laboratory. In addition, residual shear strengths were determined on conventional compacted specimens. None of these tests fully explained the differences between field and laboratory strengths and produced agreement between laboratory and field values.

17. Key Words	18. Distribution Statement
clay, Beaumont, compacted, long-term strength, differences, field, laboratory, triaxial shear tests	No restrictions. This document is available to the public through the National Technical Information Service, Springfield, Virginia 22161.

19. Security Classif. (of this report)	20. Security Classif. (of this page)	21. No. of Pages	22. Price
Unclassified	Unclassified	222	

Form DOT F 1700.7 (8-69)

FACTORS AFFECTING THE LONG TERM STRENGTH OF COMPACTED BEAUMONT CLAY

by

Roger Green
and
Stephen G. Wright

Research Report Number 436-1

Development of Design Practice and Procedures
for Determining Embankment Slope Stability

Research Project 3-8-85-436

conducted for

Texas State Department of Highways
and Public Transportation

in cooperation with the
U.S. Department of Transportation
Federal Highway Administration

by the

CENTER FOR TRANSPORTATION RESEARCH
BUREAU OF ENGINEERING RESEARCH
THE UNIVERSITY OF TEXAS AT AUSTIN

October 1986

The contents of this report reflect the views of the authors, who are responsible for the facts and the accuracy of the data presented herein. The contents do not necessarily reflect the official views or policies of the Federal Highway Administration. This report does not constitute a standard, specification, or regulation.

PREFACE

The Texas State Department of Highways and Public Transportation has experienced a number of slope failures in embankments constructed of highly plastic clays. The failures typically occur a number of years after construction and are associated with the embankment itself, rather than any feature of the foundation. Stauffer and Wright (1984) studied a number of these failures and, using strength data obtained by Gourlay and Wright (1984), showed that the shear strength measured in the laboratory on compacted specimens significantly overestimated the strength that was developed in the field. In response to this observation the present research study was initiated to understand better the reasons for the discrepancies between the field and laboratory strengths and to develop a rational basis for estimating shear strengths for design. The results of the first phases of the laboratory testing program are presented in this report.

ABSTRACT

This report describes results of an ongoing study of the stability of embankments constructed of highly plastic clays in Texas. Previous studies showed that such embankments failed by sliding many (10-30) years after construction and that the apparent shear strengths were substantially lower than the long-term shear strengths determined on the basis of laboratory tests on compacted specimens. This report presents the finding of several series of tests performed to understand better the reasons for the discrepancies between field and laboratory shear strengths. Triaxial shear tests were performed to measure the effective stress shear strength parameters on (a) undisturbed specimens taken from actual slopes which had failed, (b) specimens prepared by consolidating soil from a slurry in the laboratory, and (c) specimens prepared by packing (remolding) soil into a special mold in the laboratory. In addition, residual shear strengths were determined on conventional compacted specimens. None of these tests fully explained the differences between field and laboratory strengths and produced agreement between laboratory and field values.

SUMMARY

Previous experience has shown that the shear strength of highly plastic clays in compacted earth embankments is much lower in the field than laboratory tests suggest. In order to understand better the reasons for the discrepancies between field and laboratory strengths several series of laboratory tests were performed to measure shear strengths and compare them to field values. Laboratory tests were performed on undisturbed specimens taken from an embankment which had failed and on specimens which were prepared in the laboratory by consolidating soil from a slurry and by "packing" soil into a special mold at a high water content. Although the strengths measured on these various types of specimens were lower than those which had been measured on specimens compacted in the laboratory, the strengths still exceeded what was apparently developed in the field. Closest agreement with field observations was obtained for laboratory strengths measured at an ultimate condition (corresponding to large axial strains in triaxial compression tests) on specimens prepared by consolidation from a slurry; however, the laboratory strengths were still higher than those apparently developed in the field.

Residual shear strengths were determined using direct shear apparatus and found to be somewhat lower than values developed in the field. However, no rational basis could be found for justifying use of residual shear strengths for design of compacted earth fills.

The reasons for the discrepancies between field and laboratory strengths are still not fully understood. Further research is underway to understand and explain the reasons for the discrepancies.

IMPLEMENTATION STATEMENT

Results presented in this report do not explain the reasons for the discrepancies between shear strengths measured in the laboratory and shear strengths which can apparently be relied upon in the field for slope stability. Accordingly, it is recommended that field experience continue to be used to guide design, although it may result in excessive conservatism in at least some cases. Use of field experience as a basis for design requires that field experience with unsuccessful performance of embankments continue to be documented by the Department and disseminated to design engineers to guide them in design.

As a long-term solution, further research is recommended to understand the reasons for the discrepancy between field and laboratory strength values and to establish rational procedures for design based on laboratory testing and conventional geotechnical engineering practices for analysis and design.

TABLE OF CONTENTS

LIST OF TABLES

Table | Page

LIST OF FIGURES

Figure Page

Figure Page

Figure Page

Figure Page

Figure Page

Figure Page

Figure Page

CHAPTER ONE INTRODUCTION

A relatively large number of slope failures have occurred in District 12 of the Texas State Department of Highways and Public Transporation in embankments constructed of highly plastic "Beaumont" clay. The failures are similar in that they are relatively "shallow", and occur several years after construction. A number of slope failures of this nature are described by Stauffer and Wright (1984). In response to such failures a laboratory testing program was initiated in June of 1983 to measure effective stress shear strength properties of typical soils used in embankments which had experienced problems. The first phase of the laboratory tests and data are presented by Gourlay and Wright (1984).

The test results presented by Gourlay and Wright (1984) showed that a significant discrepancy existed between the effective stress shear strength parameters measured in the laboratory and the effective stress shear strength parameters which apparently were developed in the field. In order to better understand the reasons for the discrepancies and to develop effective stress shear strength parameters which could be used for future designs, a second phase of laboratory testing was initiated. The results fron the second phase of laboratory testing are presented in this report.

The objective of the second phase of the laboratory testing program was to determine if the discrepancies between the laboratory and field strengths could be resolved. All of the laboratory tests performed by Gourlay and Wright (1984) were performed on specimens which were compacted in the laboratory to what were judged to be conditions representative of what existed in the field at the time of construction. A considerable effort was made to obtain specimens which were representative of the field conditions; however, it is possible that the specimens did not represent field conditions sufficiently well and, thus, the observed discrepancies existed. It is also possible that some mechanism acts upon the soil in the field over a number of years which cannot be reproduced in the laboratory using conventional testing techniques.

In order to understand better and resolve the differences between the field and laboratory strengths, four distinct series of tests were initiated. The first series of tests was performed using specimens which were formed by mixing the soil with water to form a slurry, and then consolidating the slurry one-dimensionally in special tubes. The specimens were then tested using the same basic procedures as those used previously by Gourlay and Wright (1984) with the compacted specimens. The second series of tests was performed using "packed" specimens, which were formed by "packing" soil by hand into a mold at a water content which was convenient for molding specimens (the water content was significantly higher than the water content used to compact specimens in the earlier studies). Consolidated-undrained ($\bar{R}$) triaxial shear tests with pore pressure measurements were performed on the first and second series of specimens. The third series of tests was performed to measure residual, as contrasted to peak, effective stress shear strength parameters. Direct shear apparatus was used for these tests and specimens were prepared by compacting the soil into a mold. The fourth, and final series of tests was performed on undisturbed specimens taken from an embankment which had experienced sliding in the past. The embankment was located at Scott Street and I. H. 610 in Houston and was the same embankment from which the soil used in most of the preceding tests was taken. Both consolidated-undrained ($\bar{R}$) and consolidated-drained (S) triaxial tests were employed for the fourth series of tests.

CHAPTER TWO. TESTS ON SPECIMENS CONSOLIDATED FROM A SLURRY

INTRODUCTION

The first series of tests consisted of five consolidated-undrained (R) triaxial shear tests performed on specimens which were prepared by mixing soil with water to form a slurry and then consolidating the slurry one-dimensionally in tubes. The objectives of these tests were to determine if a laboratory shear strength different from that reported by Gourlay and Wright (1984) did exist and could be measured, and to obtain what Skempton (1970) termed "fully softened" shear strength parameters. Skempton stated "the fully softened shear strength parameters c and ϕ are equal numerically to the peak strength parameters of the normally consolidated clay". Skempton reported that for first time slides in fissured over-consolidated London Clay the strengths at failure corresponded to the fully softened strengths. Supporting field evidence of this has been collected and analyzed by DeLory (1957) and James (1970).

Although the studies by Skempton for slopes in the London Clay have all been for excavated and natural slopes, rather than for embankments which are of interest in the present study, the possibility that fully softened shear strength parameters would agree with the apparent field strengths was of interest. If the fully softened shear strength parameters showed good agreement with field values, the measurement of fully softened values might show promise for establishing values for design of other slopes in the future.

SPECIMEN PREPARATION

The soil used for this portion of testing was originally obtained on August 5, 1983 from an embankment at Scott Street and I. H. 610 during the first phase of this investigation. Gourlay and Wright (1984) have designated this soil as "red" clay and have classified it as highly plastic (CH under the Unified Soil Classification System) with an average liquid limit of 70 percent. The soil was air dried and processed in the same batch as that used by Gourlay and Wright for their compacted specimens.

Specimens were formed from a soil-water slurry initially containing 195 grams of air dried soil, passing a #200 sieve, at a water content of approximately 230 percent. A minus #200 sieve fraction was used so that any coarser material would not cause binding between the piston and the tube used to consolidate the specimens, and so that the coarser material would not segregate to the bottom of the specimen. Gourlay and Wright (1984) used a minus #40 sieve fraction for their triaxial specimens. Grain size analyses indicated that from five to ten percent (by weight) of the soil was removed when the minus #200 fraction was used instead of the minus #40 fraction. There was some concern that the properties of the minus #200 sieve fraction would differ from the properties of the minus #40 sieve fraction. Atterberg Limits were determined for both the minus #40 and the minus #200 sieve fraction, and the plastic and liquid limits, 20 and 65 percent, respectively, were identical for both fractions of soil.

The slurry was hydrated overnight and was then placed under a vacuum and vibrated for one hour to remove entrapped air bubbles. After deairing, the slurry was placed in a special cylindrical tube for consolidation by pouring the slurry down the side of the tube with extreme care to avoid the formation of air bubbles. During the processing of the slurry, some soil adhered in lumps to the equipment and was lost. The actual water content of the slurry when first placed in the consolidation tube was, therefore, higher than the average water content of the original slurry but was not determined.

The consolidation tubes were 18 inches in length with an inside diameter of 1.5 inches. A piston and dead weights were used to apply the vertical consolidation pressure to the upper surface of the slurry. Drainage was allowed from the top and the bottom of the specimen. Four to six load increments were used to consolidate the specimens to a final vertical pressure of 9.8 psi. A final pressure of 9.8 psi was selected to make the specimens strong enough to handle. A typical plot of the decrease in height of the slurry versus the logarithm of time is shown in Figure 2.1 for the final load increment of one of the specimens (Test 6.15). Similar plots for the other tests are included in Appendix A.

The final height of the specimens after they were consolidated in the consolidation tubes was approximately 6 inches. Only the center 3 inches of the specimen was used for triaxial testing. The specimens were extruded from

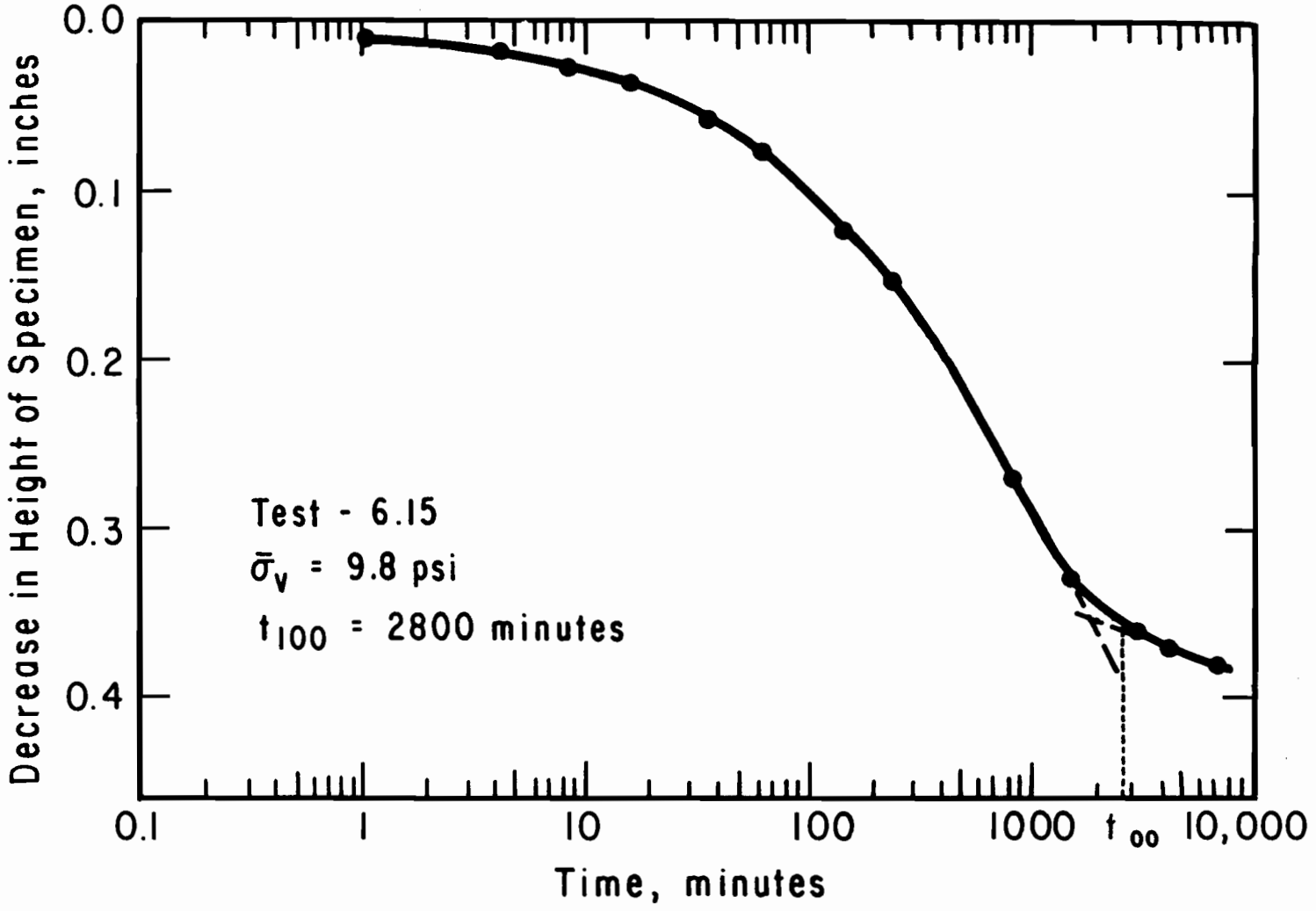

Figure 2.1. Decrease in Height of Specimen in Test 6.15 as a Function of Time, during Final Increment of One-Dimensional Consolidation - Logarithm of Time.

the bottom of the tubes with a slow steady motion. Trimming of the ends was performed as the specimen was extruded. After trimming, the specimen was placed on a paper towel, which conformed to the specimen's shape, for transporting.

Five specimens were prepared for triaxial shear tests. The dry density, water content, degree of saturation, and void ratio for each of the specimens are presented in Table 2.1. The listed values are based on the dry weight of soil after the test, and the dimensions and weight of the specimen after trimming. A measured specific gravity of solids of 2.69 was used in the calculations.

TRIAXIAL TEST SET-UP

The procedures for placing the specimen in the triaxial cell and saturating the specimen were essentially the same as those used for the compacted specimens and are described by Gourlay and Wright (1984). However, the specimens consolidated from a slurry did require more care in handling due to their higher water contents and lower strengthes. Strips of Whatman No. 1 Chromatography Paper covered approximately 50 percent of the perimeter of the specimens and served as vertical filter drains. Two latex membranes were placed onto the specimens once the filter drains were in place.

The triaxial equipment used was the same as that used by Gourlay and Wright (1984) for the compacted specimens. For Test 6.12 which was performed at an effective consolidation pressure of 1.0 psi, two accumulators were used to maintain a constant effective stress. Both accumulators were pressurized from the same source but the cell pressure accumulator was mounted 27 inches above the back pressure accumulator (27 inches of water is equal to 1.0 psi). This procedure for applying pressures was used to prevent any fluctuations in air pressures due to the air regulators or supply from effecting the stresses in the specimen. The procedure worked well and will be used for further testing at low confining pressures.

SATURATION AND CONSOLIDATION OF SPECIMENS

Approximately two weeks were required to complete the back pressure saturation and consolidation of each specimen consolidated from a slurry.

TABLE 2.1. PROPERTIES OF SPECIMENS CONSOLIDATED FROM A SLURRY AFTER EXTRUSION FROM THE TUBES.

Test	Dry Density, pcf	Water Content, percent	Degree of Saturation, percent	Void Ratio
6.12	61.5	61.0	95	1.75
6.15	70.2	51.1	99	1.40
6.11	65.1	57.9	97	1.61
6.27	66.8	57.2	100	1.51
6.10	70.8	50.9	99	1.38

Skempton's (1954) B value was measured in each specimen for every pressure increase. The pore pressure response in the specimens, when measuring Skempton's B value, was slow compared to that of the compacted specimens tested by Gourlay and Wright (1984) and a two minute response time was allowed. A response time of 30 seconds was used by Gourlay and Wright. At the end of saturation, all B values exceeded 0.96 after two minutes and the back pressures ranged from 20 to 30 psi.

The volume of water moving into and out of the specimens during back-pressure saturation and consolidation was measured in all of the tests. Typical plots of volume change during final consolidation versus both the logarithm of time and the square root of time are shown in Figures 2.2 and 2.3, respectively, for one of the tests (Test 6.12 at 1.0 psi). Similar plots are shown in Appendix A for the remaining specimens consolidated from a slurry. The times required for 100 percent primary consolidation (t_{100}) have been found graphically using the logarithm of time method and the square root of time method, and are summarized in Table 2.2.

The dry densities and water contents after consolidation were found after the completion of the triaxial tests (no volume change occurred during shear) and are presented in Table 2.3. The water contents after consolidation (just before shear) are plotted versus the logarithm of the effective consolidation pressures in Figure 2.4. Specimens consolidated in the triaxial cell to effective stresses less than approximately 10 psi were overconsolidated due to previous consolidation in the sample preparation tubes. However, the effects of overconsolidation are not evident in the data presented in Fig. 2.4; the data plot along a nearly straight line on the semi-logarithmic plot, which is indicative of normally consolidated soil.

STRAIN RATES

Rates of deformation in the consolidated-undrained ($\bar{R}$) triaxial shear tests were estimated and selected to ensure that pore water pressures would equilibriate throughout the specimen. Pore water pressures were measured at the base of the specimen and, thus, equilibration of pore water pressures through the specimen was required for meaningful interpretation of the

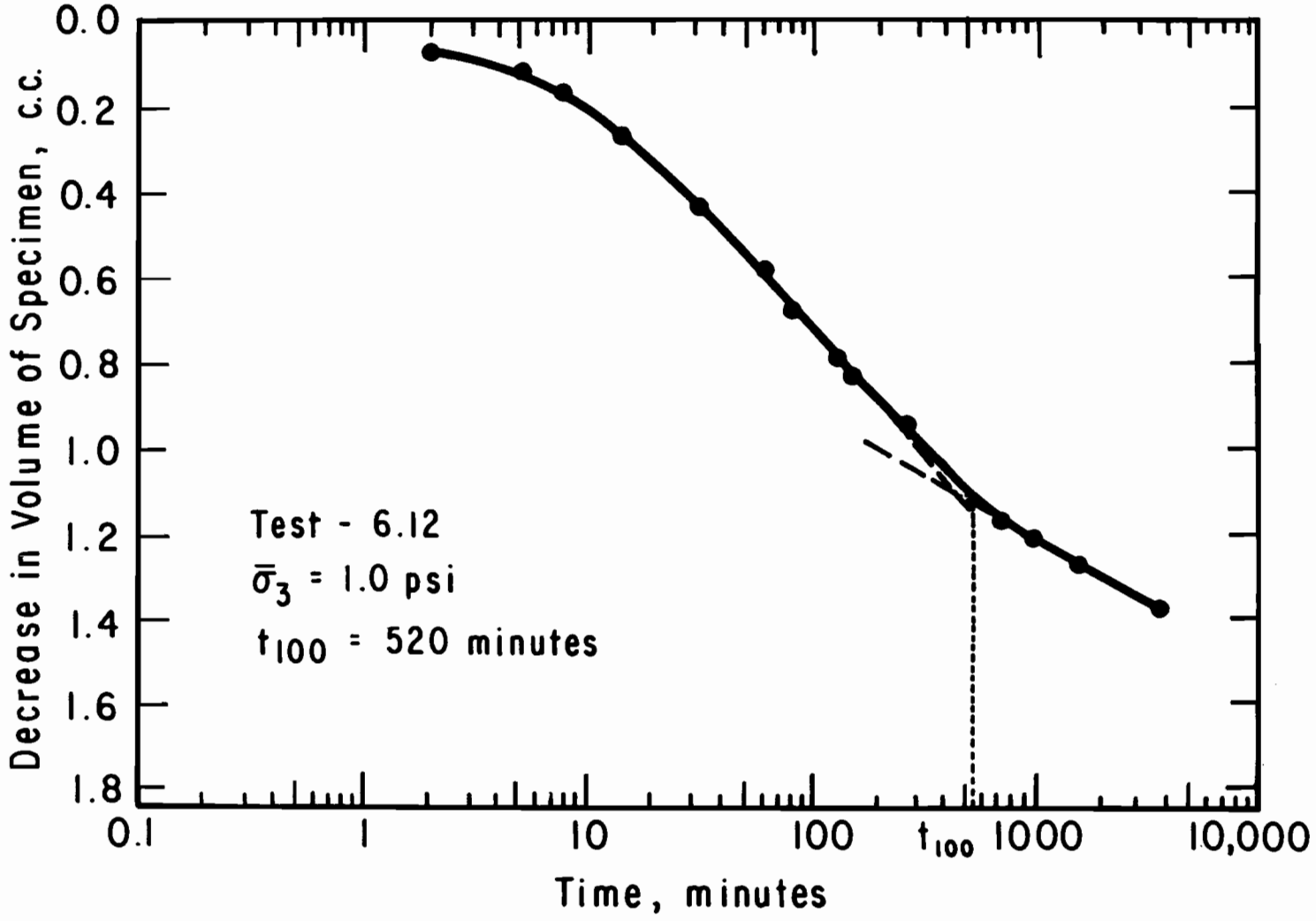

Fig. 2.2. Decrease in Pore Water Volume of Specimen in Test 6.12 as a Function of Time, during Final Consolidation - Logarithm of Time.

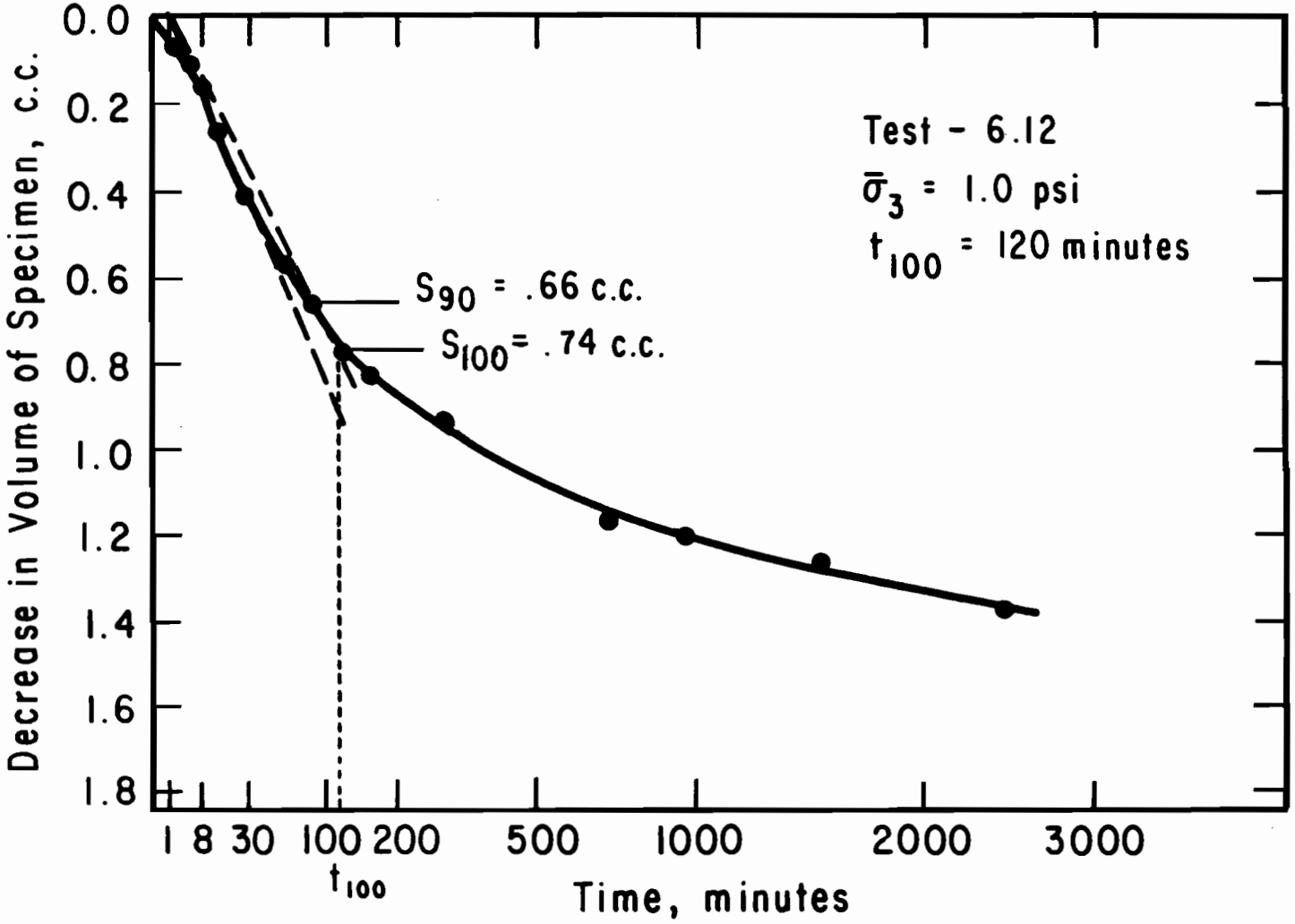

Figure 2.3. Decrease in Pore Water Volume of Specimen in Test 6.12 as a Function of Time, during Final Consolidation - Square Root of Time.

TABLE 2.2. SUMMARY OF TIMES TO THE END OF PRIMARY CONSOLIDATION BEFORE SHEAR FOR SPECIMENS CONSOLIDATED FROM A SLURRY.

Test	Effective Consolidation Pressure, psi	Square Root of Time, minutes	Logarithm of Time, minutes
6.12	1.0	120	520
6.15	4.2	115	500
6.11	10.2	270	810
6.27	14.7	670	700
6.10	20.0	N.A.*	2800

N.A.* - Theoretical S_{100} exceeded all measured values.

TABLE 2.3. PROPERTIES OF SPECIMENS CONSOLIDATED FROM A SLURRY BEFORE SHEARING.

Test	Effective Consolidation Pressure, psi	Dry Density pcf	Water Content, percent
6.12	1.0	62.2	63.3
6.15	4.2	72.3	49.2
6.11	10.2	72.8	48.7
6.27	14.7	79.0	41.8
6.10	20.0	82.0	39.0

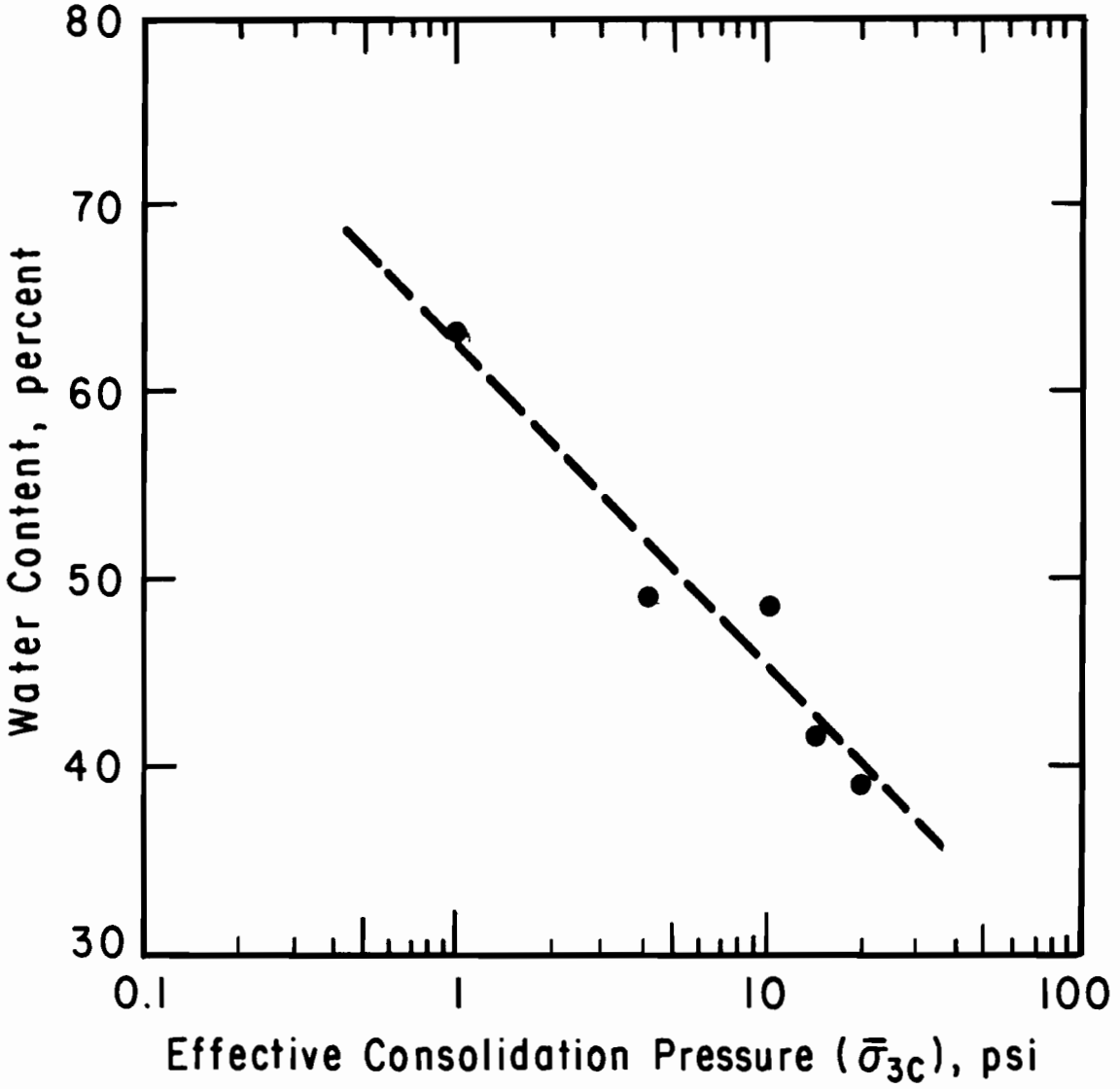

Figure 2.4. Water Content after Triaxial Consolidation versus Effective Consolidation Pressure for Specimens Consolidated from a Slurry.

results. The minimum time to failure (t_f) was estimated from the following equation given by Blight (1963):

$$t_f = \frac{0.07 \times H^2}{c_v} \tag{2.1}$$

where c_v is the coefficient of consolidation and H is one-half the specimen height during consolidation (a total specimen height of three inches was assumed). The coefficient of consolidation was calculated from the following equation presented by Bishop and Henkel (1962):

$$c_v = \frac{\pi \times H^2}{81 \times t_{100}} \tag{2.2}$$

where t_{100} is the time to the end of primary consolidation. The minimum time to failure (t_f) and the coefficient of consolidation (c_v) were calculated using Equations 2.1 and 2.2, respectively, using the t_{100} found from the logarithm of time method. The values of t_f and c_v are summarized in Table 2.4. The logarithm of time values were used because they were the larger values and therefore led to more conservative values of t_f.

The rate of shear was the same as that used by Gourlay and Wright (1984), 0.0017 in./hr., and is the slowest rate available on the Wykeham Farrance loading presses which were used. Specimens were sheared for approximately 14 days to maximum axial strains of approximately 15 percent, except for Test 6.15 which was stopped after six days with only seven percent strain due to accidental movement of the triaxial cell in the loading press.

STRESS-STRAIN BEHAVIOR

Principal stress difference, $(\sigma_1-\sigma_3)$, is plotted versus axial strain, ε, in Figure 2.5 for the five specimens consolidated from a slurry. The curves shown in Figure 2.5 are corrected for effects of piston seating errors; uncorrected curves are included in Appendix B. The method by which the principal stress values were calculated is described by Gourlay and Wright (1984); the stress values were corrected for the effects of membranes and filter paper according to Duncan and Seed (1965).

The shape of the five curves are similar in that the principal stress difference decreased after achieving a peak value and continued to decrease

TABLE 2.4. COEFFICIENT OF CONSOLIDATION AND THEORETICAL TIME TO FAILURE FOR SPECIMENS CONSOLIDATED FROM A SLURRY.

Test	Effective Consolidation Pressure, psi	Theoretical Time To Failure, minutes	Coefficient Of Consolidation, in. /minute
6.12	1.0	940	0.00067
6.15	4.2	900	0.00070
6.11	10.2	1460	0.00043
6.27	14.7	1260	0.00050
6.10	20.0	5250	0.00012

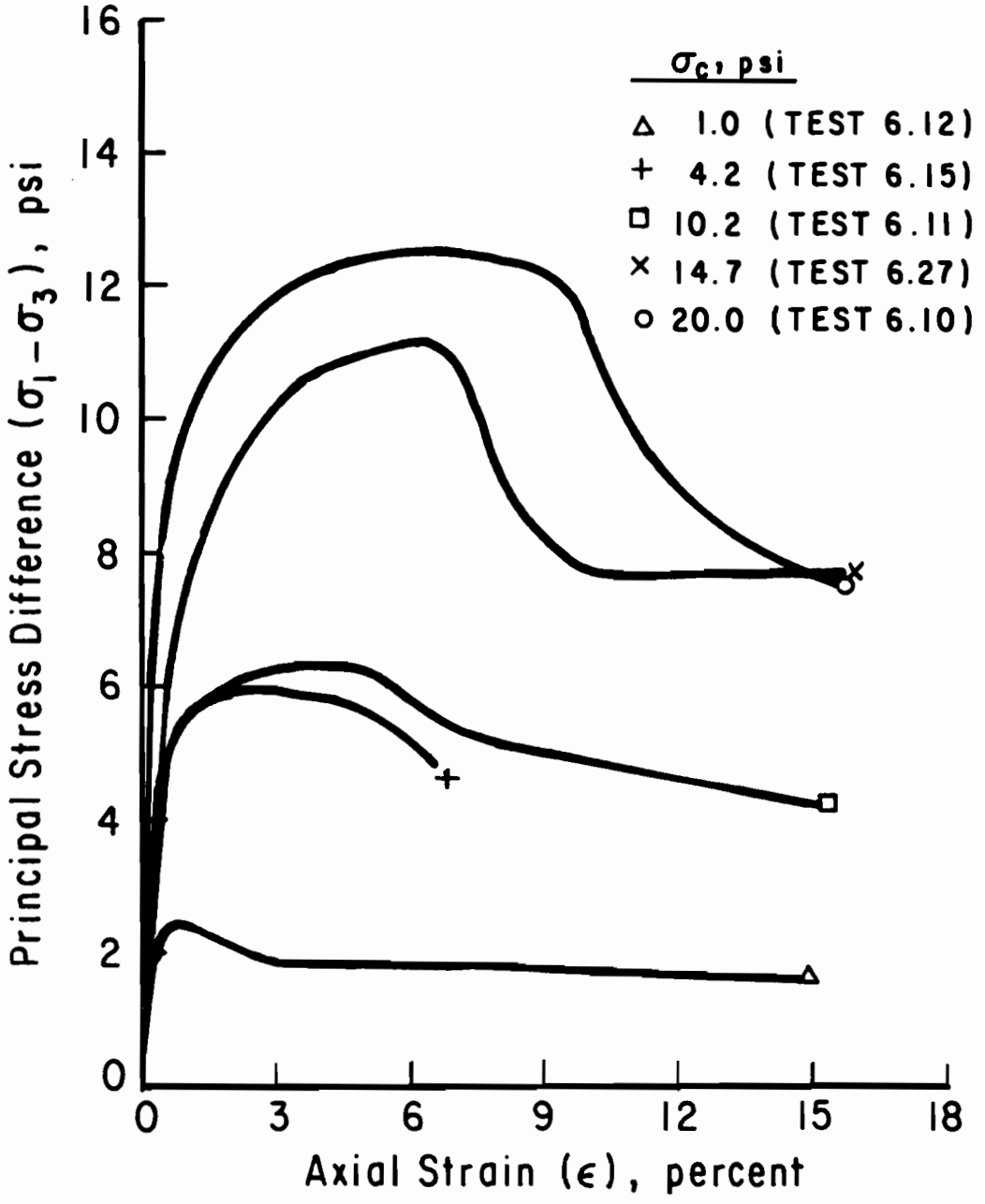

Figure 2.5. Corrected Summary Plot of Principal Stress Difference versus Axial Strain for Specimens Consolidated from a Slurry.

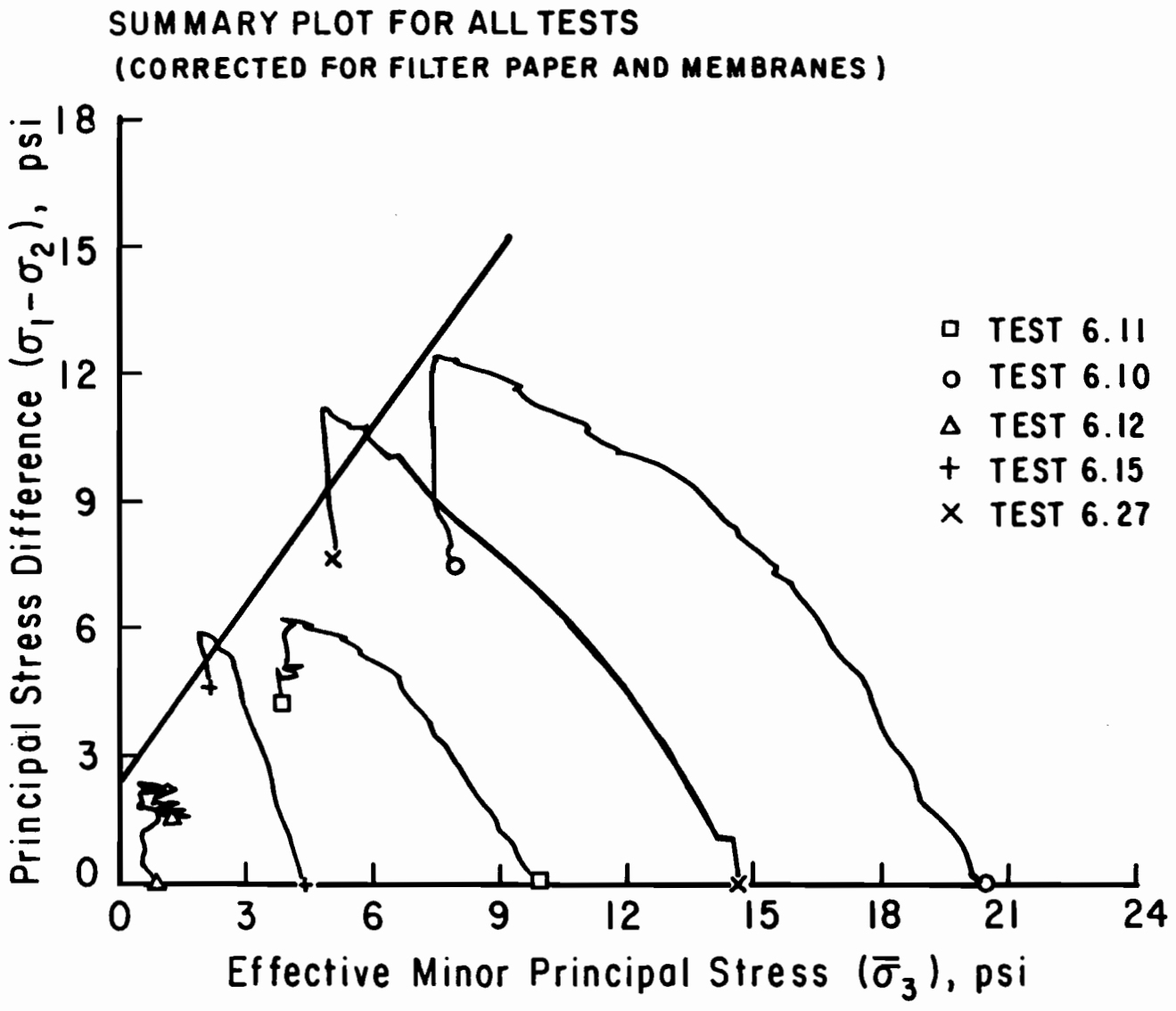

Figure 2.6. Effective Stress Paths and Failure Envelope Based on Stress Path Tangency for Specimens Consolidated from a Slurry.

TABLE 2.5. APPARENT POINTS OF STRESS PATH TANGENCY FOR SPECIMENS CONSOLIDATED FROM A SLURRY.

Test	Principal Stress Difference, psi	Effective Stress, psi
6.12	2.39	0.37
6.15	5.87	1.95
6.11	6.28	4.04
6.27	11.2	4.89
6.10	12.4	7.63

with increasing strain until the test was completed and an ultimate stress was reached. For Test 6.15, the stress would probably have decreased further than what is shown if the test had not been stopped prematurely. The amount of strain required to achieve the peak principal stress difference increased with the effective consolidation pressure on the specimen; values ranged from 0.7 percent at a consolidation pressure of 1.0 psi (Test 6.12) to 7.8 percent for a consolidation pressure of 20.0 psi (Test 6.10).

EFFECTIVE STRESS PATHS

Effective stress paths for the five specimens consolidated from a slurry are plotted in Figure 2.6 using a modified Mohr-Coulomb diagram of principal stress difference, $(\sigma_1-\sigma_3)$, versus the minor prinicpal effective stress, $\bar{\sigma}_3$. A straight line failure envelope is also shown in this figure. The envelope was chosen to represent an "average" envelope based on the criteria of stress path tangency, i.e. the envelope is tangent to the effective stress paths shown. Approximate points of tangency were estimated and a linear regression analysis was used to fit the line shown. The values of principal stress difference, $(\sigma_1-\sigma_3)$, and effective minor principal stress, $\bar{\sigma}_3$, used in the linear regression are listed in Table 2.5.

FAILURE ENVELOPES

Stress Path Tangency Envelope

The straight line failure envelope shown in Figure 2.6 has a slope, $\bar{\psi}$, of 54 degrees and an intercept, $\bar{d}$, of 340 psf. The corresponding effective stress shear strength parameters, $\bar{\phi}$ and $\bar{c}$, on a Mohr-Coulomb diagram were computed from the following equations:

$$\bar{\phi} = \sin^{-1}\left(\frac{\tan\bar{\psi}}{2 + \tan\bar{\psi}}\right) \qquad (2.3)$$

$$\bar{c} = \bar{d} \times \left(\frac{1 - \sin\bar{\phi}}{2 \times \cos\bar{\phi}}\right) \qquad (2.4)$$

The computed friction angle, $\bar{\phi}$, is 24 degrees and the cohesion value, $\bar{c}$, is 110 psf. For specimens of compacted red clay, Gourlay and Wright (1984)

report a friction angle and cohesion of 20 degrees and 270 psf, respectively. The difference in the friction angles is 4 degrees, which is small, while the difference in the cohesion value is 160 psf, and is significant.

To determine the effect of the difference in the friction angles on the cohesion, a modified linear regression analysis was performed in which the friction angle of the specimens consolidated from a slurry was required to be the same as that reported by Gourlay and Wright (1984), 20 degrees. A cohesion of 160 psf was found from the modified linear regression; the straight line failure envelope corresponding to a friction angle of 20 degrees is shown in Figure 2.7. Even with equal friction angles, a significant difference of 110 psf exists between the cohesion reported by Gourlay and Wright and that found for the specimens consolidated from a slurry. This indicates that the difference between the strengths reported by Gourlay and Wright and the fully softened shear strengths lies primarily in the cohesion intercept.

The specimens consolidated in the triaxial cell to effective stresses lower than 9.8 psi were over-consolidated due to the effective stresses present during one-dimensional consolidation; because of this the cohesion intercept reported for the series of tests on specimens consolidated from a slurry possibly was higher than that for the normally-consolidated soil. A linear regression was performed on the points of stress path tangency for the three tests on specimens which were normally-consolidated, Tests 6.10, 6.11, and 6.27, and the computed friction angle, $\bar{\phi}$, was 24 degrees and the cohesion value, $\bar{c}$, was 100 psf. The cohesion value based on only the data for the normally-consolidated specimens does not significanty differ from that reported for the complete series of tests, 110 psf.

Ultimate Envelope

To determine if a difference exists between the shear strength parameters at stress path tangency and those at large strains where the specimen is in a more remolded state a linear regresion was also performed using the final points of the stress paths. Test 6.15 was excluded from this regression due to the premature conclusion of the test. The effective stress paths and the average straight line failure envelope for the ultimate points are shown in Figure 2.8. The failure envelope show in Figure 2.8 has an intercept, $\bar{d}$, of

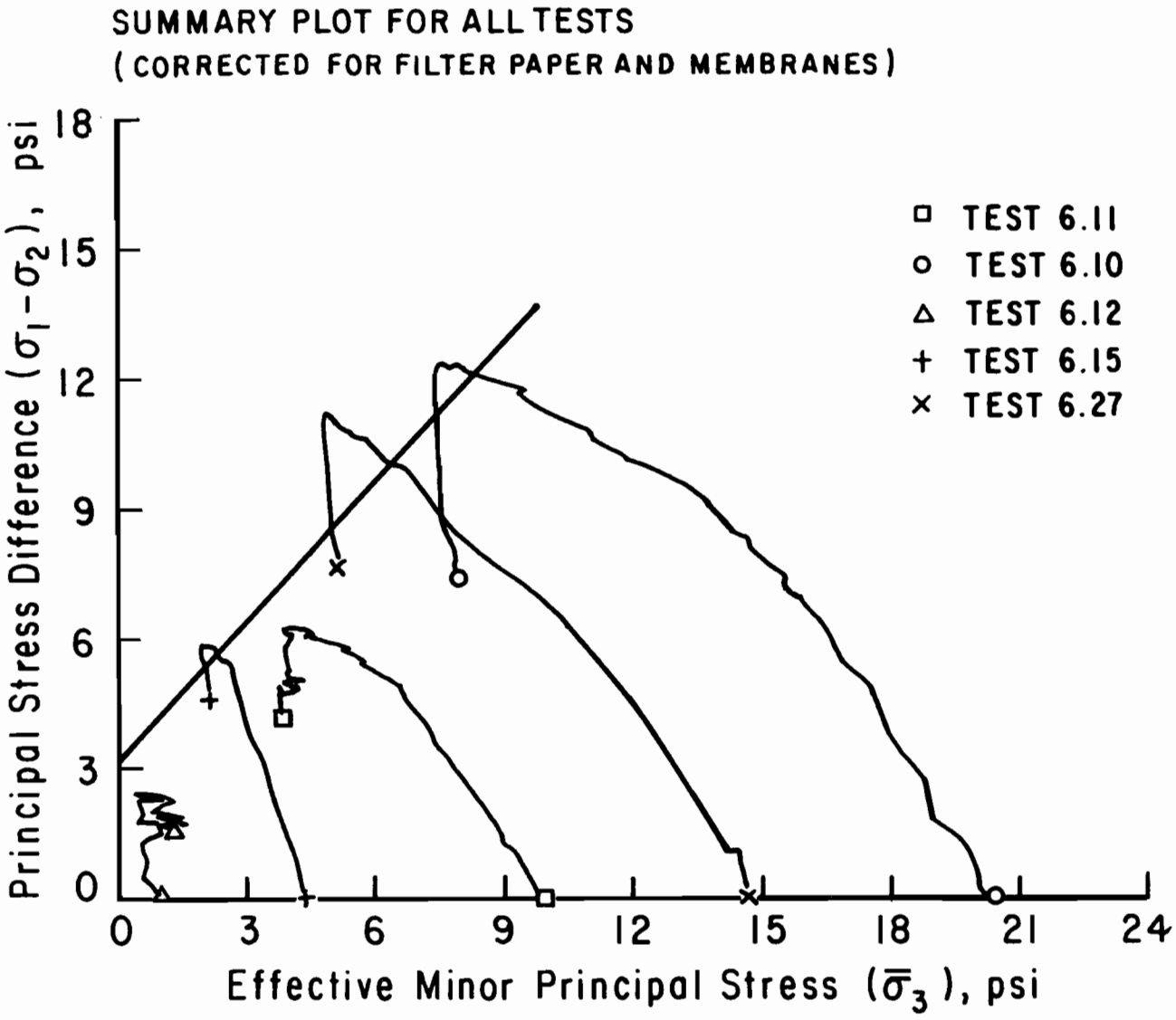

Figure 2.7. Effective Stress Paths and Failure Envelope based on a Friction Angle of 20 Degrees for Specimens Consolidated from a Slurry.

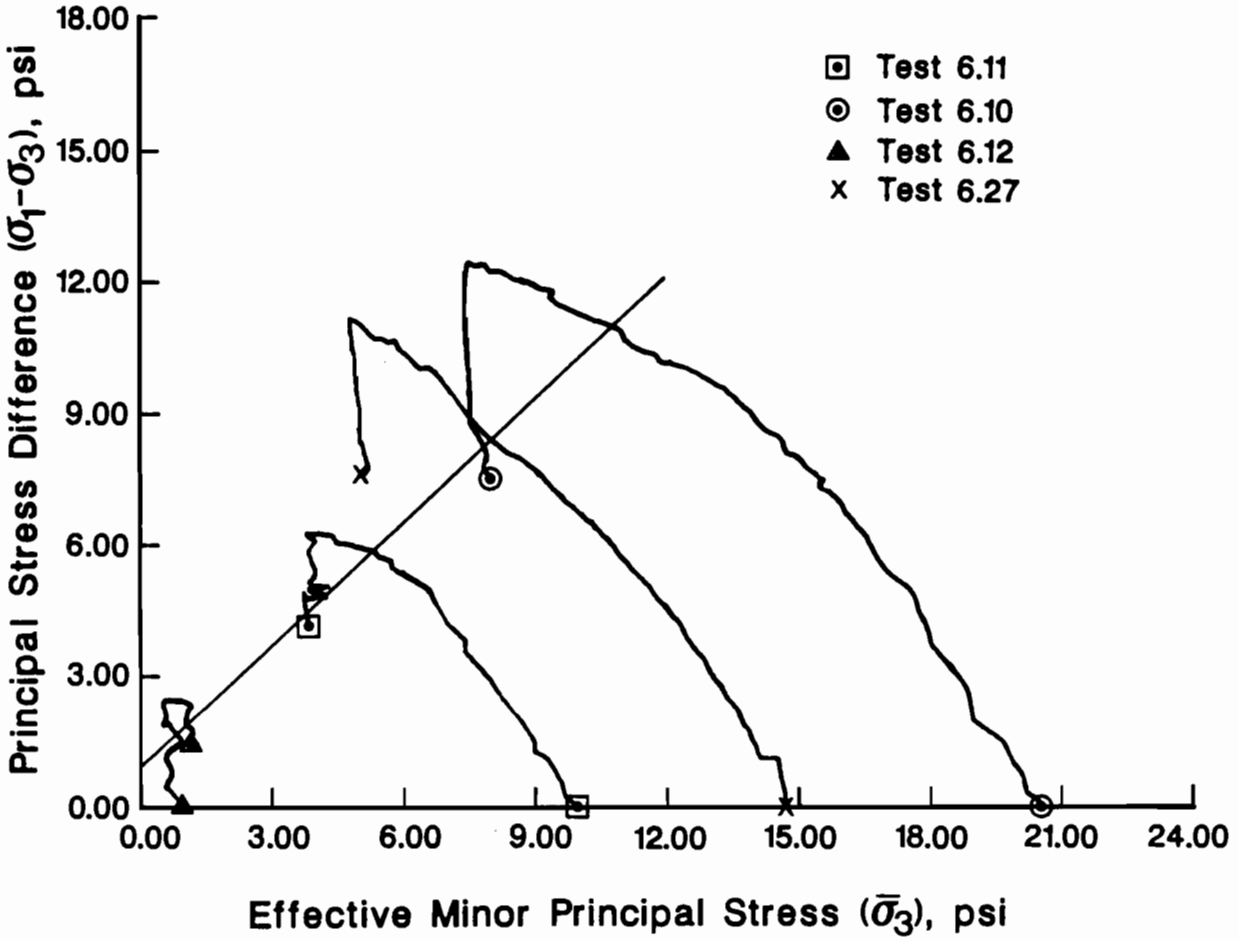

Figure 2.8. Effective Stress Paths and Failure Envelope based on Ultimate Values for Specimens Consolidated from a Slurry.

140 psf and a slope, $\bar{\psi}$, of 43 degrees. The corresponding effective stress shear strength parameters, $\bar{\phi}$ and $\bar{c}$, are 18 degrees and 50 psf, respectively. These values are significantly lower than the values of $\bar{\phi}$ and $\bar{c}$ found for the stress path tangency envelope, 24 degrees and 110 psf, respectively.

TIME TO FAILURE

The axial strain and time to failure for the specimens consolidated from a slurry are presented in Table 2.6 for both the points of stress path tangency and peak principal stress difference. In general, the principal stress difference began to decrease at the point of stress path tangency and the peak principal stress difference and stress path tangency occurred at nearly the same point in the shear test. Also included in Table 2.6 are the minimum theoretical times to failure, t_f, calculated from Equation 2.1. A comparison of the minimum theoretical times to failure and the actual times to failure for both the points of peak principal stress difference and stress path tangency shows that the actual times to failure are nearly equal or exceed the minimum times computed from Eq. 2.1. Accordingly, the shearing rate used (0.0017 in./hr.) should have been adequate to ensure full equilization of pore water pressures throughout the specimen.

TABLE 2.6. AXIAL STRAIN AND TIME TO FAILURE FOR SPECIMENS CONSOLIDATED FROM A SLURRY USING STRESS PATH TANGENCY AND PEAK STRESS FAILURE CRITERIA.

Test	Effective Consolidation Pressure, psi	Stress Path Tangency		Peak Stress Difference		Theoretical Time To Failure, minutes
		Strain, percent	Time, minutes	Strain, percent	Time, minutes	
6.12	1.0	0.9	1140	0.7	890	940
6.15	4.2	3.3	3980	3.3	3980	900
6.11	10.2	5.9	7340	5.3	6580	1460
6.27	14.7	6.3	8100	6.3	8100	1260
6.10	20.0	7.1	8600	7.8	9510	5250

CHAPTER THREE. TESTS ON "PACKED" SPECIMENS

INTRODUCTION

The second series of tests was performed on specimens which were prepared by "packing" soil into a special mold to form a cylindrical specimen. Four such specimens were tested in consolidated-undrained (R) triaxial tests with pore pressure measurements. The purpose of the second series of tests was to develop a procedure which might produce specimens with similar shear strength properties to those formed by a slurry mixture of soil and water, but which would require much less time to prepare. The specimens which were consolidated from a slurry required approximately 30 days to prepare prior to triaxial testing; while the packed specimens could be prepared in approximately three days. The actual packing of the soil required less than one hour. Both the soil used for the packed specimens and the triaxial shear test procedures were identical to those used with the specimens which were consolidated from a slurry, with one exception; a minus #40 sieve fraction was used for the packed specimens instead of a minus #200 sieve fraction. Coarser material was allowed for the packed specimens since binding and segregation would not be a problem in the packing mold as it was in the consolidation tubes used for consolidating specimens from a slurry.

SPECIMEN PREPARATION

The mold shown in Figure 3.1 was fabricated specially for preparing the packed specimens. The mold was made from acrylic tubing and had an inside diameter of 1.5 inch. The piston was also acrylic and was machined to fit snugly in the mold but still retain freedom of movement. With the piston at the base of the mold, the maximum length of soil which could be placed in the mold was 3.5 inches. A stainless steel rod was attached to the piston to control the position of the piston. The base, through which the rod passed, was made of brass and housed a screw which, when tightened, fixed the position of the piston in the mold. A small hole was bored in the base to allow movement of air between the base and the piston.

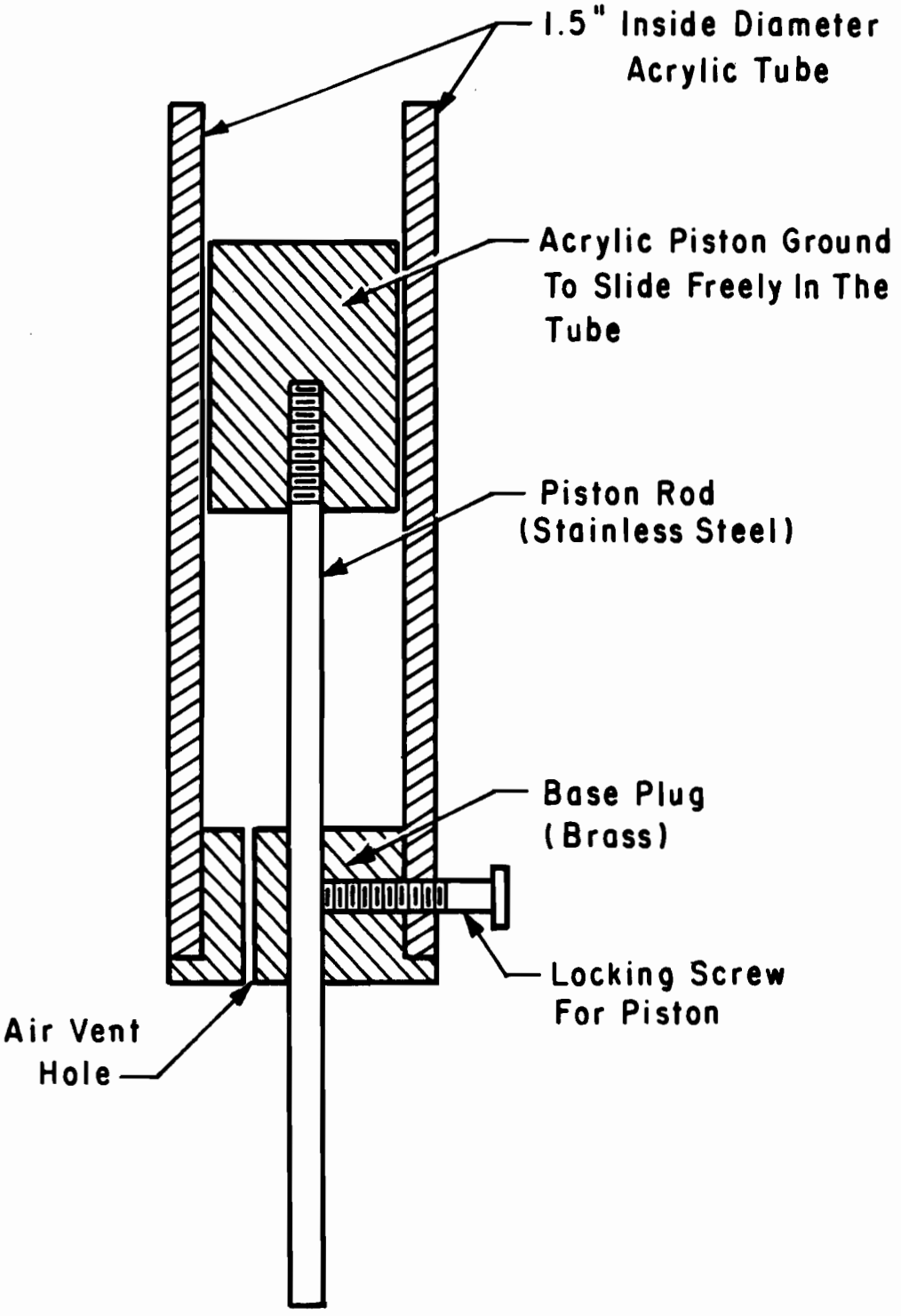

Figure 3.1. Mold Used to Prepare Packed Specimens.

Several specimens were prepared on a preliminary basis before specimens were prepared for the shear tests. These preliminary specimens were prepared using various water contents and procedures for placing the soil in the mold to arrive at an optimum set of procedures for preparation of the specimens to be used in the triaxial tests. It was observed that the wetter the soil, the easier it was to place in the mold without forming air voids; however, difficulties were encountered in handling the specimens at water contents much higher than 60 percent. For these reasons, water contents in the range of from 50 to 60 percent were selected. In order to produce uniform specimens the soil was prepared at a water content of 60 percent and allowed to hydrate in a moisture room at The University of Texas for one day before packing was begun. Some water loss from the soil occurred during the packing process which resulted in slighty lower water contents than as originally prepared.

The soil for the packed specimens was placed into the mold using several layers to form a 3 inch high specimen. Specimens were prepared using both five lifts and eight lifts. The layers were placed according to the following procedure; a small spatula was used repeatedly to spread a small portion of each lift onto the upper surface inside the mold until the layer was completed. Soil placement began at the side of the mold and progressed inward. At the completion of a layer, the surface was trimmed and a 1.48 inch diameter rod was placed onto the soil to push the specimen down into the mold as the piston was lowered. The piston was only lowered enough so that the next lift could be placed. The piston was then fixed, the rod removed, and the next layer begun. The rod had to be twisted repeatedly to free it from the soil, otherwise the packed soil would be pulled from the mold. The top of the final layer was trimmed in the mold so that no trimming would be required outside of the mold. After trimming the specimen, the piston was used to slowly extrude the specimen from the mold.

Specimens formed using eight lifts were generally easier to prepare without voids than those specimens formed in five lifts. Therefore, eight lifts were selected for the preparation of subsequent specimens. The dry density, water content, degree of saturation, and void ratio of several of the better quality preliminary packed specimens are listed in Table 3.1. These properties were calculated in the same manner as those for the specimens

TABLE 3.1. PROPERTIES OF PRELIMINARY PACKED SPECIMENS.

Specimen	Number Of Lifts	Dry Density, pcf	Water Content, percent	Degree Of Saturation, percent	Void Ratio
1 / 2	5	71.7	48.4	97	1.35
1 / 3	5	69.7	52.0	99	1.42
2 / 1	8	67.6	53.8	97	1.49
2 / 2	8	67.9	54.0	98	1.48
2 / 3	8	67.1	54.6	98	1.51

TABLE 3.2. INITIAL PROPERTIES OF TESTED PACKED SPECIMENS.

Test	Dry Density, pcf	Water Content, percent	Degree of Saturation, percent	Void Ratio
6.13	65.9	57.2	99	1.56
B.8	68.1	54.5	100	1.48
B.10	65.4	59.2	100	1.58
B.9	69.3	53.6	100	1.43

consolidated from a slurry in Chapter 2. They are comparable to the properties of the specimens consolidated from a slurry listed in Table 2.1.

Four additional specimens were prepared by packing for use in triaxial testing. The dry density, water content, degree of saturation, and void ratio of these specimens are listed in Table 3.2. The packed specimens were found to be significantly weaker than the specimens consolidated from a slurry even though the initial dry densities and water contents of both types of specimens were very similar. The packed specimens were weaker apparantly because they were freshly remolded and were, therefore, subject to a lower effective stress than the specimens consolidated from a slurry; similar low strengths would be expected in the specimens consolidated from a slurry if they were remolded.

TRIAXIAL TEST SET-UP

The procedure for setting up the specimens in the triaxial cell was the same procedure used for the specimens consolidated from a slurry. However, one change in procedure was required due to the softness of the packed specimens. Originally, the membranes were rolled onto the specimens from the base pedestal to remove excess air from between the membrane and the specimen. This operation caused excessive deformations at the base of the packed specimens. To prevent this from occurring, a vacuum membrane expander was used to place the membranes over the specimens. More air was entrapped with this method; however, this could not be avoided without damaging the specimen.

SATURATION AND CONSOLIDATION OF SPECIMENS

The back pressure saturation and consolidation procedures were identical to those used for the specimens consolidated from a slurry. The pore water pressure response, when measured to determine Skempton's (1954) B value, was slow and a two minute response time was allowed as with the specimens consolidated from a slurry. At the end of saturation, all the B values exceeded 0.99 after two minutes and back pressures ranged from 10 to 35 psi.

As with the specimens consolidated from a slurry, the volume of water moving into and out of the specimens during back-pressure saturation and consolidation was measured for all tests. The volume change during final consolidation for one of the tests (Test B.8 at 4.7 psi) is plotted versus the

logarithm of time in Figure 3.2 and versus the square root of time in Figure 3.3. Similar plots for the other tests are included in Appendix A. The times required for 100 percent primary consolidation (t_{100}) were found graphically using the logarithm of time method and the square root of time method, and are summarized in Table 3.3.

The dry densities and water contents after consolidation were found after the completion of the triaxial tests (no volume change occurred during shear) and are presented in Table 3.4. Water contents after consolidation (just before shear) are plotted versus the logarithm of the effective consolidation pressures in Figure 3.4. The data group along a straight line. Also included in Figure 3.4 are the data for the specimens consolidated from a slurry. In general the water contents of the packed specimens are lower than those for the specimens consolidated from a slurry at any given effective consolidation pressure.

STRAIN RATES

The procedure for shearing the specimens which were prepared by packing was identical to that used for the specimens consolidated from a slurry. The rate of shear used for the packed specimens was 0.0017 in./hr. which was the same rate as used for the shearing of the specimens consolidated from a slurry. Specimens were sheared for approximately 12 days and axial strains of at least 14 percent were achieved.

The theoretical minimum times to failure, t_f, and the coefficients of consolidation, c_v, for the packed specimens were calculated using Eqs. 2.1 and 2.2, respectively; these are listed in Table 3.5, along with the corresponding values for the specimens consolidated from a slurry. As with the specimens consolidated from a slurry, the values of time based on the logarithm (rather than the square root) plots listed in Table 3.3 were used because they were larger values and therefore led to more conservative values of t_f. The times to failure shown in Table 3.5 were generally lower for the packed specimens than for the specimens consolidated from a slurry at corresponding effective consolidation pressures; the strain rate used previously (0.0017 in./hr.) should, therefore, have been more than adequate to ensure that pore water pressures would equilibriate throughout the packed specimen.

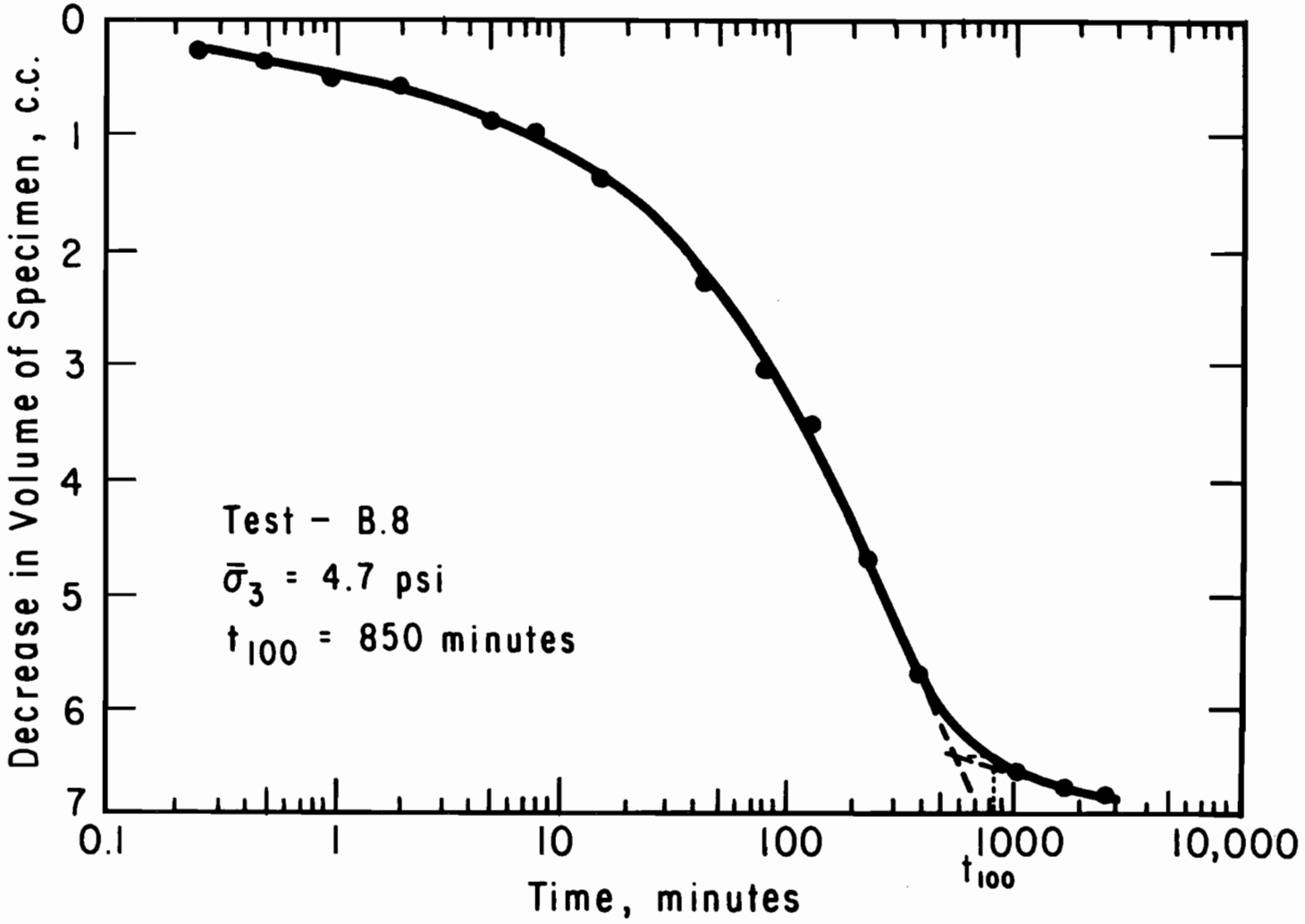

Figure 3.2. Decrease in Pore Water Volume of Specimen in Test B.8 as a Function of Time, during Final Consolidation - Logarithm of Time.

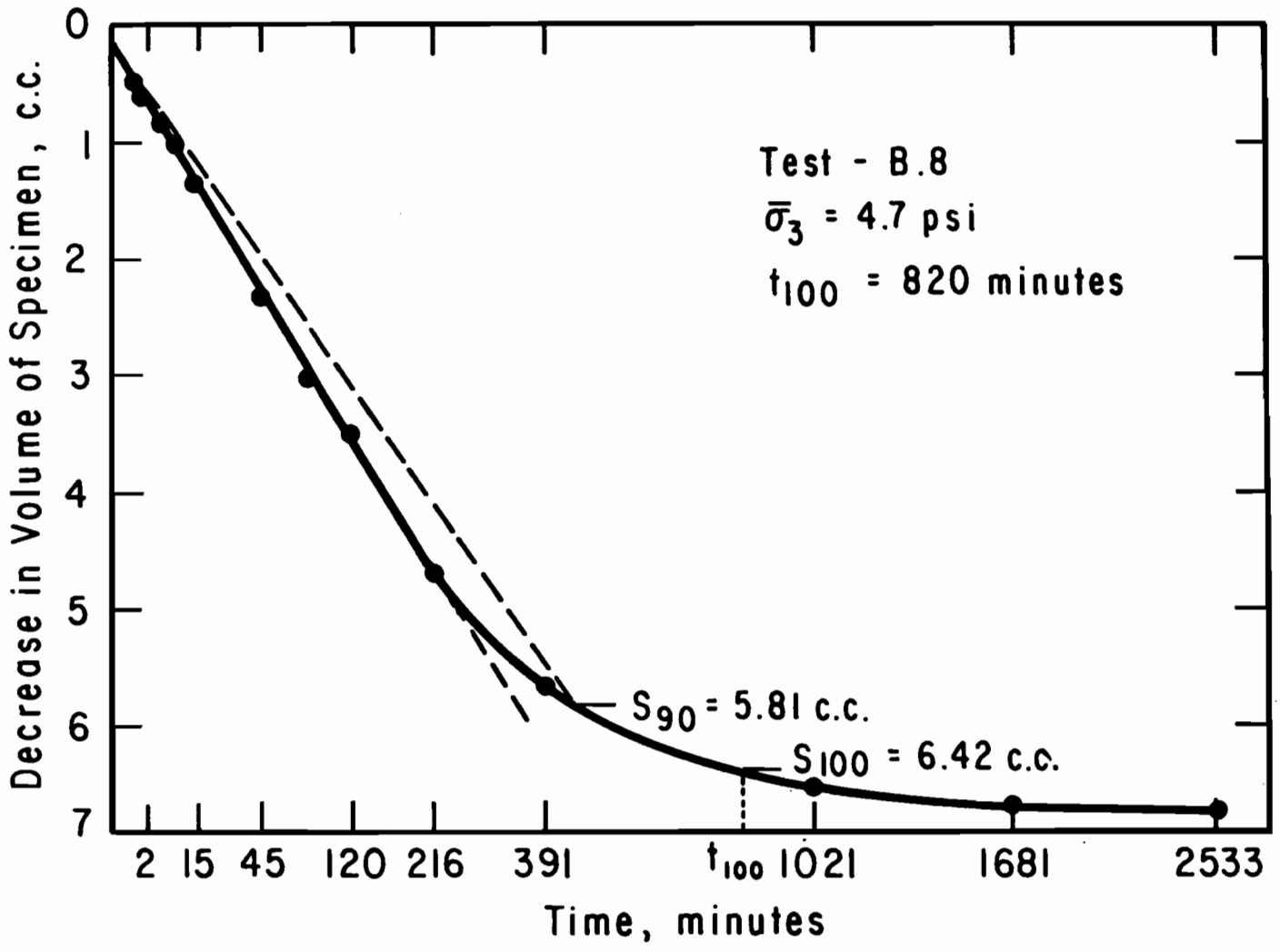

Figure 3.3. Decrease in Pore Water Volume of Specimen in Test B.8 as a Function of Time, during Final Consolidation - Square Root of Time.

TABLE 3.3. SUMMARY OF TIMES TO THE END OF PRIMARY CONSOLIDATION BEFORE SHEAR FOR PACKED SPECIMENS.

Test	Effective Consolidation Pressure, psi	Square Root of Time, minutes	Logarithm of Time, minutes
6.13	1.0	N.A.*	360
B.8	4.7	820	850
B.10	12.0	N.A.*	480
B.9	20.0	710	1050

N.A.* - Theoretical S_{100} exceeded all measured values.

TABLE 3.4. PROPERTIES OF PACKED SPECIMENS BEFORE SHEARING.

Test	Effective Consolidation Pressure, psi	Dry Density pcf	Water Content, percent
6.13	1.0	68.8	53.6
B.8	4.7	76.7	44.3
B.10	12.0	80.8	40.2
B.9	20.0	85.9	35.6

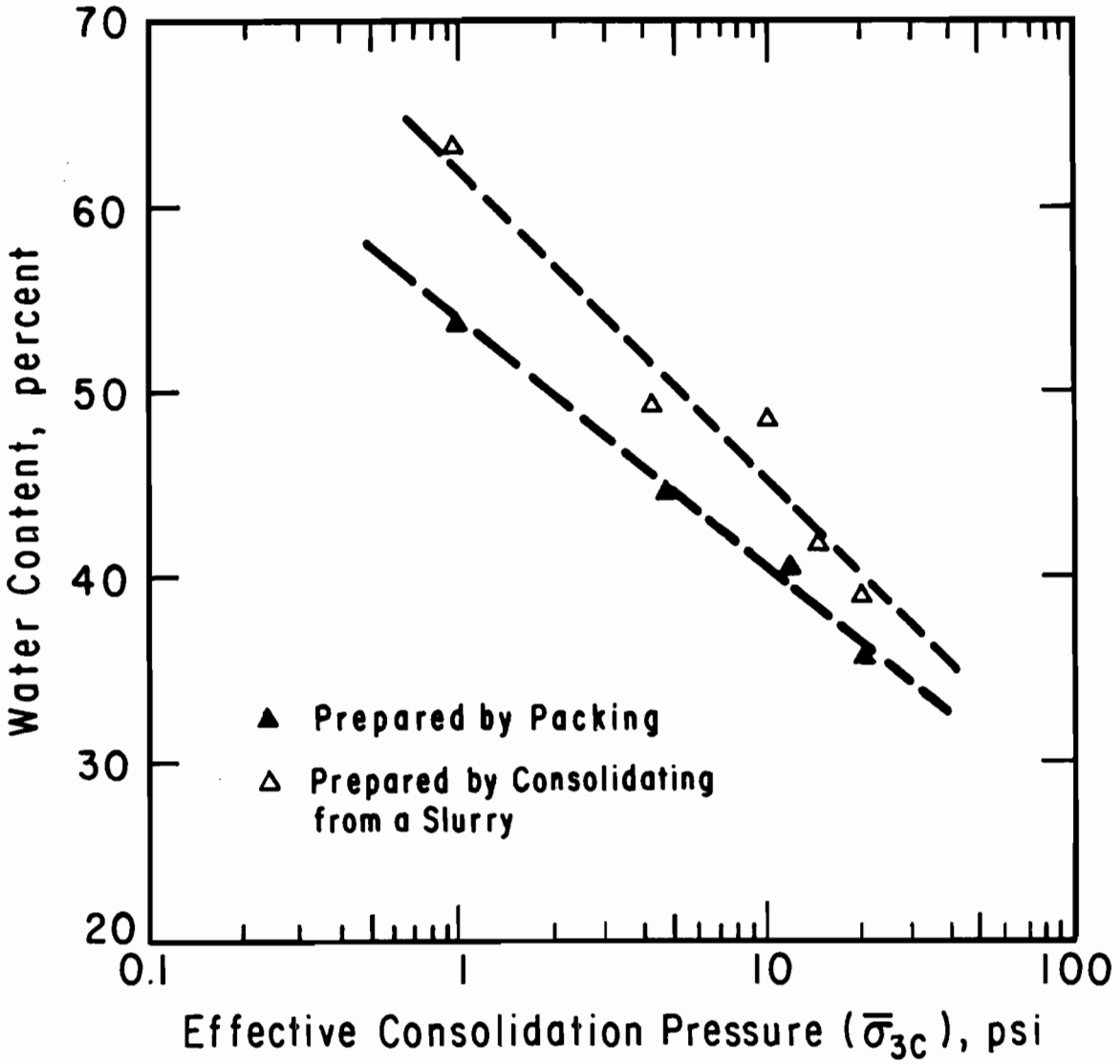

Figure 3.4. Water Content after Triaxial Consolidation versus Effective Consolidation Pressure for Specimens Prepared by Packing and Consolidating from a Slurry.

TABLE 3.5. COMPARISON OF MINIMUM THEORETICAL TIMES TO FAILURE AND COEFFICIENTS OF CONSOLIDATION FOR PACKED SPECIMENS AND SPECIMENS CONSOLIDATED FROM A SLURRY

Packed				Consolidated From A Slurry			
Test	Effective Consolidation Pressure, psi	Theoretical Time To Failure, minutes	Coefficient Of Consolidation, $in.^2$/minute	Test	Effective Consolidation Pressure, psi	Theoretical Time To Failure, minutes	Coefficient Of Consolidation $in.^2$/minute
6.13	1.0	650	0.00097	6.12	1.0	940	0.00067
B.8	4.7	1540	0.00041	6.15	4.2	900	0.00070
B.10	12.0	860	0.00073	6.11	12.0	1460	0.00043
B.9	20.0	1910	0.00033	6.27	14.7	1260	0.00050
				6.10	20.0	5250	0.00012

STRESS-STRAIN BEHAVIOR

Principal stress difference, $(\sigma_1-\sigma_3)$, is plotted versus axial strain, ε, in Figure 3.5 for the four consolidated-undrained triaxial tests on packed specimens. The curves shown in Figure 3.5 are corrected for effects of piston seating errors; uncorrected curves are shown in Appendix B. The axial strain corresponding to the peak principal stress difference increased slightly from 4.0 to 6.5 percent with the effective consolidation pressure; however, the increase was slight. Little change occurred in the principal stress difference once the peak was reached except in Test B.9; Test B.9 at a consolidation pressure of 20.0 psi shows a significant decrease in stress.

EFFECTIVE STRESS PATHS

Effective stress paths for the four packed specimens are plotted in Figure 3.6 using a modified Mohr-Coulomb diagram of principal stress difference, $(\sigma_1-\sigma_3)$, versus effective confining stress, $\bar{\sigma}_3$. The stress paths are all similar in that the pore water pressure of the specimens increased until the peak principal stress difference was reached. After the peak value was reached, the principal stress difference decreased while the pore water pressure decreased slightly. The point of stress path tangency occurs at the same point as the peak principal stress difference, and the two failure criteria yield identical results.

FAILURE ENVELOPES

Stress Path Tangency Envelope

A straight line failure envelope corresponding to the "average" line tangent to the effective stress paths is shown in Figure 3.6. This envelope was found from a linear regression of the apparent points of stress path tangency. The values of principal stress difference and effective confining stress used in the linear regression are listed in Table 3.6. The line has an intercept, $\bar{d}$, of 240 psf and a slope, $\bar{\psi}$, of 50 degrees. The corresponding conventional Mohr-Coulomb effective stress shear strength parameters, $\bar{\phi}$ and $\bar{c}$, are 22 degrees and 80 psf, respectively.

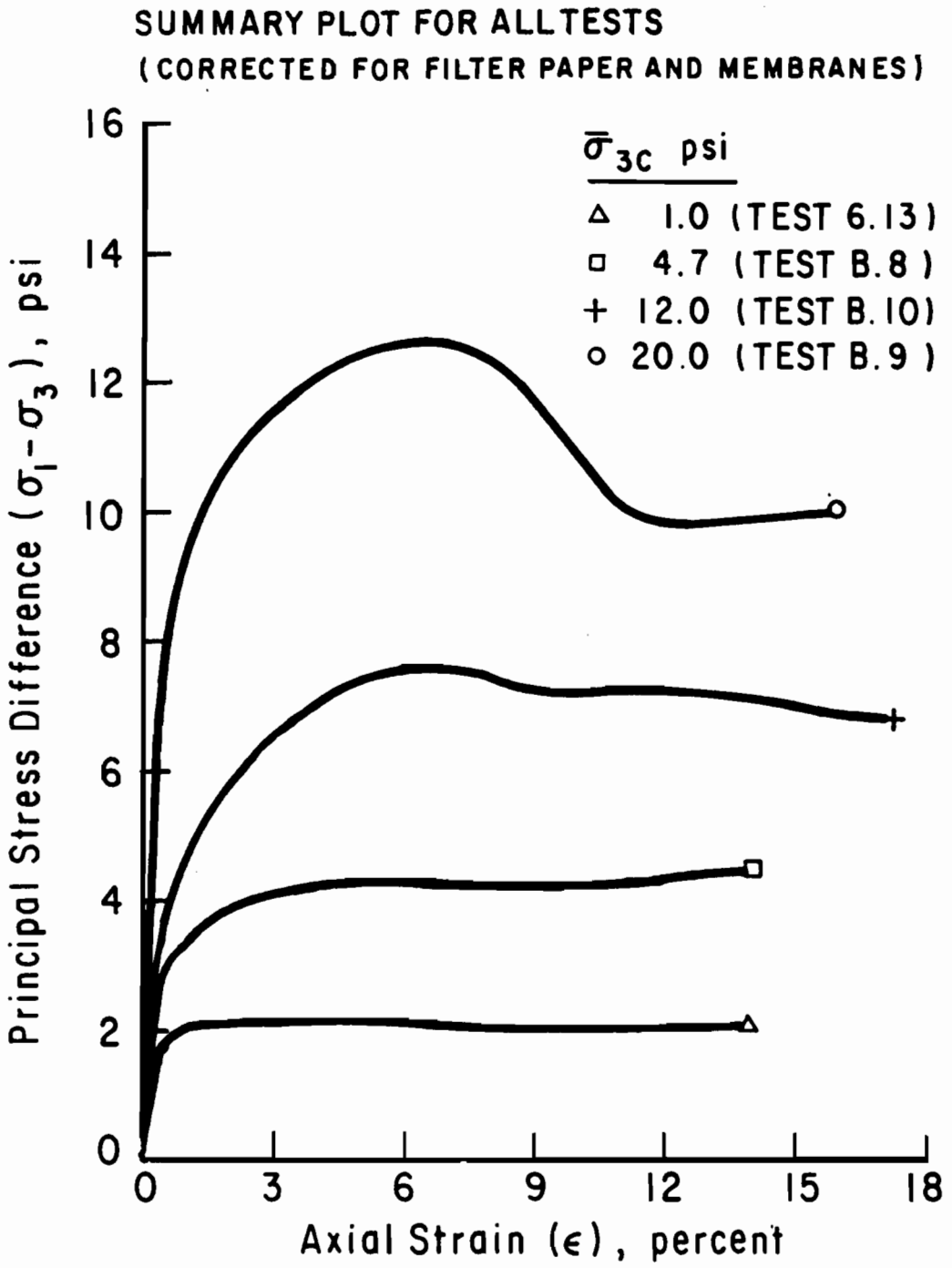

Figure 3.5. Corrected Summary Plot of Principal Stress Difference versus Axial Strain for Specimens Prepared by Packing.

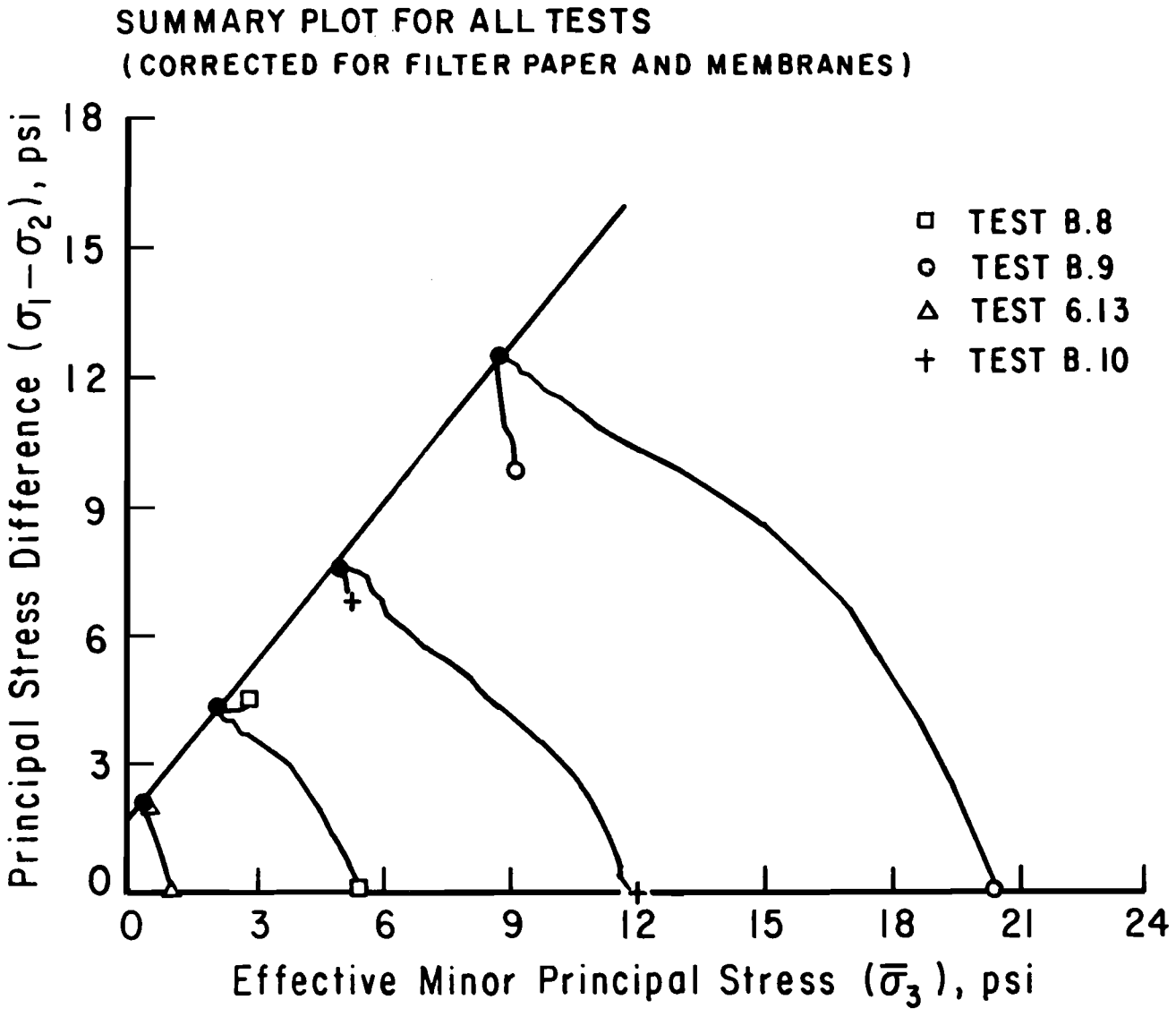

Figure 3.6. Effective Stress Paths and Failure Envelope based on Stress Path Tangency for Specimens Prepared by Packing.

TABLE 3.6. APPARENT POINTS OF STRESS PATH TANGENCY FOR PACKED SPECIMENS.

Test	Principal Stress Difference, psi	Effective Stress, psi
6.13	2.15	0.35
B.8	4.30	2.10
B.10	7.50	5.05
B.9	12.50	8.85

Ultimate Envelope

The "ultimate" shear strength parameters of the packed specimens were determined by performing a linear regression on the final points of the stress paths. The effective stresspaths for the packed specimens and the average straight line failure envelope corresponding to the "ultimate" points is shown in Figure 3.7. The failure envelope has a slope, $\bar{\psi}$, of 42 degrees and an intercept, $\bar{d}$, of 260 psf. The corresponding Mohr-Coulomb shear strength parameters, $\bar{\phi}$ and $\bar{c}$, are 18 degrees and 90 psf, respectively.

COMPARISON WITH SPECIMENS CONSOLIDATED FROM A SLURRY

One of the primary purposes of testing packed specimens was to develop a procedure which might produce specimens with effective stress shear strength properties similar to those of the specimens consolidated from a slurry. The friction angles and cohesion values, $\bar{\phi}$ and $\bar{c}$, corresponding to stress path tangency and ultimate conditions are listed in Table 3.7 for specimens consolidated from a slurry and packed specimens. At stress path tangency both the friction angle and cohesion value of the specimens consolidated from a slurry were only slightly more than those of the packed specimens (by 2 degrees and 30 psf, respectively). At the "ultimate" conditions the friction angles of both types of specimens are very similar, (18 degrees) while the cohesion value of the packed specimens is slightly greater (by 40 psf) than that of the specimens consolidated from a slurry.

The points of stress path tangency and the stress path tangency failure envelopes are shown in Figure 3.8 for both the specimens consolidated from a slurry and the packed specimens. The limits for a confidence of 75 percent are shown in Figure 3.8 for the failure envelope of the specimens consolidated from a slurry (i.e. the probability that the failure envelope lies somewhere between these limits is 75 percent). The failure envelope of the packed specimens lies within these limits and, thus, differences between the failure envelopes appear minimal. Therefore, specimens prepared by packing soil into a mold yield shear strength parameters similar to those found in specimens consolidated from a slurry.

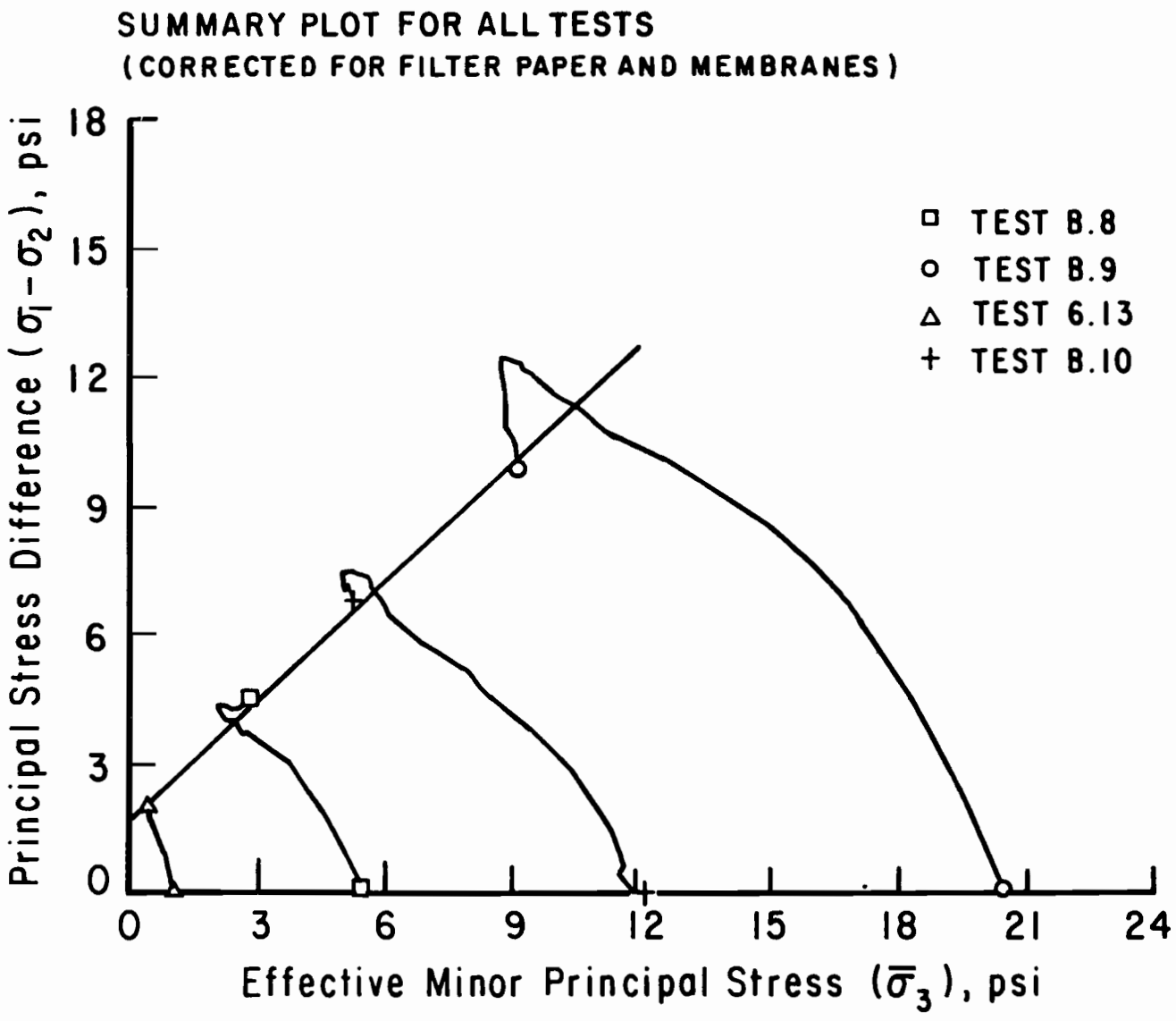

Figure 3.7. Effective Stress Paths and Failure Envelope based on Ultimate Values for Specimens Prepared by Packing.

TABLE 3.7. COMPARISON OF EFFECTIVE STRESS SHEAR STRENGTH PARAMETERS FOR SPECIMENS PREPARED BY BOTH CONSOLIDATING FROM A SLURRY AND PACKING.

Specimen Type	Stress Path Tangency		Ultimate	
	Friction Angle, degrees	Cohesion, psf	Friction Angle, degrees	Cohesion, psf
Consolidated from a Slurry	24	110	18	50
Packed	22	80	18	90

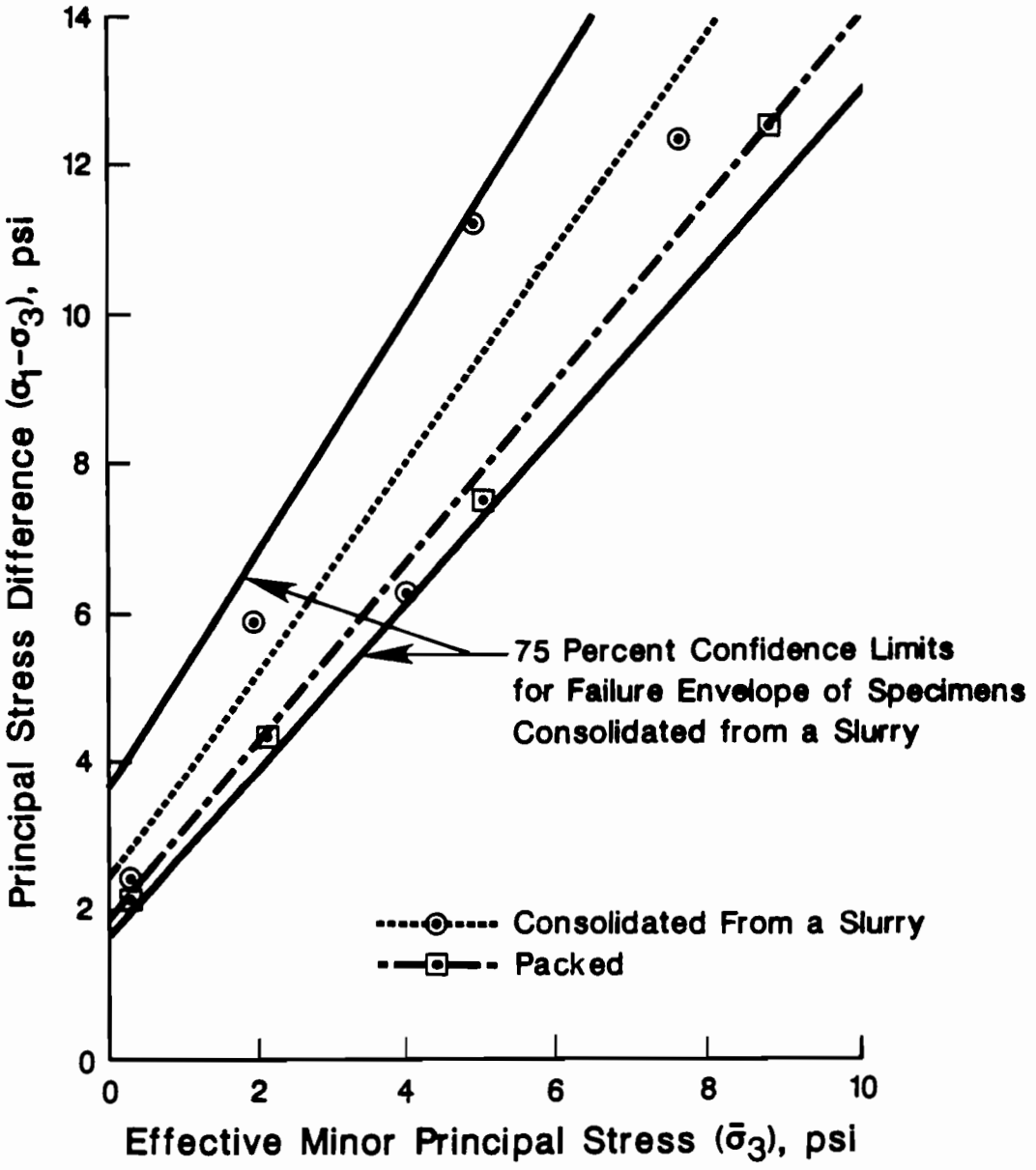

Figure 3.8. Stress Path Tangency Failure Envelopes for Specimens Prepared by Packing and Consolidating from a Slurry, and 75 Percent Confidence Limits based on Specimens Consolidated from a Slurry.

CHAPTER FOUR. RESIDUAL DIRECT SHEAR TESTS

INTRODUCTION

The third series of tests consisted of nine drained direct shear tests on compacted specimens of soil from the Scott Street and I. H. 610 embankment. Skempton (1964) first showed that residual shear strengths, rather than the peak shear strengths, were the governing strengths for the long-term stability of slopes in the London Clay. Although residual shear strengths are associated generally with large deformations and no such movements were observed in the embankments presently of interest, residual shear strengths were judged to be of some interest for comparison with the shear strengths which were developed in the field.

Skempton (1964) measured the residual shear strength in slow, drained direct shear tests, where the residual shear strength was defined as the shear strength developed at large displacements. He actually "cycled" the deformation until a minimum strength was found, which he called the residual shear strength. This method of determining the residual shear strength is discussed by Heley and MacIver (1971) and by Townsend and Gilbert (1976). The concept of residual shear strengths has been widely accepted and applied in slope stability calculations; however, the concept has not generally been applied to compacted fill slopes. Most applications have been made to natural soil deposits and either excavated slopes, natural slopes, or embankment foundations, rather than to compacted fill materials themselves.

SPECIMEN PREPARATION

Specimens for the direct shear tests were compacted in the laboratory using a compaction mold which was specially designed and fabricated for this testing program. The mold has an inside diameter of 2.5 inches, which produces a specimen of the correct final diameter to fit the direct shear box. A drawing of the mold is shown in Fig 4.1. Specimens were compacted in the mold to a "target" dry density of 96.3 pcf and a water content of 24 percent. These values (96.3 pcf and 24 percent) were determined by Gourlay and Wright

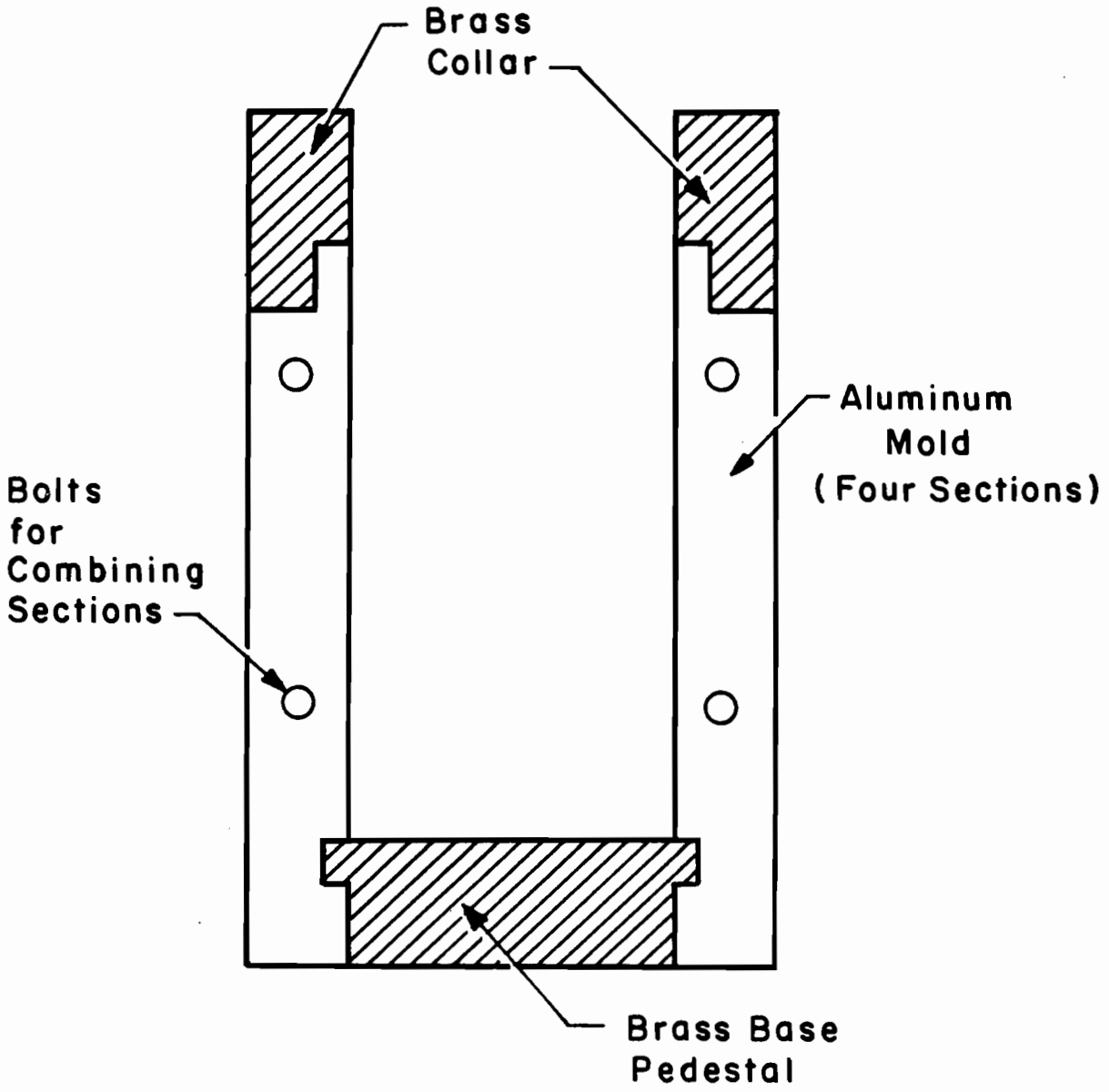

Figure 4.1. Four Section Mold Used to Compact 2.5 Inch Diameter Direct Shear Specimens.

TABLE 4.1. PROPERTIES OF DIRECT SHEAR SPECIMENS AFTER COMPACTION.

Test	Dry Density, pcf	Water Content, percent	Degree of Saturation, percent	Void Ratio
DS-1	98.9	24.1	92	0.70
DS-2	97.4	24.1	89	0.73
DS-3	97.5	24.4	90	0.73
DS-4	97.3	23.8	87	0.73
DS-5	97.6	23.4	87	0.73
DS-6	96.6	22.7	82	0.74
DS-7	97.2	22.4	82	0.73
DS-8	98.3	23.4	88	0.72
DS-9	94.6	22.4	77	0.78
Mean	97.3	23.4	86	0.73
Standard Deviation	1.20	0.76	4.7	0.02

(1984) to be appropriate for the "red" clay from the Scott Street and I. H. 610 embankment based on Texas SDHPT Test Method Tex-113-E. The values were used as "target" values by Gourlay and Wright.

A 2.15 pound hammer with a cylindrical face 1.5 inches in diameter was used to compact the specimens. The soil was compacted in four equal lifts using six hammer blows per lift. Each hammer blow consisted of dropping the hammer a distance of 12 inches and then moving the face of the hammer to another position on the specimen. The surface of each lift was scarified before the next lift was placed. Each lift contained approximately 42 grams of wet soil which had been prepared the previous day at the desired water content; the soil was forced by hand through a #40 sieve immediately prior to compaction. The first three lifts completed the specimen while the fourth lift provided material which could be trimmed to ensure a smooth specimen surface; this trimmed soil was used to determine the as-compacted water content. Using three lifts for the specimen itself ensured that the failure plane which was induced through the middle of the specimen in the direct shear test would not coincide with a lift boundary. After the fourth lift was compacted the mold was disassembled and a stainless steel ring with an inside diameter of 2.5 inches and a height of 0.816 inches was placed over the specimen so that the upper surface could be trimmed.

The as-compacted properties for the nine specimens on which direct shear tests were performed are summarized in Table 4.1. This table includes the dry density, water content, void ratio, and degree of saturation values for each specimen. The void ratio and degree of saturation were calculated using a measured specific gravity of solids of 2.69.

TEST PROCEDURES

Two different devices were used for the direct shear tests: a Wykeham Farrance (Model- WF25301) direct shear device and an Engineering Laboratory Equipment (Model- EL28-009) direct shear device. The vertical load was applied to the specimen in the Wykeham Farrance apparatus by a 10:1 lever arm and to the specimen in the Engineering Laboratory Equipment apparatus by a loaded hanger. A calibrated proving ring was mounted on each device to

measure the horizontal shearing load on the specimen. The rate of shear on both devices could be controlled and equivalent rates used.

Specimens were set-up in the direct shear devices immediately after compaction. Specimens were first consolidated and then sheared at a rate which was judged to be sufficiently slow to ensure that no excess pore-water pressures were developed.

Specimens were consolidated vertically using a single load increment. No free water was made available to the specimens at the beginning of consolidation in order to prevent the specimens from swelling before the application of the vertical load. However, immediately after the load was applied, distilled water was introduced into the direct shear box. Numerous refillings of the direct shear box with distilled water were required throughout the test to replenish the water lost by evaporation.

Time-settlement data were recorded during the consolidation phase of each test. However, the data were of little use in defining when the end of consolidation occurred. Seating problems, movement of the soil into grooves in the upper and lower confining plates, and some swelling of the specimen caused the data to be somewhat erratic.

Gibson and Henkel (1954) suggested that the time to failure, t_f, required in a direct shear test to ensure that excess pore-water pressures are not developed can be calculated from the following equation:

$$t_f = \frac{H^2}{2 \times c_b \times (1-U)} \tag{4.1}$$

where H is one-half the specimen height, c_b is the coefficient of consolidation, and U is the degree of excess pore-water dissipation corresponding approximately to the degree of drainage (a value of U equal to at least 0.95 is recommended by Gibson and Henkel). Although the erratic consolidation data precluded determining the coefficient of consolidation from the current tests, Gibson and Henkel suggest that values found from direct shear tests and triaxial tests are essentially the same. While this may not be entirely true, due to impeded drainage in the triaxial test, only triaxial test data were available. The minimum coefficient of consolidation reported

by Gourlay and Wright (1984) for triaxial specimens prepared from this soil at similar densities and water contents was 0.0012 in.^{2}/min.

Using the coefficient of consolidation reported by Gourlay and Wright (1984) and a specimen height of 0.816 inches (H = 0.816/2 = 0.408 inches), the theoretical minimum time to failure calculated from Eq. 4.1 is 1390 minutes. However, the amount of deformation required for this soil to reach failure in a direct shear test was not known and, therefore, an appropriate shear deformation rate could not be calculated in advance of testing. To be conservative, specimens were sheared at a rate of 0.0017 in./hr. which was the slowest rate possible on the direct shear devices. Prior to shearing the specimens, the upper and lower halves of the direct shear box were separated by 0.05 inches to prevent contact between the halves which would result in friction and, thus, erroneous data.

Large cumulative shear deformations were achieved in the specimens by alternating the direction of deformation in the direct shear device. The shear stress was measured for both directions of shear. As the upper and lower halves of the direct shear specimen were displaced, a change in the area of the horizontal shear plane between the two halves of the specimen occurred. The change in area was considered when the shear stress was calculated. For a circular direct shear specimen with a diameter of 2.5 inches, as was used in these tests, the area of shear is found from the following equation:

$$A = 0.0545 \times \cos^{-1}\left(\frac{\Delta}{2.5}\right) - 1.25 \times \Delta \times \sin\left[\cos^{-1}\left(\frac{\Delta}{2.5}\right)\right] \qquad (4.2)$$

where the displacement, Δ, is in inches, the angle is in degrees, and the shearing area, A, is in square inches. The derivation of Eq. 4.2 is included in Appendix C.

TEST RESULTS

A typical plot of measured shear stress, t, versus cumulative shear deformation is shown in Figure 4.2 for Test DS-3 at a vertical consolidation pressure of 11.6 psi. Similar plots for the remaining direct shear tests are included in Appendix D. The figures all typically show a rapid increase in shear stress during the first cycle until the value corresponding to the peak

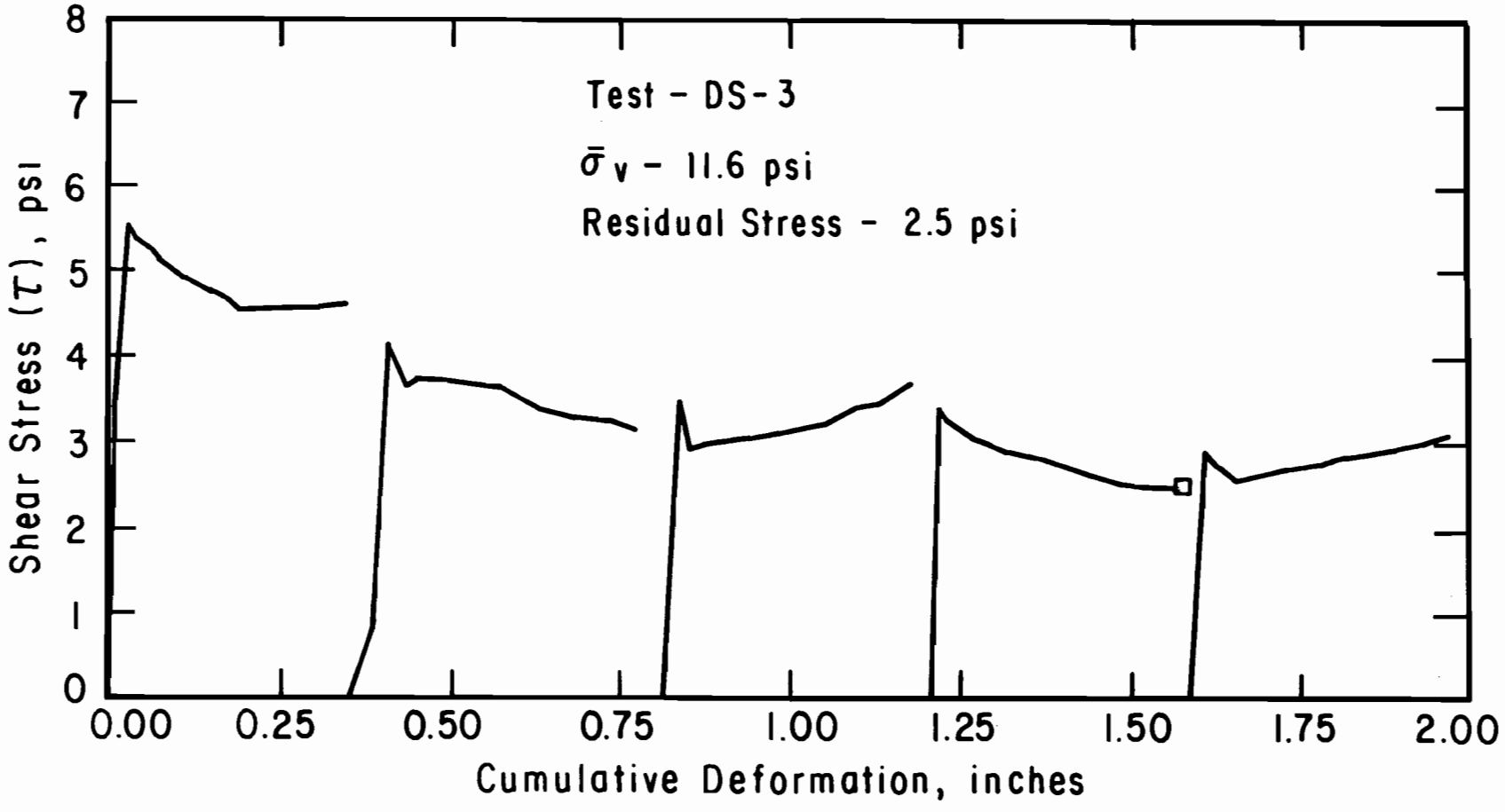

Figure 4.2. Horizontal Shear Stress versus Cumulative Deformation for Direct Shear Test DS-3.

is achieved. A subsequent decrease in shear stress occurs after the peak value. A similar pattern is observed each time the direction of shear is reversed; however, the later peaks are of a much lower magnitude than that which occurs in the first cycle. The stress following each peak tends to decrease as the number of cycles increase until a relatively constant stress is maintained between cycles. The minimum stress found during the test, once the peak for that cycle had been passed, was considered to be the residual strength of the specimen.

Each cycle consisted of deforming the specimen approximately 0.25 inches and then returning it to the point of zero deformation. Deformations up to 0.35 inches were used in the first three tests; however, at these large deformations small lumps of soil occasionally slaked from the gap between the halves of the direct shear box and the upper half of the direct shear box tended to tilt excessively. Each direct shear test lasted approximately 1.5 months. Average cumulative deformation for the specimens was approximately 1.7 inches.

Plots of shear stress versus cumulative deformation occasionally revealed erratic behavior with sudden increases in the shear stress during a cycle and significant differences in stresses between cycles. These erratic data were attributed to two separate factors: Tilting of the upper halves of the direct shear boxes and O-ring friction on the piston used to measure the horizontal load in the Wykeham Farrance device. The tilting of the upper halves of the boxes was believed to be due to volume changes in the specimens during shear and eccentric horizontal loading. Excessive tilting resulted in contact between the upper and lower halves of the boxes which yielded the unrealisticaly high shear stresses. When this occurred the gap between the boxes (0.05 inches) was reset and shearing was continued. Piston friction in the Wykeham Farrance device varied with the direction of movement and resulted in the differences in shear stress between cycles in several of the tests. The lower values of stress are believed to be correct. Significant piston friction occurred in three of the earlier tests, Tests DS-1, DS-2, and DS-4, before the friction was discovered and the results from these tests are viewed with caution.

The "time to failure" in each of the direct shear tests was defined to be the time from the start of shear until the first peak in the shear stress

occurred. The times to failure defined in this manner for all nine tests were averaged and the average was found to be 1200 minutes. This time is slightly less than the theoretical minimum time to failure calculated from Eq. 4.1 (1390 minutes). However, the coefficient of consolidation used in the calculation was believed to be conservative and therefore the rate of shear used (0.0017 in./hr.) should have adequately ensured that no excess pore water pressures developed during the course of the test.

At the completion of each test, the specimen was returned to the point of zero deformation, the water surrounding the specimen was drained, and the vertical load was removed. The direct shear device was then disassembled and a final water content was determined. The vertical effective stress, final dry density, and final water content for the nine direct shear specimens are listed in Table 4.2. The final dry densities were calculated from the initial weight of dry solids, the final water content and assuming a final degree of saturation of 100 percent. The final water contents of the specimens are plotted versus the effective vertical consolidation pressures on the specimens in Figure 4.3. For Tests DS-1, DS-2, and DS-3 the water contents listed in Table 4.2 and shown in Figure 4.3 are probably higher than those which existed in the center of the specimens. Small zones of very wet soil were encountered near the top, bottom, and side of the specimens where effective stresses were probably not uniform, and these zones were included in the final water contents for the first three tests (DS-1, DS-2, and DS-3). For all subsequent tests a wire saw was used to trim the outer, wetter zones from the specimen so a truer representation of the final water content in the shear zone could be obtained.

SHEAR STRENGTHS

Peak Shear Strength

The peak shear stresses for the nine direct shear specimens are summarized in Table 4.3 and plotted in a Mohr-Coulomb diagram in Figure 4.4. A linear regression was performed and the Mohr-Coulomb peak effective stress shear strength parameters, $\bar{c}$ and $\bar{\phi}$, were found to be 260 psf (1.8 psi) and 21 degrees, respectively. The failure envelope corresponding to these values is shown in Figure 4.4. These peak shear strength parameters are comparable to

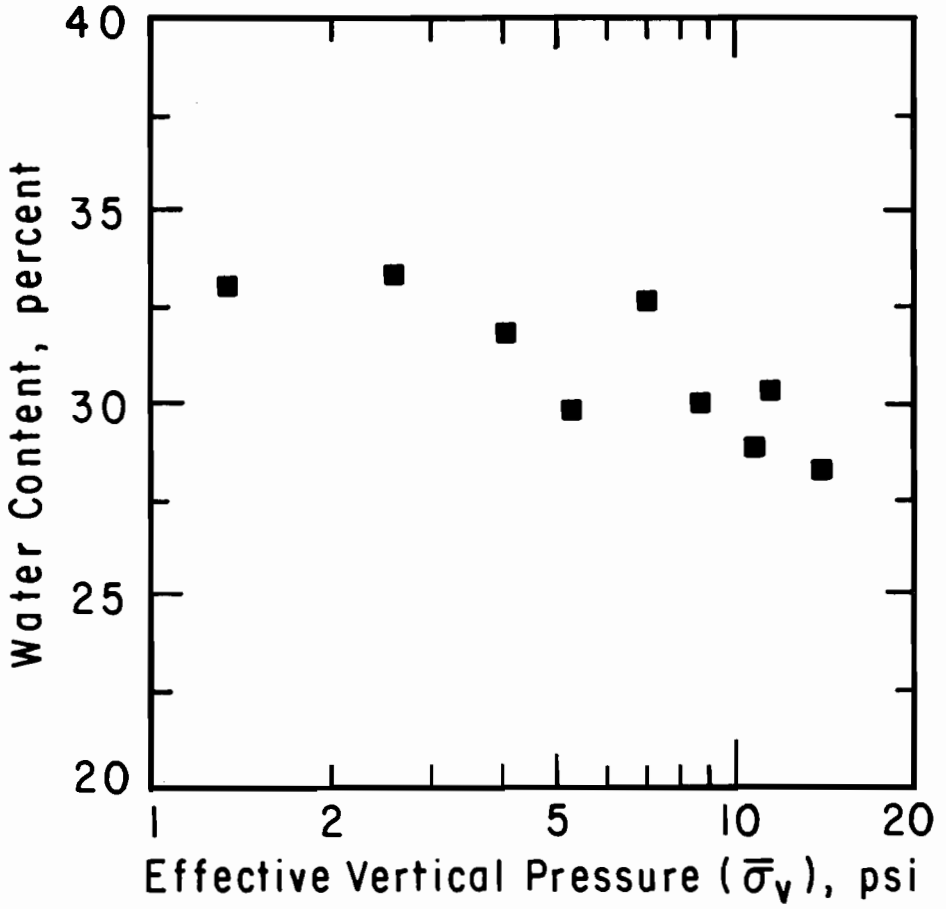

Figure 4.3. Water Content after Completion of Test versus Effective Vertical Stress for Compacted Direct Shear Specimens.

TABLE 4.2. PROPERTIES OF DIRECT SHEAR SPECIMENS AFTER SHEARING.

Test	Effective Vertical Stress, psi	Dry Density, pcf	Water Content, percent
DS-8	1.3	89.1	33.0
DS-7	2.6	88.9	33.2
DS-2	4.0	90.7	31.7
DS-4	5.2	93.2	29.9
DS-1	7.3	89.3	32.8
DS-5	8.9	93.0	30.0
DS-6	11.3	94.7	28.9
DS-3	11.6	92.5	30.4
DS-9	14.1	95.7	28.2

TABLE 4.3. PEAK SHEAR STRESSES FOUND FOR DIRECT SHEAR SPECIMENS.

Test	Effective Vertical Stress, psi	Peak Horizontal Stress, psi
DS-8	1.3	1.7
DS-7	2.6	2.3
DS-2	4.0	4.4
DS-4	5.2	3.2
DS-1	7.3	6.2
DS-5	8.9	5.4
DS-6	11.3	6.3
DS-3	11.6	5.6
DS-9	14.1	7.2

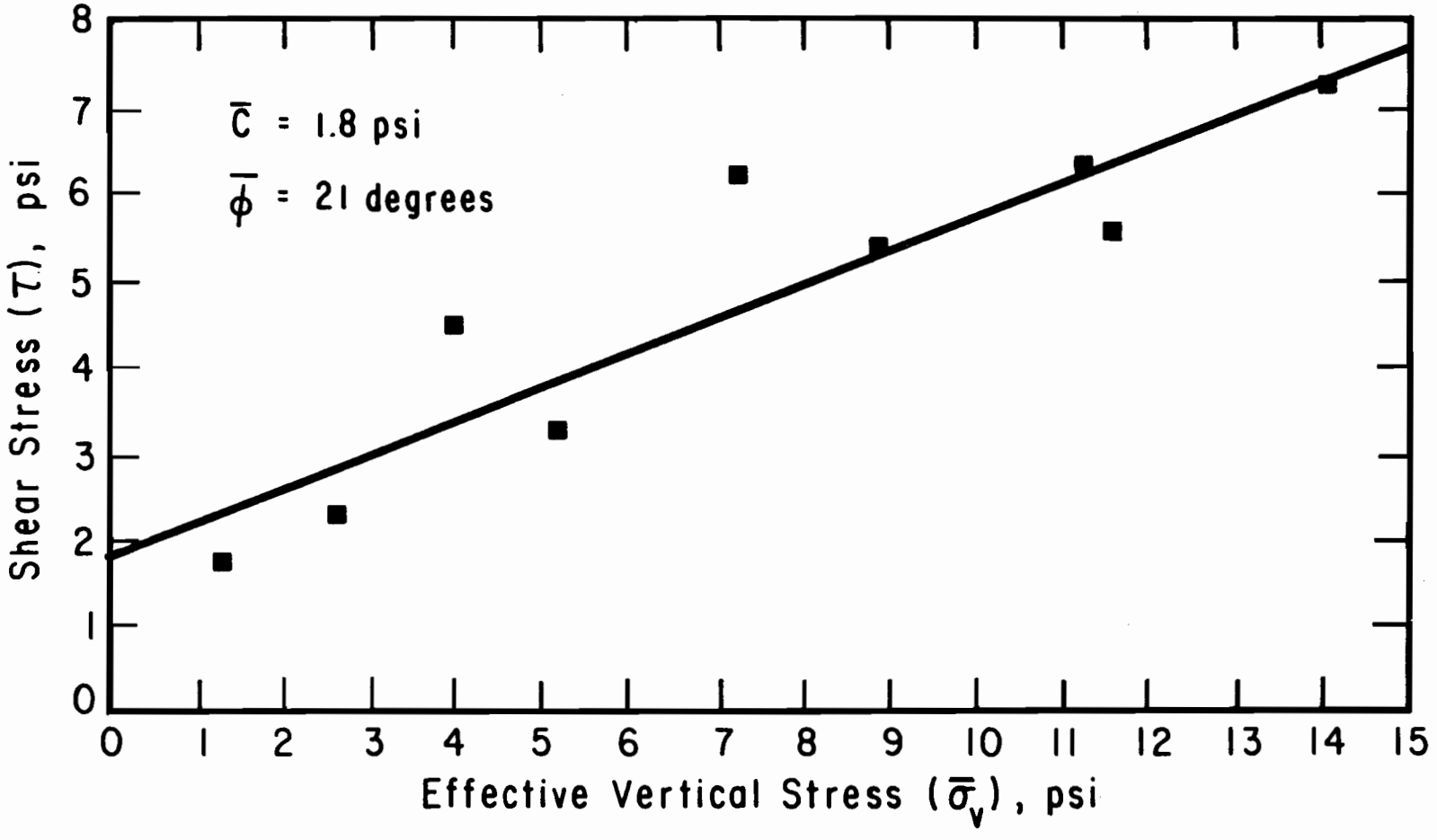

Figure 4.4. Mohr-Coulomb Failure Envelope based on Peak Shear Stress Values for Compacted Direct Shear Specimens.

the values of 270 psf for $\bar{c}$ and 20 degrees for $\bar{\phi}$, reported by Gourlay and Wright (1984) based on triaxial tests on similar specimens.

Residual Shear Strength

Residual shear stresses from the direct shear tests are listed in Table 4.4 and plotted in a Mohr-Coulomb diagram in Figure 4.5. A linear regression yielded residual effective stress shear strength parameters, $\bar{c}_r$ and $\bar{\phi}_r$, of 100 psf (0.7 psi) and 12 degrees, respectively. The failure envelope corresponding to these values is shown in Figure 4.5.

The residual shear strengths derived from Tests DS-1, DS-2, and DS-4 are questionable due to piston friction during the tests, and another linear regression was performed in which these tests were excluded. The cohesion and friction angle, $\bar{c}_r$ and $\bar{\phi}_r$, found from the second linear regression are 16 psf (0.11 psi) and 14 degrees, respectively. The failure envelope corresponding to these values is shown in Figure 4.6. The failure envelope shown in Figure 4.6 appears to fit the plotted residual shear stresses much better than the failure envelope shown in Figure 4.5 where Tests DS-1, DS-2, and DS-4 were included.

Focht and Sullivan (1969) have reported the residual strengths, $\bar{c}_r$ and $\bar{\phi}_r$, of undisturbed Beaumont clay to be 0 psf and 15 degrees, respectively, based on both field and laboratory observations. To determine if a residual cohesion value of zero is appropriate for the current direct shear tests, a modified linear regression was performed using the values listed in Table 4.4 (results of Tests DS-1, DS-2, and DS-4 were excluded) in which the cohesion value was required to be zero. The friction angle found from this linear regression is 14 degrees. The failure envelope found from this regression is shown in Figure 4.7. The failure envelope shown in Figure 4.7 for a cohesion value of zero appears to actually fit the data at low effective pressures better than the failure envelope shown in Figure 4.6, which was based on a linear regression.

Based on the results of the direct shear tests, the residual friction angle of compacted Beaumont clay tested in this study appears to be approximately 14 degrees. Although some uncertainty exists in the residual cohesion of the soil, the value can be considered negligible when compared to the peak cohesion of 260 psf.

TABLE 4.4. RESIDUAL SHEAR STRESSES FOUND FOR DIRECT SHEAR SPECIMENS.

Test	Effective Vertical Stress, psi	Residual Horizontal Stress, psi
DS-8	1.3	0.4
DS-7	2.6	0.7
DS-2	4.0	2.1
DS-4	5.2	2.1
DS-1	7.3	3.2
DS-5	8.9	2.6
DS-6	11.3	3.1
DS-3	11.6	2.5
DS-9	14.1	3.5

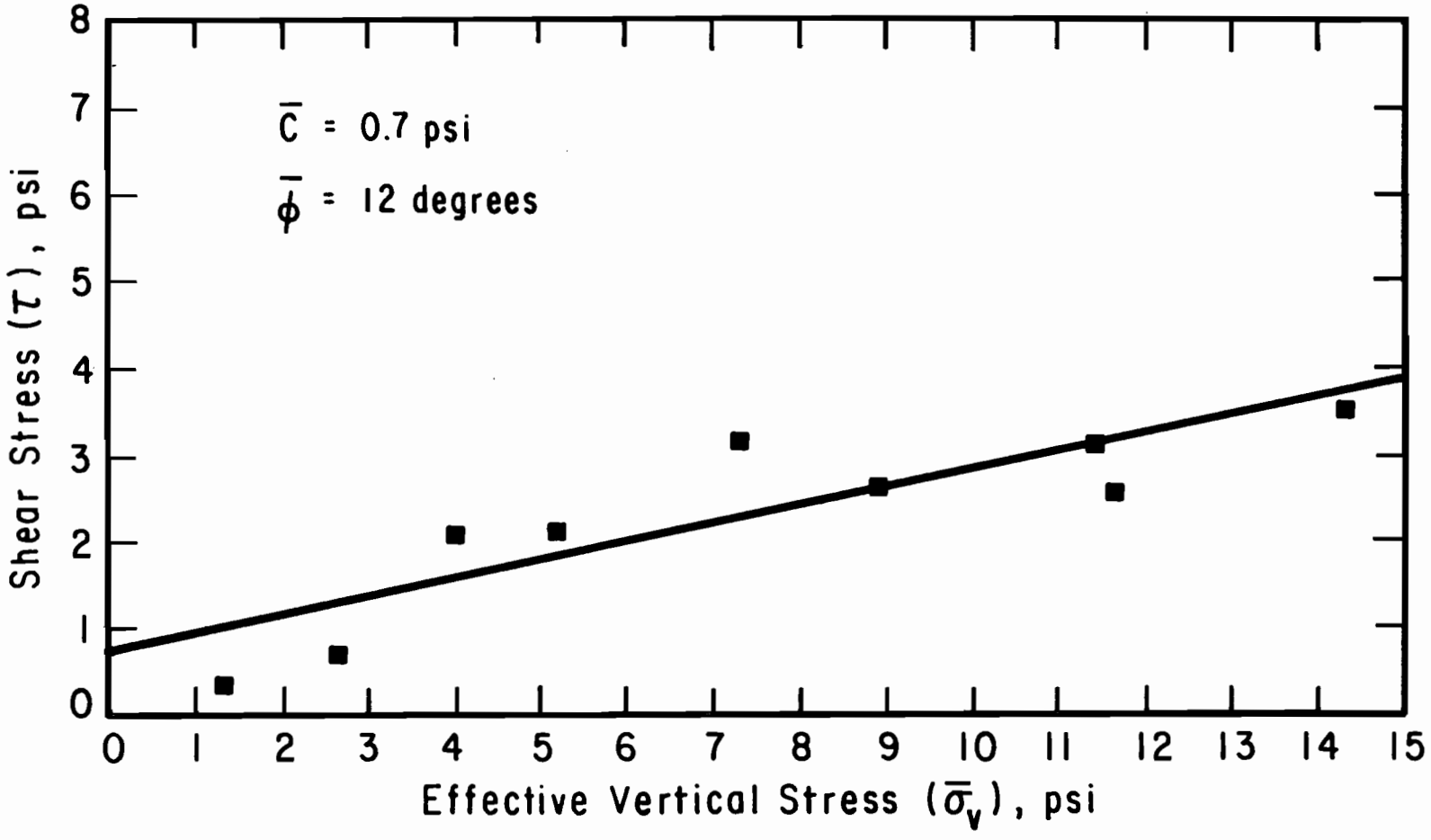

Figure 4.5. Mohr-Coulomb Failure Envelope based on Residual Shear Stress Values for Compacted Direct Shear Specimens.

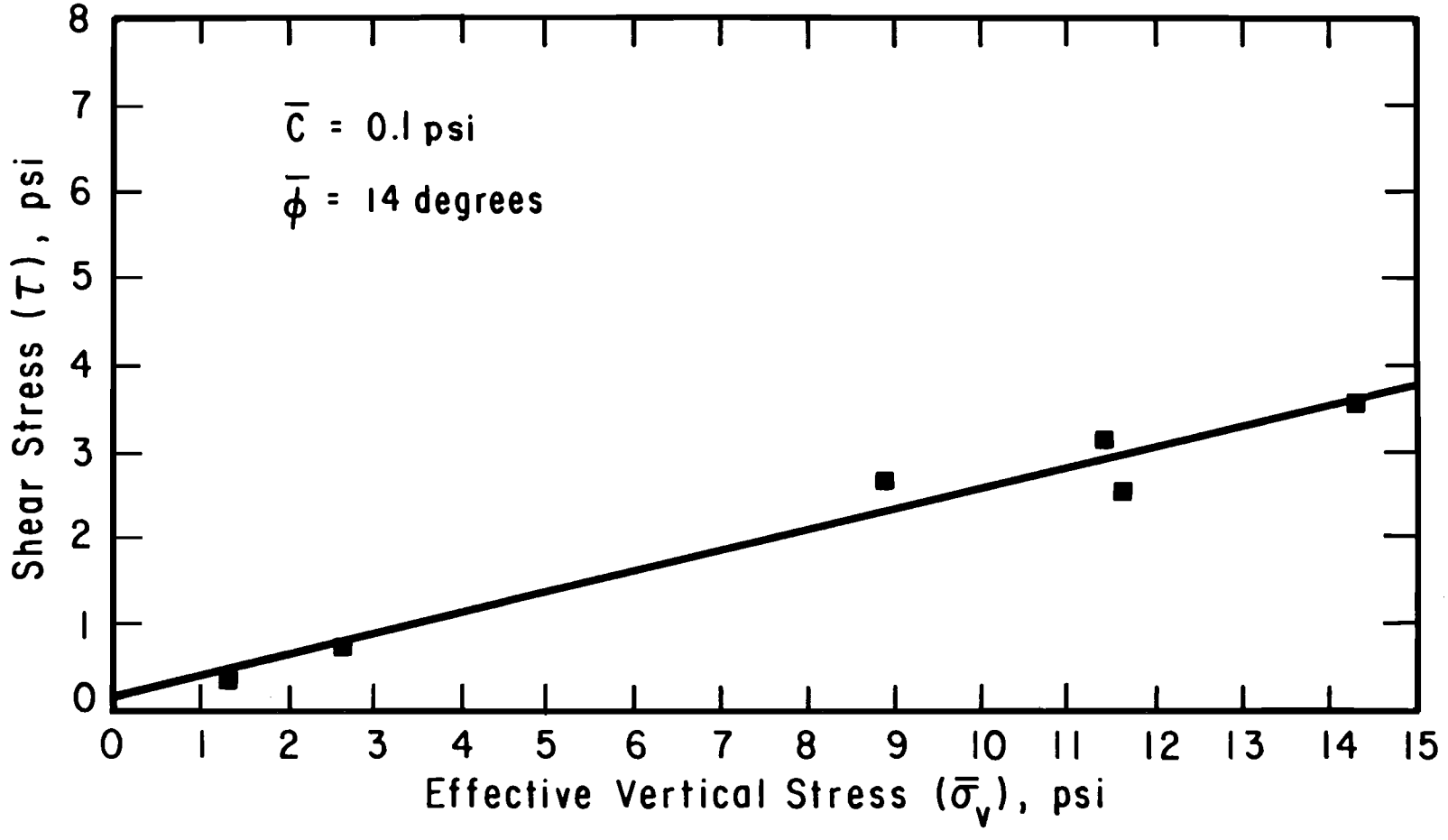

Figure 4.6. Mohr-Coulomb Failure Envelope based on Residual Shear Stress Values for Compacted Direct Shear Specimens, Excluding Tests DS-1, DS-2, and DS-4.

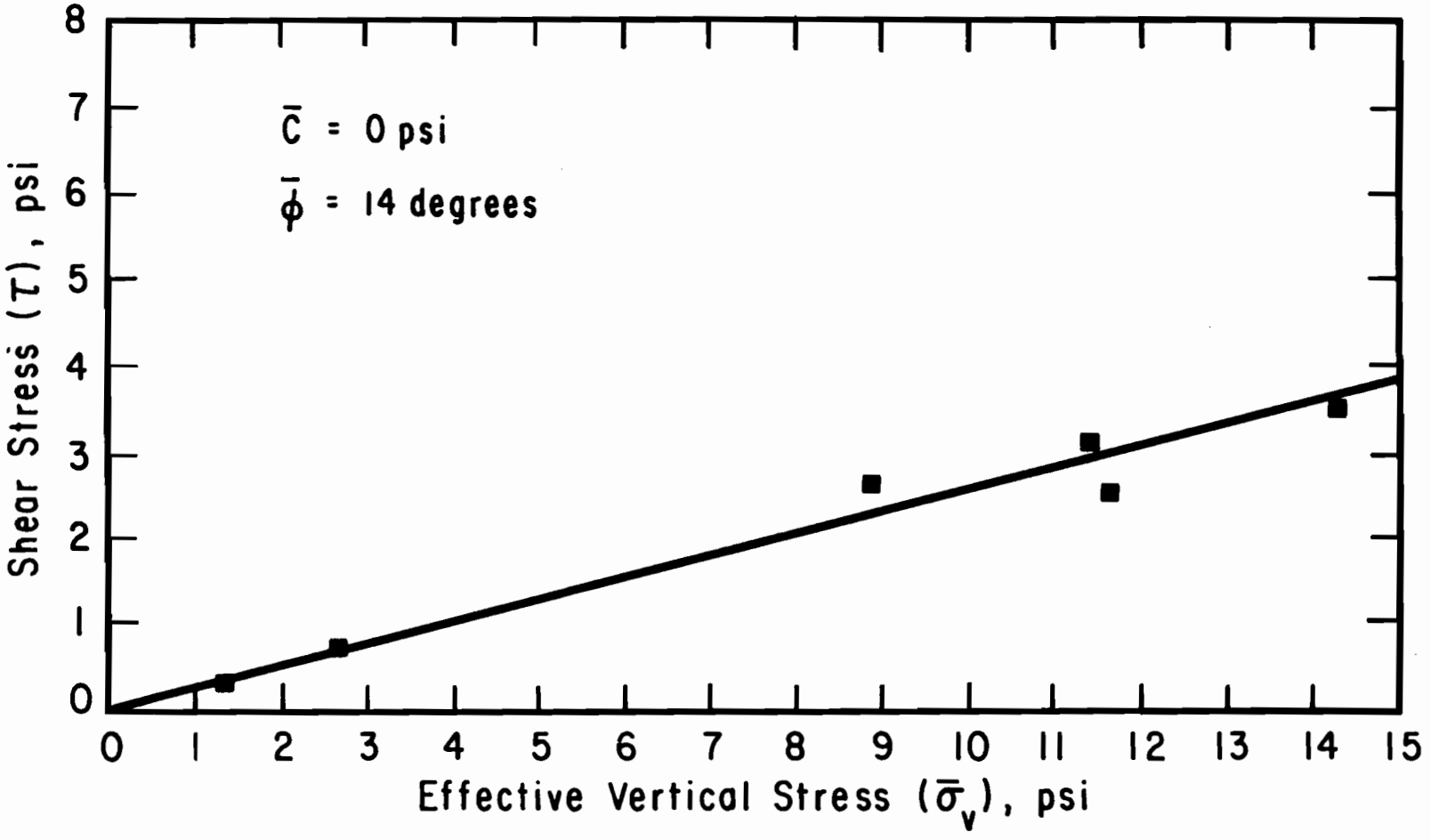

Figure 4.7. Mohr-Coulomb Failure Envelope based on Residual Shear Stress Values for Compacted Direct Shear Specimens (Cohesion Intercept Forced to Zero).

CHAPTER FIVE. UNDISTURBED SOIL SAMPLING

INTRODUCTION

All of the tests described in the preceding chapters in addition to those reported by Gourlay and Wright (1984) were performed on laboratory prepared specimens. It was recognized at an early stage that some of the discrepancies between the field and laboratory shear strength values might be due to the fact that laboratory prepared specimens, for one or more reasons, did not reproduce the conditions in the field. As a result, undisturbed specimens were taken from the Scott Street and I. H. 610 embankment and returned to the University of Texas for testing as part of the second stage of laboratory testing. The field exploration and sampling to obtain undisturbed samples is described in this chapter and the results of triaxial shear tests performed on undisturbed specimens are presented in the next chapter.

UNDISTURBED SAMPLING

Undisturbed Shelby tube samples were obtained from the portion of the embankment at the north-east corner of I. H. 610 and Scott Street. Southwestern Laboratories, Inc. performed the drilling and sampling on May 1, 1984, under the supervision and direction of personnel from the University of Texas.

The drill rig used was a CME-55 mounted rig on an all-terrain vehicle. Due to the steep inclination of the slope there was some difficulty in placing the drill rig in certain locations; an anchor was therefore required above the slope to secure the drill rig. For this purpose a laden water truck was parked on the shoulder of the freeway, at the crest of the slope, with a cable attached to the drill rig. The drill rig was levelled by three hydraulic jacks mounted on the all-terrain vehicle. A slight inclination was observed in several of the boreholes but the inclination was considered negligible.

The Shelby tubes used to recover the samples were 2.5 feet in length with an outside diameter of 2.92 inches. Initially tubes with a wall thickness of 0.096 inches were used for sampling, but after 21 samples were recovered the

supply of tubes at the sampling site was depleted and additional tubes had to be delivered. The delivered tubes were almost identical to the initial tubes but had a wall thickness of 0.070 inches. The first and second tubes had area ratios of 13.2 percent and 10.8 percent, respectively.

Ten borings were made in the slope; five were located slightly east of the slide area and the remaining were located inside of the unrepaired slide mass. The location of the borings and the approximate slide mass with respect to the slope are shown in Figure 5.1. A depth of penetration of six feet was used for seven of the borings and a depth of eight feet was used for the remaining three. Stauffer and Wright (1984) reported that this slope failure was shallow and, thus, deeper borings were not considered to be necessary. Each tube was pushed a distance of 2.0 feet and the lengths of recovery varied from 0.7 feet to 2.0 feet. In order to avoid recovery problems, the tube was twisted while still in the ground to free the sampled soil from the bottom of the boring. A complete list of the recovered samples is given in Table 5.1.

The samples from the first boring, designated BH#1, were extruded with a horizontally oriented extruder at the site in order to inspect the quality of the samples. The extruded samples appeared to be generally of good quality; however, they tended to break apart. Consequently, all subsequent samples were left in the tubes until they could be transported to The University of Texas for extrusion and examination. Both ends of the tubes were sealed with paraffin and a plastic cap immediately after the tubes were removed from the ground. The tubes were stored in a moisture room at The University of Texas at Austin until they were extruded.

SPECIMEN EXTRUSION

Prior to extrusion, the Shelby tube was cut with a hacksaw slightly above the paraffin at the top of the tube to reduce the distance through which the soil would have to be pushed. After cutting the tube, the paraffin was removed from both ends of the tube. The tube was then placed in a frame which fixed the tube in a vertical position, and a hand operated hydraulic jack was used to extrude the soil. A steel plate with a diameter of 2.7 inches was attached to the piston to push the soil. The soil was extruded vertically in

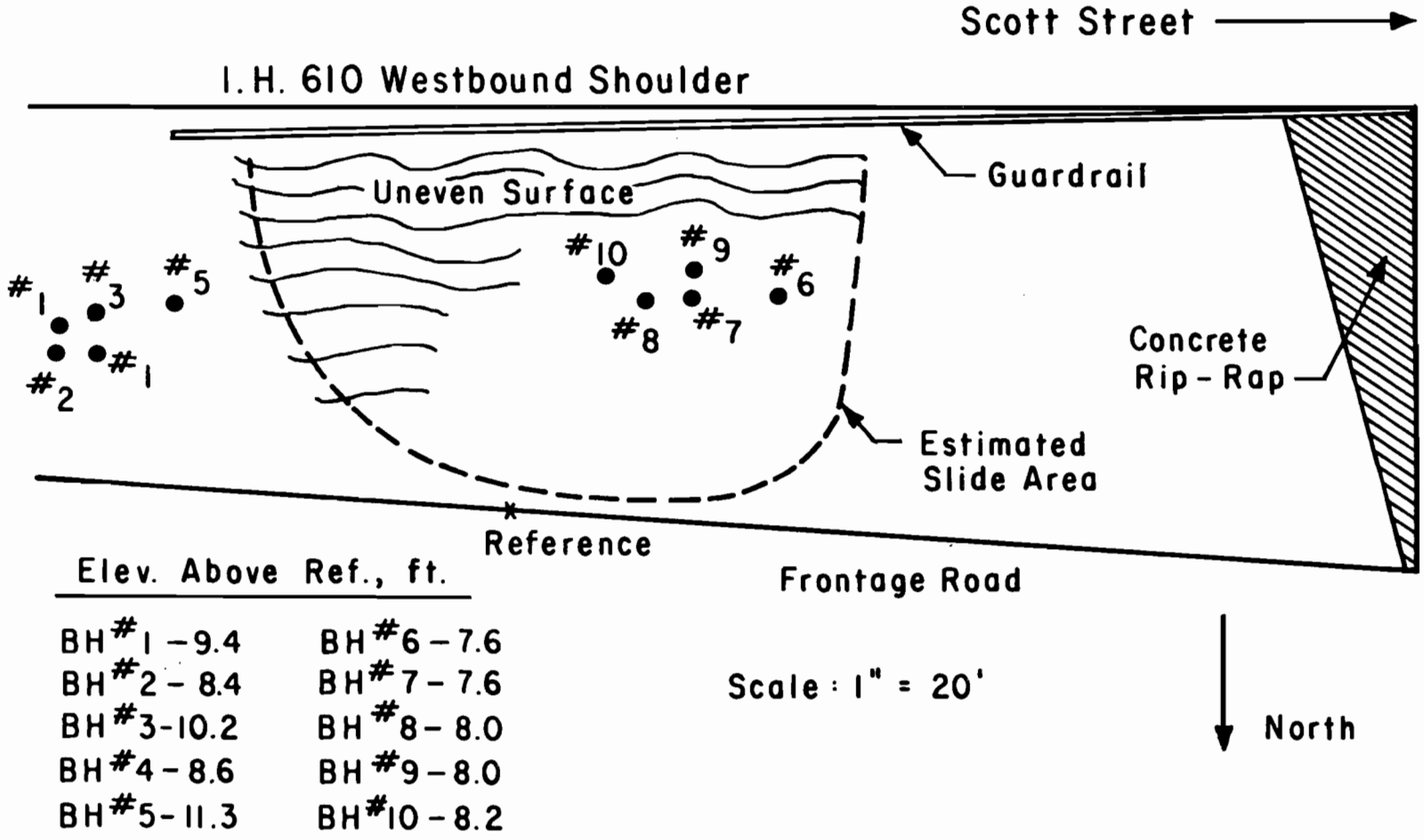

Figure 5.1. Plan View of Failed Embankment at Intersection of I. H. 610 and Scott Stress in Houston, Texas.

TABLE 5.1. LIST OF RECOVERED SAMPLES EXAMINED IN THE LABORATORY.

Boring	Tip Depth of Shelby Tube, feet	Length of Recovery, feet
BH#2	2.2	2.1
	5.0	1.7
	7.0	1.3
BH#3	2.0	1.4
	4.0	1.1
	6.0	1.2
BH#4	2.0	0.7
	4.0	1.0
	6.0	1.8
BH#5	2.1	2.1
	4.0	2.0
	6.0	1.8
	8.0	1.8
BH#6	2.0	2.0
	4.1	1.9
	6.0	2.0
BH#7	2.0	1.9
	4.0	1.3
	6.0	1.9
	8.0	2.0
BH#8	2.0	2.0
	4.0	1.5
	6.0	1.8
BH#9	2.0	1.2
	4.0	1.2
	6.0	2.0
	8.0	2.0
BH#10	2.0	2.0
	4.0	2.0
	5.8	1.8

the same direction as it was originally pushed into the tube. Some compression of the soil was observed during the extrusion process.

Some sections of soil approximately two to three inches in length were extruded, and removed from the top of the tube with a sharp knife for classification and measurement of water content and density. Other sections of approximately 5 inches in length were obtained for triaxial testing whenever consistent, trimmable soil was encountered. The preparation and testing of the triaxial specimens is discussed in the following chapter.

SOIL PROFILES

The soil profiles for Borings BH#2 through BH#10 are included in Appendix E, along with plots of water content and dry density versus depth. Some gaps exist in the soil profiles due to incomplete sample recovery in the Shelby tubes. Two distinct soil colors appear in the soil profiles, grey and red. Gourlay and Wright (1984) also report the two distinct soil colors in their findings. Variations in these two colors (red and grey) existed, and small quantities of soil with other colors, such as tan and brown, were observed. Rarely was a soil with homogeneous color encountered; pockets of different colored soil were usually included in any section of soil. Calcareous nodules and organics, such as grass and roots, were encountered quite often throughout the embankment. Silt and silty clay pockets were occasionally encountered. The soil used to construct the embankment was known to be miscellaneous fill from the Houston area; therefore, even though the soil used to construct the embankment was all Beaumont clay, some variation in the color and properties of the soil was expected.

The soil profiles from the location outside of the slide area, BH#2 through BH#5, show the colors of the soil as being well mixed with no obvious signs of layering. The soil profiles from the locations within the slide area, BH#6 through BH#10, show the colors of the soil as being well segregated. From these borings the profile of the slide area can be generalized as highly organic grey clay from zero to one feet, red clay from two to five feet, and grey clay below a depth of five feet. The lower grey layer tended to be very stiff and have lower water contents than in the other layers; therefore the possibility that the failure occurred below a depth of

five feet seems unlikely. The soil above a depth of six feet had a uniform texture with relatively few visible voids, but below a depth of six feet large voids and distinct peds were visible; therefore, it appears that changes in the macro-structure of the soil were limited to a depth of approximately six feet in this embankment.

FAILURE SURFACE

After sufficient triaxial specimens from within the slide area had been tested, 10 sample tubes remained from the slide area. These 10 tubes represented three complete borings and it was decided to use these tubes to obtain a more detailed profile of water content and Atterberg Limits with depth. The focus was to locate the failure zone by finding the depth in which the soil contained an unsually high water content or liquid limit. The three borings which were examined were BH#6, BH#8, and BH#9. The water contents and Atterberg Limits found for BH#6, BH#8, and BH#9 are shown versus depth in Figures 5.2, 5.3, and 5.4, respectively. All of the Atterberg Limits were determined according to ASTM (1982) standards.

The Atterberg Limits shown for BH#6, BH#8, and BH#9 vary greatly even for soil with the same color. The plastic limit for the red clay varied from 11 to 25 percent, and for the grey clay from 9 to 25 percent. The liquid limit for the red clay varied from 48 to 76 percent, and for the grey clay from 40 to 52 percent. The liquid limits found by Gourlay and Wright (1984) during their field investigation, 50 percent for the grey clay and 70 percent for the red clay, agree well with those given here except for the wider variation in values discovered in the present investigation. For boring BH#6 the highest liquid limits, approximately 76 percent, were found between the depth of three to five feet, and for BH#9 between four and five feet; no soil in this depth range was recovered for BH#8. The depths at which the maximum water contents were found were 4.5 feet for BH#6, 4.8 feet for BH#8, and 3.8 feet for BH#9. These depths correspond well to the depths in which the high liquid limits were encountered.

The positions of the borings taken from within the slide mass are shown relative to the cross-section of the slide mass in Figure 5.5. The circular surface shown in Figure 5.5 is the same surface used by Stauffer and Wright

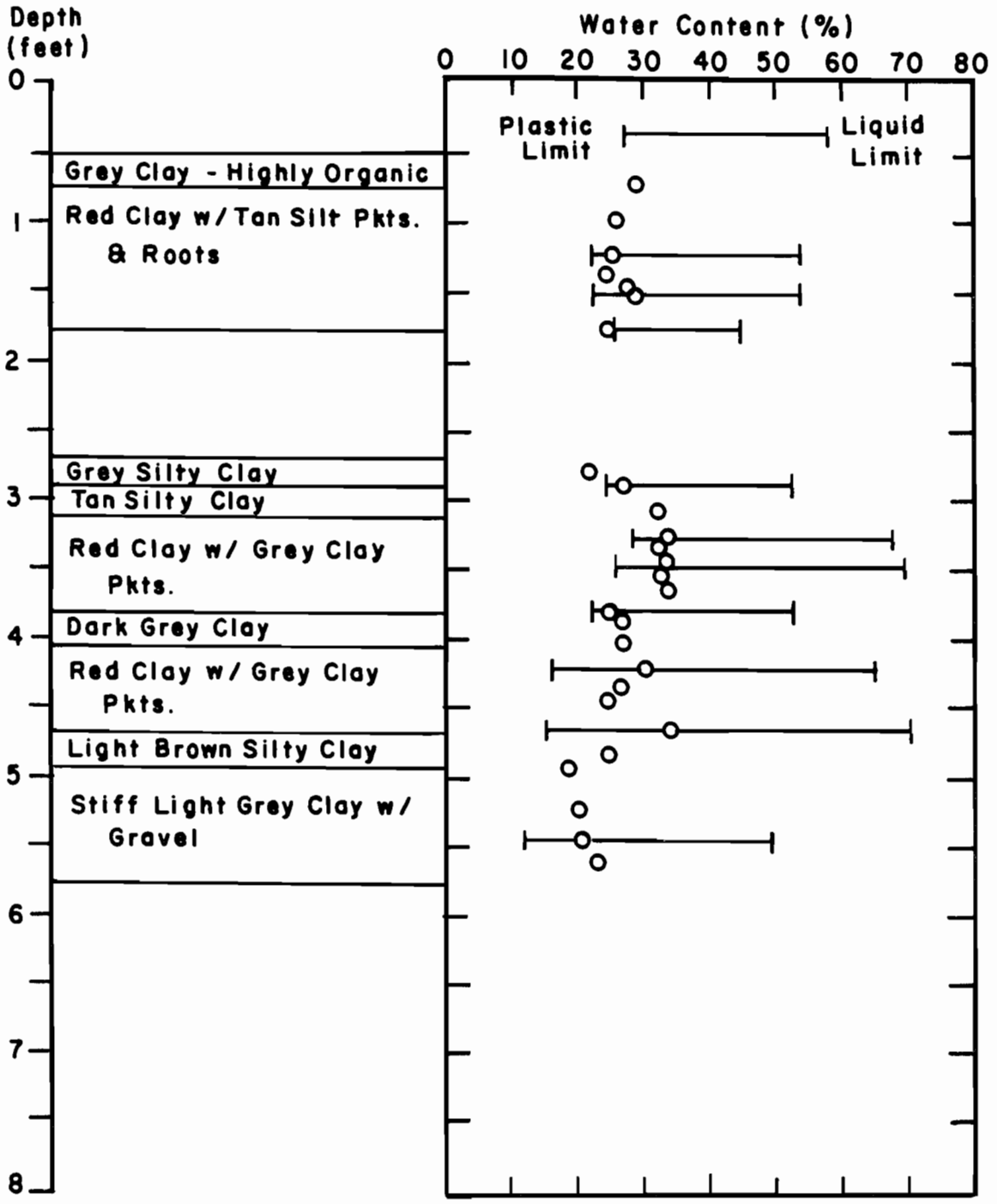

Figure 5.2. Soil Profile for Boring BH#6 at I. H. 610 and Scott Street Embankment.

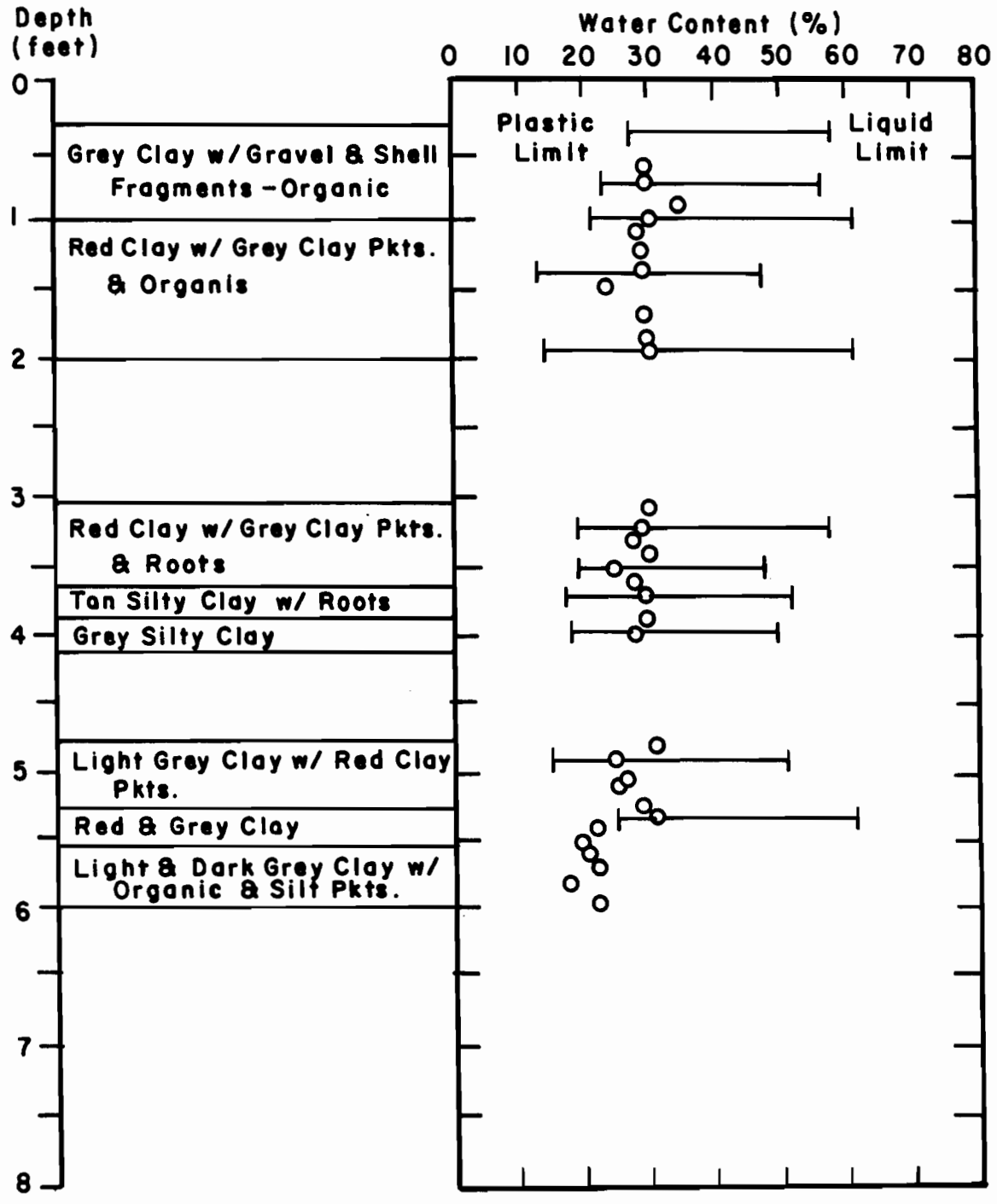

Figure 5.3. Soil Profile for Boring BH#8 at I. H. 610 and Scott Street.

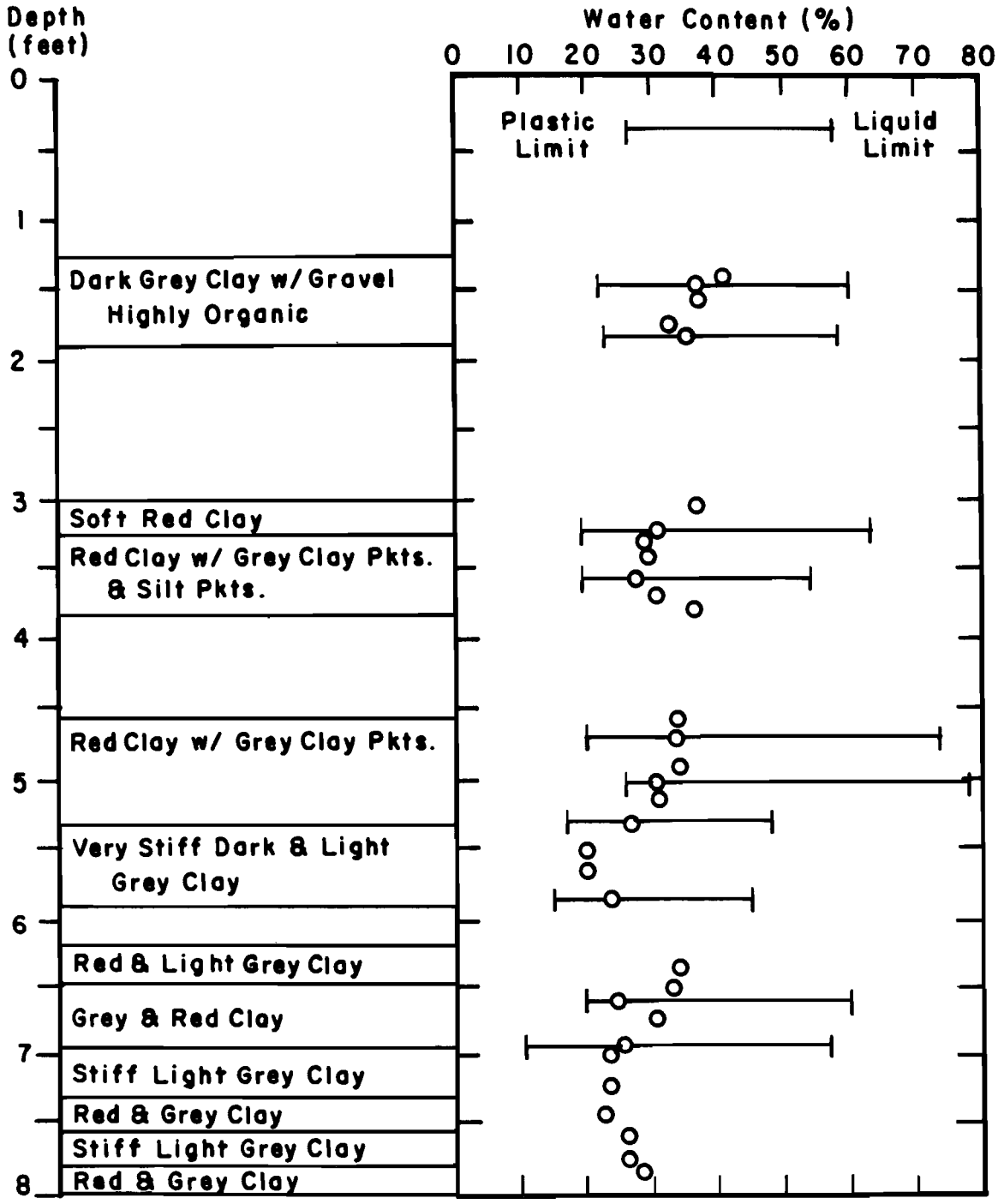

Figure 5.4. Soil Profile for Boring BH#9 at I.H. 610 and Scott Street.

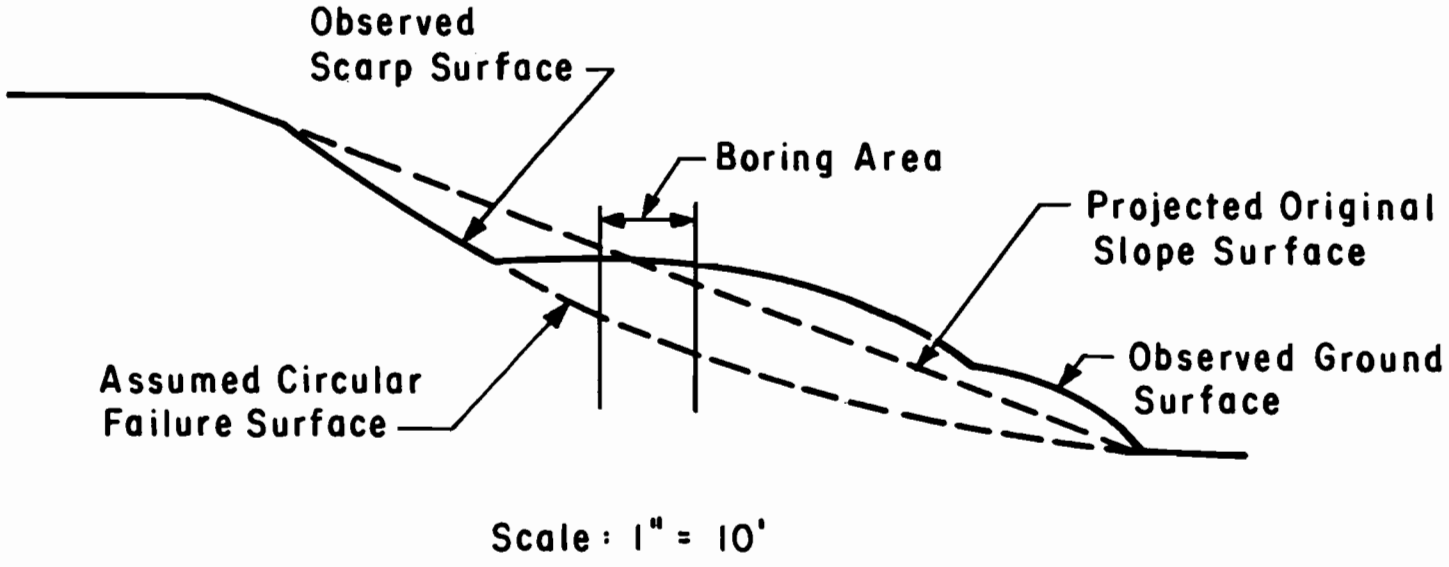

Figure 5.5. Cross-Section of Failed Embankment at Intersection of I. H. 610 and Scott Street Showing Approximate Location of Borings (Profile from Stauffer and Wright, 1984).

(1984) for back-calculation of strength values. Based on this estimated failure surface, the failure plane should have passed through the boring area at a depth of between 3.0 feet and 5.0 feet which is a zone of red clay. High liquid limits were found in this region making the failure surface estimated by Stauffer and Wright (1984) appear reasonable. However, there is a great deal of scatter in the water contents obtained from the borings and the failure surface cannot be identified by an abrupt change in water content; sampling was performed over one year after the data of failure and redistribution of water throughout the slope has probably occurred removing the zone of high water content which was expected.

CHAPTER SIX. TESTS ON UNDISTURBED SPECIMENS

INTRODUCTION

The fourth series of tests was performed on undisturbed specimens from the Scott Street and I. H. 610 embankment. The purpose of this series of tests was to compare the effective stress shear strength parameters of undisturbed specimens to both those measured on specimens prepared in the laboratory and those back-calculated from the slope and slide geometry in the field. Seventeen consolidated-undrained (R) triaxial shear tests and three consolidated-drained (S) triaxial shear tests were performed. Procedures for preparing the specimens, properties of the specimens, and results of the shear tests are discussed in this chapter.

SPECIMEN PREPARATION

Undisturbed samples were examined as they were extruded to obtain relatively homogeneous specimens with little or no organic material, calcareous nodules, or gravel for use in the triaxial shear tests. After extrusion, the approximately 2.8 inch diameter sample was trimmed to a diameter of 1.5 inch for triaxial shear testing. A soil trimming "lathe" and wire saw were used to trim the specimens in the conventional manner. Water contents and Atterberg Limits were determined from a portion of the trimmings. Small calcareous nodules and gravel were often encountered during the trimming process and had to be removed. The voids remaining after their removal were carefully filled with soil and retrimmed to prevent irregularities in the specimens.

A miter box was used to trim the ends of the specimen to a final length of three inches. The specimen was then weighed, and the height and diameter measured with a caliper. The specimen was then wrapped with cellophane and placed in a humid area for approximately one hour while the final preparations were made of the triaxial apparatus. Unlike the specimens which were consolidated from a slurry and the packed specimens, the undisturbed specimens were quite firm and easy to handle.

SPECIMEN PROPERTIES

The test specimens were separated into three groups based on color and location in the slope as follows:

- Group A - Grey clay from outside of the slide area.
- Group B - Red clay from outside of the slide area.
- Group C - Red clay from within the slide area.

No specimens of grey clay from within the slide area could be obtained because all of the grey clay encountered in this area was either highly organic or contained large calcareous nodules. Group C, the red clay from within the slide area, was of the greatest interest because it was the primary soil along the failure surface of the slide. Although the specimens were grouped by color, they were rarely homogeneous and usually contained pockets of different colored soil.

The dry density, water content, degree of saturation, and void ratio of the triaxial specimens immediately after trimming along with the Atterberg Limits which were found from the trimmed soil, are listed in Tables 6.1, 6.2, and 6.3 for Groups A, B, and C, respectively. The properties listed in Tables 6.1 through 6.3 have been calculated from the dry weight of solids after the completion of the triaxial tests. The specific gravities of solids for the red and grey clay were determined to be 2.69 and 2.64, respectively. The Atterberg Limits listed in Tables 6.1 through 6.3 reveal some variation for the specimens within the same soil group.

SATURATION AND CONSOLIDATION OF SPECIMENS

The procedures for set-up, back pressure saturation, and consolidation of the undisturbed triaxial specimens were similar to those used for all the previous triaxial specimens and are given by Gourlay and Wright (1984). Approximately two weeks were required to complete back pressure saturation and consolidation of each specimen. The pore water pressures, when measured to determine Skempton's (1954) B value, required only a few seconds to reach equilibrium after the increase in the cell pressure. For this reason a 30 second response time was used to measure the B value instead of the two minute response time which was used for the specimens discussed in previous chapters. At the end of back pressure saturation the B values found for the undisturbed

TABLE 6.1. PROPERTIES OF UNDISTURBED GREY CLAY SPECIMENS FROM OUTSIDE THE SLIDE AREA AFTER TRIMMING.

Test	Boring	Depth, ft.-in.	Dry Density, pcf	Water Content, percent	Degree Of Saturation, percent	Void Ratio	Plastic Limit, percent	Liquid Limit, percent
6.22	BH#2	6'-4"	103.1	22.1	98	0.60	19	51
6.20	BH#3	3'-0"	98.6	24.8	98	0.67	19	54
6.24	BH#4	3'-6"	97.3	27.0	100	0.70	9	49
6.25	BH#4	5'-5"	99.5	25.2	100	0.66	20	54
B.11	BH#5	1'-9"	94.3	27.0	96	0.75	22	52
6.14	BH#5	3'-7"	99.2	24.0	96	0.66	17	46

TABLE 6.2. PROPERTIES OF UNDISTURBED RED CLAY SPECIMENS FROM OUTSIDE THE SLIDE AREA AFTER TRIMMING.

Test	Boring	Depth, ft.-in.	Dry Density, pcf	Water Content, percent	Degree Of Saturation, percent	Void Ratio	Plastic Limit, percent	Liquid Limit, percent
6.23	BH#2	4'-7"	97.7	24.4	91	0.72	20	59
B.18	BH#3	1'-8"	111.2	18.2	96	0.51	20	53
6.26	BH#4	4'-11"	94.2	29.1	99	0.79	22	64
B.13	BH#5	5'-2"	96.5	27.9	100	0.74	18	65
6.16	BH#5	5'-7"	93.5	30.3	100	0.80	18	65
B.14	BH#5	7'-6"	97.1	25.2	93	0.73	22	72

TABLE 6.3. PROPERTIES OF UNDISTURBED RED CLAY SPECIMENS FROM WITHIN THE SLIDE AREA AFTER TRIMMING.

Test	Boring	Depth, ft.-in.	Dry Density, pcf	Water Content, percent	Degree Of Saturation, percent	Void Ratio	Plastic Limit, percent	Liquid Limit, percent
B.15	BH#7	1'-3"	96.4	26.5	96	0.75	16	52
6.17	BH#7	3'-0"	91.9	29.1	94	0.83	16	48
6.18	BH#7	5'-0"	90.7	31.4	99	0.86	22	66
6.21	BH#10	1'-4"	86.8	30.2	86	0.94	27	73
B.16	BH#10	2'-6"	96.6	27.3	99	0.74	19	55
6.19	BH#10	3'-4"	92.2	30.4	99	0.83	19	55
B.17	BH#10	4'-5"	93.5	28.4	96	0.80	17	49

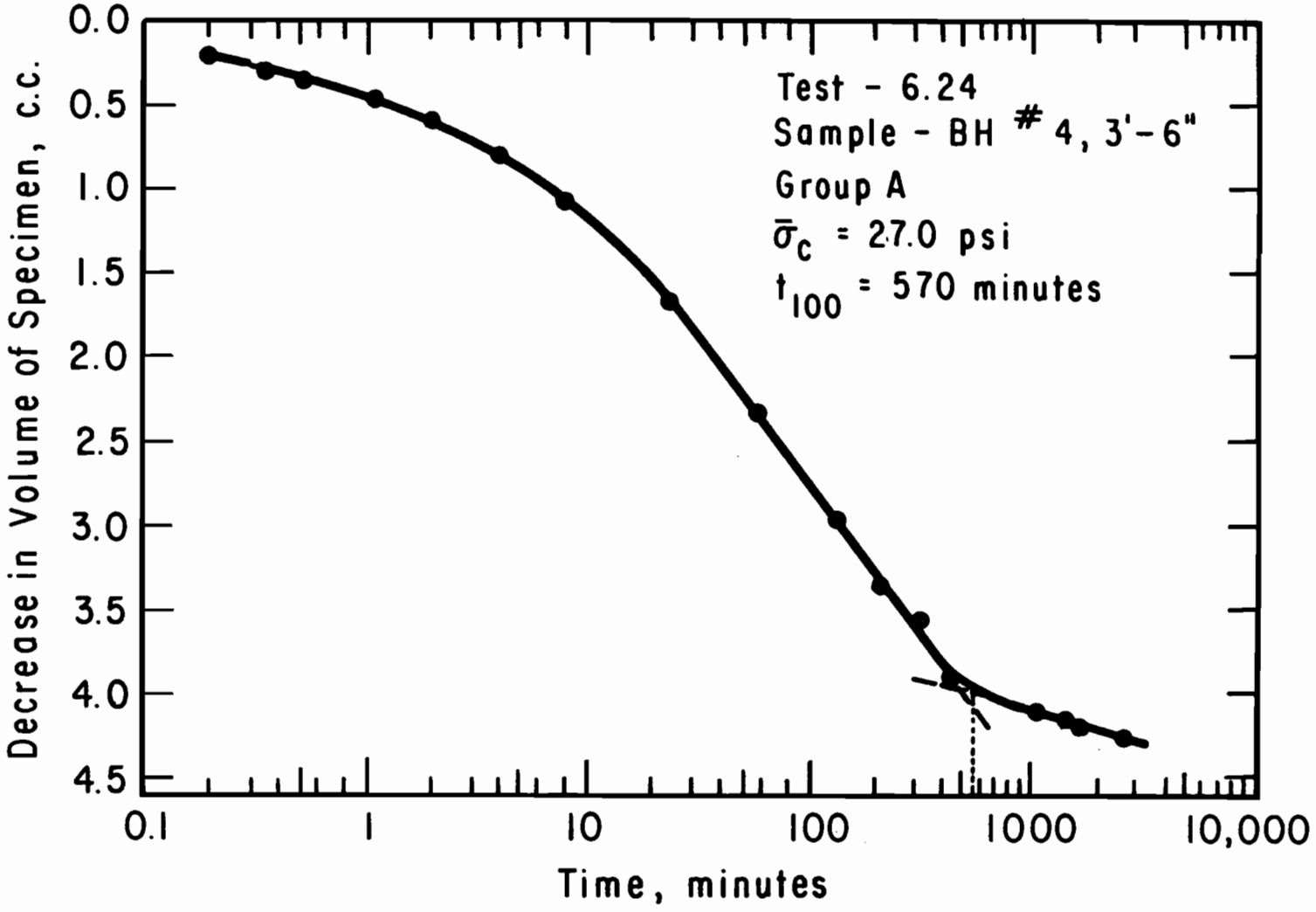

Figure 6.1. Decrease in Pore Water Volume of Specimen in Test 6.24 as a Function of Time, during Final Consolidation - Logarithm of Time.

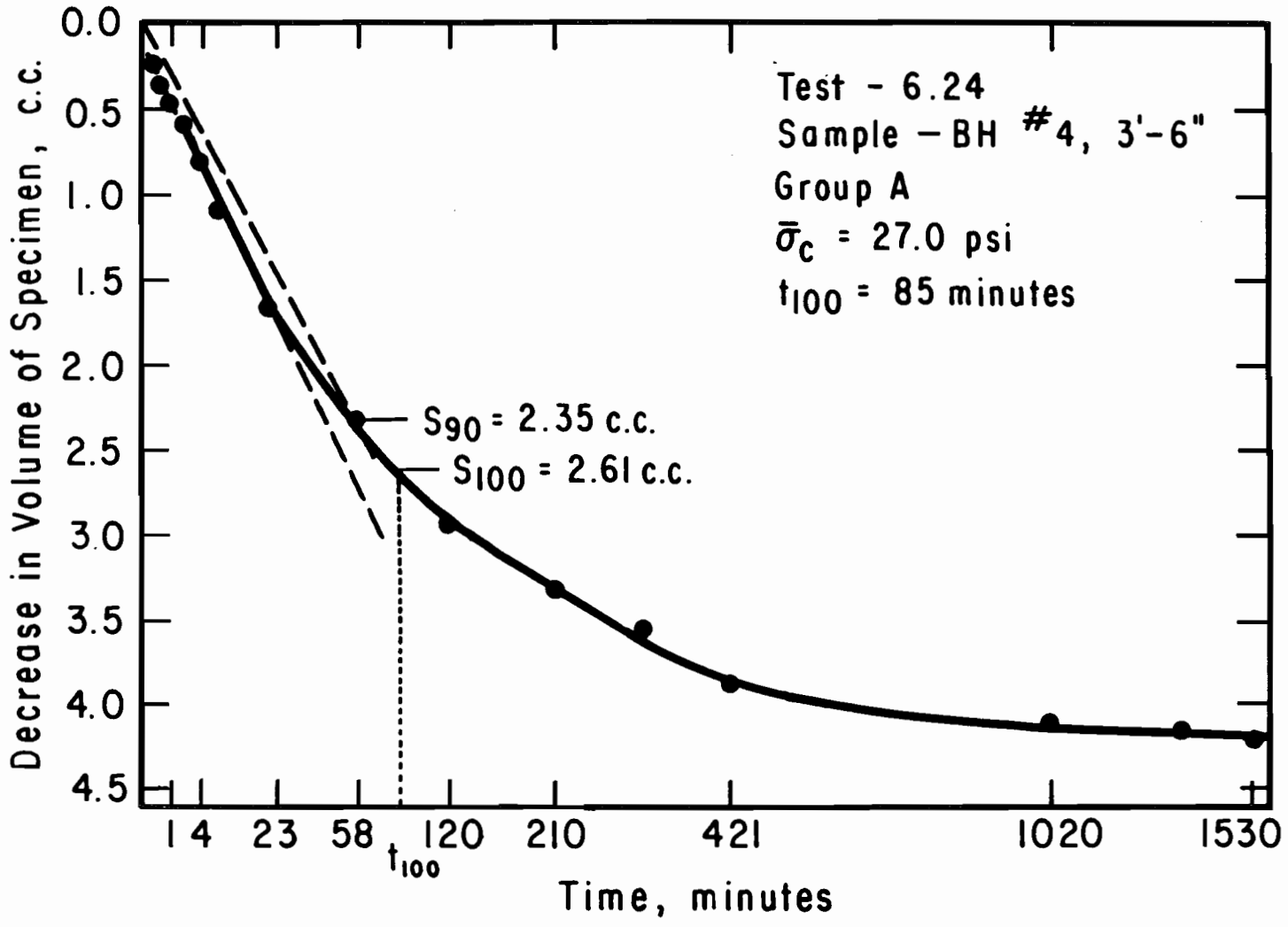

Figure 6.2. Decrease in Pore Water Volume of Specimen in Test 6.24 as a Function of Time, during Final Consolidation - Square Root of Time.

TABLE 6.4. SUMMARY OF TIMES TO THE END OF PRIMARY CONSOLIDATION BEFORE SHEAR FOR UNDISTURBED SPECIMENS

Test	Effective Consolidation Pressure, psi	Square Root of Time, minutes	Logarithm of Time, minutes
6.14	4.0	34	200
6.17	4.8	69	280
B.12	15.0	140	850
B.13	15.0	20	500
B.16	15.0	34	380
6.22	20.0	30	340
B.18	22.0	350	600
B.17	22.0	80	440
6.24	27.0	85	570

TABLE 6.5. PROPERTIES OF GREY CLAY SPECIMENS FROM OUTSIDE THE SLIDE AREA BEFORE SHEARING.

Test	Effective Consolidation Pressure, psi	Dry Density pcf	Water Content, percent
6.20	1.0	97.7	26.1
6.14	4.0	98.5	25.1
B.11	9.0	99.5	24.8
6.25	12.0	97.6	26.0
B.12	15.0	97.9	25.9
6.22	20.0	102.7	22.8
6.24	27.0	98.8	25.1

TABLE 6.6. PROPERTIES OF RED CLAY SPECIMENS FROM OUTSIDE THE SLIDE AREA BEFORE SHEARING.

Test	Effective Consolidation Pressure, psi	Dry Density, pcf	Water Content, percent
6.26	1.0	96.1	27.9
6.16	1.0	87.8	34.0
6.23	5.6	98.2	26.5
B.14	9.0	96.3	27.7
B.13	15.0	95.6	28.2
B.18	22.0	109.2	20.1

TABLE 6.7. PROPERTIES OF RED CLAY SPECIMENS FROM WITHIN THE SLIDE AREA BEFORE SHEARING.

Test	Effective Consolidation Pressure, psi	Dry Density, pcf	Water Content, percent
6.19	1.0	88.6	33.4
6.18	4.0	89.1	32.9
6.17	4.8	92.6	30.4
6.21	5.5	82.8	38.4
B.15	9.0	98.3	26.5
B.16	15.0	99.1	25.9
B.17	22.0	96.2	27.8

specimens ranged from 0.97 to 1.0, and the back pressures ranged from 15 to 44 psi.

The volume of water moving into and out of the specimens was measured during back pressure saturation and consolidation. The undisturbed specimens tended to swell, and only nine of the 20 triaxial specimens yielded usable consolidation data. The specimens with usable data were typically consolidated with an effective confining stress of 15 psi or more; however, two specimens with confining stresses of 4.0 psi and 4.8 psi also yielded usable data. Typical plots of volume change during final consolidation versus both the logarithm of time and square root of time are shown in Figures 6.1 and 6.2, respectively, for Test 6.24 (27.0 psi). Other tests yielding usable consolidation data included Tests 6.14 (4.0 psi); 6.17 (4.8 psi); B.12, B.13, and B.16 (15.0 psi); 6.22 (20.0 psi); and B.17 and B.18 (22.0 psi). Similar plots for these tests are included in Appendix A.

The times required to complete 100 percent consolidation (t_{100}) were found graphically using both the logarithm of time and the square root of time methods, and are summarized in Table 6.4. An examination of the values listed in Table 6.4 does not reveal a trend for the time to complete primary consolidation to increase with an increase in the consolidation stress on the specimen. Such a trend was noted for both the specimens consolidated from a slurry, Table 2.2, and the packed specimens, Table 3.3. The times for the specimens consolidated from a slurry and the packed specimens are also significantly larger at comparable consolidation stresses than those listed in Table 6.4, which indicates that excess pore water pressures should have equilibriated much faster in the undisturbed specimens than in the laboratory prepared specimens.

The effective confining stress, dry density, and water content of the triaxial specimens after final consolidation are listed in Tables 6.5, 6.6 and 6.7 for Groups A, B, and C, respectively. The dry density was calculated after the completion of the test based upon the water content and dry weight of solids in the specimen. Tests 6.19, 6.20, and 6.25 were run as consolidated-drained tests, and the water contents for these tests have been adjusted for the change in volume of water during shear. Water content after final consolidation versus effective consolidation stress is plotted in Figure 6.3.

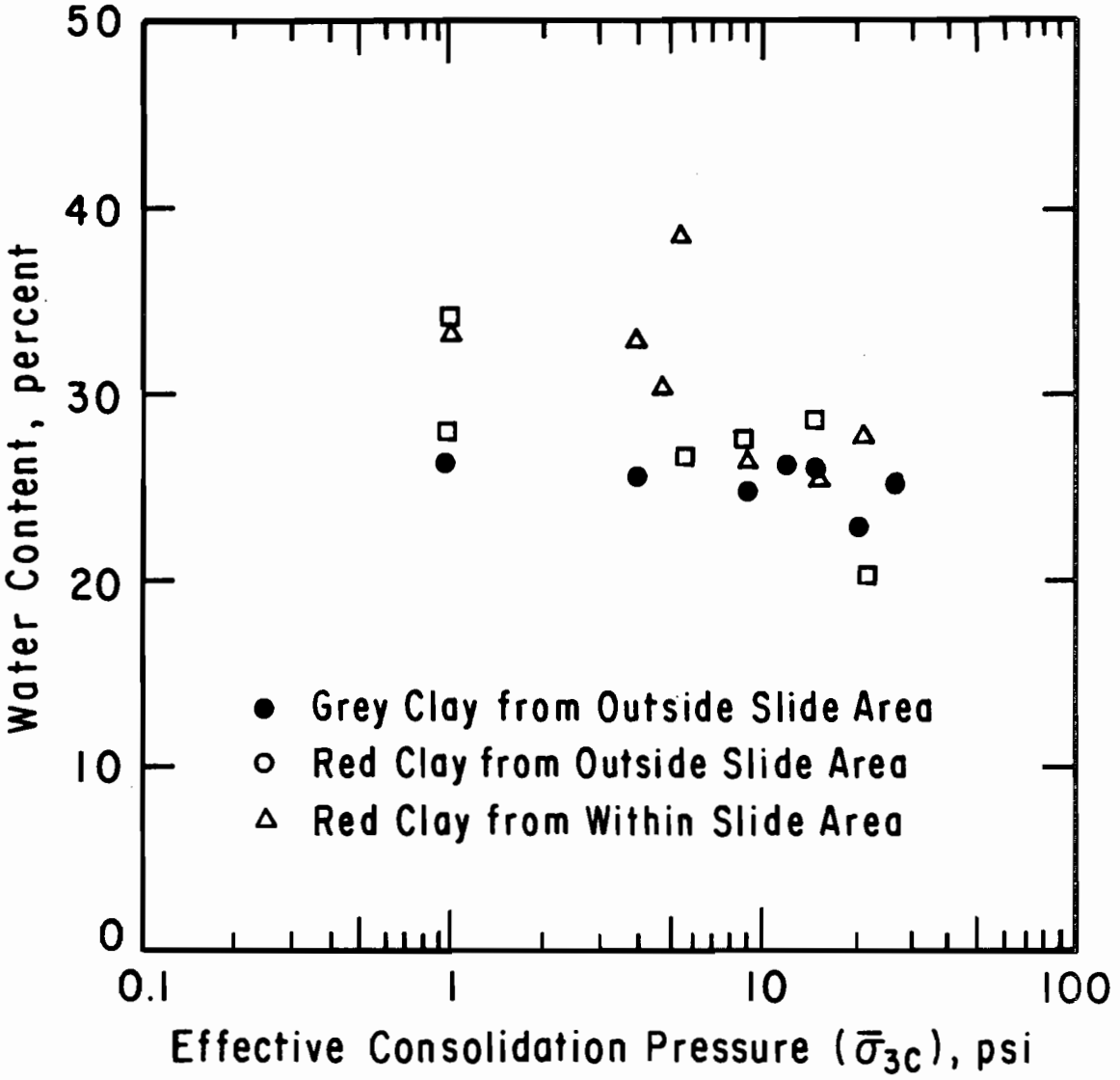

Figure 6.3. Water Content after Triaxial Consolidation versus Effective Consolidation Pressure for Undisturbed Specimens.

STRESS-STRAIN BEHAVIOR

Plots of principal stress difference, $(\sigma_1-\sigma_3)$, versus axial strain, e, in the consolidated-undrained ($\bar{R}$) tests are shown in Figures 6.4, 6.5, and 6.6 for groups A, B, and C, respectively. The curves shown in Figures 6.4, 6.5, and 6.6 are corrected for effects of piston seating errors; uncorrected curves are included in Appendix B. The shape of the curves in these plots are very similar. The curves indicate a slow increase in the principal stress difference throughout the test with no decrease in stress at large strains.

Tests 6.20, 6.26, and 6.19 belonging to Groups A, B, and C, respectively, were run as consolidated-drained (S) triaxial tests at an effective confining pressure stress of 1.0 psi. The stress-strain curves for these tests are shown in Figure 6.7. The principal stress difference in each tests reachs a peak at approximately one percent strain and then drops to a constant ultimate value.

EFFECTIVE STRESS PATHS

The effective stress paths for the grey clay from outside of the slide (Group A), the red clay from outside of the slide (Group B), and the red clay from inside the slide mass (Group C) are shown in Figures 6.8, 6.9, and 6.10, respectively, using the same type of modified Mohr-Coulomb diagram as was used in previous chapters. The stress paths for the undrained tests all show an increase in the pore pressure initially with a subsequent decrease in the pore pressure as the point of stress path tangency is approached.

FAILURE ENVELOPES

A straight line corresponding to the "average" line tangent to the stress paths was obtained for each group and is plotted with the effective stress paths for that group. The values of principal stress difference and effective confining stress which were used in the linear regression calculations to obtain these lines are listed in Tables 6.8, 6.9, and 6.10 for Groups A, B, and C, respectively. The intercept of the lines ($\bar{d}$) and their slopes angles ($\bar{\psi}$) are tabulated in Table 6.11 along with the conventional Mohr-Coulomb shear strength parameters, $\bar{c}$ and $\bar{\phi}$, which were calculated from Eqs. 2.3 and 2.4.

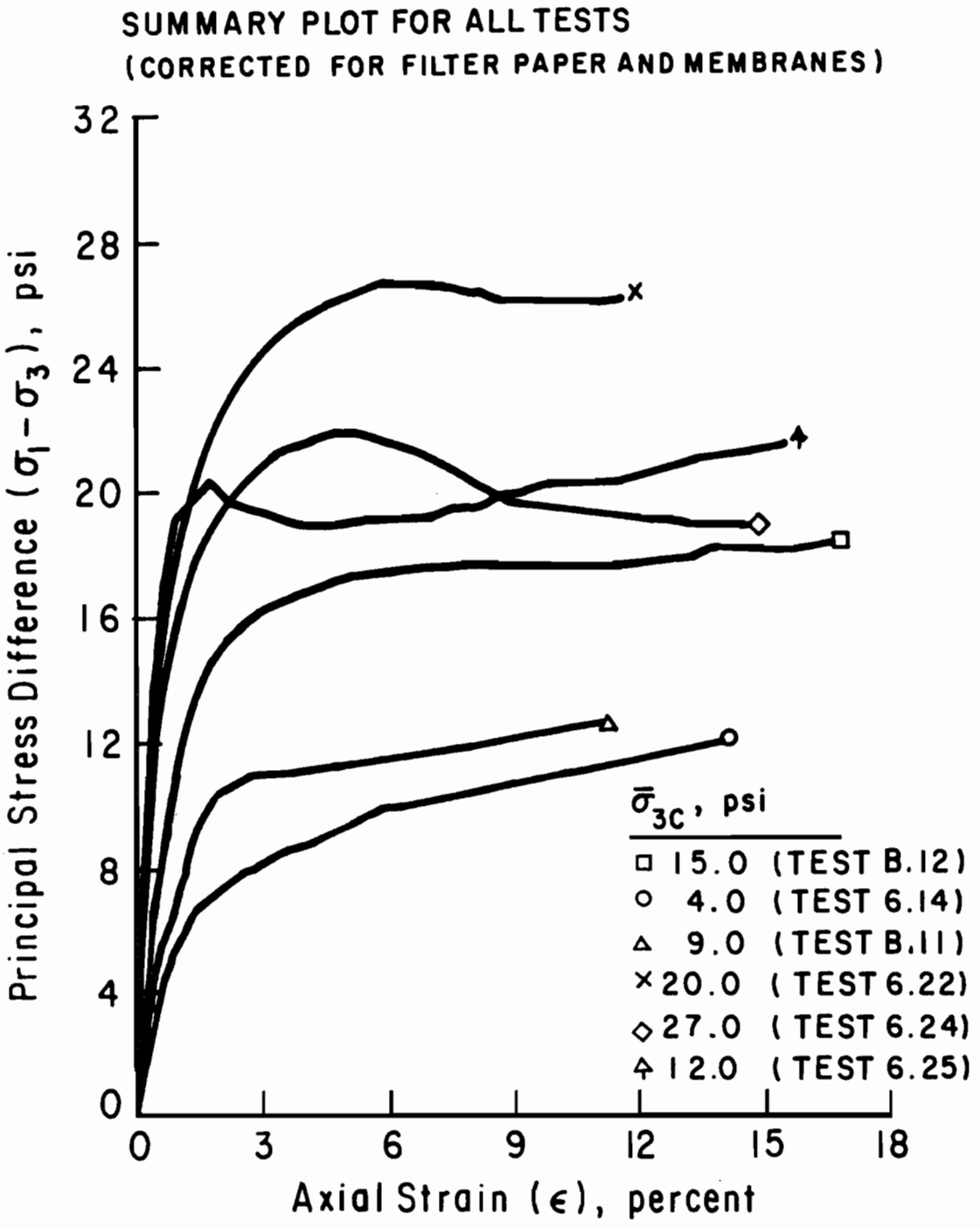

Figure 6.4. Corrected Summary Plot of Principal Stress Difference versus Axial Strain for Undisturbed Grey Clay Specimens from Outside of Slide Area (Consolidated-Undrained Triaxial Tests).

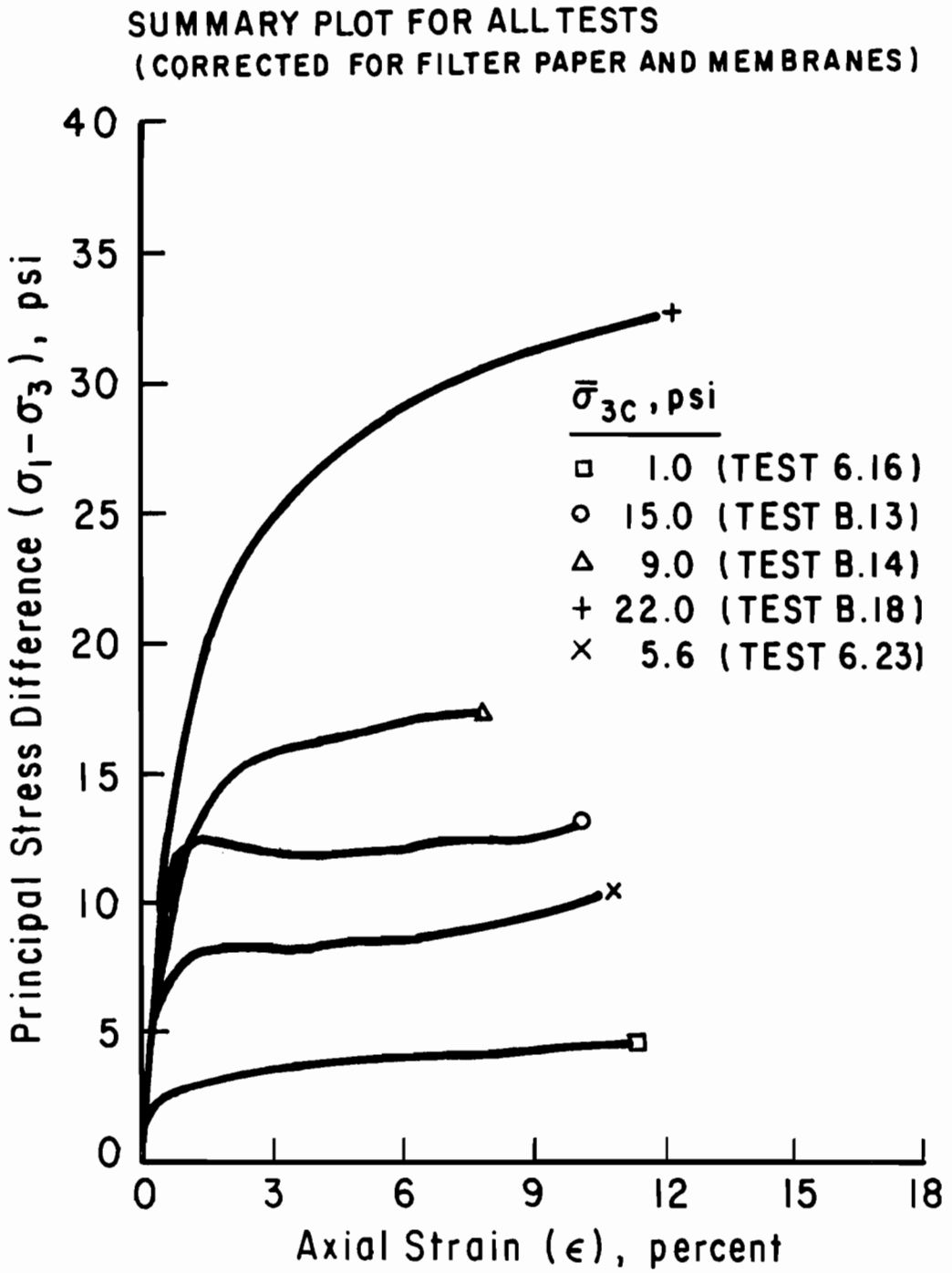

Figure 6.5. Corrected Summary Plot of Principal Stress Difference versus Axial Strain for Undisturbed Red Clay Specimens from Outside of Slide Area (Consolidated-Undrained Triaxial Tests).

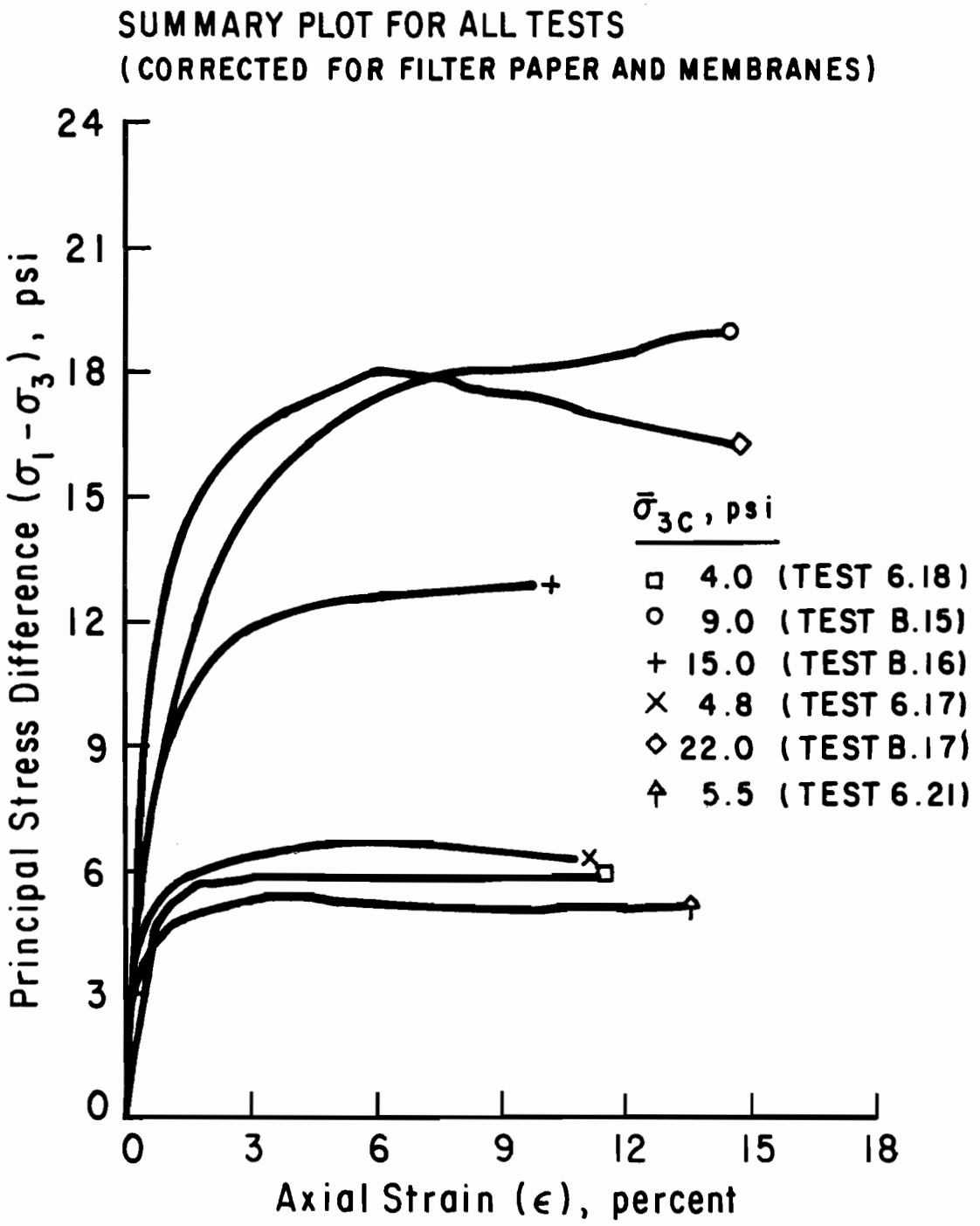

Figure 6.6. Corrected Summary Plot of Principal Stress Difference versus Axial Strain for Undisturbed Red Clay Specimens from Within Slide Area (Consolidated-Undrained Triaxial Tests).

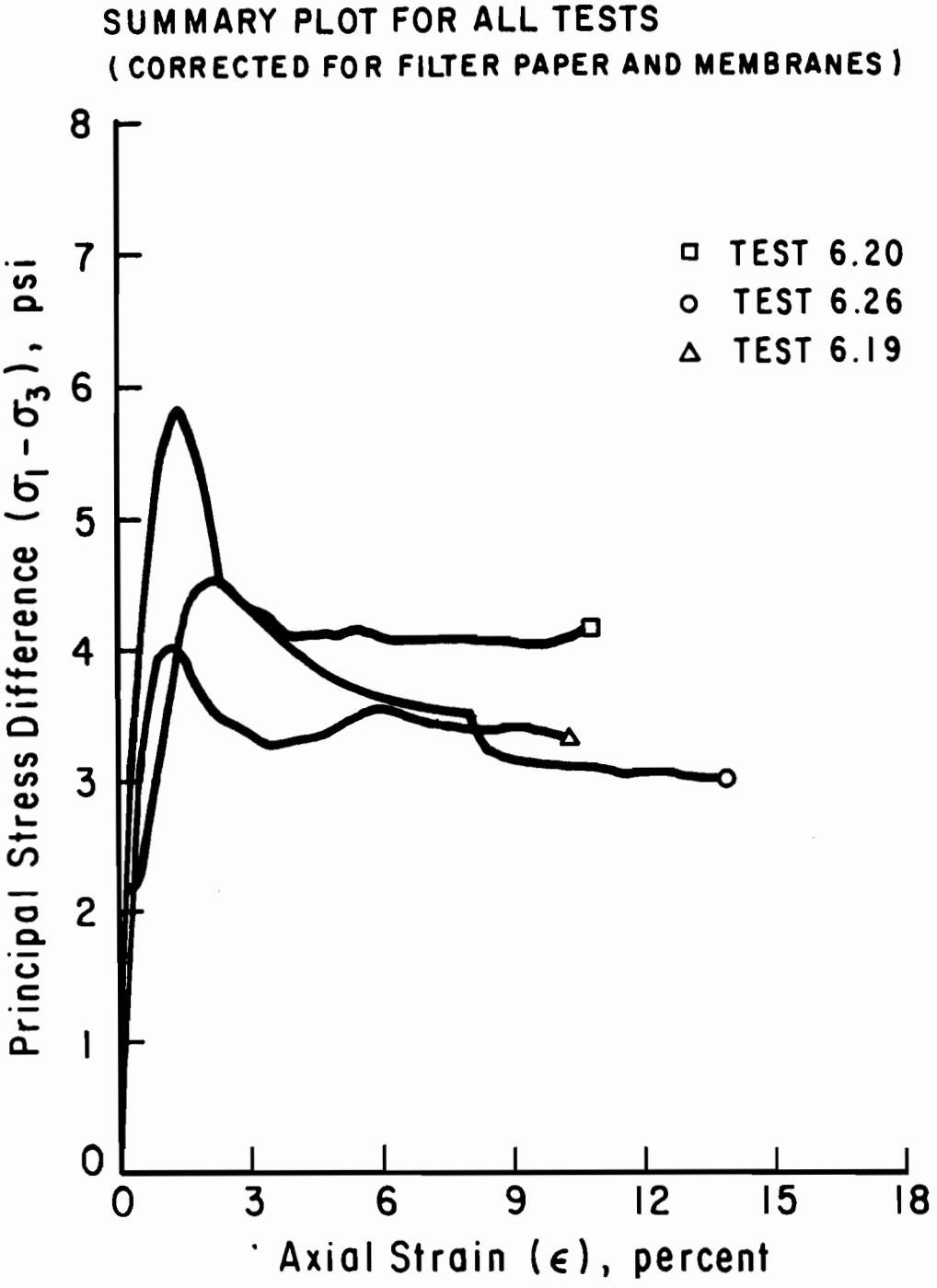

Figure 6.7. Corrected Summary Plot of Principal Stress Difference versus Axial Strain for Undisturbed Specimens Consolidated to 1.0 psi (Consolidated-Drained Triaxial Tests).

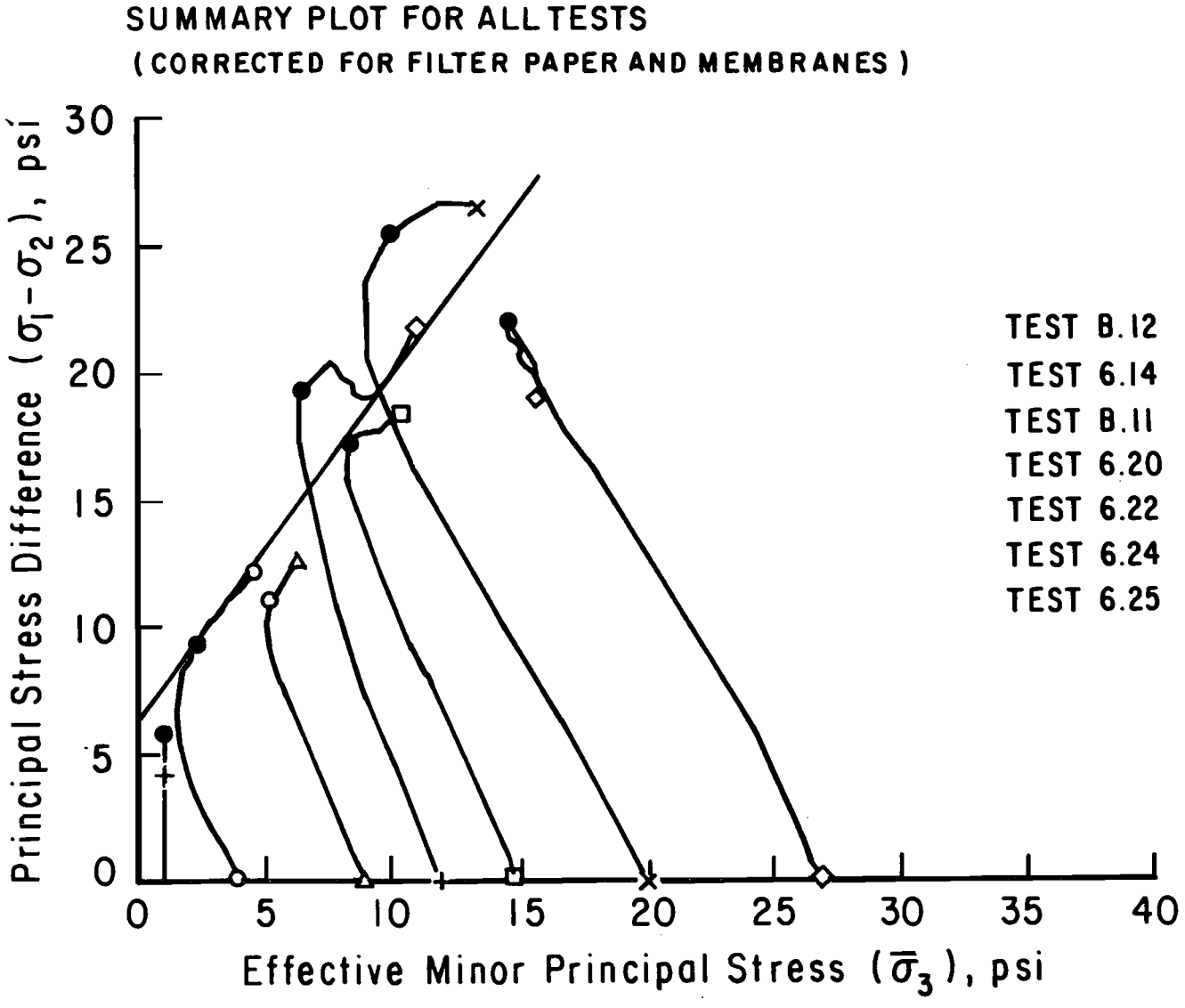

Figure 6.8. Effective Stress Paths and Failure Envelope based on Stress Path Tangency for Undisturbed Grey Clay Specimen from Outside of Slide Area.

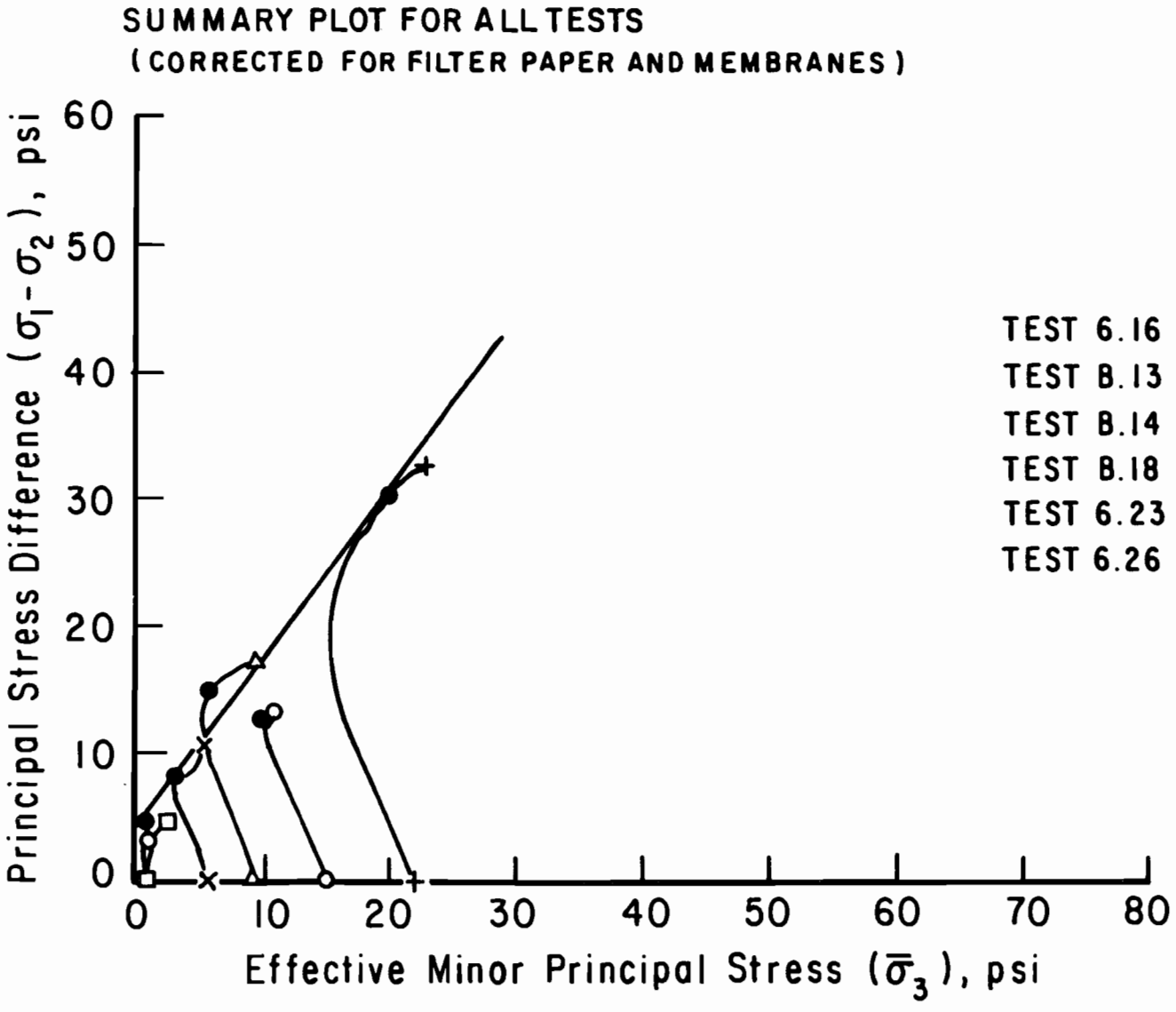

Figure 6.9. Effective Stress Paths and Failure Envelope based on Stress Path Tangency for Undisturbed Red Clay Specimens from Outside of Slide Area.

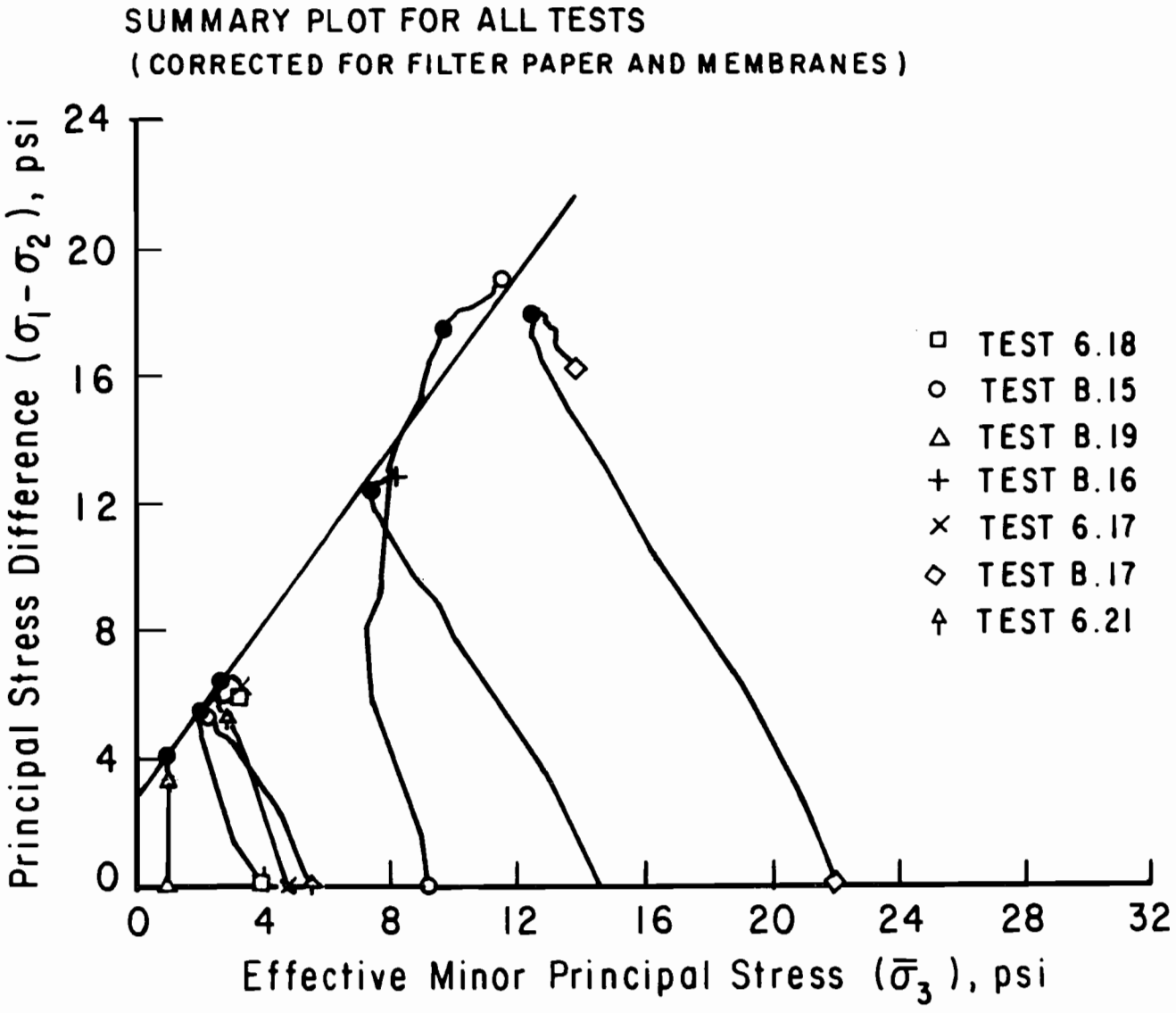

Figure 6.10. Effective Stress Paths and Failure Envelope based on Stress Path Tangency for Undisturbed Red Clay Specimens from Within Slide Area.

TABLE 6.8. APPARENT POINTS OF STRESS PATH TANGENCY FOR GREY CLAY SPECIMENS FROM OUTSIDE OF THE SLIDE AREA.

Test	Principal Stress Difference, psi	Effective Stress, psi
6.20	5.8	1.0
6.14	8.9	2.3
B.11	10.6	5.2
6.25	19.3	6.6
B.12	17.3	8.5
6.22	25.1	10.0
6.24	21.8	14.8

TABLE 6.9. APPARENT POINTS OF STRESS PATH TANGENCY FOR RED CLAY SPECIMENS FROM OUTSIDE OF THE SLIDE AREA.

Test	Principal Stress Difference, psi	Effective Stress, psi
6.16	3.1	0.8
6.26	4.5	1.0
6.23	8.1	3.0
B.14	14.9	6.9
B.13	12.5	9.8
B.18	30.3	20.2

TABLE 6.10. APPARENT POINTS OF STRESS PATH TANGENCY FOR RED CLAY SPECIMENS FROM OUTSIDE OF THE SLIDE AREA.

Test	Principal Stress Difference, psi	Effective Stress, psi
6.19	4.0	1.0
6.18	5.6	2.2
6.17	6.4	2.6
6.21	5.3	2.2
B.15	17.4	9.8
B.16	12.4	7.5
B.17	18.0	12.5

TABLE 6.11. EFFECTIVE STRESS SHEAR STRENGTH PARAMETERS FOR UNDISTURBED SPECIMENS.

Specimen Type	Slope, degrees	Intercept, psf	Friction Angle, degrees	Cohesion, psf
Grey Clay from Outside of the Slide Area	53	920	23	300
Red Clay from Outside of the Slide Area	53	440	23	150
Red Clay from Within the Slide Area	53	400	23	130

The red clay specimens were separated into two groups, Group B outside of the slide area and Group C inside of the slide area, to examine if the location of sampling had any influence on the effective stress shear strength parameters of the red clay. The friction angles of Groups B and C, 23 degrees, are very similar, and the cohesion values, 150 and 130 psf, respectively, are only slightly different. From these comparisons it appears that the effective stress shear strength parameters of the red clay from outside and inside the slide area are essentially the same.

Gourlay and Wright (1984) reported a difference between the effective stress shear strength parameters of red and grey clay specimens prepared in the laboratory. The friction angles of the red and grey clay specimens were similar, 20 degrees, but the cohesion value of the grey clay, 390 psf, exceeded that of the red clay, 270 psf. This same trend exists for the undisturbed red and grey clay specimens: The friction angles of the three groups of undisturbed specimens are very similar, 23 degrees, but the cohesion value of the grey clay in Group A, 300 psf, exceeds the cohesion values of the red clay in Groups B and C, 150 and 130 psf, respectively.

The liquid limits of the red clay specimens ranged from 48 percent to 73 percent. To determine the effect of the liquid limit on the effective stress shear strength parameters, several of the red clay specimens were divided into two groups; one group consists of specimens with liquid limits at or below 55 percent; the second group consists of specimens with liquid limits at or above 65 percent. A maximum value of 55 percent and a minimum value of 65 percent were chosen for the two groups so that each group would contain sufficient specimens to define a respective failure envelope. The liquid limits of the specimens in the two groups are summarized in Table 6.12.

The effective stress paths for the six specimens with liquid limits at or below 55 percent are plotted in Figure 6.11 along with the "average" line tangent to the stress paths. The effective stress paths for the five specimens with liquid limits at or above 65 percent are similarly plotted in Figure 6.12. The intercept, $\bar{d}$, and slope, $\bar{\psi}$, of the straight line failure envelopes shown in Figures 6.11 and 6.12 are listed in Table 6.13 along with the conventional Mohr-Coulomb shear strength parameters, $\bar{c}$ and $\bar{\phi}$, calculated from Eqs. 2.3 and 2.4.

TABLE 6.12. SPECIMENS USED TO DETERMINE THE EFFECT OF THE LIQUID LIMIT ON THE SHEAR STRENGTH OF RED CLAY

Liquid Limit at or Below 55 Percent		Liquid Limit at or Above 65 Percent	
Test	Liquid Limit, percent	Test	Liquid Limit, percent
6.19	55	6.16	65
6.17	48	6.18	66
B.15	52	6.21	73
B.16	55	B.14	72
B.17	49	B.13	65
B.18	53		

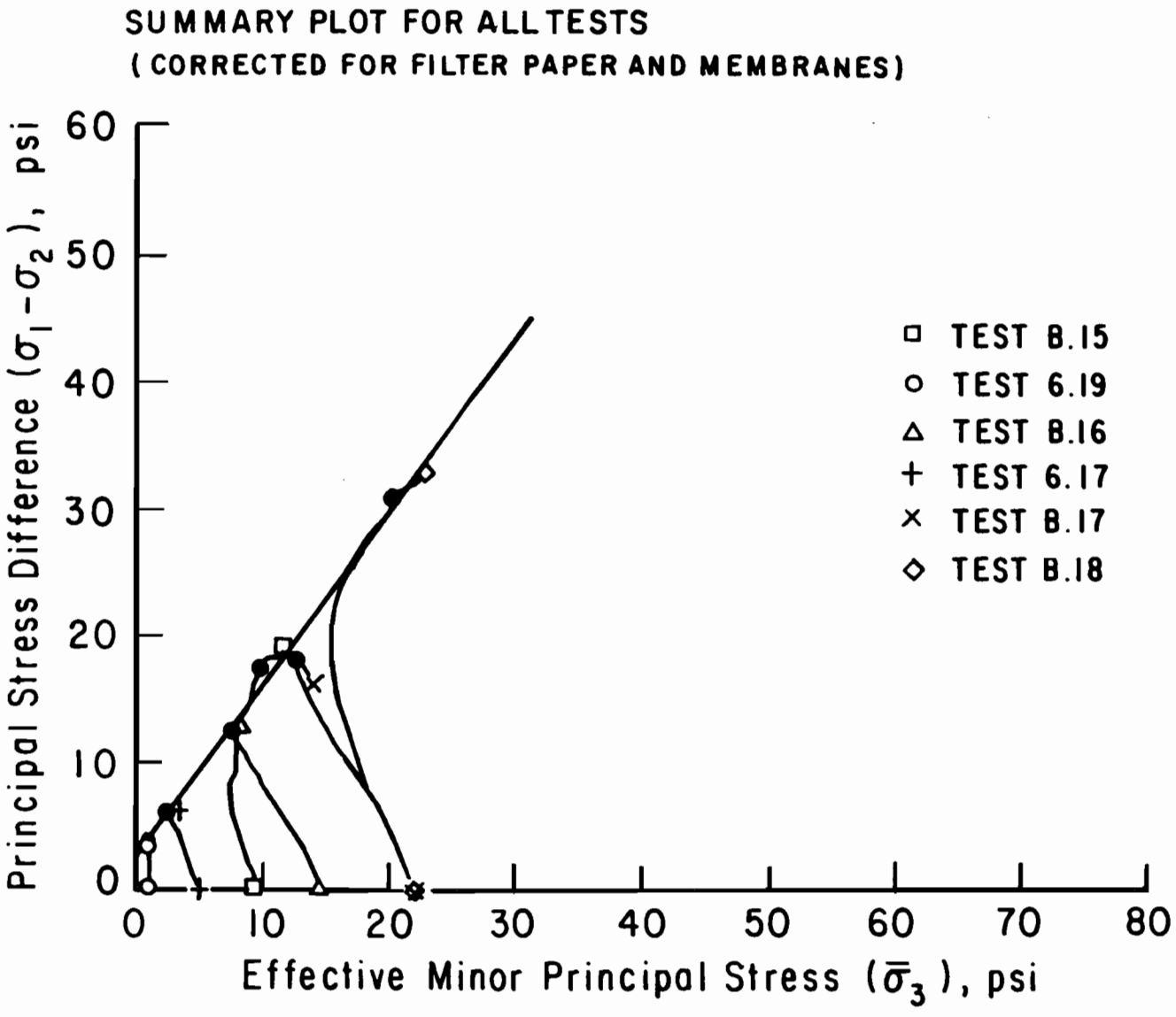

Figure 6.11. Effective Stress Paths and Failure Envelope based on Stress Path Tangency for Undisturbed Red Clay Specimens with Liquid Limits at or Below 55 Percent.

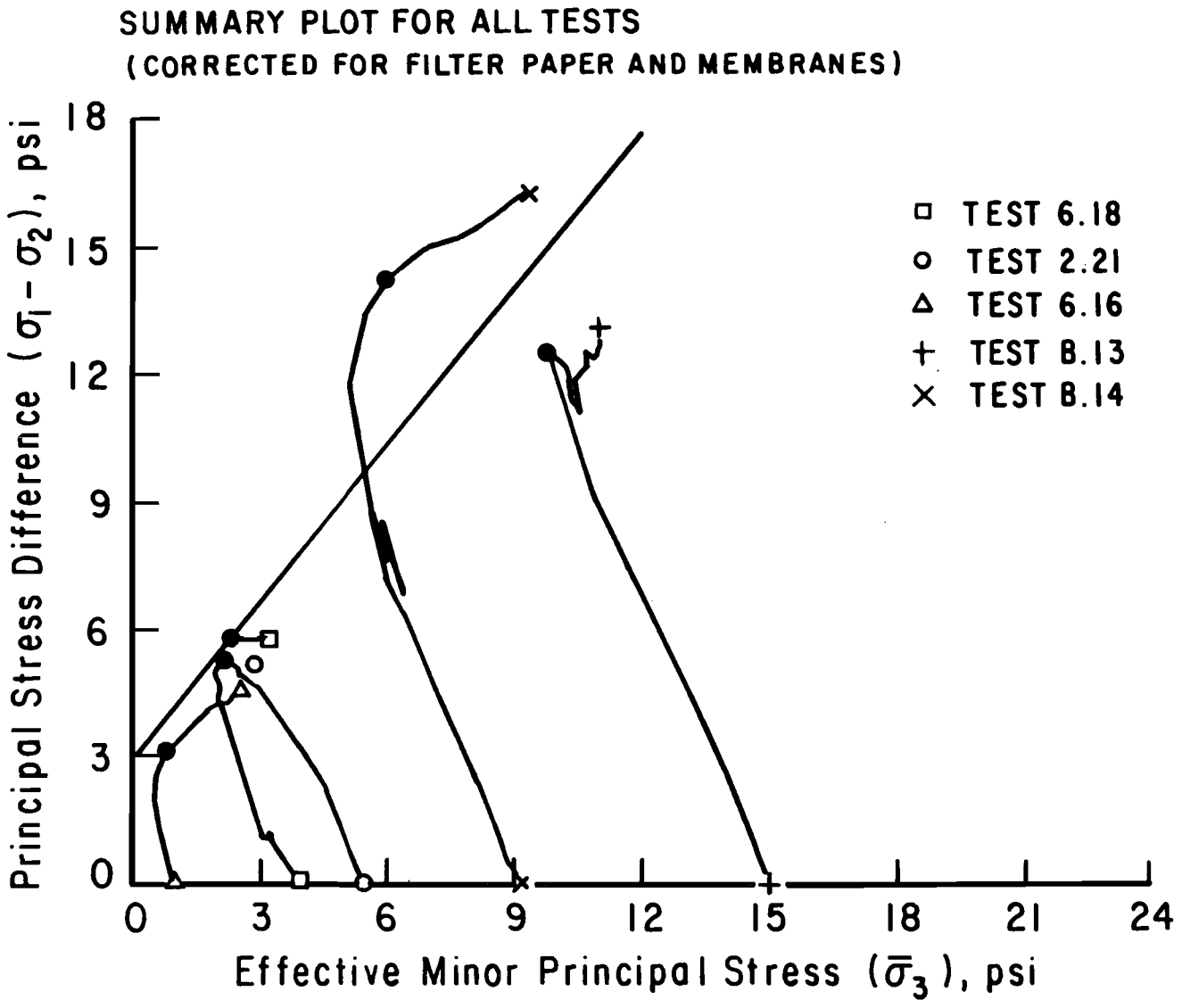

Figure 6.12. Effective Stress Paths and Failure Envelope based on Stress Path Tangency for Undisturbed Red Clay Specimens with Liquid Limits at or Above 65 Percent.

TABLE 6.13. SHEAR STRENGTH PARAMETERS BASED ON LIQUID LIMITS.

Liquid Limit	Slope, degrees	Intercept, psf	Friction Angle, degrees	Cohesion, psf
At Or Above 65 Percent	50	420	22	140
At Or Below 55 Percent	53	390	24	130

The friction angle for specimens with liquid limits at or above 65 percent is 22 degrees, which is 2 degrees lower than the friction angle of 24 degrees for specimens with liquid limits at or below 55 percent. The cohesion value for specimens with liquid limits at or above 65 percent is 140 psf, which is 10 psf higher than the cohesion value of 130 psf for specimens with liquid limits at or below 55 percent. The difference in effective stress shear strength parameters among the red clay specimens is small even though the liquid limits varied.

CHAPTER SEVEN. COMPARISON OF SHEAR STRENGTH PARAMETERS

INTRODUCTION

The effective stress shear strength parameters determined for various tests and specimens described in Chapters 2 through 6 are compared and discussed in this Chapter. In addition, the results of the tests performed in the current study are compared to the results of the tests performed by Gourlay and Wright (1984) on compacted specimens of red clay. The measured shear strength parameters are also compared to those back-calculated from the slope failure at I. H. 610 and Scott Street as reported by Stauffer and Wright (1984).

TRIAXIAL TESTS ON LABORATORY PREPARED SPECIMENS

Consolidated-undrained triaxial shear tests with pore-pressure measurements were performed on three types of laboratory prepared specimens: (1) compacted specimens (Gourlay and Wright, 1984), (2) specimens consolidated from a slurry, and (3) packed specimens. The effective stress cohesion values and friction angles, $\bar{c}$ and $\bar{\phi}$, of the three types of specimens were based on the stress path tangency failure criteria. The effect stress shear strength parameters at ultimate conditions were determined for the specimens prepared by packing and consolidating from a slurry.

Stress Path Tangency Failure Criteria

The effective stress shear strength parameters based on the stress path tangency failure criteria, $\bar{\phi}$ and $\bar{c}$, are listed in Table 7.1 for the three types of laboratory prepared specimens. The differences among the friction angles for the three types of specimens are negligible. However, the cohesion value of the compacted specimens (270 psf) is significantly larger than those of the specimens prepared by both consolidating from a slurry and packing (110 and 80 psf, respectively). Preparing specimens by compaction yields a much higher cohesion value than the two other methods of preparing specimens, while

TABLE 7.1. PEAK EFFECTIVE STRESS SHEAR PARAMETERS FOUND FROM TRIAXIAL TESTS ON SPECIMENS PREPARED IN THE LABORATORY

Specimen Type	Friction Angle, degrees	Cohesion, psf
Compacted (Gourlay and Wright, 1984)	20	270
Consolidated from a Slurry	24	110
Packed	22	80

preparing specimens by consolidating from a slurry and packing yield similar cohesion values.

Stauffer and Wright (1984) back-calculated an effective stress friction angle of 19 degrees and a cohesion value of 7 psf for a failed embankment constructed of compacted Beaumont clay. The back-calculated friction angle is similar to those found from laboratory prepared specimens. However, the back-calculated cohesion value is negligible in contrast to any of the cohesion values found in the laboratory; particularly in contrast to the cohesion value of 270 psf found for compacted specimens.

Ultimate Condition

Friction angles based on ultimate values of principal stress difference and effective minor principal stress for the specimens prepared by consolidation from a slurry and packing are similar, 18 degrees. The corresponding cohesion intercepts are 50 psf for specimens prepared by consolidation from a slurry and 90 psf for specimens prepared by packing. The ultimate friction angles slightly decreased from the peak values listed in Table 7.1 based on the stress path tangency failure criteria. The ultimate cohesion value of 90 psf for the packed specimens changed very little from the value of 80 psf based on stress path tangency; however, the cohesion value for the specimens consolidated from a slurry significantly decreased from 110 to 50 psf.

Because of the decrease in the cohesion value of the specimens consolidated from a slurry at large strains the ultimate effective stress shear strength parameters for the specimens consolidated from a slurry may be more appropriate for what Skempton (1970) refers to as "fully softened" shear strength parameters. The reason for a decrease in the cohesion value of the specimens consolidated from a slurry is not clearly known; a possible explanation is the time required to prepare the specimens consolidated from a slurry exceeded the time required for the other types of specimens by four to five weeks, and age hardening occurred during this period.

The ultimate friction angles for the specimens prepared by packing and consolidating from a slurry are similar to the friction angle back-calculated by Stauffer and Wright (1984), 19 degrees. Only the ultimate cohesion value

for the specimens consolidated from a slurry, 50 psf, approaches the back-calculated value of 7 psf.

TRIAXIAL TESTS ON UNDISTURBED SPECIMENS

A series of consolidated-undrained (R) and consolidated-drained (S) triaxial tests were performed on undisturbed specimens from a failed embankment which was examined by Stauffer and Wright (1984). The purpose of these tests was to compare the undisturbed effective stress shear strengths to those both back-calculated and found from specimens prepared in the laboratory. Though three groups of undisturbed specimens were tested, attention was focused on the tests on specimens sampled from within the slide mass.

A friction angle of 23 degrees was found for the undisturbed specimens, which is similar to values found for both laboratory prepared specimens and by back-calculation from field data. A cohesion value of 130 psf was determined, and is similar to the value reported for both the specimens prepared by packing and consolidating from a slurry. Assuming the soil in the field originally possessed a cohesion similar to that found from triaxial tests on compacted specimens, 270 psf, a significant decrease in the cohesion of the soil has obviously occurred; however, the cohesion found from the undisturbed specimens is still significantly larger than that observed in the field.

Factors in the triaxial test which could contribute to higher cohesions being measured in the laboratory than in the field include: (1) a rate of shear too high to allow complete pore-pressure equalization, (2) larger effects on measured stresses due to membranes and filter drains than are currently corrected for (Duncan and Seed, 1965), (3) increased friction in the loading piston during shear due to lateral movement of the top loading platten, (4) a differenct failure plane orientation than existed in the field, and (5) changes in pore-water chemistry during saturation and consolidation. The effects of these factors on measured strength are believed to be negligible; however, further detailed examination of these factors in future studies is desirable.

RESIDUAL DIRECT SHEAR TESTS ON COMPACTED SPECIMENS

The residual effective stress shear strength parameters, ϕ_r and c_r, for compacted red clay were found to be 14 degrees and approximately 0 psf, respectively. The significant difference between the residual shear strength values found from direct shear tests and the peak values found in triaxial tests is due to direct shear specimens undergoing much larger deformations than triaxial specimens. The cohesion value back-calculated by Stauffer and Wright (1984), 7 psf, and residual cohesion value are similar; both are negligible in contrast to cohesion values measured in triaxial tests. A significant difference of 5 degrees exists between the residual friction angle and back-calculated friction angle, 19 degrees.

FACTORS OF SAFETY BASED ON LABORATORY SHEAR STRENGTHS

Factors of safety against slope failure were calculated for the I. H. 610 and Scott Street embankment based on the effective stress shear strengths found from laboratory tests. The purpose of these calculations was to compare the factors of safety based on laboratory shear strengths to that of unity which existed at the time of failure. Factors of safety were calculated using the program UTEXAS (Roecker and Wright, 1984).

The effective stress shear strength parameters found from tests on 1) compacted specimens, 2) specimens consolidated from a slurry, 3) packed specimens, 4) undisturbed red clay specimens from within the slide area, and 5) residual direct shear specimens are listed in Table 7.2 along with their corresponding factors of safety. Zero pore water pressures were assumed for the calculations. The factors of safety based upon peak shear strengths found from triaxial tests all significantly exceeded unity. The ultimate effective stress shear strength parameters for the specimens consolidated from a slurry yield a factor of safety slightly greater the one. The factor of safety based on residual shear strength is less than unity and would have predicted failure.

Further calculations were performed to determine what pore pressure conditions would be necessary for the laboratory shear strengths to yield a factor of safety of unity. Positive pore pressures were examined in terms of the pore pressure parameter, r_u, defined by Bishop and Morgenstern (1960) as:

TABLE 7.2. FACTORS OF SAFETY AGAINST SLOPE FAILURE BASED ON EFFECTIVE STRESS SHEAR STRENGTH PARAMETERS DETERMINED IN THE LABORATORY

Specimen Type	Friction Angle, degrees	Cohesion, psf	Factor of Safety
Compacted (Gourlay and Wright, 1984)	20	270	2.2
Consolidated from a Slurry (Peak)	24	110	1.9
Consolidated from a Slurry (Ultimate)	18	50	1.2
Packed	22	80	1.6
Undisturbed Red Clay from Within the Slide Area	23	130	1.9
Residual Direct Shear	14	0	0.7

$$r_u = \frac{u}{z \cdot \gamma} \tag{7.1}$$

where u is the pore pressure at a point, γ is the total unit weight of soil above the point, and z is the vertical distance from the ground surface to the point.

The shear strength parameters found from triaxial tests are listed in Table 7.3 along with the corresponding values of r_u necessary to yield factors of safety of unity. The values of r_u listed in Table 7.3 for the peak shear strength values generally are much larger than those associated with even the least favorable seepage conditions in a slope and, thus, it is doubtful that the peak shear strength values found from triaxial tests would predict failure even under extreme pore pressure conditions. The r_u value of 0.20 listed for the ultimate shear strength values of the specimens consolidated from a slurry is reasonable.

TABLE 7.3. BISHOP AND MORGENSTERN (1960) PORE PRESSURE PARAMETER, r_u, NECESSARY TO OBTAIN A FACTOR OF SAFETY OF UNITY

Specimen Type	Friction Angle, degrees	Cohesion, psf	r_u
Compacted (Gourlay and Wright, 1984)	20	270	0.88
Consolidated from a Slurry (Peak)	24	110	0.57
Consolidated from a Slurry (Ultimate)	18	50	0.20
Packed	22	80	0.47
Undisturbed Red Clay from Within the Slide Area	23	130	0.60

CHAPTER EIGHT. SUMMARY, CONCLUSIONS AND RECOMMENDATIONS

SUMMARY

Gourlay and Wright (1984) indicated that the conventional method of obtaining effective stress shear strength parameters for embankment design employing triaxial tests on compacted specimens, over-estimates the long-term shear strength of compacted Beaumont clay. They reported a cohesion value and friction angle of 270 psf and 20 degrees, respectively, in terms of effective stress. Stauffer and Wright (1984) back-calculated the effective stress shear strength parameters of compacted Beaumont clay from a number of embankment slope failures and found that while the back-calculated friction angle of 19 degrees was comparable to the value measured by Gourlay and Wright, the effective stress cohesion intercept was negligible. Thus, the principal discrepancy appeared to lie in the effective stress cohesion intercept.

Four series of tests were performed as part of the current study to understand better and resolve the differences between the field and laboratory shear strengths. Tests included three series of consolidated-undrained triaxial shear tests with pore water pressure measurements on specimens (1) prepared in the laboratory by consolidation of soil from a slurry, (2) prepared in the laboratory by "packing" soil into a special mold, and (3) sampled from a failed embankment in an undisturbed state. In addition, direct shear tests were performed on specimens compacted in the laboratory to determine residual shear strength parameters.

Factors of safety were calculated for an embankment which had previously failed using the effective stress shear strength parameters found in this study, and assuming zero pore pressures. All the factors of safety based on peak shear strengths were significantly greater than unity. The ultimate effective stress shear strength parameters of the specimens consolidated from a slurry yielded a factor of safety slightly greater than unity, and appear more appropriate than the peak values for what Skempton (1970) describes as "fully softened" shear strength parameters. The factor of safety calculated using the residual shear strength was less than unity and would have predicted

failure, however, there is no rational basis for adopting residual shear strengths for design.

Soil profiles from a failed embankment were examined, and no irregularities which would contribute to the failure were found. The approximate depth of the slide surface was found from the soil profiles, and compares well to the depth estimated by Stauffer and Wright (1984).

CONCLUSIONS

Significant discrepancies exist between the effective stress shear strength parameters determined in the laboratory and those found in the field. These discrepancies occur primarily in the cohesion intercept, rather than in the friction angle. The discrepancies are greatest when the laboratory specimens are prepared by compaction. Tests on undisturbed specimens from the field yield a lower cohesion value than tests on laboratory compacted specimens; however, the undisturbed specimens still yield a cohesion intercept which is relatively large compared to what appears to exist after long times in the field. Tests on specimens prepared by packing and consolidation from a slurry produced comparable values of shear strengths, which are lower than those measured on undisturbed specimens. However, these (packed and slurry consolidated) specimens also produced strengths which exceeded those which are apparently eventually developed in the field. Effective stress shear strength parameters based on ultimate (large axial strain) conditions in the specimens consolidated from a slurry produced the closest agreement with what was observed in the field, although strengths were still somewhat overestimated.

Although specimens consolidated from a slurry appear to produce the most promising values for the shear strength parameters in terms of agreement with field observations, a fundamental problem exists in using this approach for determining the strength of soil in the normally consolidated state as suggested by Skempton. The problem is especially pronounced when the objective is to determine the strength at low stresses and, particularly, the existence of a low cohesion intercept. In order to prepare samples in the laboratory with sufficient strength to enable them to be handled and tested, they must be consolidated to pressures of at least several hundred psf. If the cohesion intercept is to be determined for such samples in a normally

consolidated state, they must be tested at confining stresses at least as high and, probably, several times as high as the maximum stress to which they were consolidated in the sample preparation phase. Consequently, the cohesion intercept must be estimated by extrapolating the strength envelope measured at higher stresses back to the origin. If the stresses used in testing are at least several hundred psf and, perhaps several thousand psf, and the cohesion intercept is only a few ten's of psf, at most, substantial error may be introduced in determining the effective cohesion intercept. An alternative is to perform tests at lower stresses; however, the soil will then be overconsolidated if specimens are prepared at the normal pressures needed to facilitate handling. The use of an ultimate strength may be an alternative for determining strengths of the soil corresponding to normally consolidated conditions, although this remains to be established.

RECOMMENDATIONS

Based on the results of the testing performed and presented in this report two types of recommendations are made. The first type pertain to recommendations for current design practice; the second type pertain to recommendations for further study. With regard to current design practice it is recommended that laboratory strength values not be relied upon for design of embankments constructed of high plasticity clays such as the Beaumont clay. Instead it is recommended that results of field observations and experience be used to guide current design. In the case of the Beaumont clay experience suggests that an effective stress friction angle of no more than 20 degrees and, perhaps, as low as 15 degrees should be used and that the effective cohesion intercept be assumed to be zero.

Further research is needed to understand the reasons for the discrepancies between strengths measured in the laboratory and those eventually developed in the field. One possible factor which was not investigated in the studies presented in this report is the effects of repeated wetting and drying on soil properties. Separate studies are being conducted to examine the effects of repeated wetting and drying. Until the reasons for the differences between the strengths measured in the laboratory and the strengths developed in the field are better understood, design must be

based on limited field experience and will probably be excessively conservative. More fundamental procedures for design are needed.

BIBLIOGRAPHY

ASTM (1982), Annual Book of ASTM Standards: Part 19, American Society for Testing and Materials, Philadelphia, 710 p.

Bishop, A.W. and Henkel, D.J. (1962), The Measurement of Soil Properties in the Triaxial Test, Second Edition, Edward Arnold, London, 1962, 228 p.

Bishop, A.W. and Morgenstern, Norbert (1960), "Stability Coefficients for Earth Slopes," Geotechnique, Vol 10, No. 4, pp. 129-151.

Blight, G.E. (1963), "The Effect of Nonuniform Pore Pressures on Laboratory Measurements of the Shear Strength of Soils," ASTM Special Technical Publication No. 361, pp. 173-184.

Delory, F.A. (1957), "Long Term Stability of Slopes in Over Consolidated Clays," Ph.D. Thesis, University of London.

Duncan, J.M. and Seed, H.B. (1965), "Errors in Strength Tests and Recommended Corrections," Report No. TE 65-4, Department of Civil Engineering, University of California, Berkeley, California, 1965.

Focht, J.A. Jr. and Sullivan, R.A. (1969), "Two Slides in Overconsolidated Pleistocene Clays," Proceedings, Seventh International Conference on Soil Mechanics and Foundations Engineering, Mexico, 1969, Vol II, pp. 571-576.

Gibson, R.E. and Henkel, D.J. (1954), "Influence of Duration of Tests at Constant Rate of Strain on Measured 'Drained' Strength," Geotechnique, Vol 4, No. 1, pp. 6-15.

Gourlay, A.W. and Wright, S.G. (1984), "Initial Laboratory Study of the Shear Strength Properties of Compacted, Highly Plastic Clays Used for Highway Embankment Construction in the Area of Houston, Texas," A Report on Laboratory Testing Performed Under Interagency Contract Nos. (82-83) 2187 and (84-85) 1026, Center for Transportation Research, The University of Texas at Austin.

Heley, W. and MacIver, B.N. (1971), "Engineering Properties of Clay Shales," U.S. Army Waterway Experimental Station Vicksburg, Technical Report No. S-71-6, 1971, 89 p.

James, P.M. (1970), "Time Effects and Progressive Failure in Clay Slopes," Ph.D Thesis, University of London.

Lambe, T.W. (1961), "Residual Pore Pressures in Compacted Clay," Proceedings, Fifth International Conference on Soil Mechanics and Foundation Engineering, Paris, 1961, Vol I, pp. 207-212.

Olson, R.E. and Langfelder, L.J. (1965), "Pore Water Pressures in Compacted Clay," Proceedings, American Society of Civil Engineers Journal of Soil Mechanics and Foundation Engineering, Vol 91, No. SM4, pp. 127-150.

Roecker, J.D. and Wright, S.G. (1984), "UTEXAS (University of Texas Analysis of Slopes) - A Program for Slope Stability Calculations," Research Report No. 353-1, Center for Transportation Research, The University of Texas at Austin.

Skempton, A.W. (1954), "The Pore Pressure Coefficients A and B," Geotechnique, Vol 4, No. 4, pp. 143-147.

Skempton, A.W. (1964), "Long-Term Stability of Clay Slopes," Geotechnique, Vol 14, No. 2, pp. 77-102.

Skempton, A.W. (1970), "First-Time Slides in Over-Consolidated Clays," Geotechnique, Vol 20, No. 3, pp. 320-324.

Stauffer, P.A. and Wright, S.G. (1984), "An Examination of Earth Slope Failures in Texas," Research Report No. 353-3F, Center for Transportation Research, The University of Texas at Austin.

Texas SDHPT (1978), Manual of Testing Procedures, Texas State Department of Highways and Public Transportation, Austin, Texas.

Townsend, F.C. and Gilbert, P.A. (1976), "Effects of Specimen Type on the Residual Strength of Clay and Clay Shales," ASTM Special Technical Publication No. STP-599, 1976, pp. 43-65.

Wright, S.G. (1983), "Report on Research and Interim Recommendations for Embankment Slope Design in District 12," Technical Memorandum Under Interagency Contract (82-83) 2187, Center for Transportation Research, The University of Texas at Austin.

APPENDICES

APPENDIX A

Appendix A contains the consolidation results, which are not presented in the main text, for all the specimens in this phase of testing. These include the specimens consolidated from a slurry, the specimens prepared by packing, and the undisturbed specimens.

Plots are included for:

1. The change in height of slurry versus the logarithm of time for the specimens consolidated from a slurry (Tests 6.10, 6.11, 6.12, and 6.27).

2. The change in volume during final triaxial consolidation versus both the logarithm of time and the square root of time for the specimens consolidated from a slurry (Tests 6.15, 6.11, 6.27, and 6.10).

3. The change in volume during final triaxial consolidation versus both the logarithm of time and the square root of time for the specimens prepared by packing (Tests 6.13, B.10, and B.9).

4. The change in volume during final triaxial consolidation versus both the logarithm of time and the square root of time for the undisturbed specimens (Tests 6.14, 6.17, B.12, B.13, B.16, 6.22, B.18, and B.17).

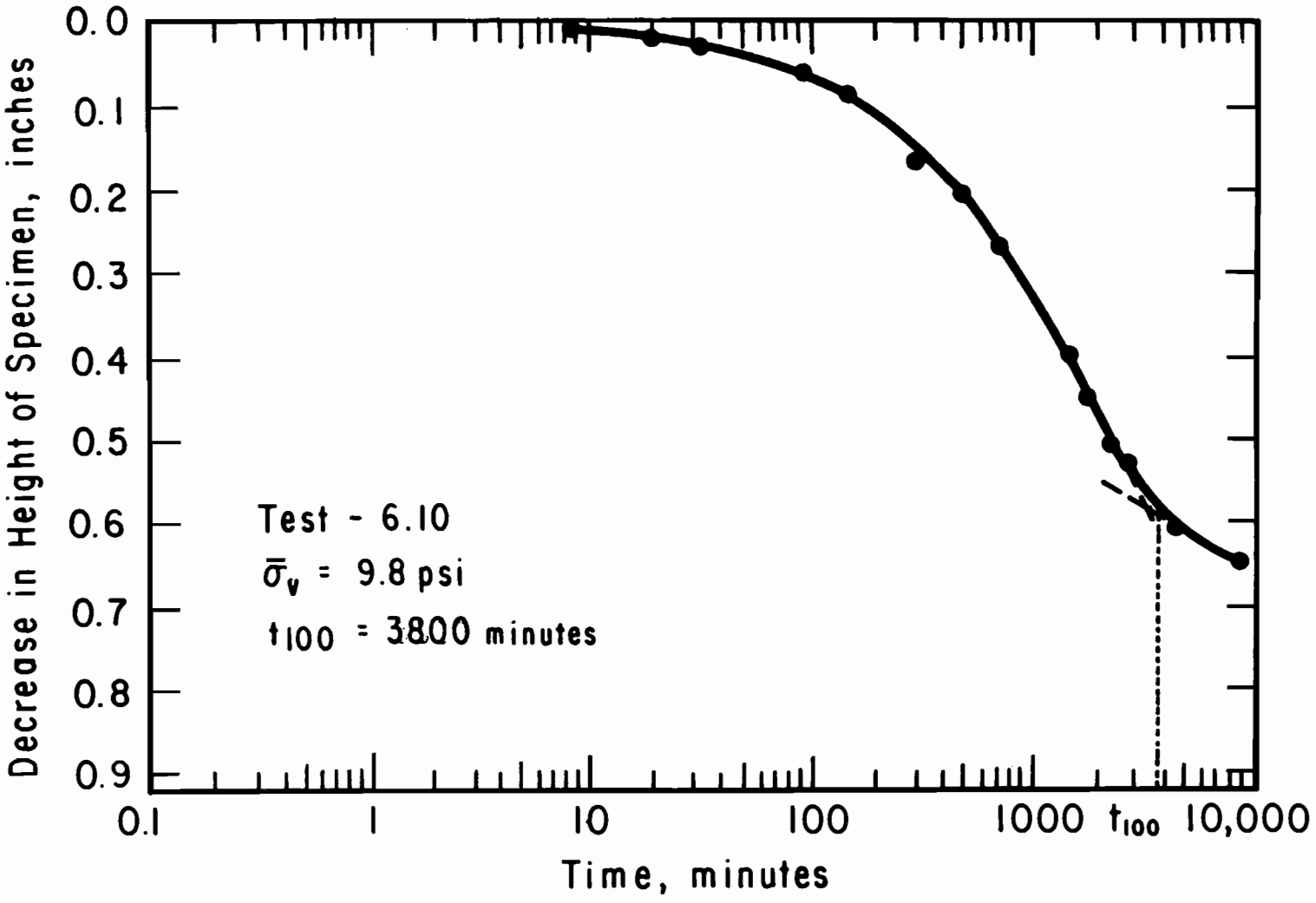

Figure A.1.1. Decrease in Height of Specimen in Test 6.10 as a Function of Time, during Final Increment of One-Dimensional Consolidation - Logarithm of Time.

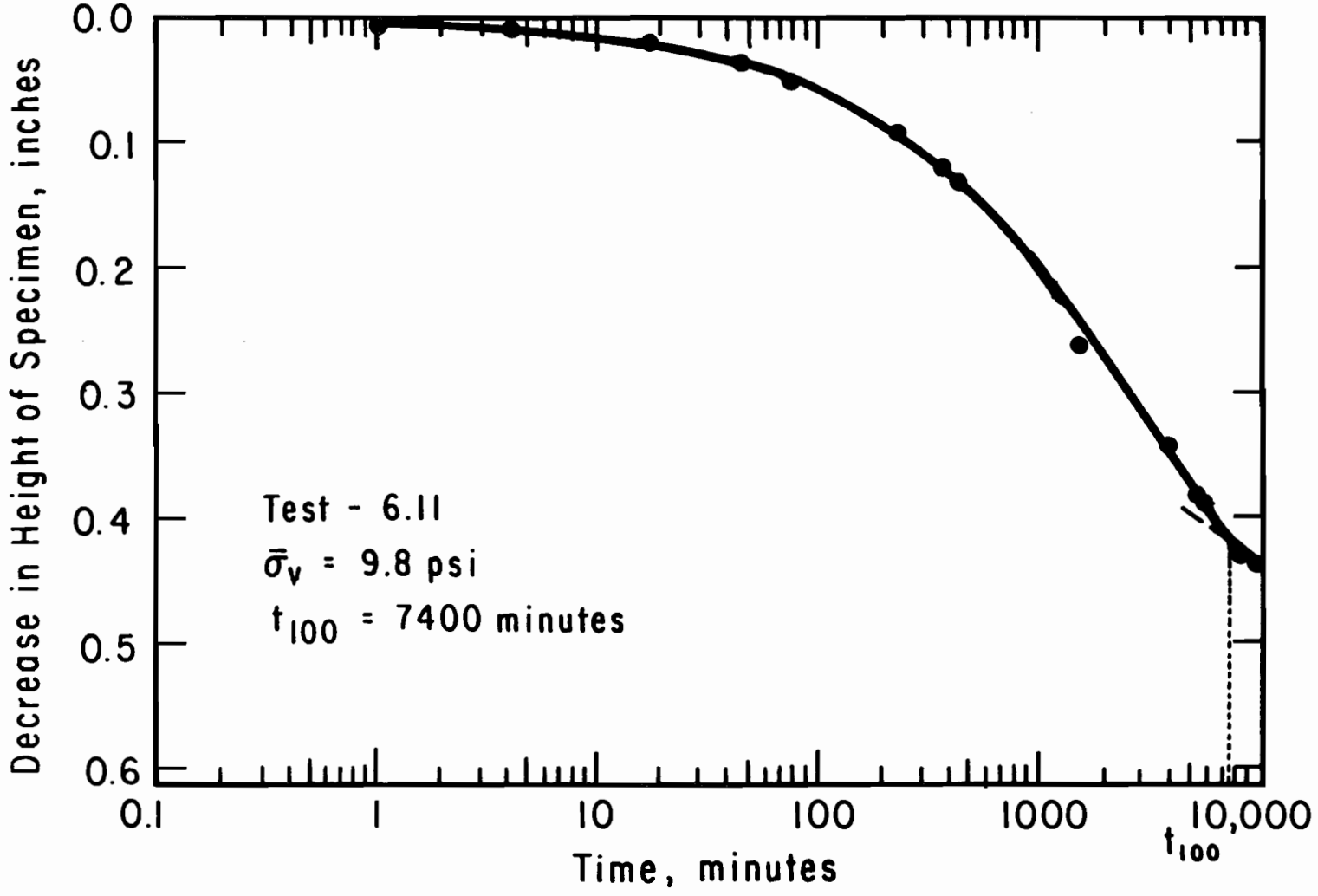

Figure A.1.2. Decrease in Height of Specimen in Test 6.11 as a Function of Time, during Final Increment of One-Dimensional Consolidation - Logarithm of Time.

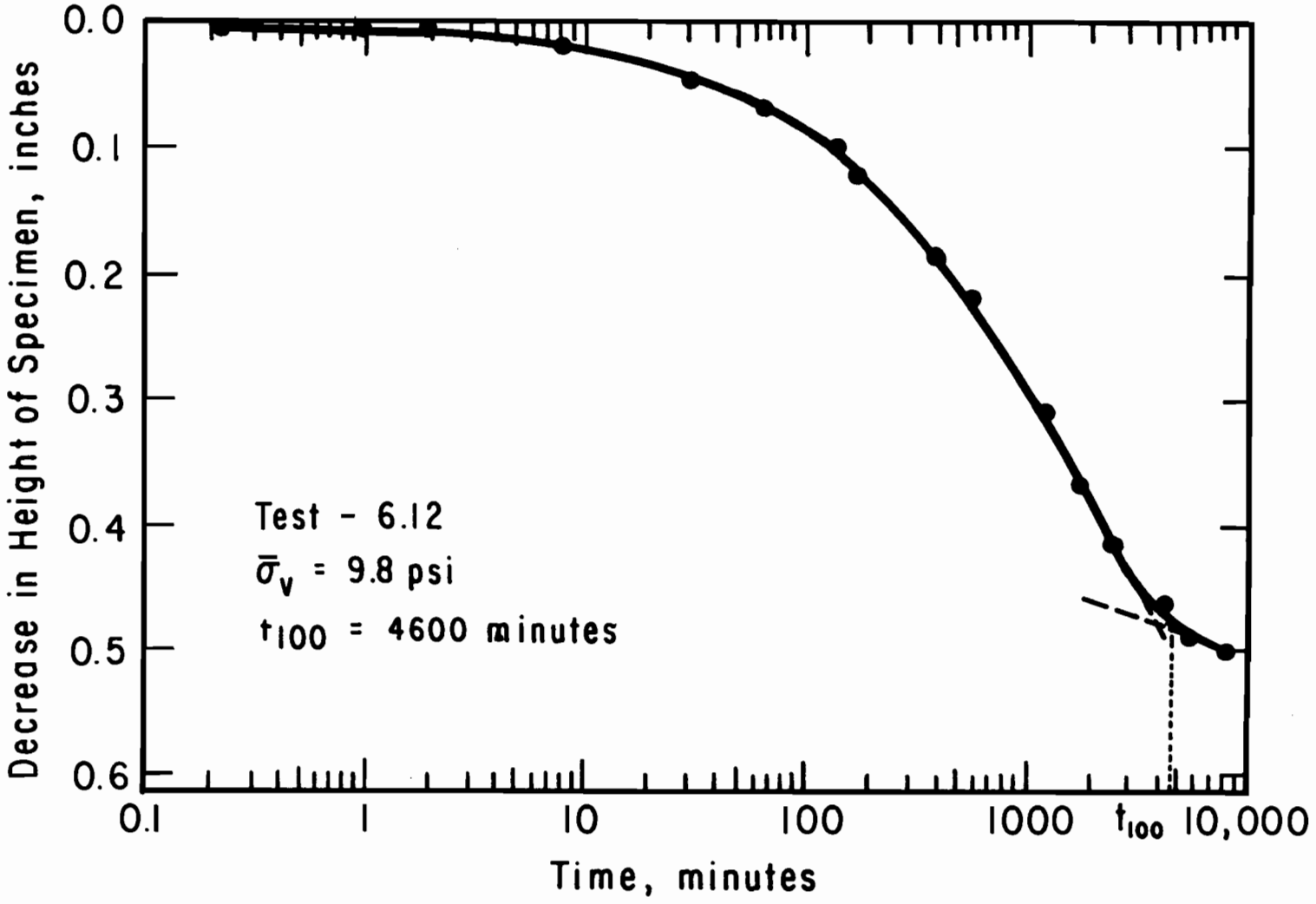

Figure A.1.3. Decrease in Height of Specimen in Test 6.12 as a Function of Time, during Final Increment of One-Dimensional Consolidation - Logarithm of Time.

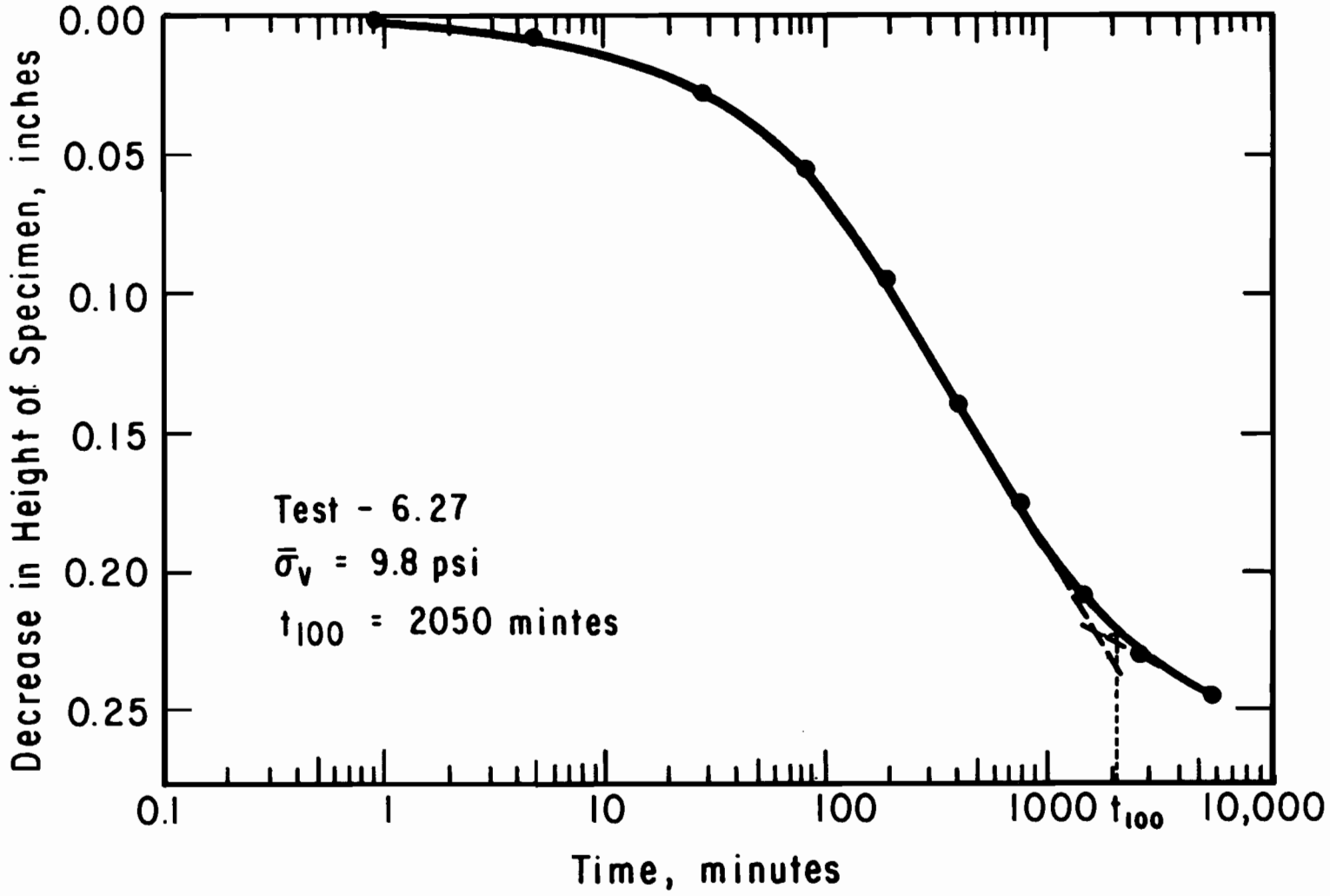

Figure A.1.4. Decrease in Height of Specimen in Test 6.27 as a Function of Time, during Final Increment of One-Dimensional Consolidation - Logarithm of Time.

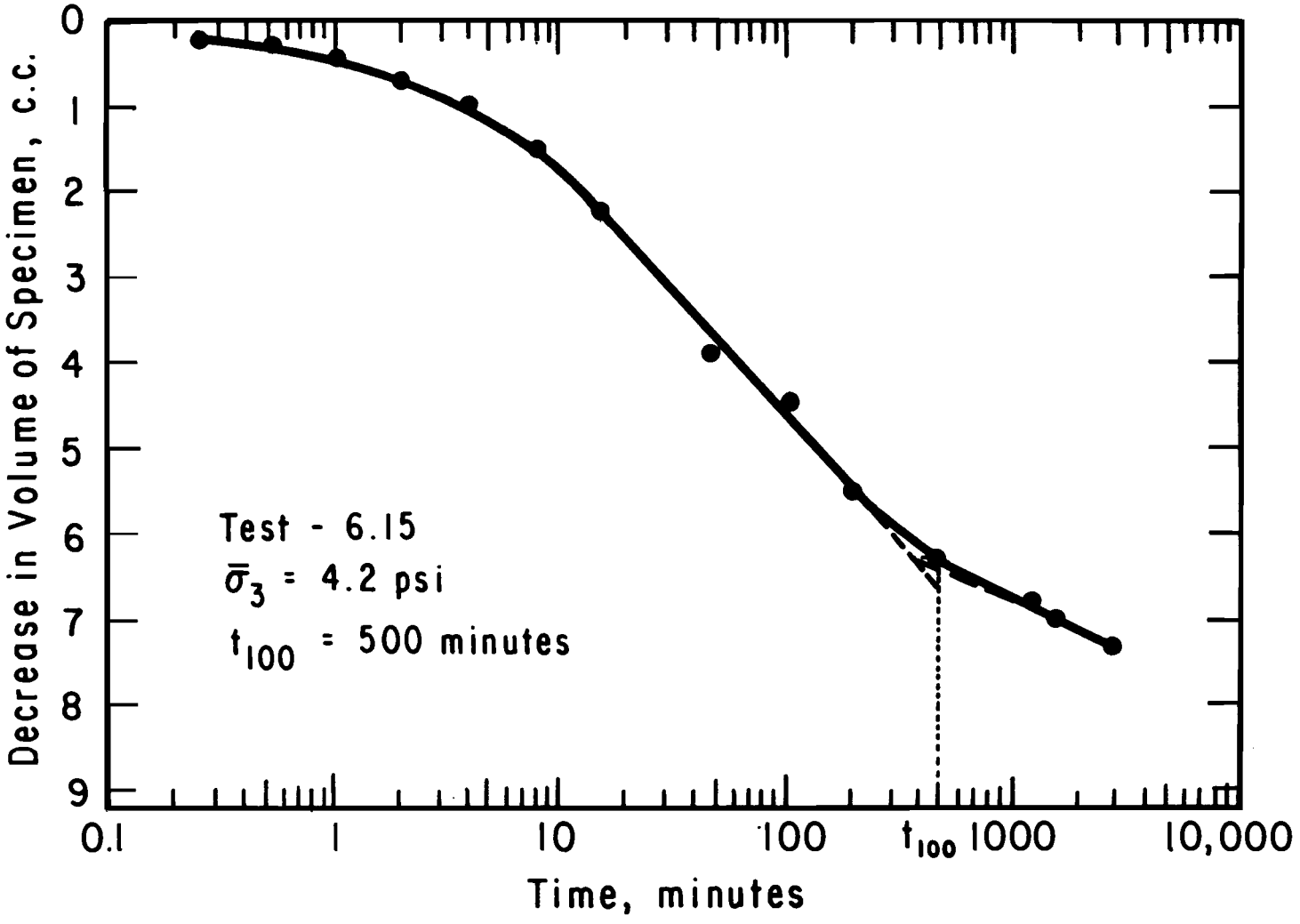

Figure A.2.1. Decrease in Pore Water Volume of Specimen in Test 6.15 as a Function of Time, during Final Consolidation - Logarithm of Time.

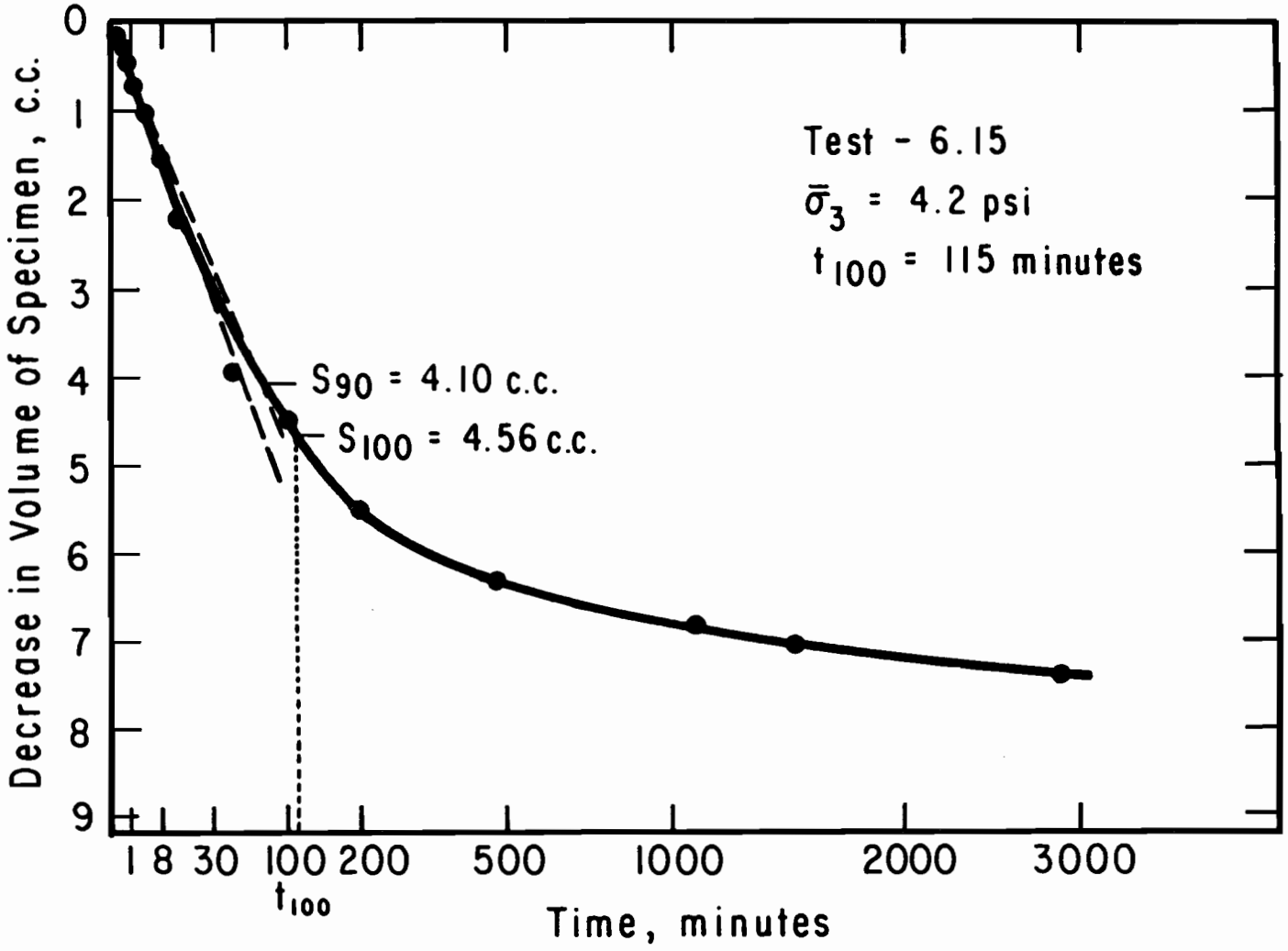

Figure A.2.2. Decrease in Pore Water Volume of Specimen in Test 6.15 as a Function of Time, during Final Consolidation - Square Root of Time.

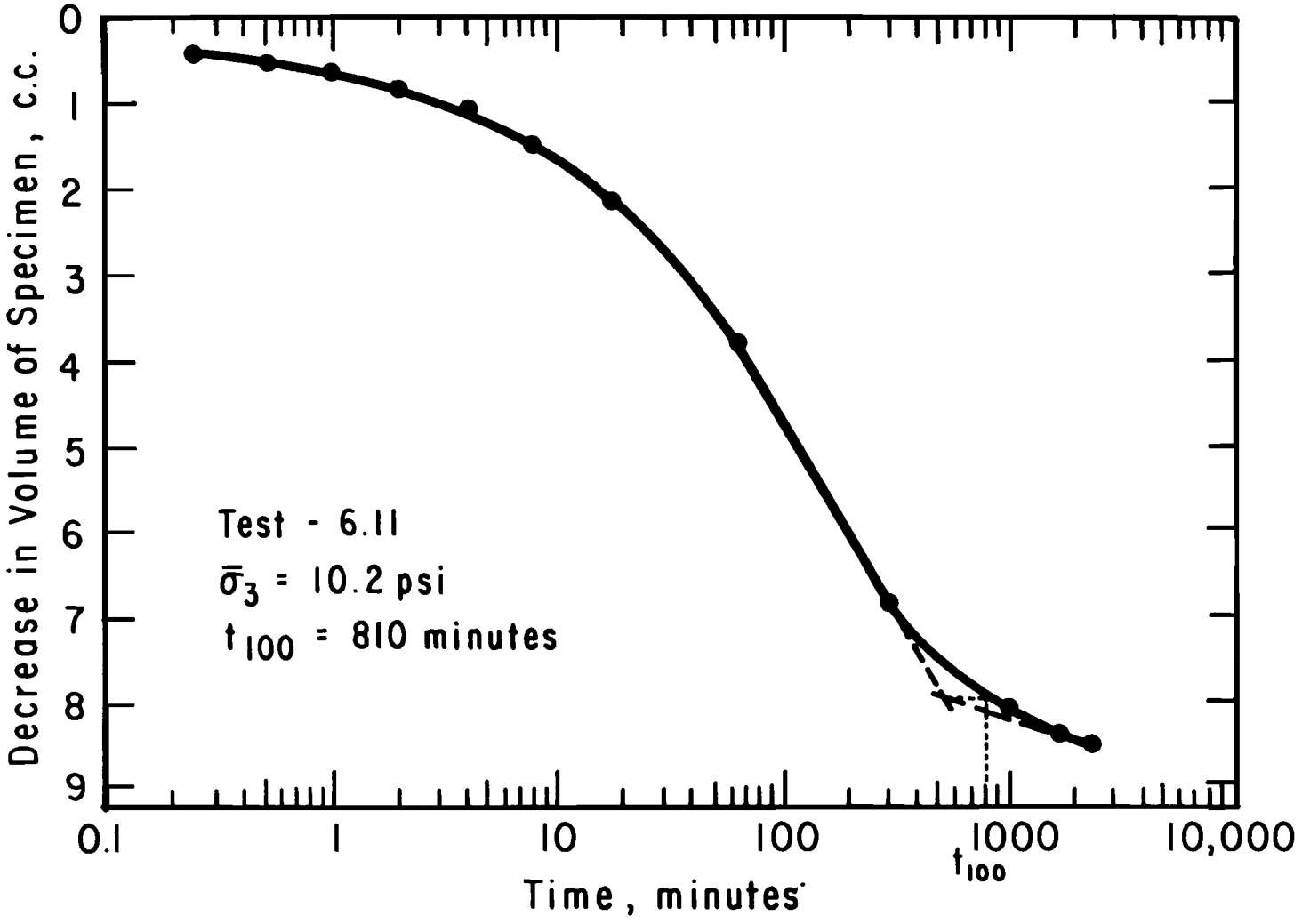

Figure A.2.3. Decrease in Pore Water Volume of Specimen in Test 6.11 as a Function of Time, during Final Consolidation - Logarithm of Time.

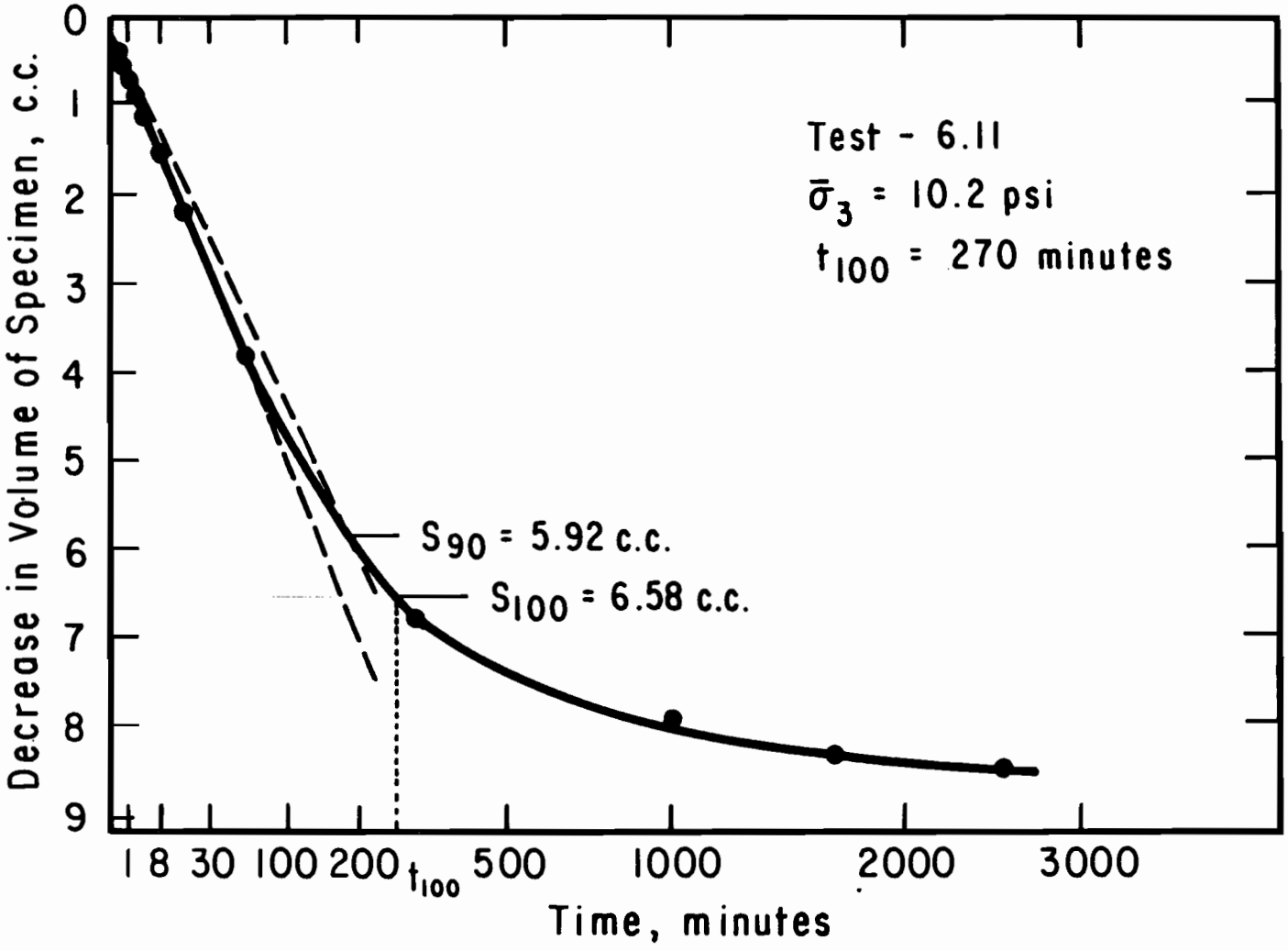

Figure A.2.4. Decrease in Pore Water Volume of Specimen in Test 6.11 as a Function of Time, during Final Consolidation - Square Root of Time.

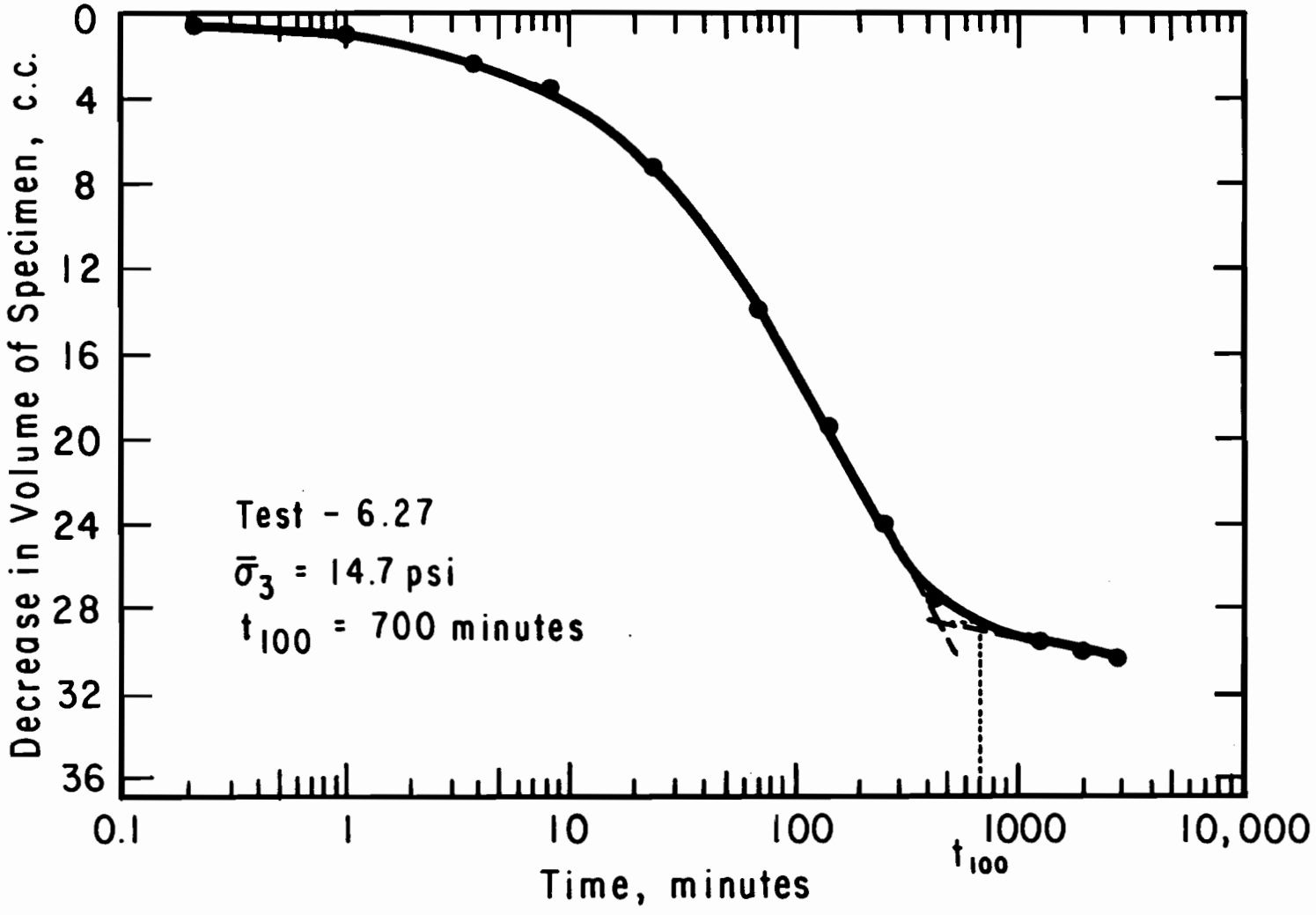

Figure A.2.5. Decrease in Pore Water Volume of Specimen in Test 6.27 as a Function of Time, during Final Consolidation - Logarithm of Time.

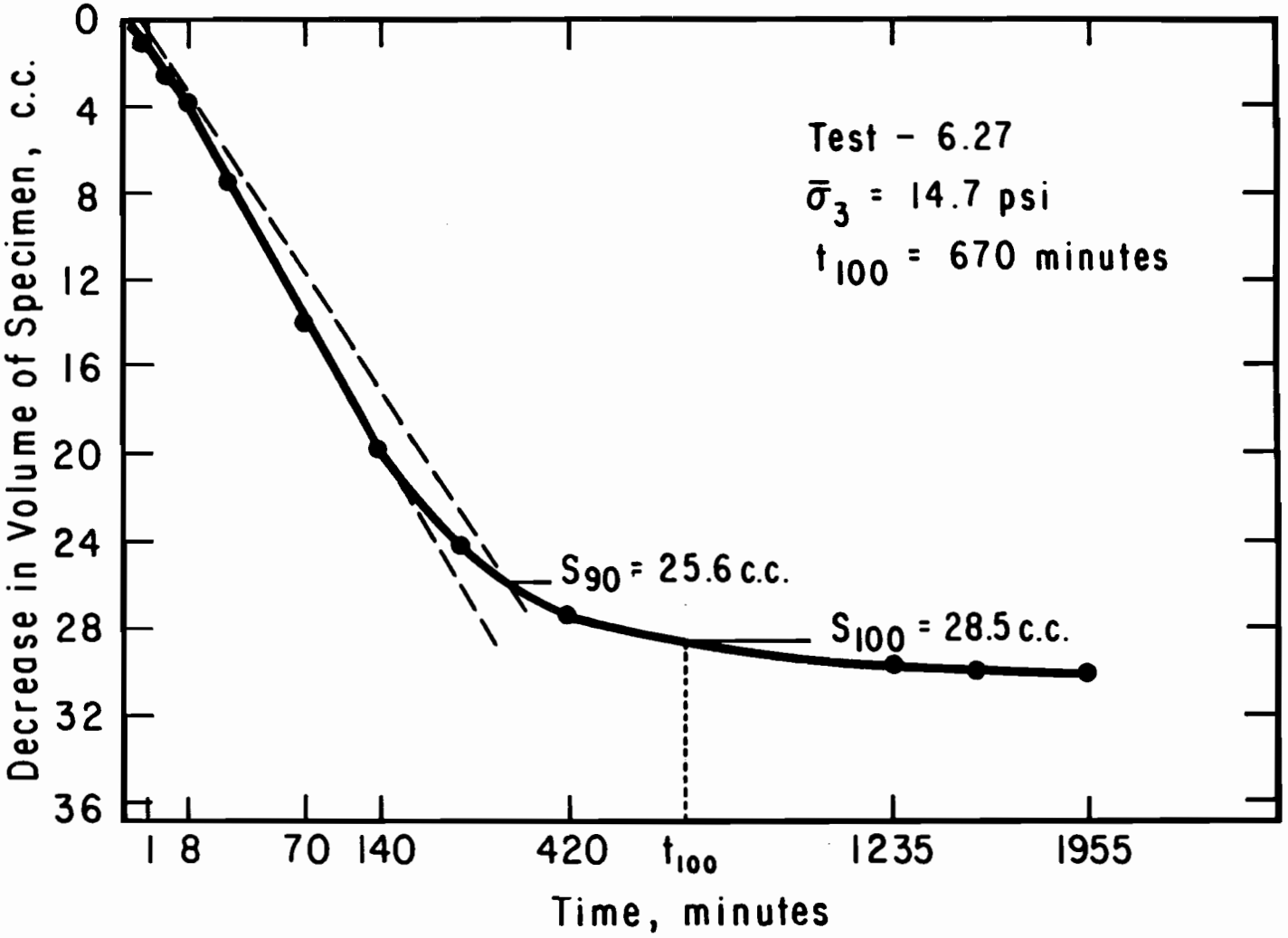

Figure A.2.6. Decrease in Pore Water Volume of Specimen in Test 6.27 as a Function of Time, during Final Consolidation - Square Root of Time.

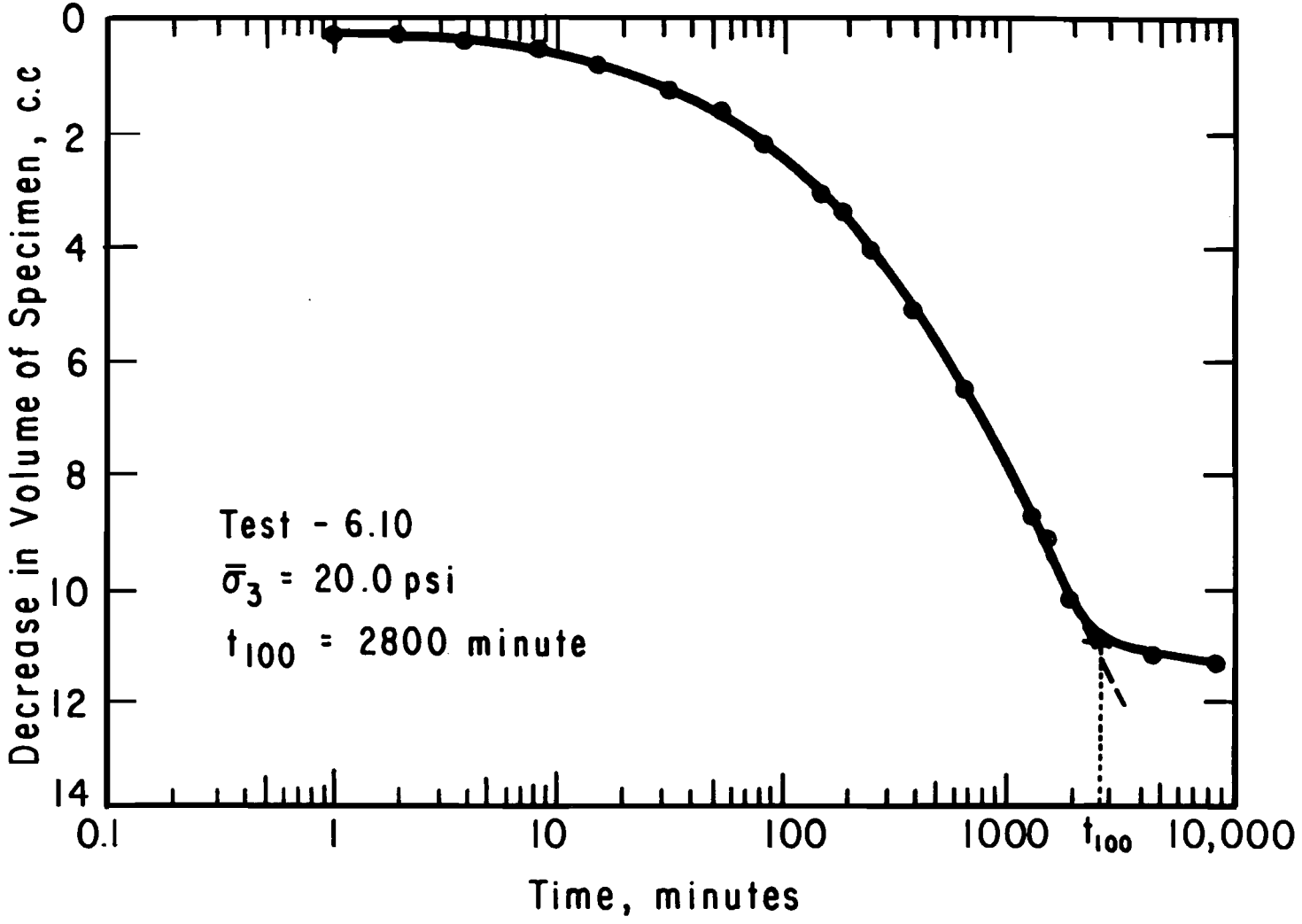

Figure A.2.7. Decrease in Pore Water Volume of Specimen in Test 6.10 as a Function of Time, during Final Consolidation - Logarithm of Time.

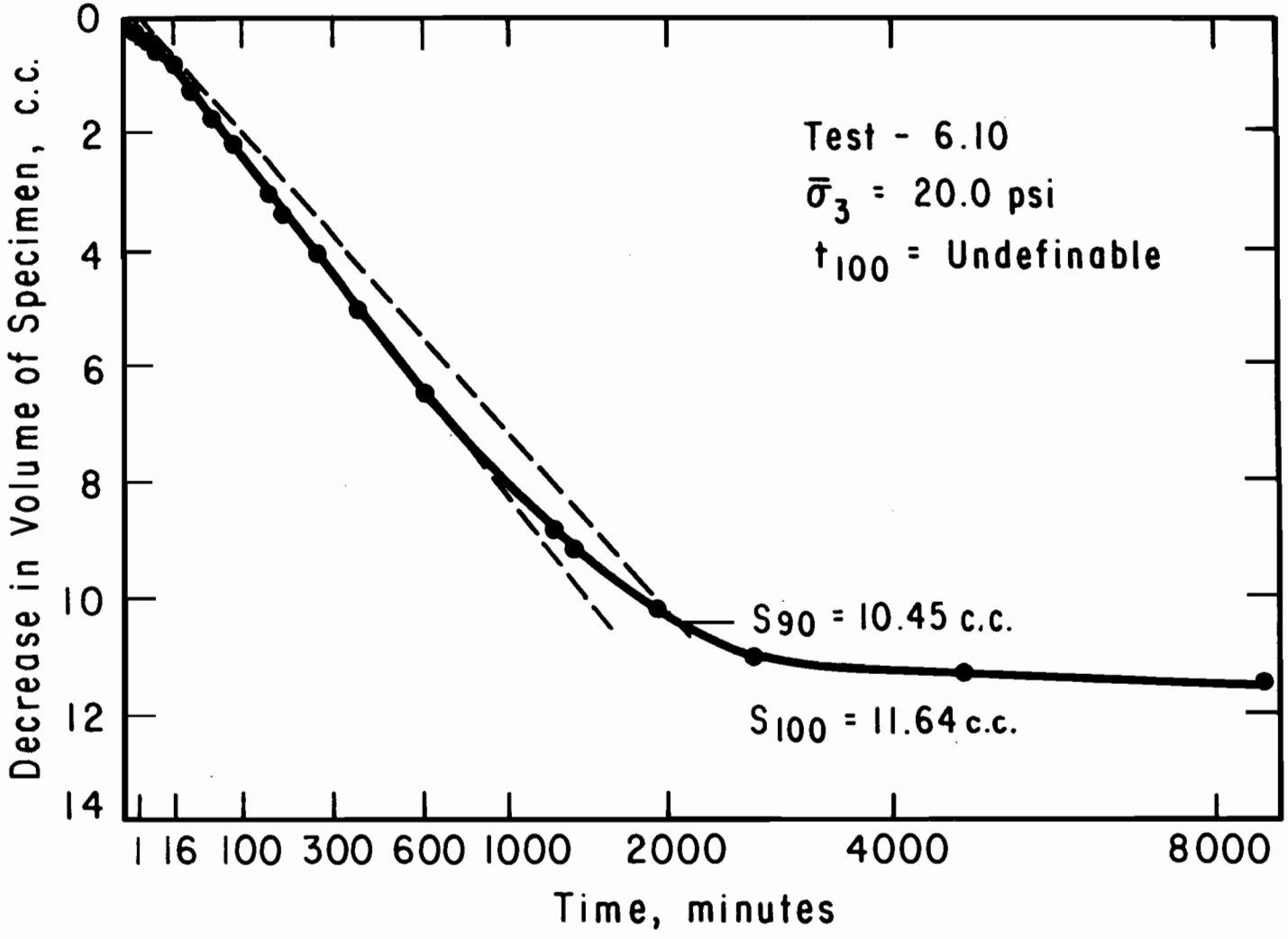

Figure A.2.8. Decrease in Pore Water Volume of Specimen in Test 6.10 as a Function of Time, during Final Consolidation - Square Root of Time.

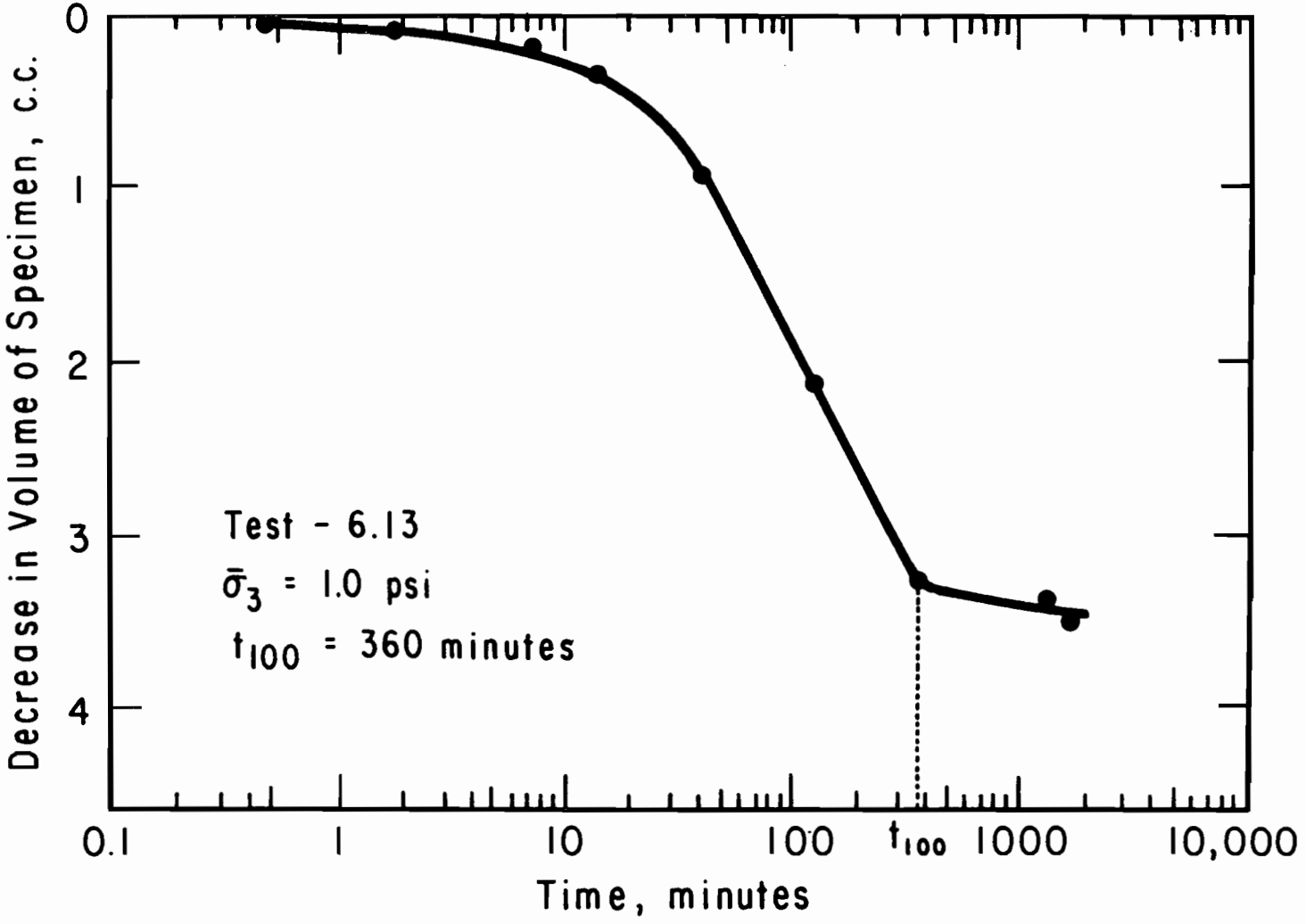

Figure A.3.1. Decrease in Pore Water Volume of Specimen in Test 6.13 as a Function of Time, during Final Consolidation - Logarithm of Time.

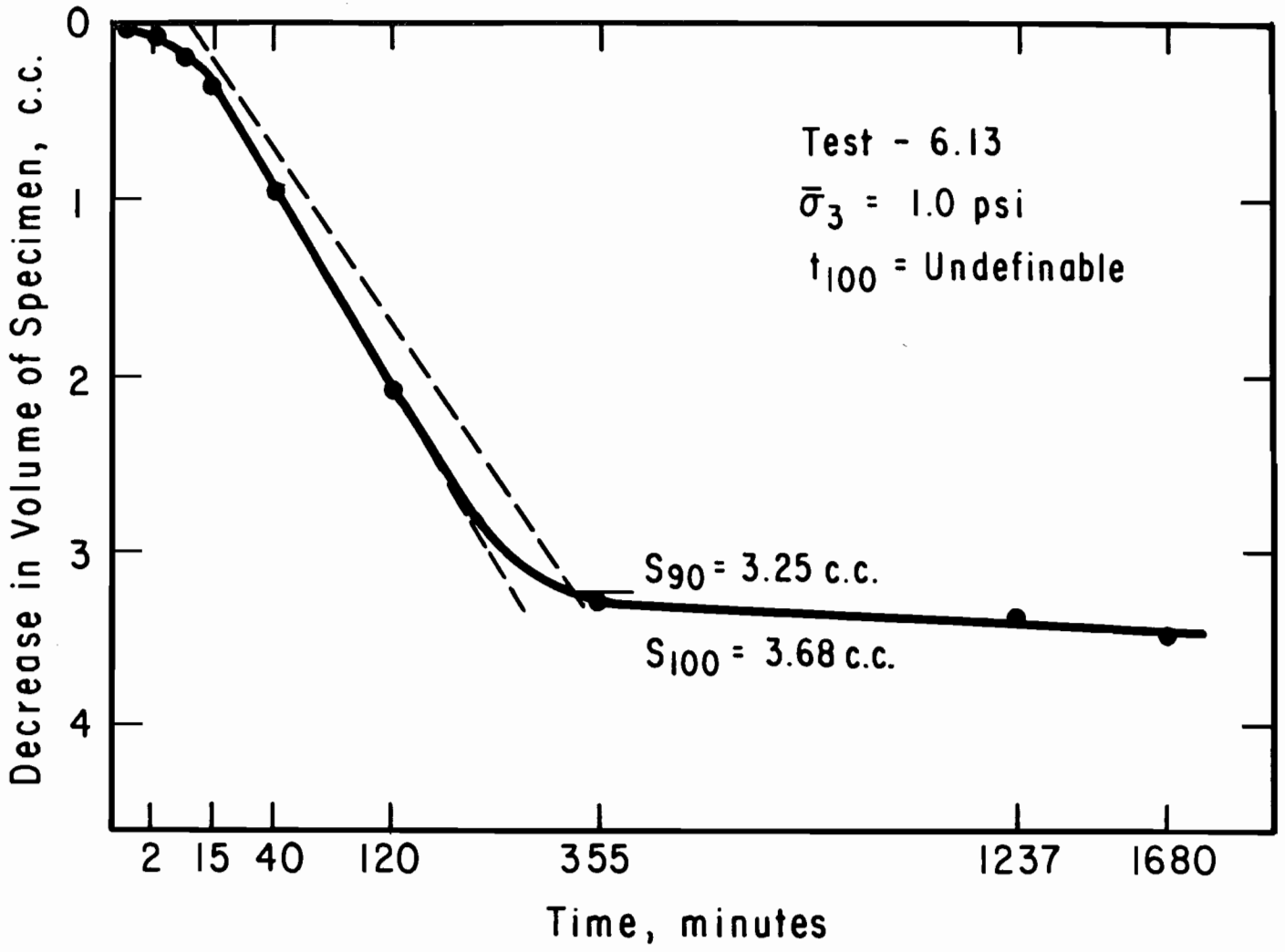

Figure A.3.2. Decrease in Pore Water Volume of Specimen in Test 6.13 as a Function of Time, during Final Consolidation - Square Root of Time.

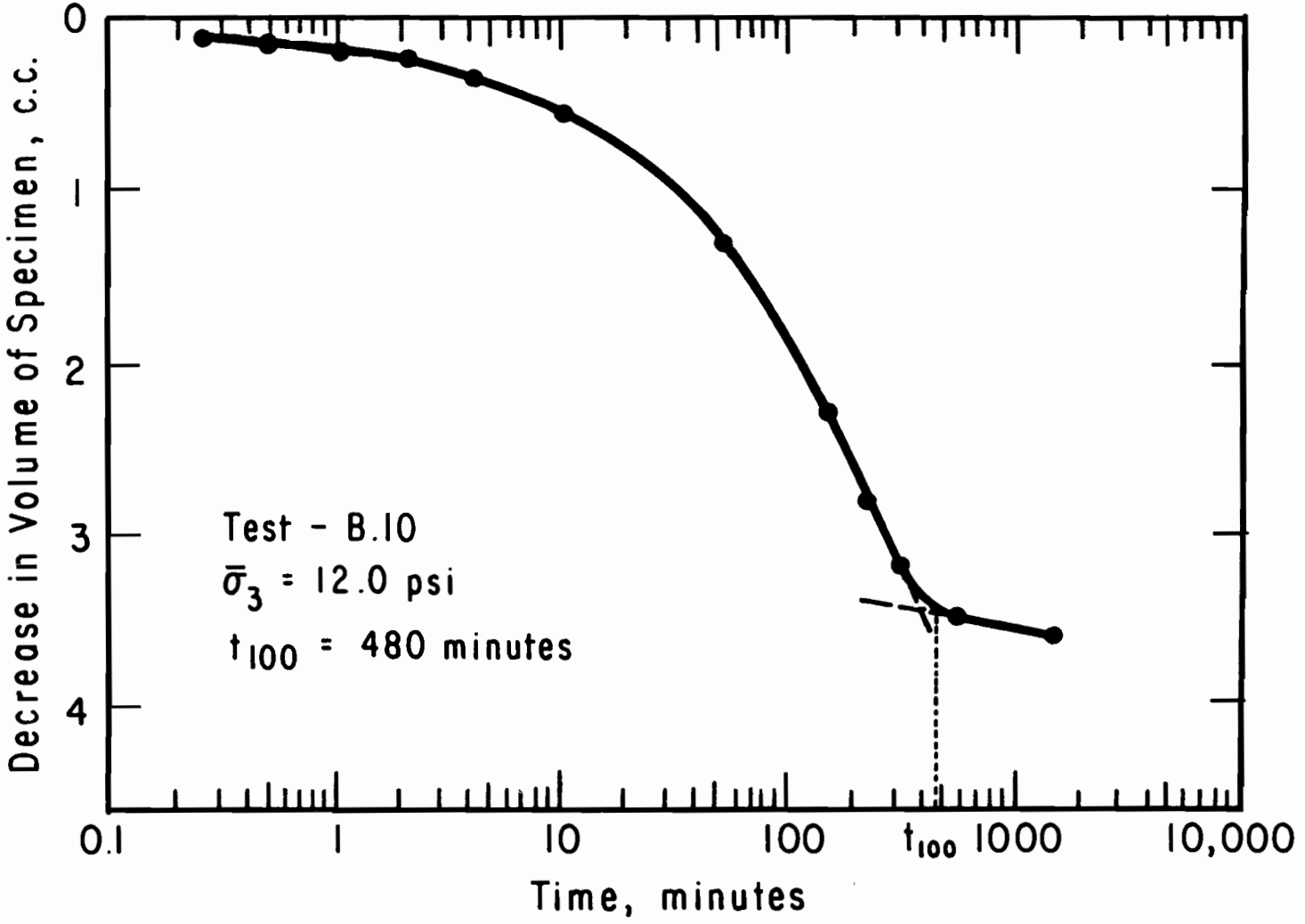

Figure A.3.3. Decrease in Pore Water Volume of Specimen in Test B.10 as a Function of Time, during Final Consolidation - Logarithm of Time.

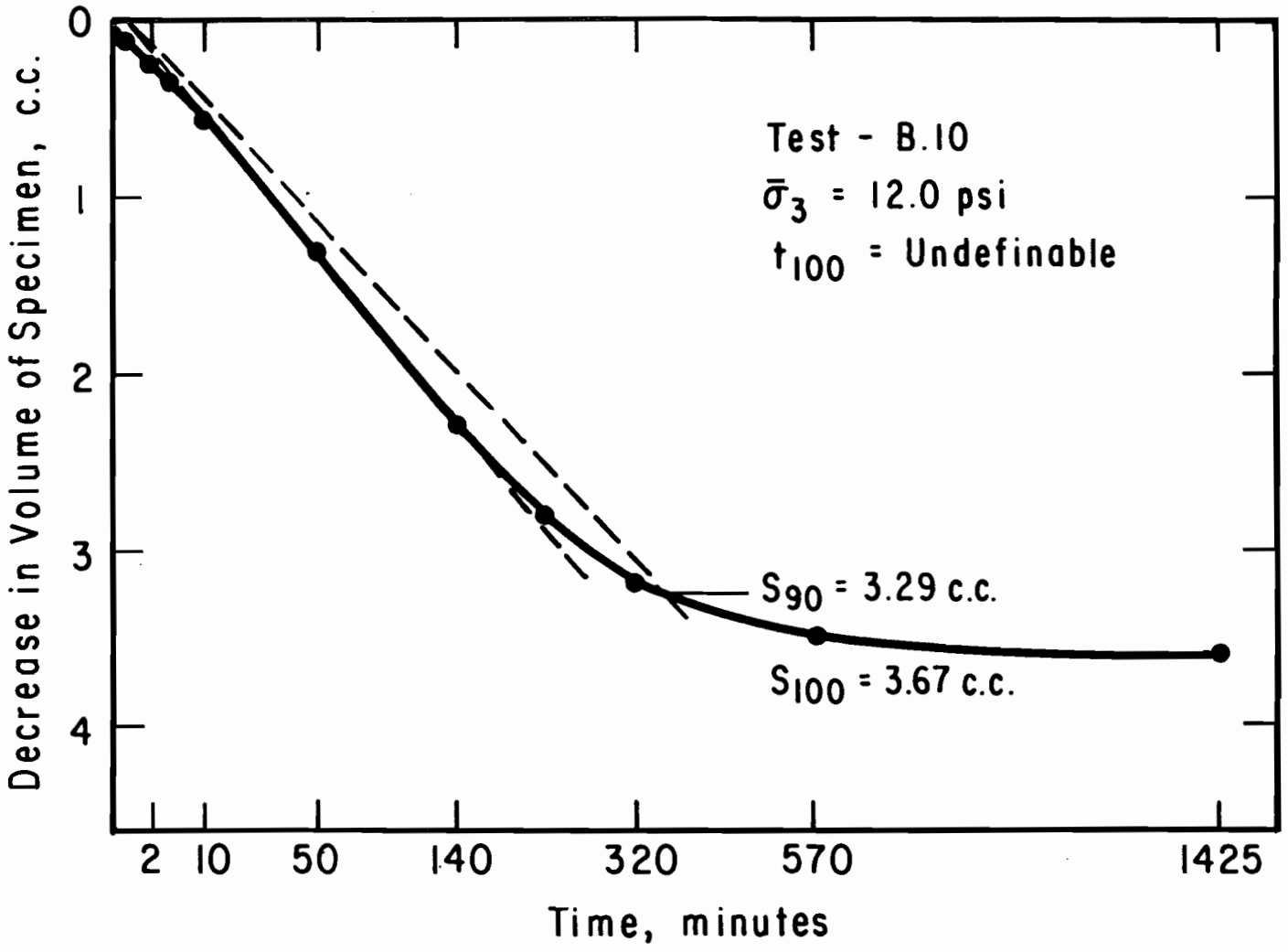

Figure A.3.4. Decrease in Pore Water Volume of Specimen in Test B.10 as a Function of Time, during Final Consolidation - Square Root of Time.

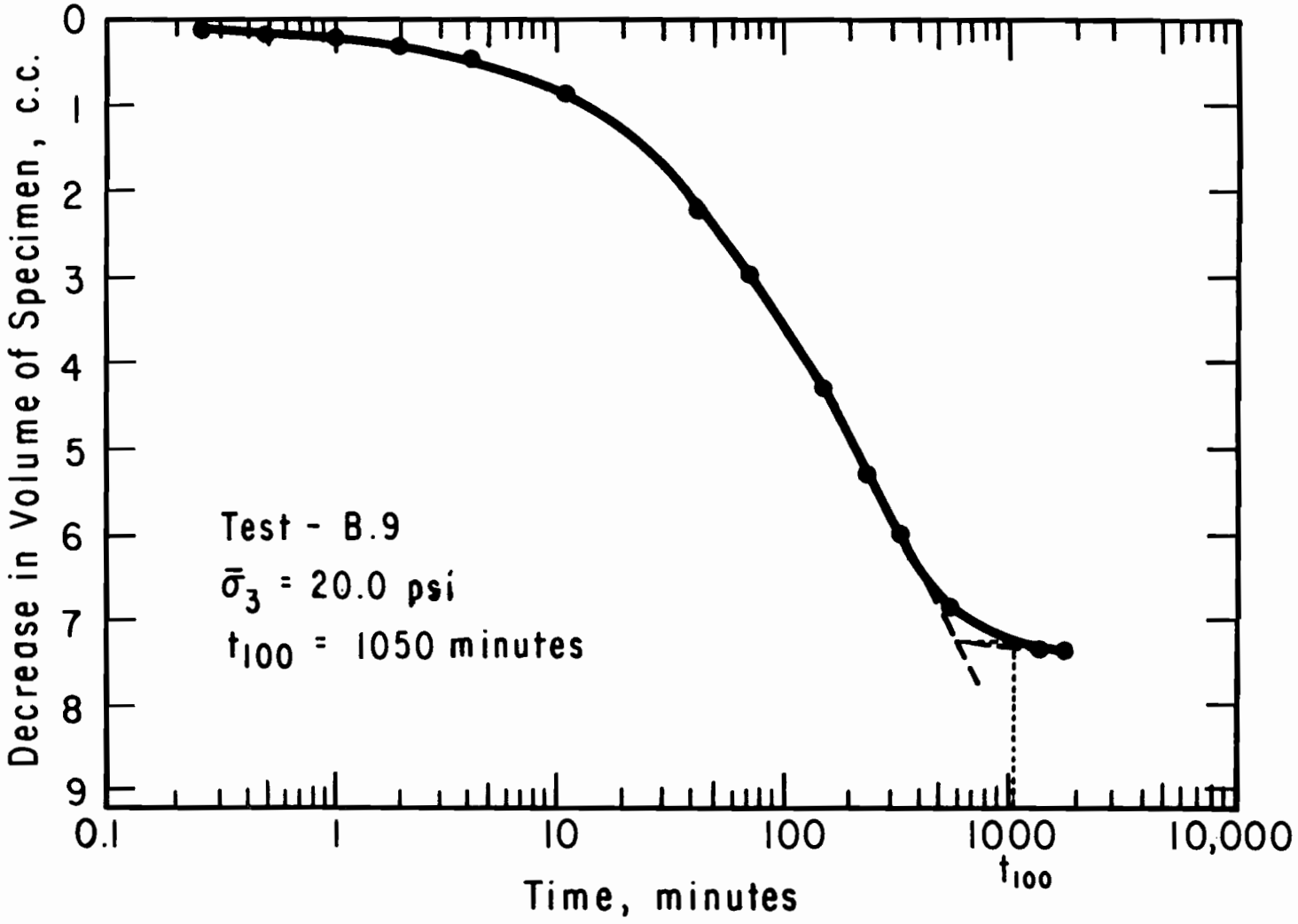

Figure A.3.5. Decrease in Pore Water Volume of Specimen in Test B.9 as a Function of Time, during Final Consolidation - Logarithm of Time.

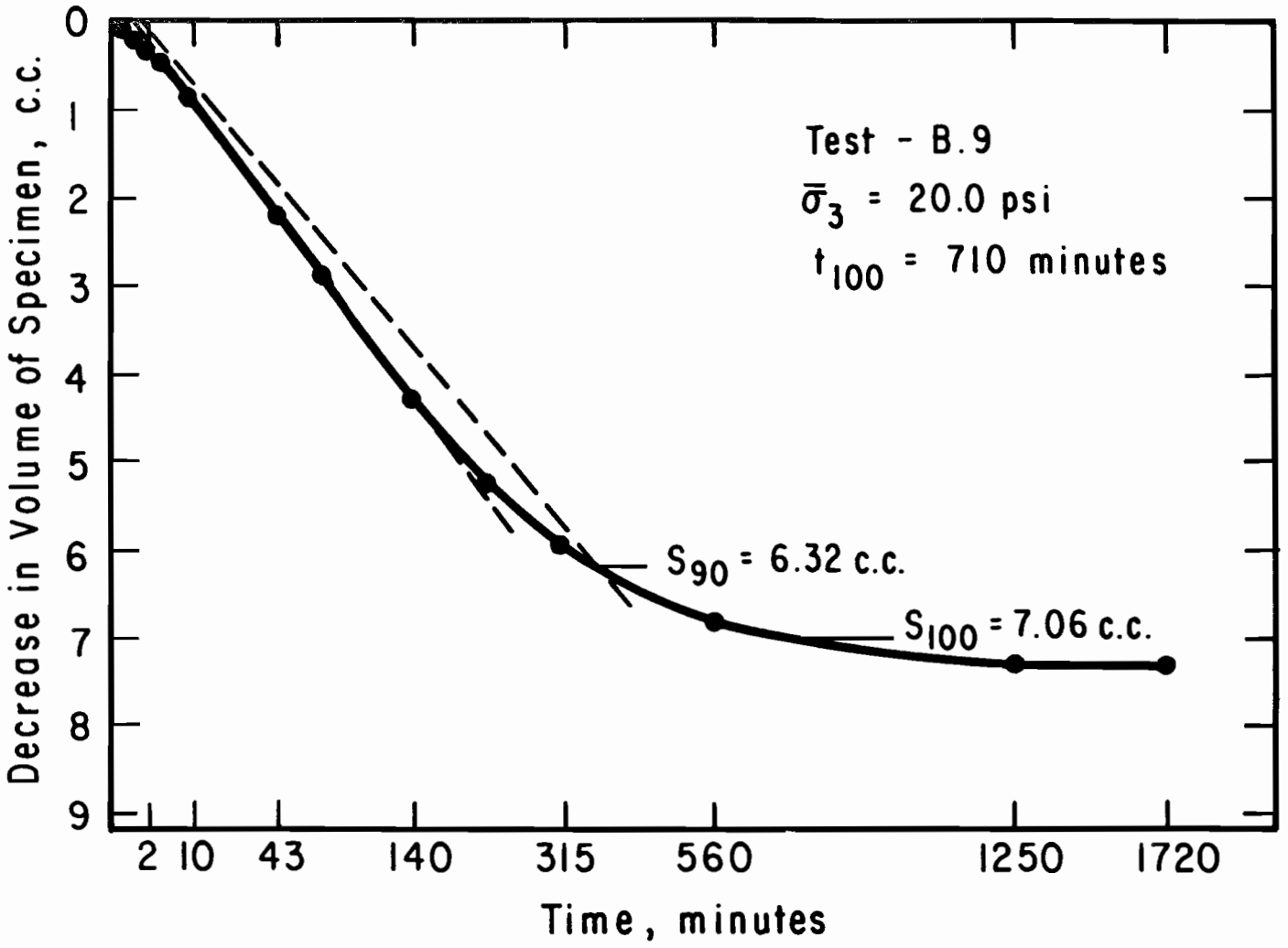

Figure A.3.6. Decrease in Pore Water Volume of Specimen in Test B.9 as a Function of Time, during Final Consolidation - Square Root of Time.

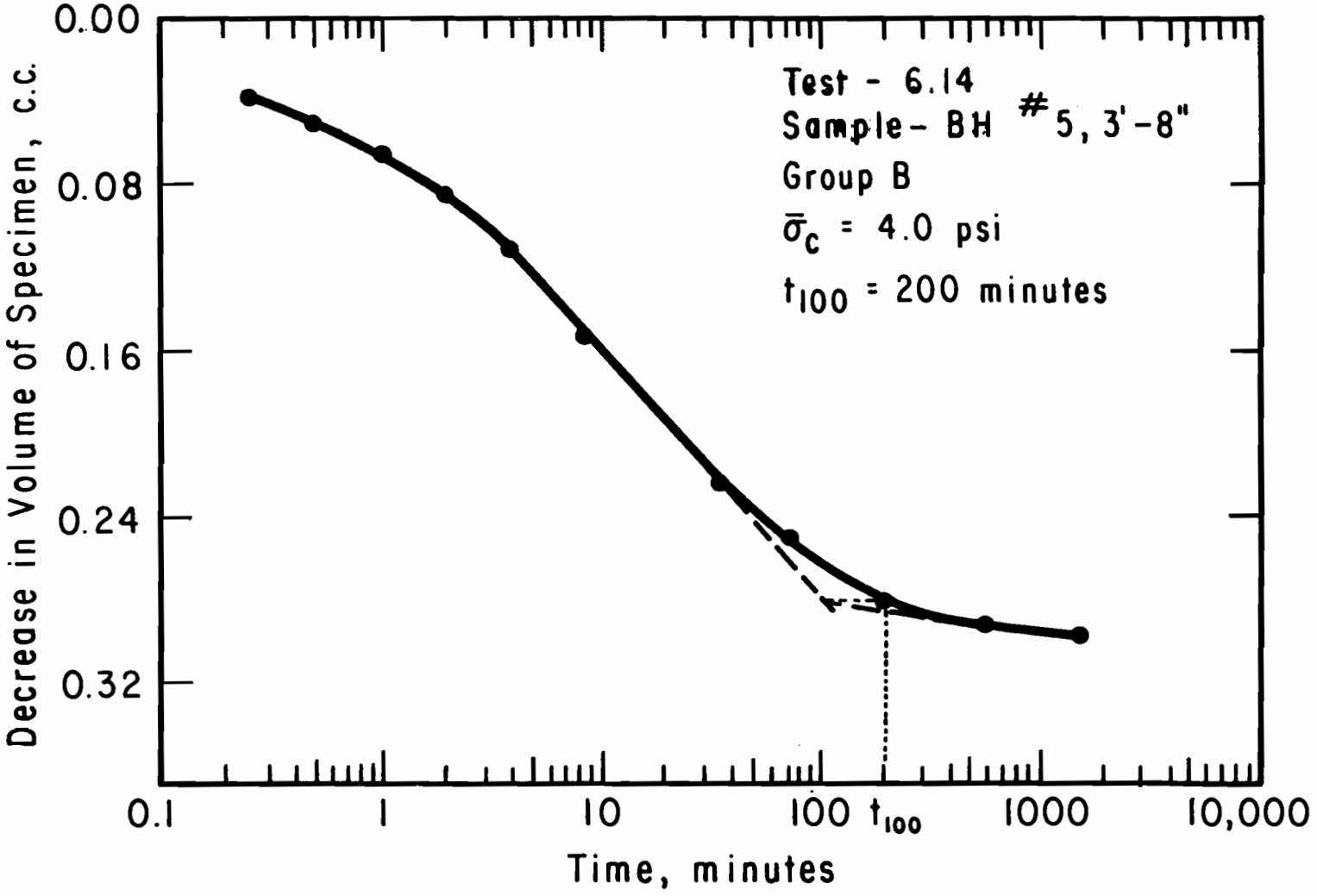

Figure A.4.1. Decrease in Pore Water Volume of Specimen in Test 6.14 as a Function of Time, during Final Consolidation - Logarithm of Time.

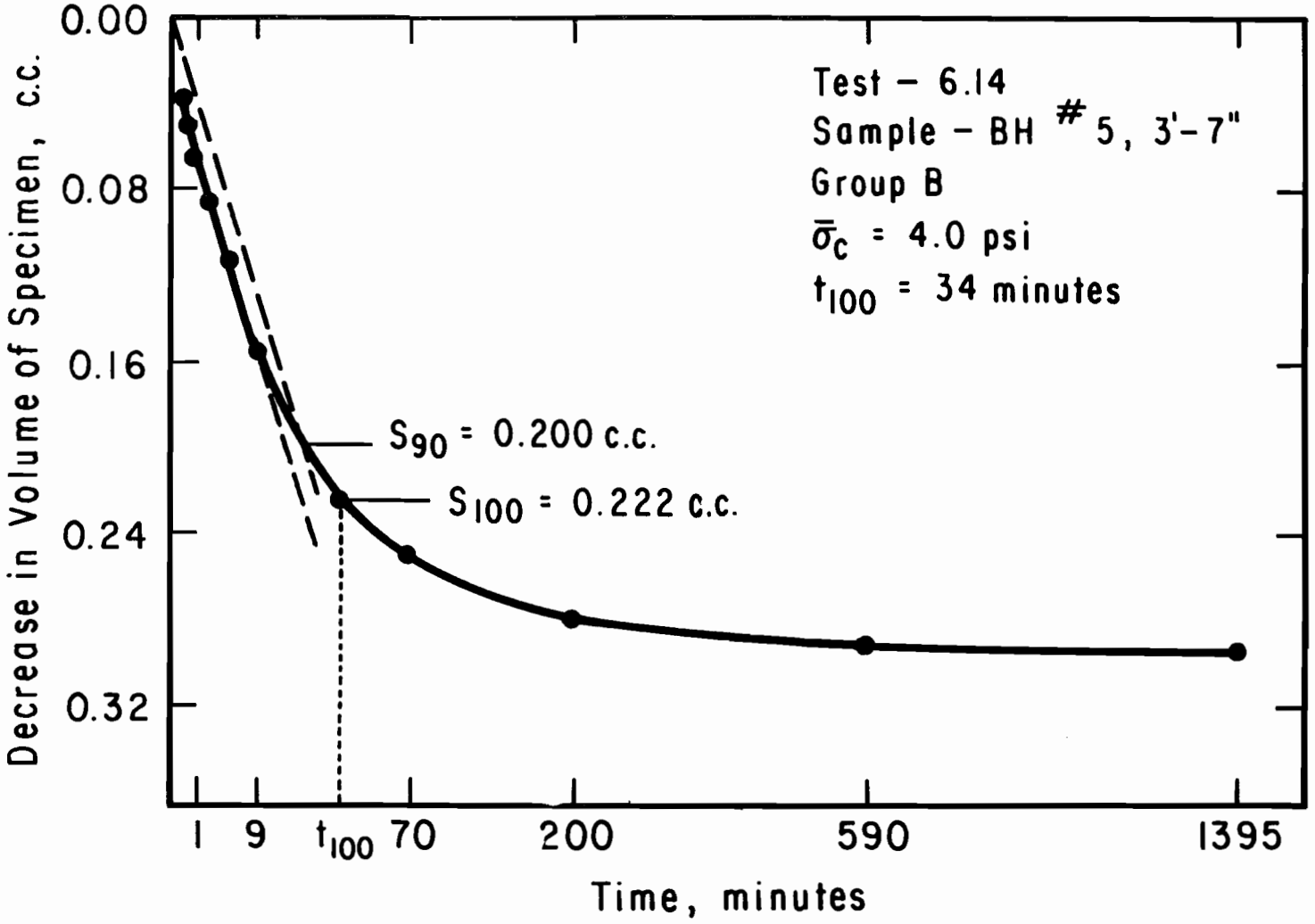

Figure A.4.2. Decrease in Pore Water Volume of Specimen in Test 6.14 as a Function of Time, during Final Consolidation - Square Root of Time.

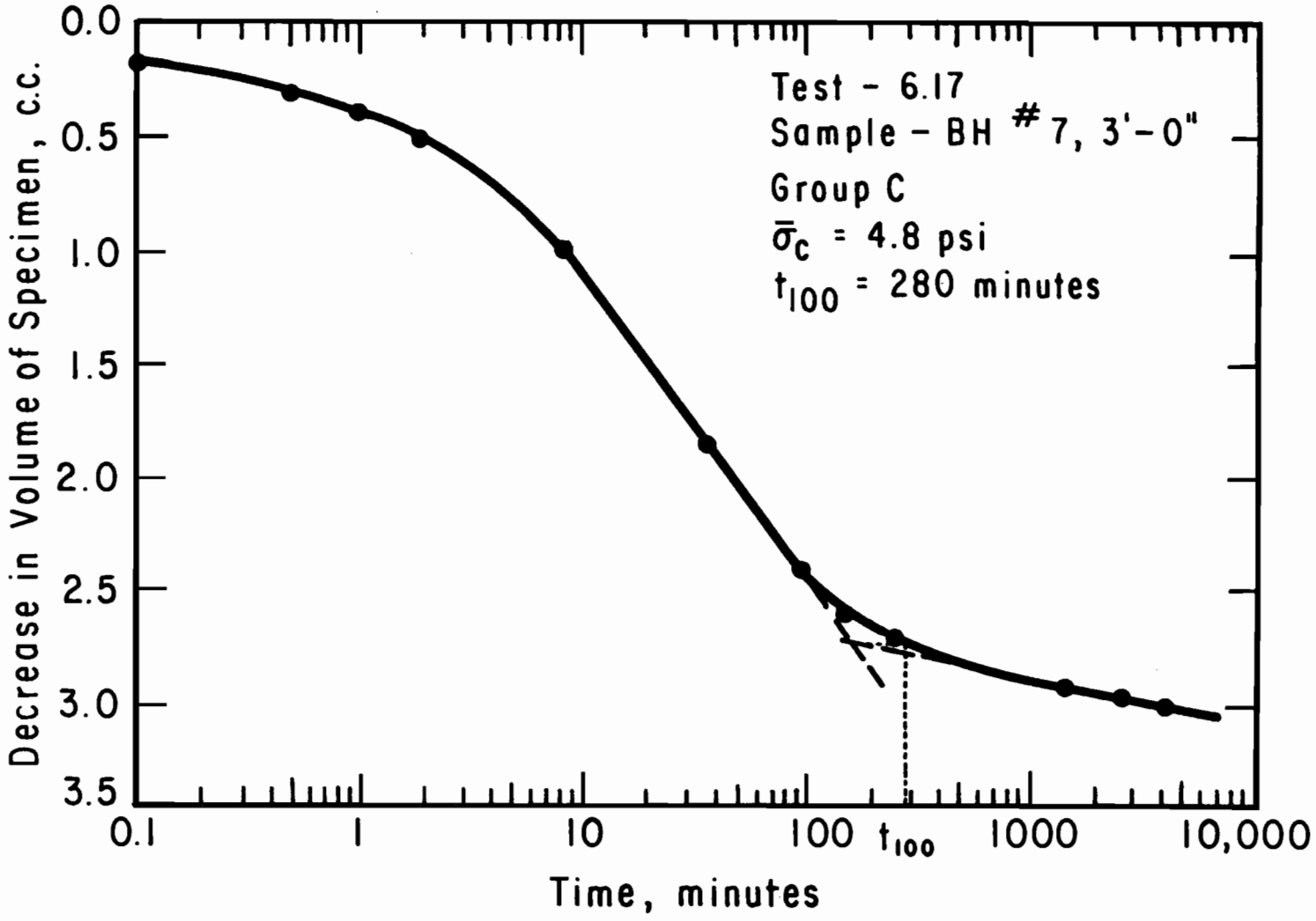

Figure A.4.3. Decrease in Pore Water Volume of Specimen in Test 6.17 as a Function of Time, during Final Consolidation - Logarithm of Time.

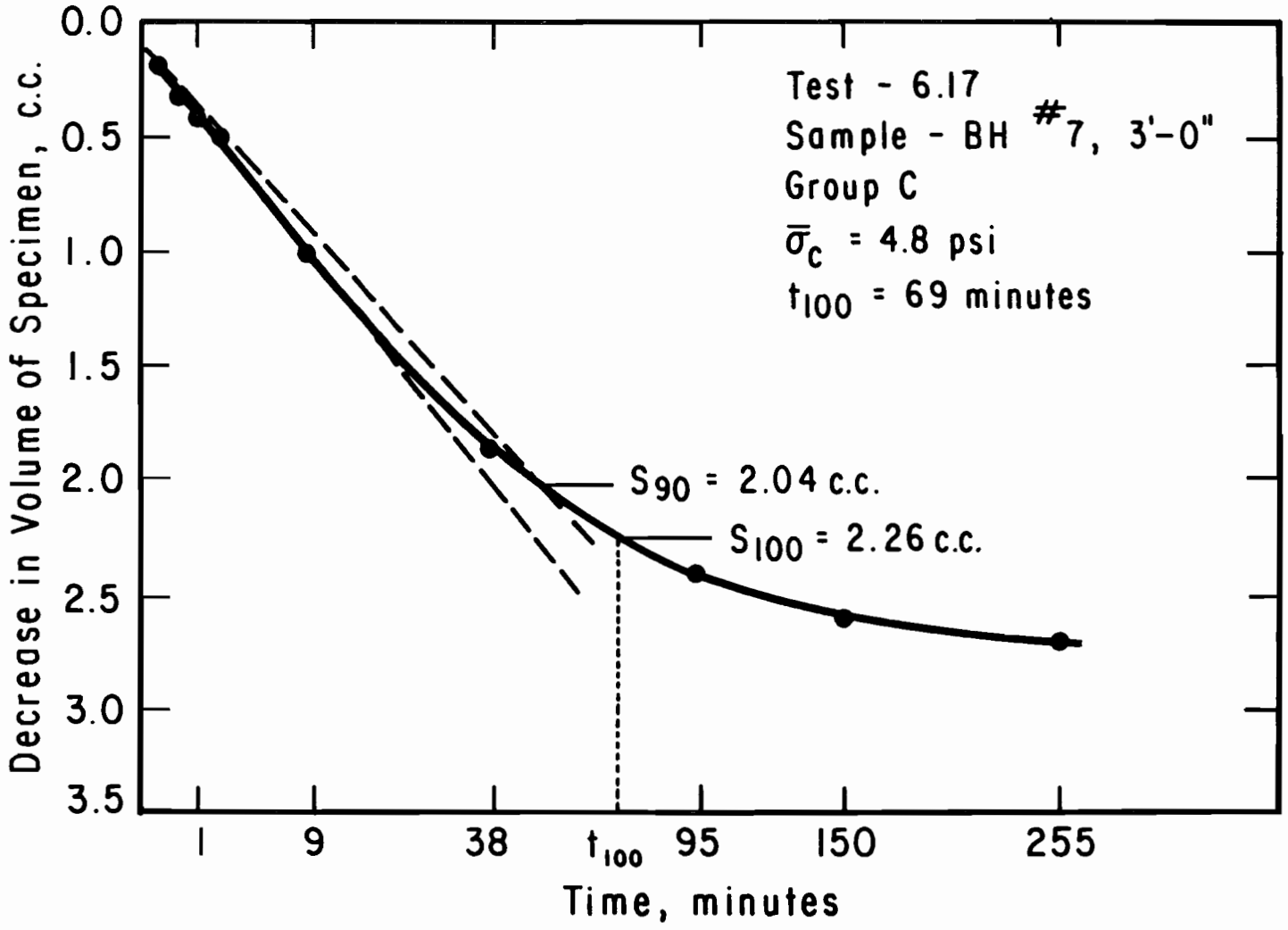

Figure A.4.4. Decrease in Pore Water Volume of Specimen in Test 6.17 as a Function of Time, during Final Consolidation - Square Root of Time.

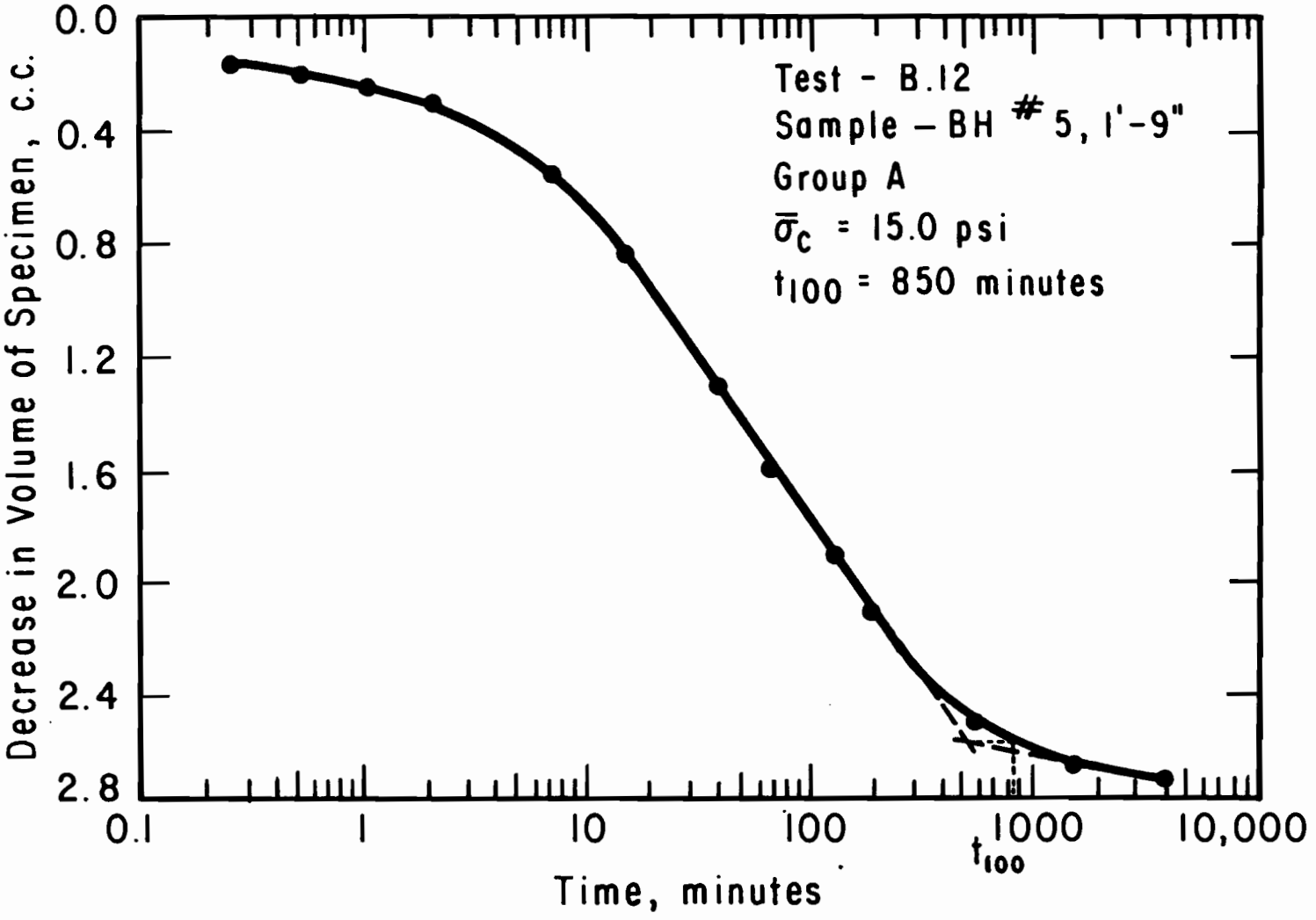

Figure A.4.5. Decrease in Pore Water Volume of Specimen in Test B.12 as a Function of Time, during Final Consolidation - Logarithm of Time.

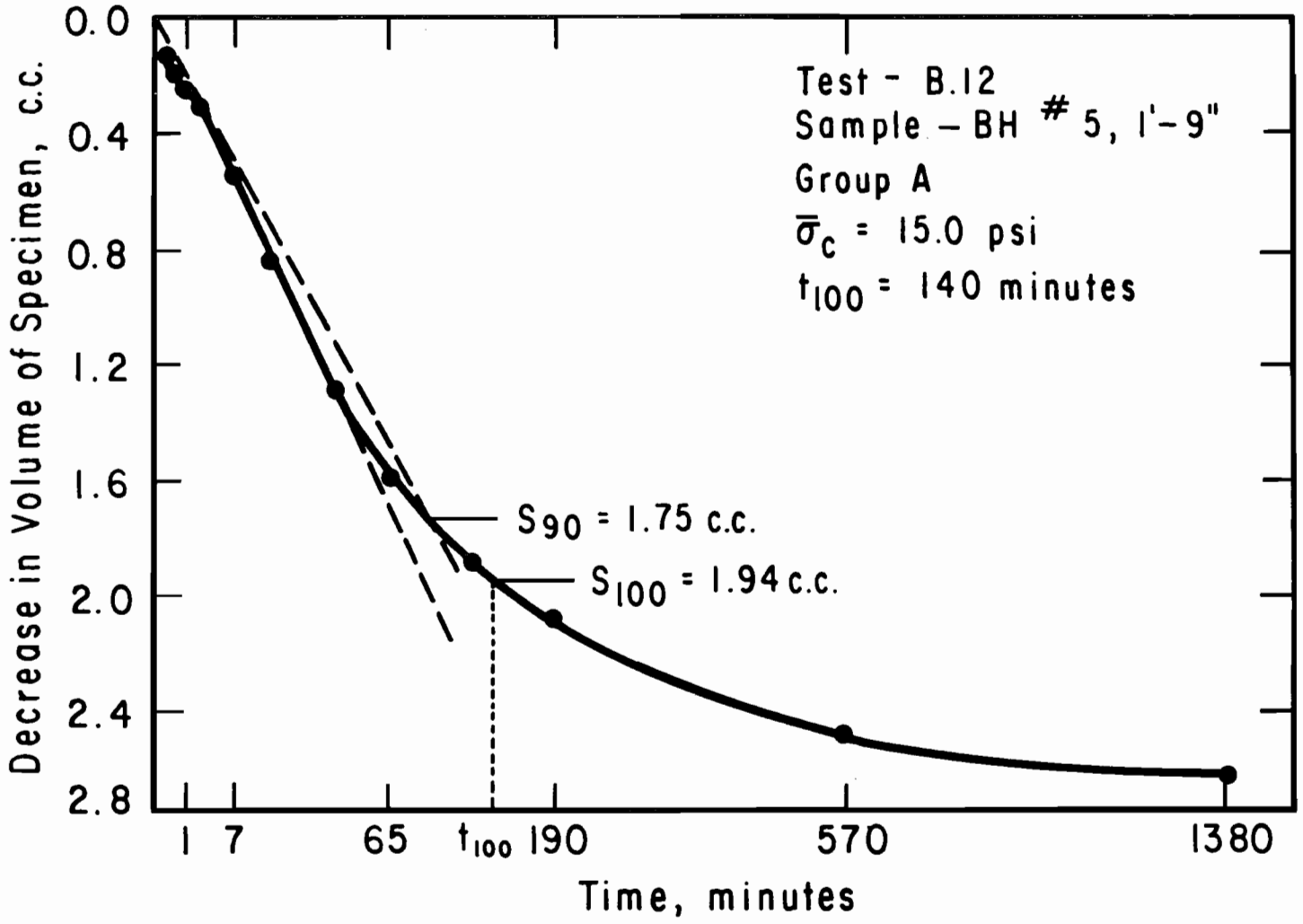

Figure A.4.6. Decrease in Pore Water Volume of Specimen in Test B.12 as a Function of Time, during Final Consolidation - Square Root of Time.

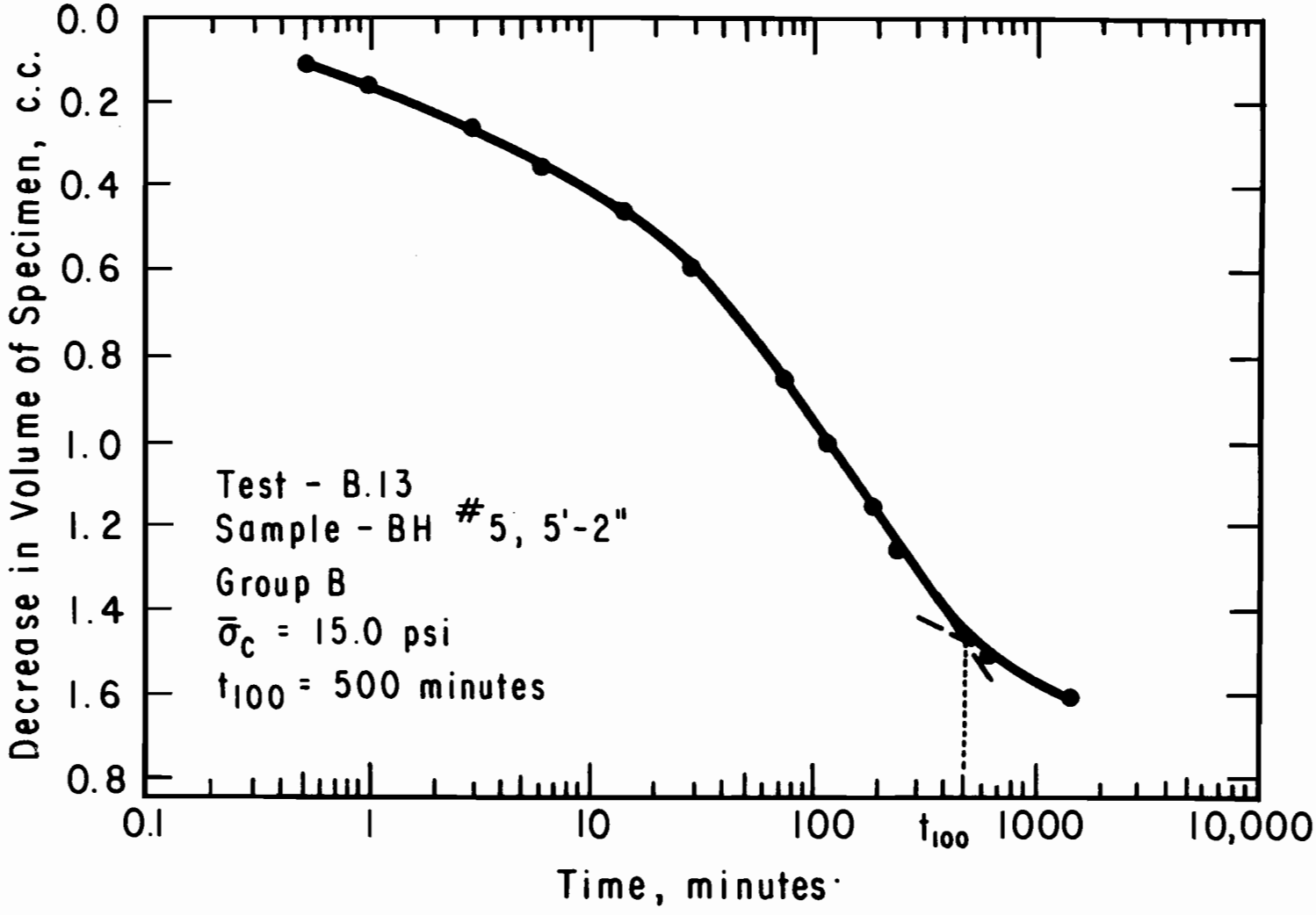

Figure A.4.7. Decrease in Pore Water Volume of Specimen in Test B.13 as a Function of Time, during Final Consolidation - Logarithm of Time.

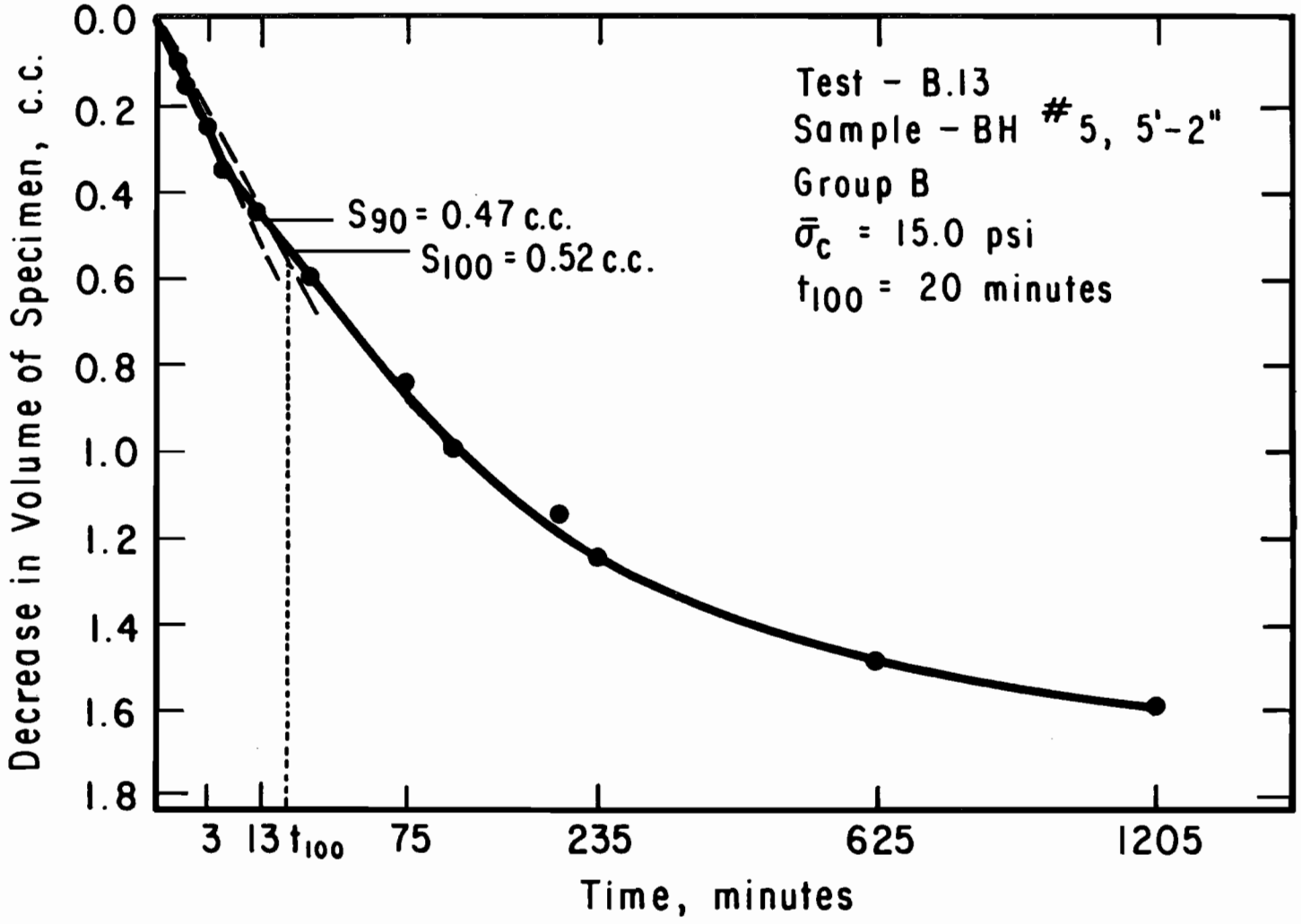

Figure A.4.8. Decrease in Pore Water Volume of Specimen in Test B.13 as a Function of Time, during Final Consolidation - Square Root of Time.

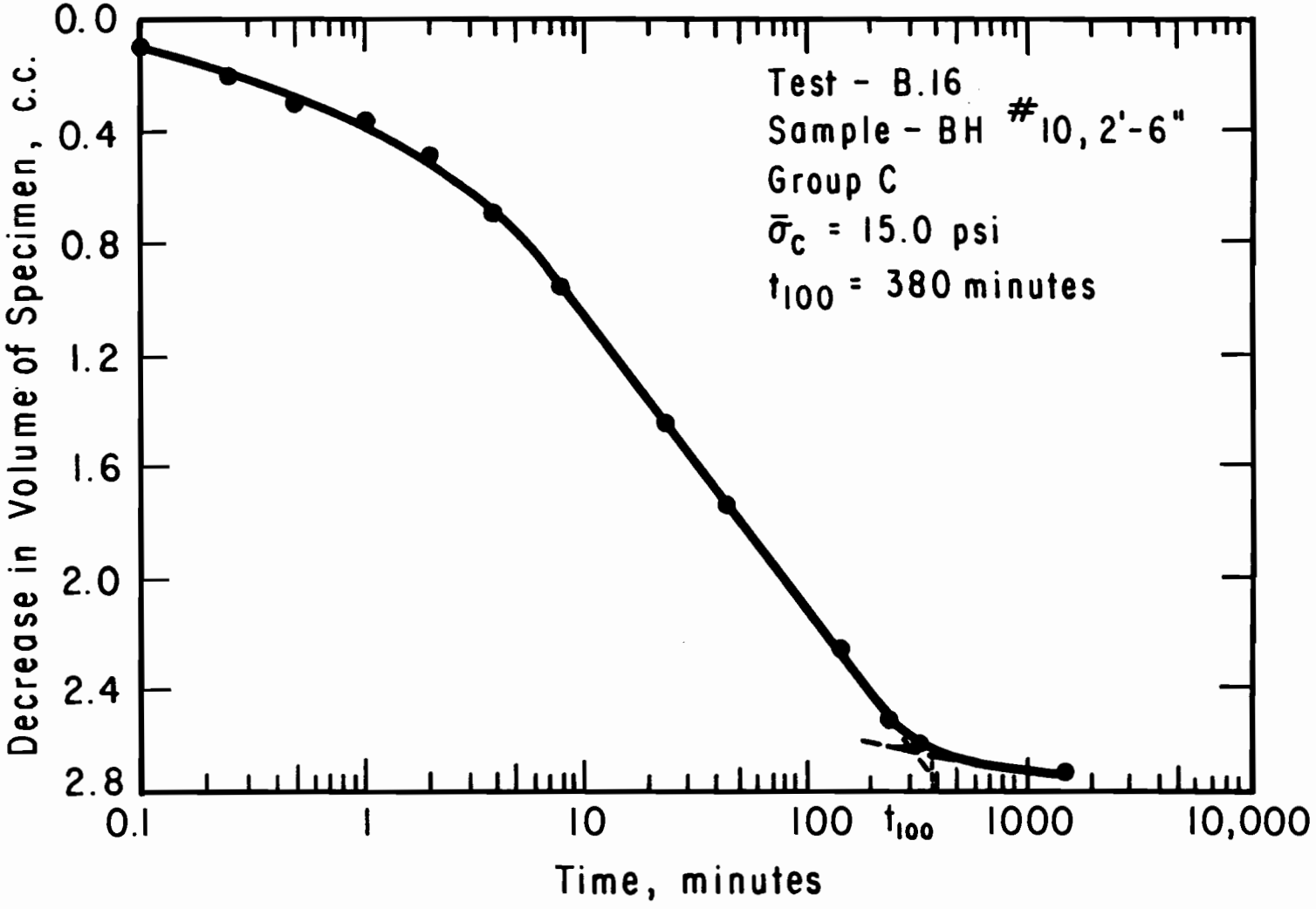

Figure A.4.9. Decrease in Pore Water Volume of Specimen in Test B.16 as a Function of Time, during Final Consolidation - Logarithm of Time.

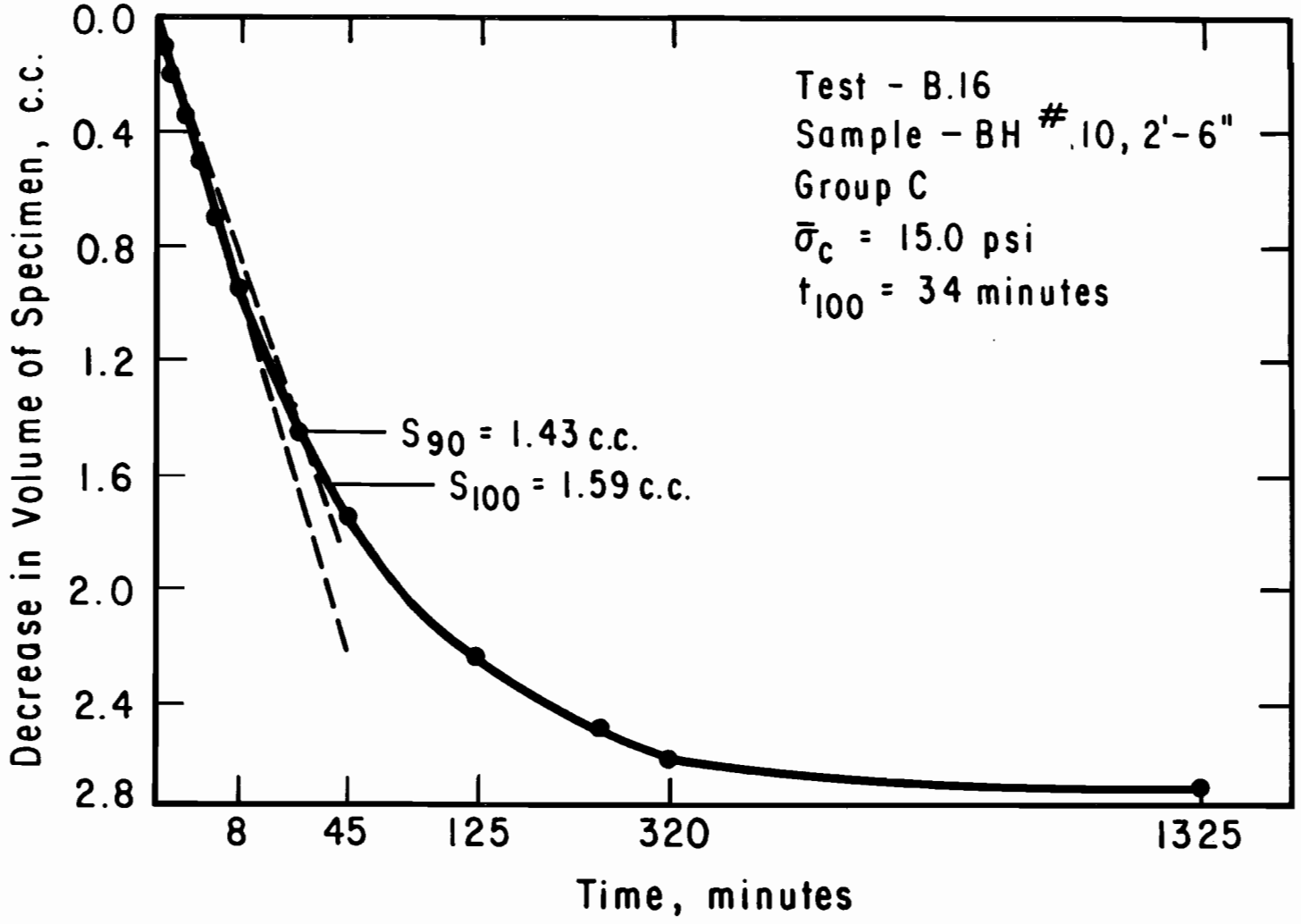

Figure A.4.10. Decrease in Pore Water Volume of Specimen in Test B.16 as a Function of Time, during Final Consolidation - Square Root of Time.

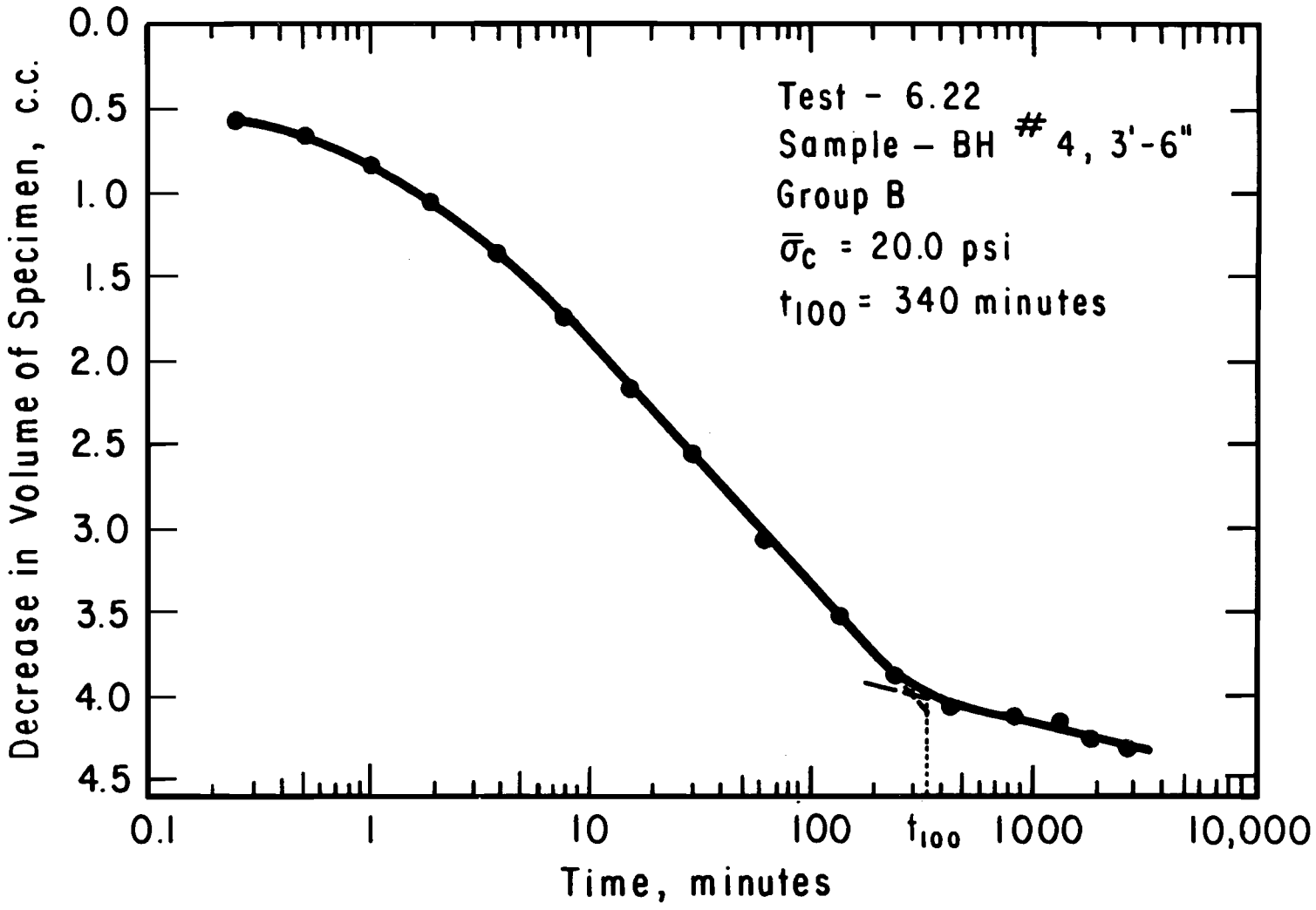

Figure A.4.11. Decrease in Pore Water Volume of Specimen in Test 6.22 as a Function of Time, during Final Consolidation - Logarithm of Time.

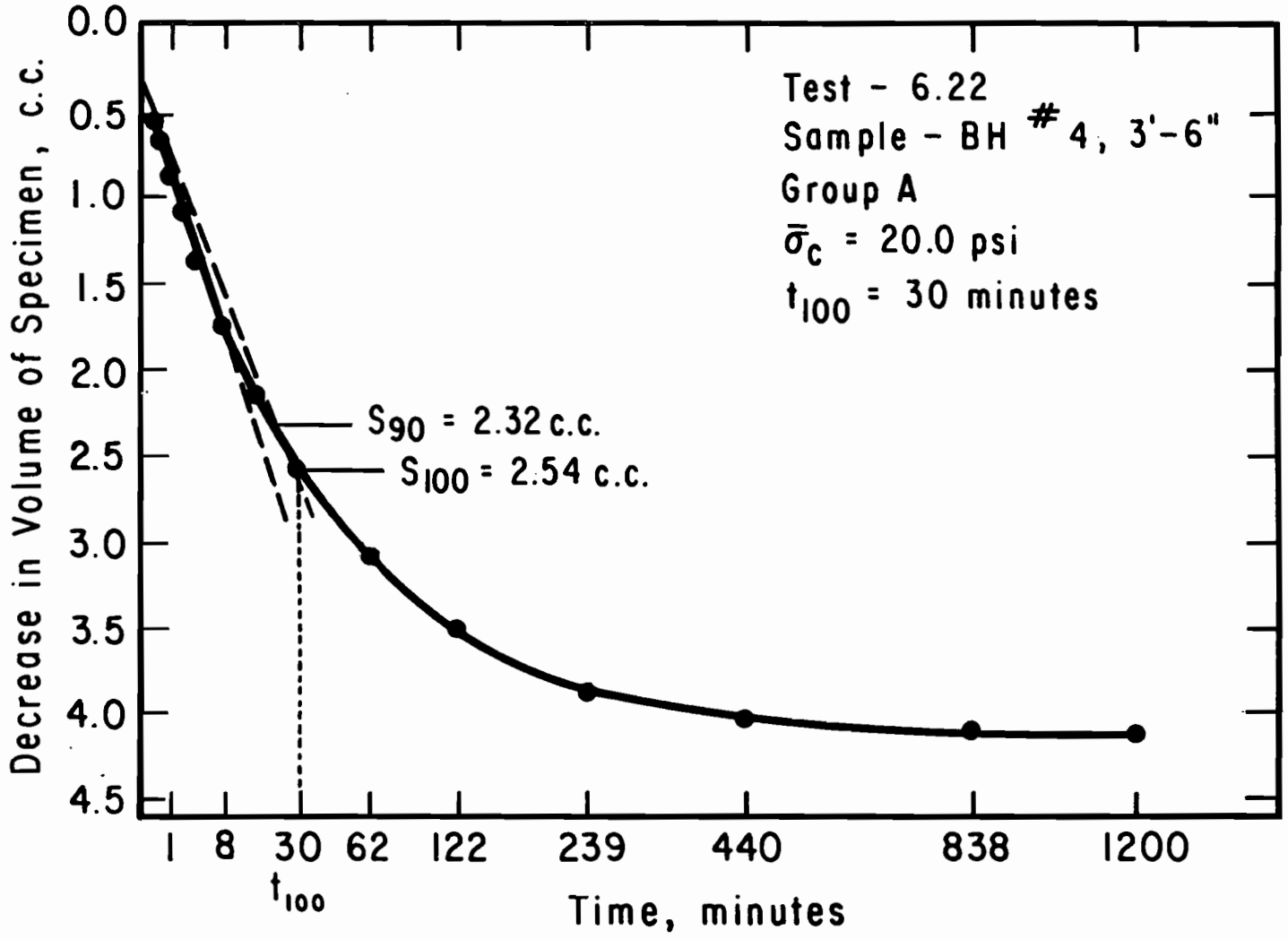

Figure A.4.12. Decrease in Pore Water Volume of Specimen in Test 6.22 as a Function of Time, during Final Consolidation - Square Root of Time.

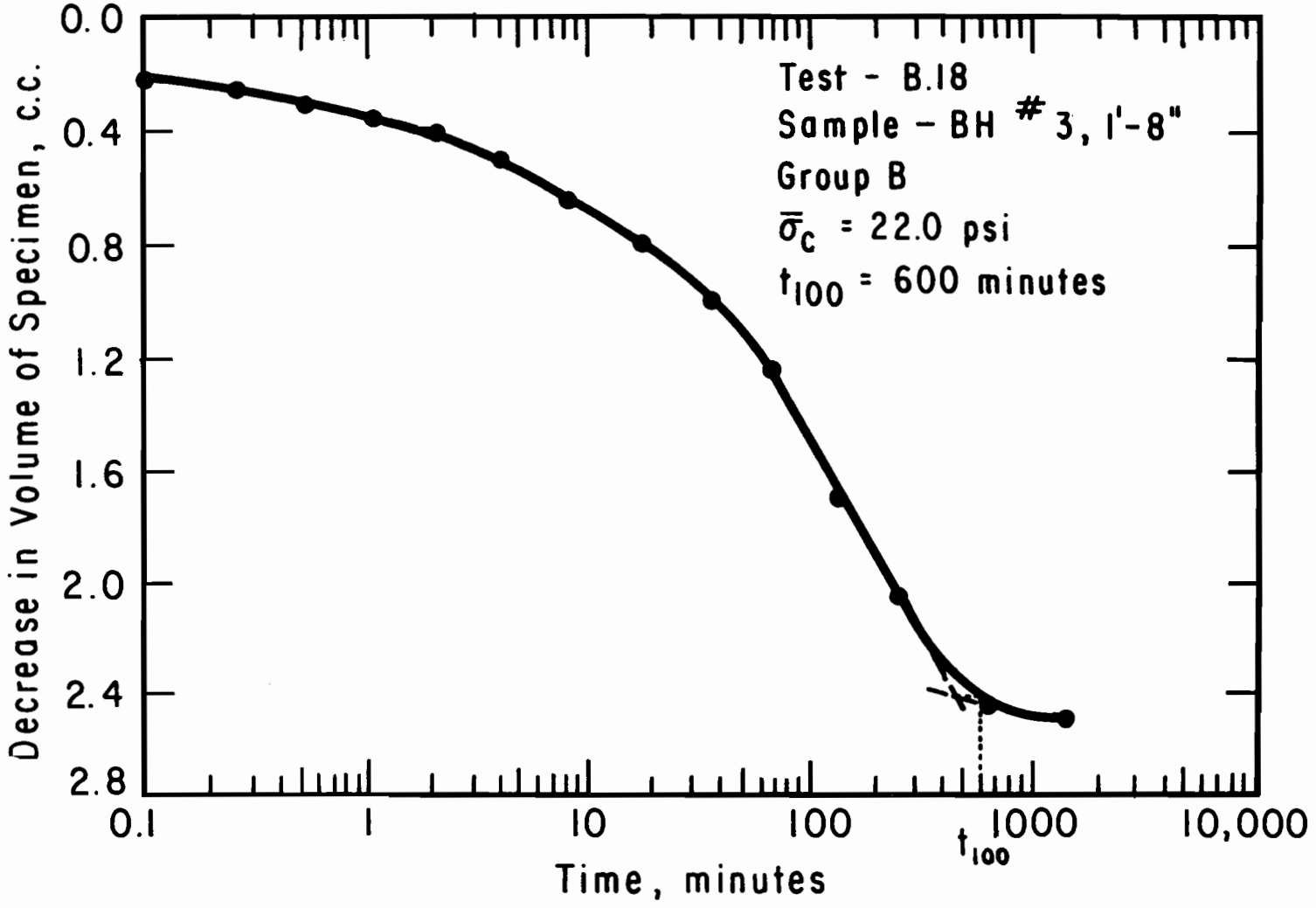

Figure A.4.13. Decrease in Pore Water Volume of Specimen in Test B.18 as a Function of Time, during Final Consolidation - Logarithm of Time.

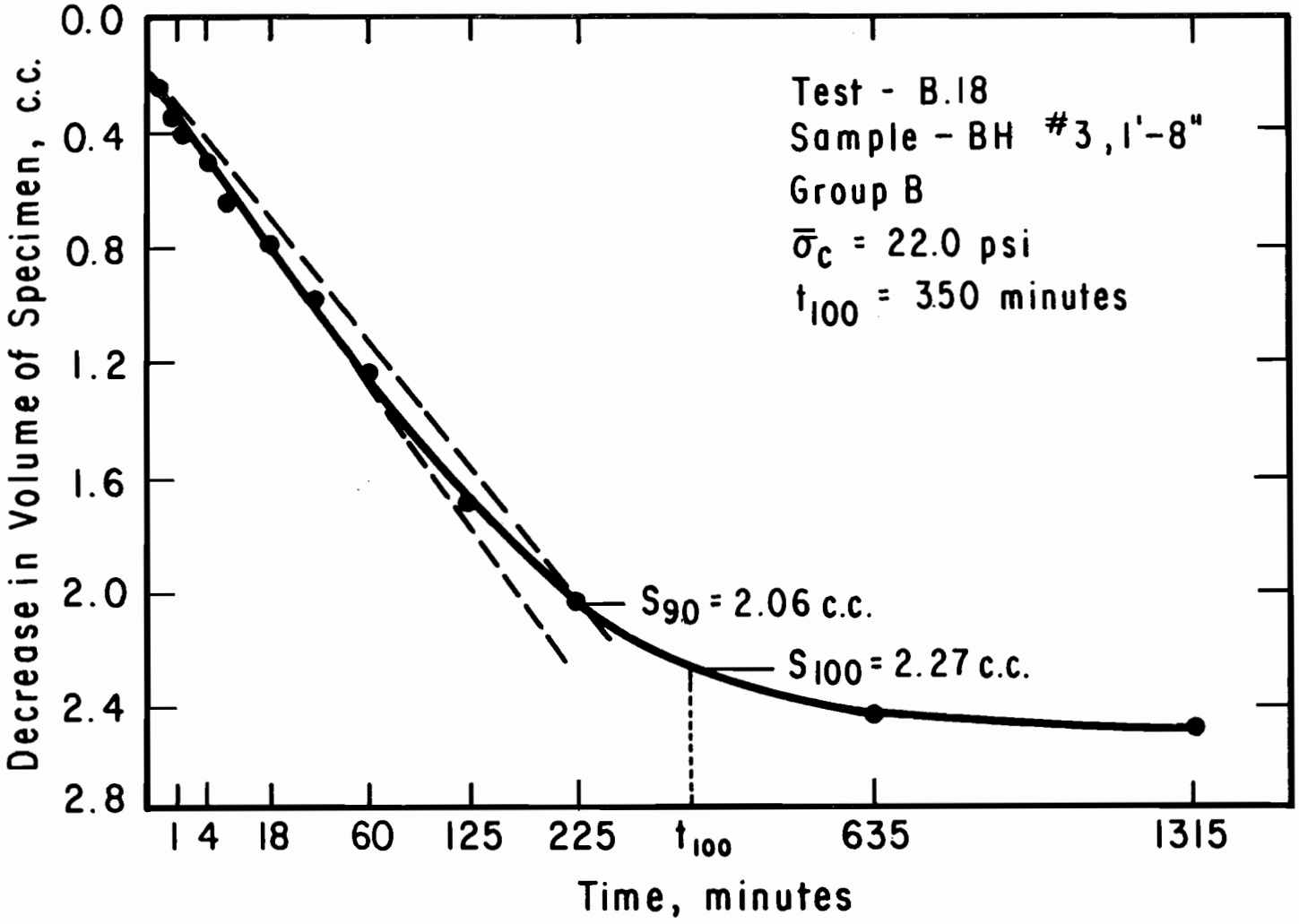

Figure A.4.14. Decrease in Pore Water Volume of Specimen in Test B.18 as a Function of Time, during Final Consolidation - Square Root of Time.

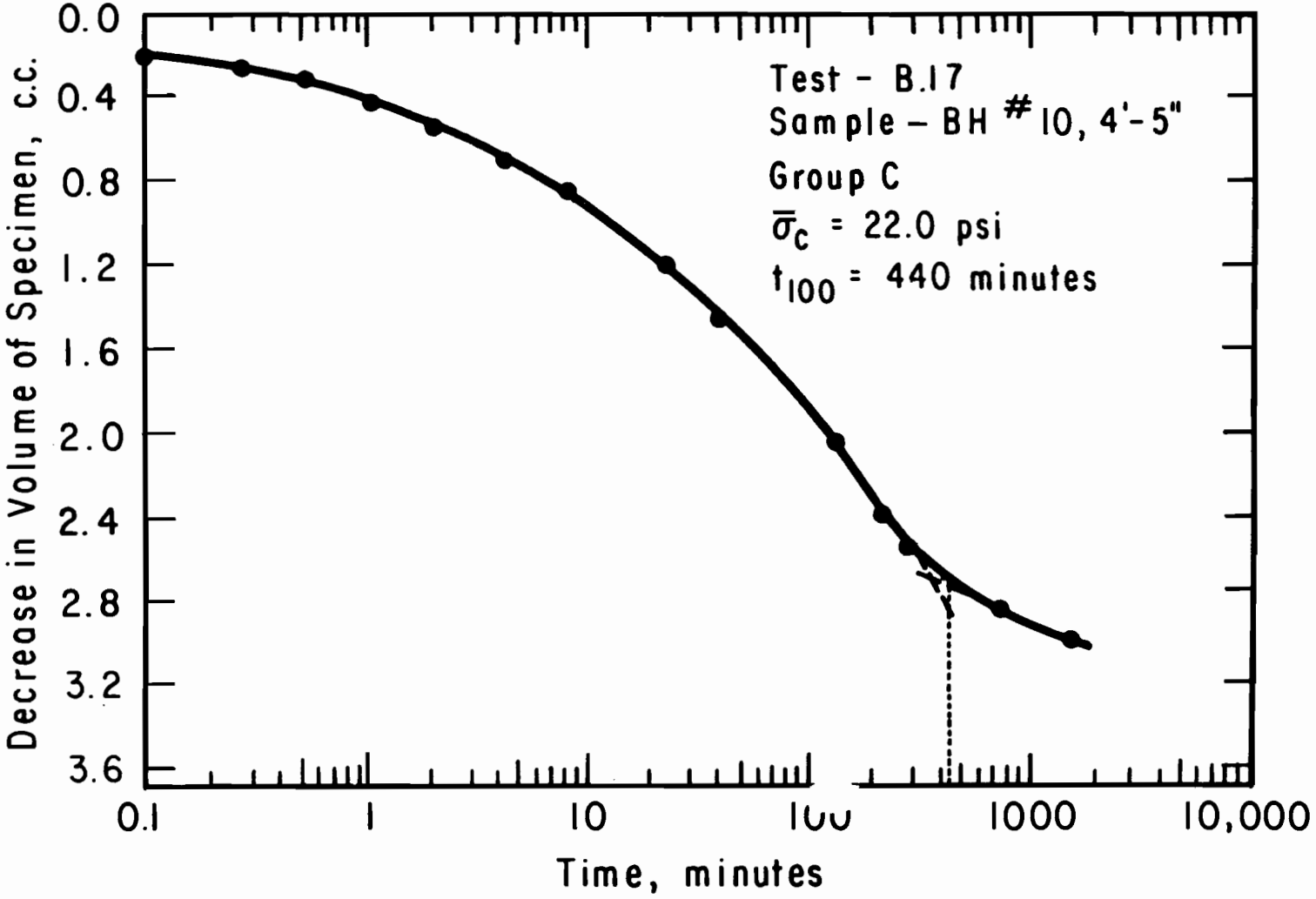

Figure A.4.15. Decrease in Pore Water Volume of Specimen in Test B.17 as a Function of Time, during Final Consolidation - Logarithm of Time.

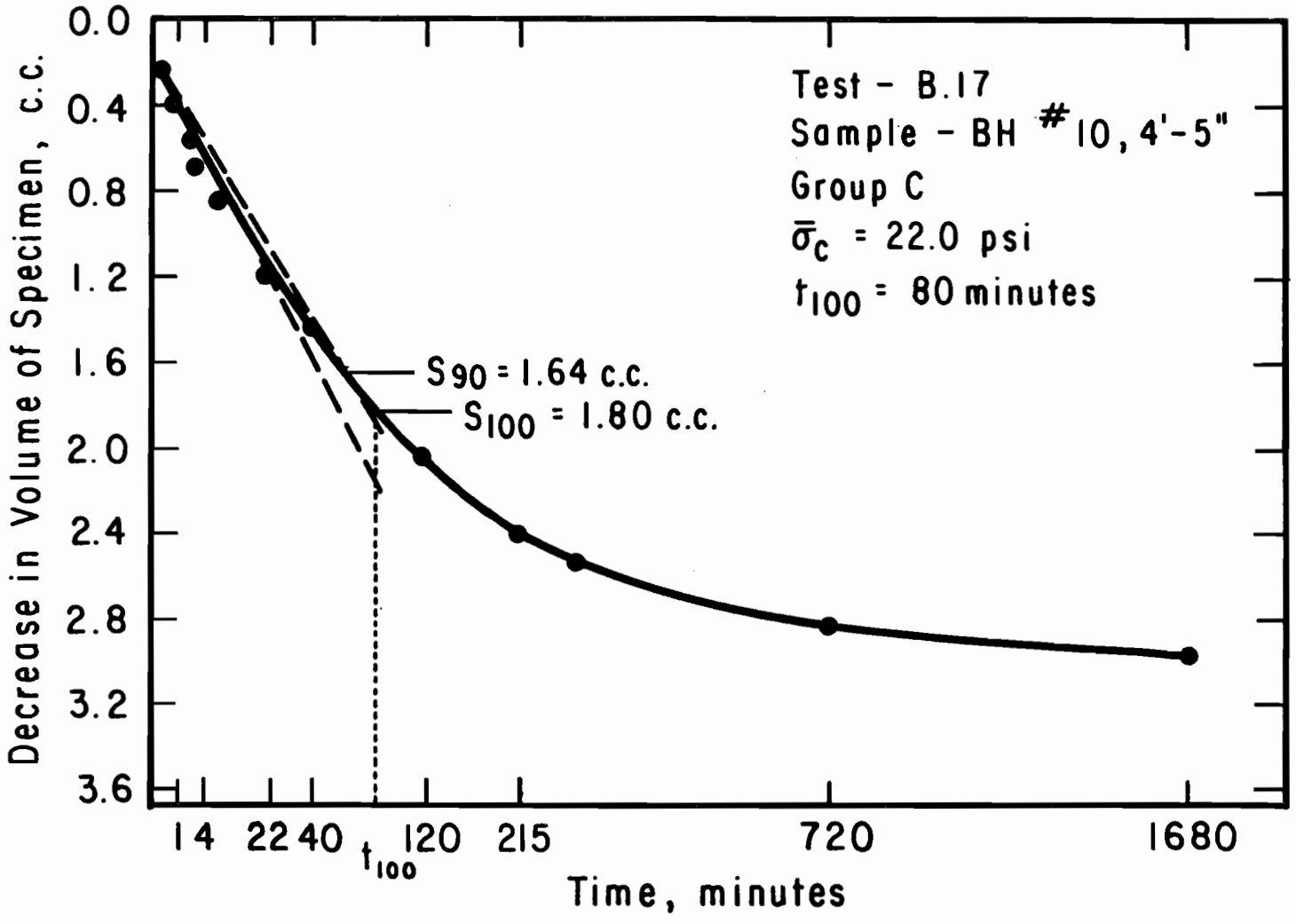

Figure A.4.16 Decrease in Pore Water Volume of Specimen in Test B.17 as a Function of Time, during Final Consolidation - Square Root of Time.

APPENDIX B

Appendix B contains the uncorrected summary plots of stress versus strain, over the full range of strains and over the first 1.5 percent of strain, for all the triaxial tests performed in this phase of testing. These include the tests on the specimens consolidated from a slurry, the specimens prepared by packing, and the undisturbed specimens.

Summary plots are included for:

1. The specimens consolidated from a slurry (Tests 6.12, 6.15, 6.11, 6.27, and 6.10).

2. The specimens prepared by packing (Tests 6.13, B.8, B.10, and B.9).

3. The undisturbed specimens of grey clay from outside of the slide, Group A (Tests 6.20, 6.14, B.11, 6.25, B.12, 6.22, and 6.24).

4. The undisturbed specimens of red clay from outside of the slide, Group B (Tests 6.26, 6.16, 6.23, B.14, B.13, and B.18).

5. The undisturbed specimens of red clay from within the slide, Group C (Tests 6.19, 6.18, 6.17, 6.21, B.15, B.16, and B.17).

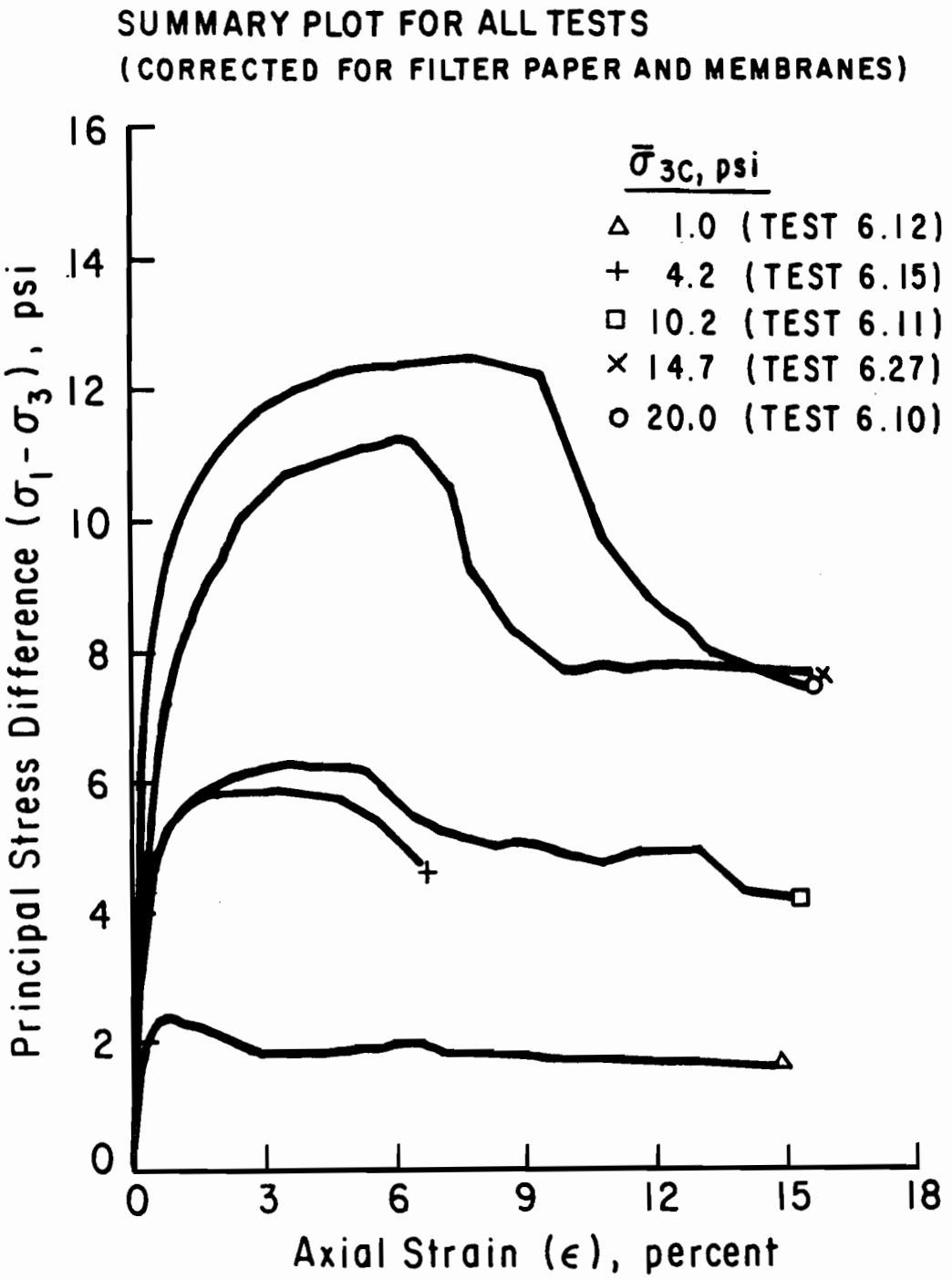

Figure B.1.1. Uncorrected Summary Plot of Principal Stress Difference versus Axial Strain for Specimens Consolidated from a Slurry.

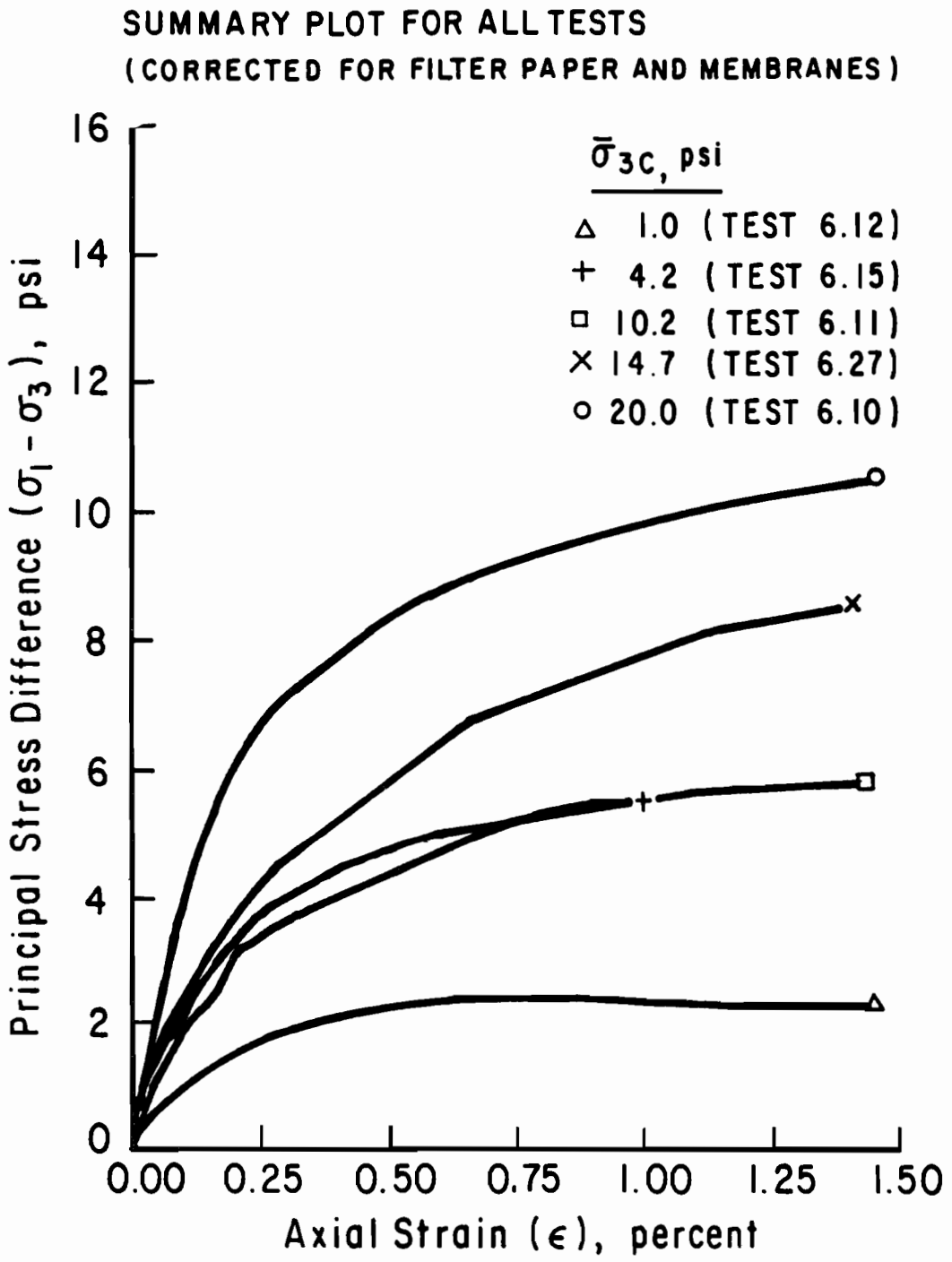

Figure B.1.2. Uncorrected Summary Plot of Principal Stress Difference versus Axial Strain for Specimens Conslidated from a Slurry(Low Strains).

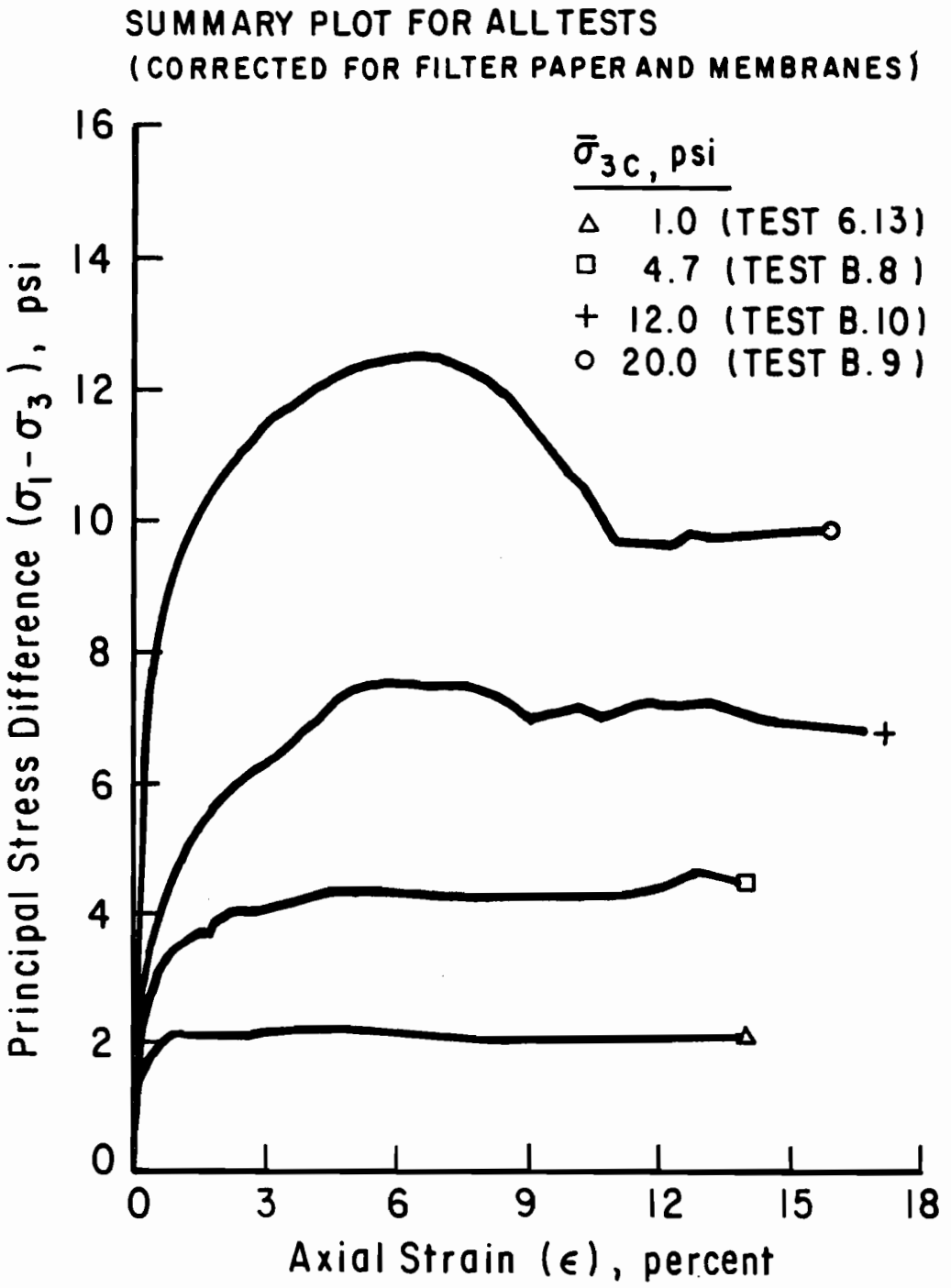

Figure B.2.1. Uncorrected Summary Plot of Principal Stress Difference versus Axial Strain for Specimens Prepared by Packing.

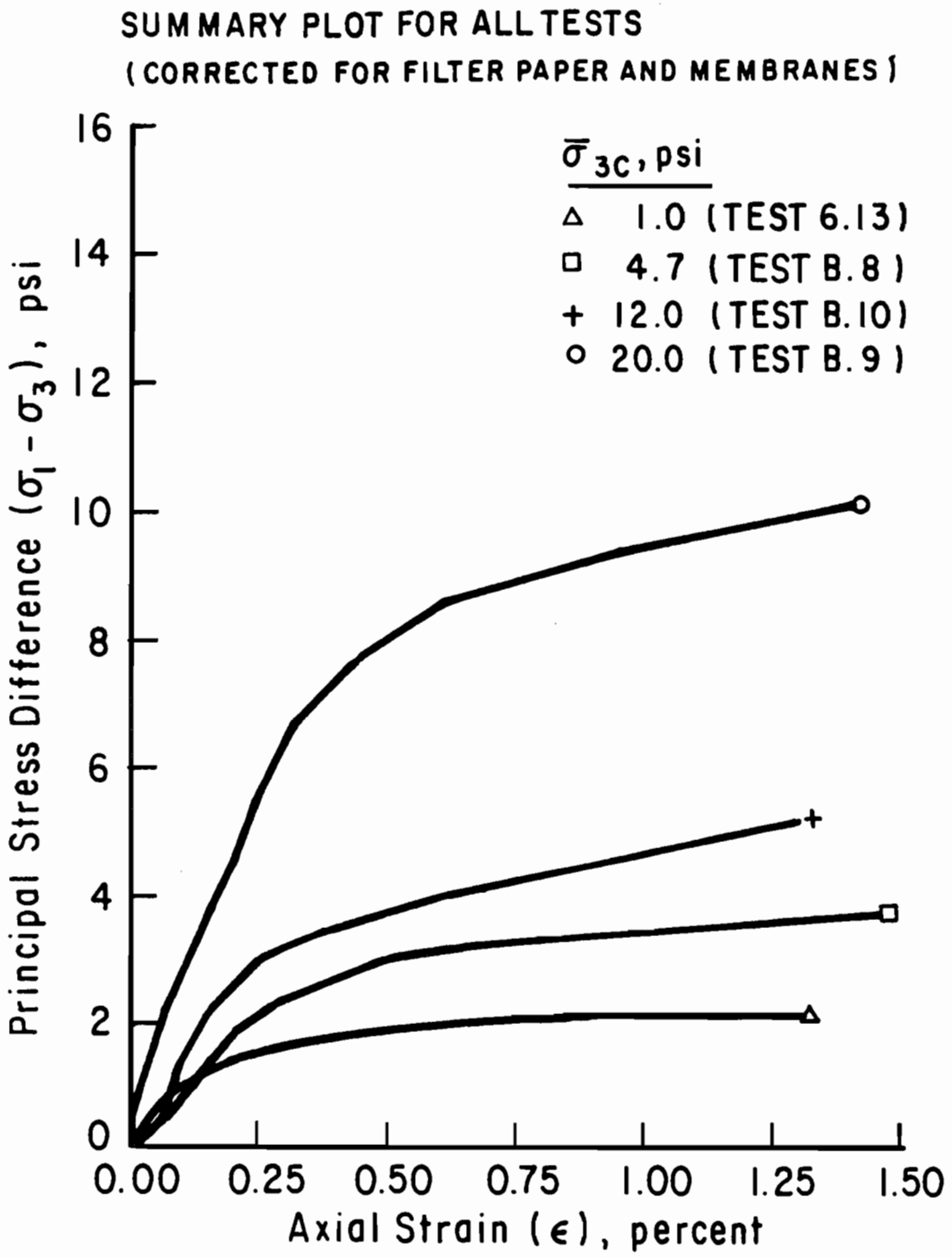

Figure B.2.2. Uncorrected Summary Plot of Principal Stress Difference versus Axial Strain for Specimens Prepared by Packing (Low Strains).

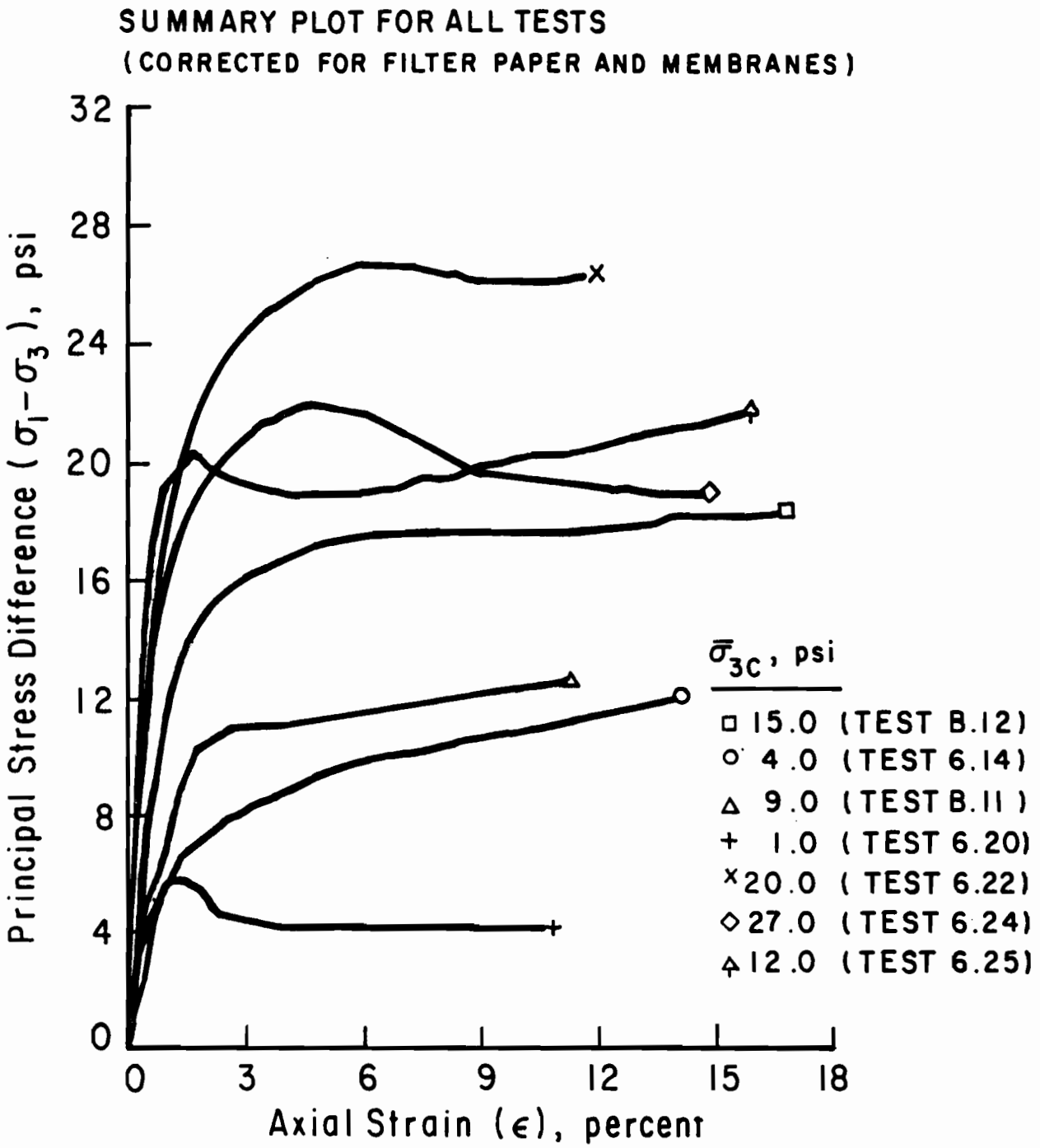

Figure B.3.1. Uncorrected Summary Plot of Principal Stress Difference versus Axial Strain for Undisturbed Grey Clay Specimens from Outisde the Slide Area.

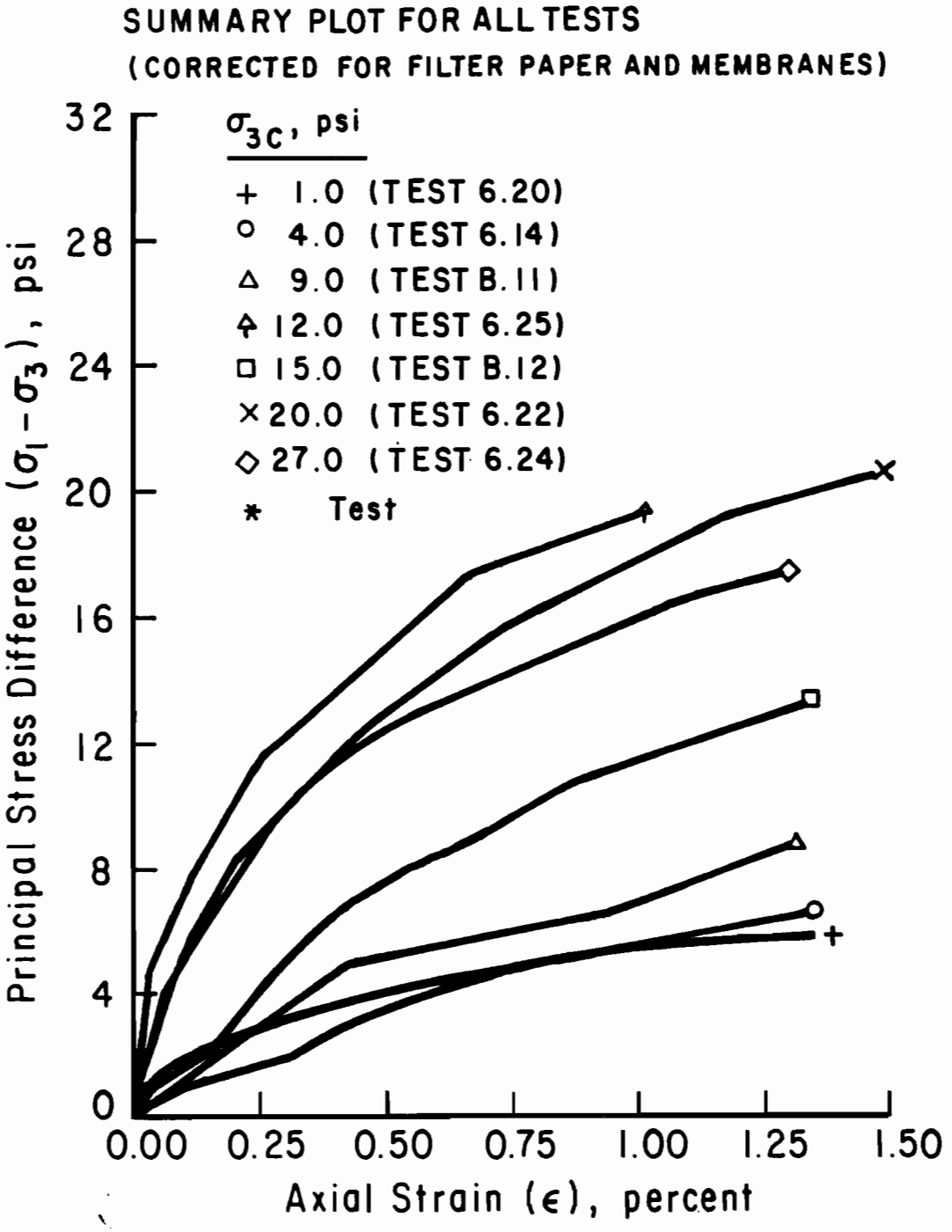

Figure B.3.2. Uncorrected Summary Plot of Principal Stress Difference versus Axial Strain for Undisturbed Grey Clay Specimens from Outside the Slide Area (Low Strains).

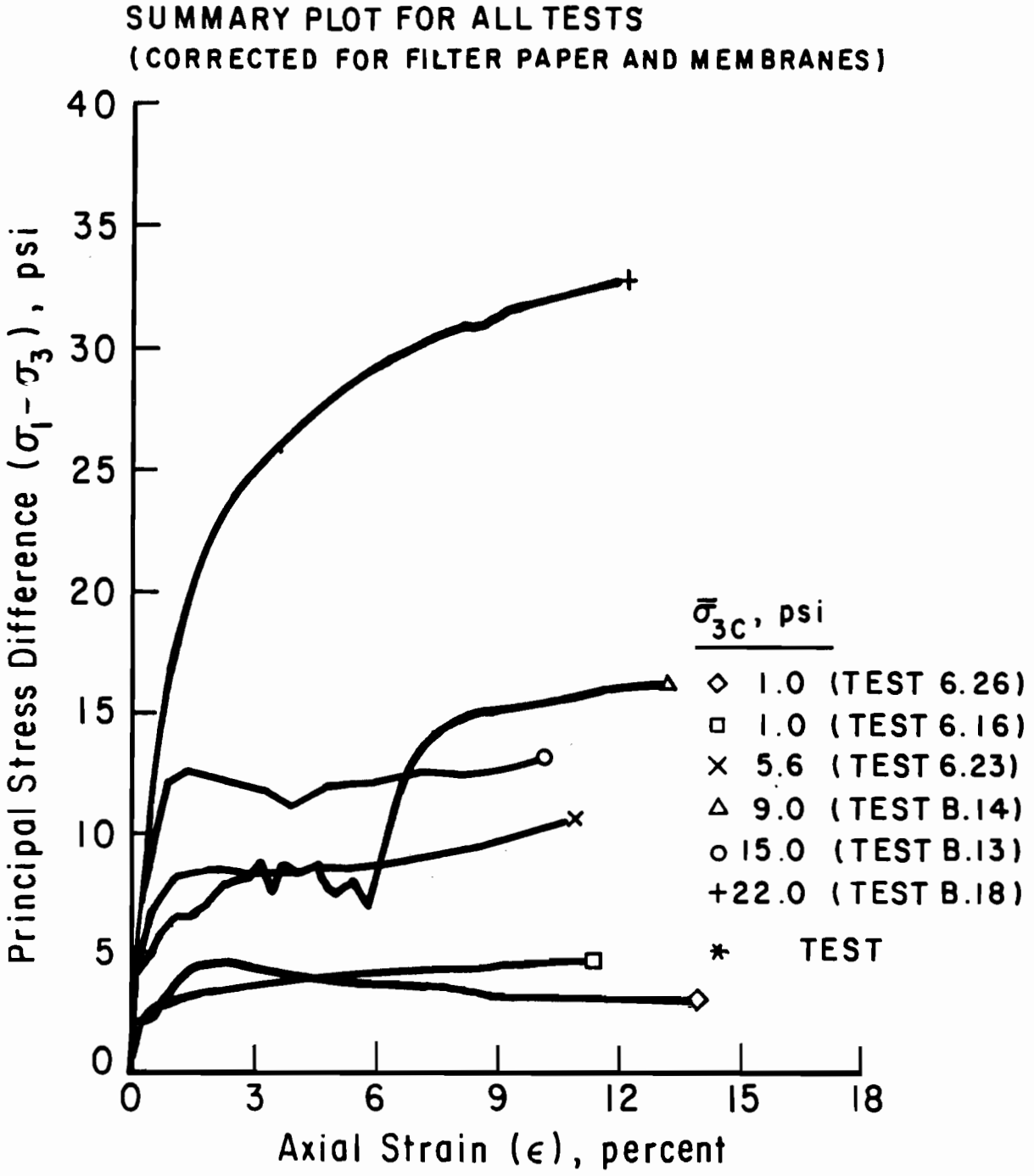

Figure B.4.1. Uncorrected Summary Plot of Principal Stress Difference versus Axial Strain for Undisturbed Red Clay Specimens from Outside the Slide Area.

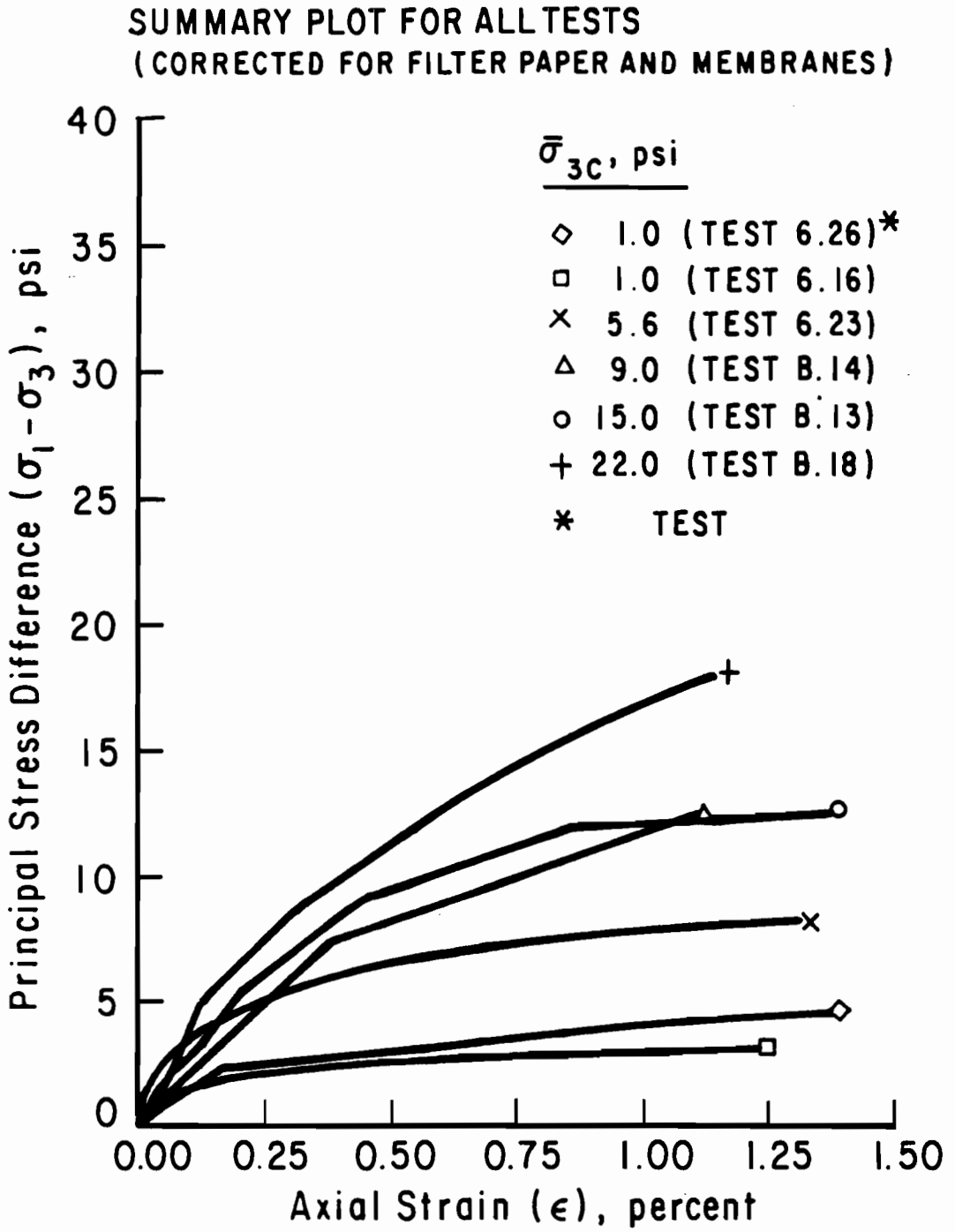

Figure B.4.2. Uncorrected Summary Plot of Principal Stress Difference versus Axial Strain for Undisturbed Red Clay Specimens from Outisde the Slide Area (Low Strains).

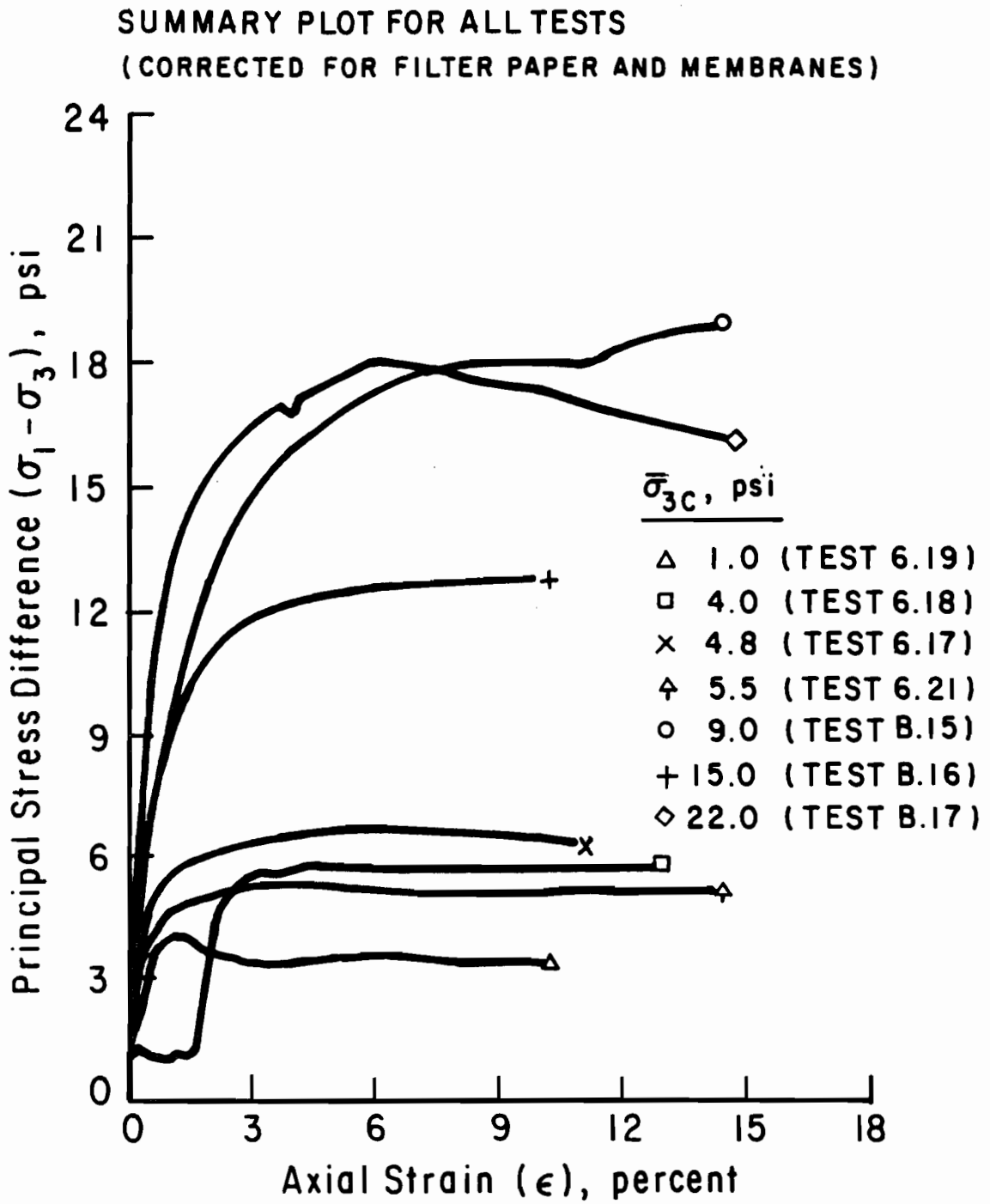

Figure B.5.1. Uncorrected Summary Plot of Principal Stress Difference versus Axial Strain for Undisturbed Red Clay Specimens from Within the Slide Area.

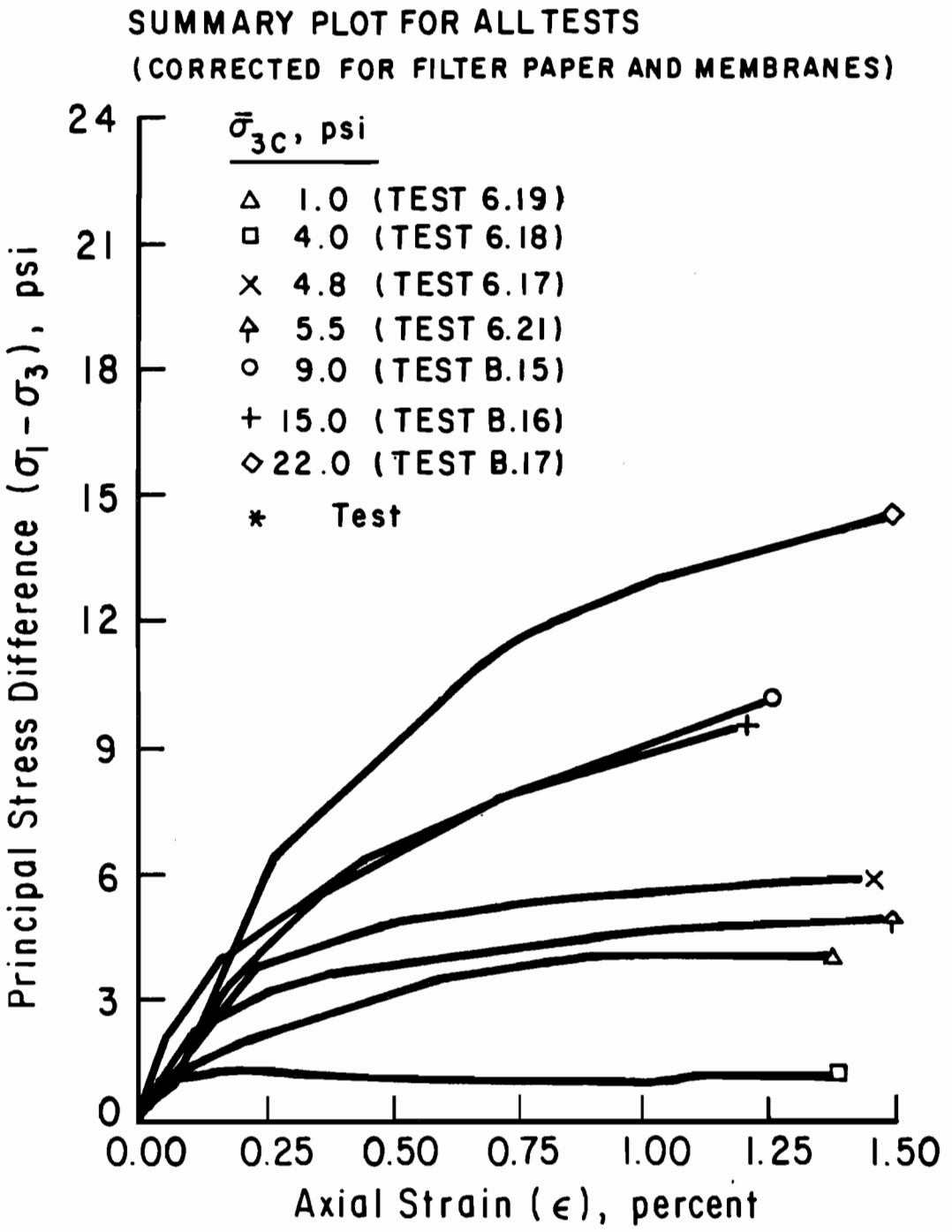

Figure B.5.2. Uncorrected Summary Plot of Principal Stress Difference versus Axial Strain for Undisturbed Red Clay Specimens from Within the Slide Area (Low Strains).

APPENDIX C. DERIVATION OF THE AREA CORRECTION FOR DIRECT SHEAR TESTS

The following derivation of the area correction for direct shear tests comes from the laboratory notes presented by Dr. D.E. Daniel to the CE 392L class, "Measurement of Soil Properties", at the University of Texas at Austin. The area correction is required because as the upper and lower halves of a direct shear specimen are displaced a change in the area of shear occurs. This change must be considered when the shear stress is calculated. The shearing area of a circular direct shear specimen at a given displacement, Δ, is shown in Figure C.1. One-half of this area is shown in Figure C.2, and is the area OABC minus the area OAC. These areas are given by the following equations where all angles are in units of degrees:

$$A_{OABC} = \frac{2 \times \alpha}{360} \times \pi \times R^2 \qquad (C.1)$$

$$A_{OAC} = \frac{1}{2} \times b \times h = R \times (\sin \alpha) \times (\frac{1}{2} \times \Delta) \qquad (C.2)$$

where the angle, α, is given by:

$$\alpha = \cos^{-1} (\frac{1}{2} \times \Delta/R) \qquad (C.3)$$

The total of area of of contact, A, shown in Figure C.1 is therefore:

$$A = 2 \times (A_{OABC} - A_{OAC}) = \frac{\alpha}{90} \times \pi R^2 - \Delta \times R \times \sin \alpha \qquad (C.4)$$

Noting that the original area, A_o, is given by:

$$A_o = \pi \times R^2 \qquad (C.5)$$

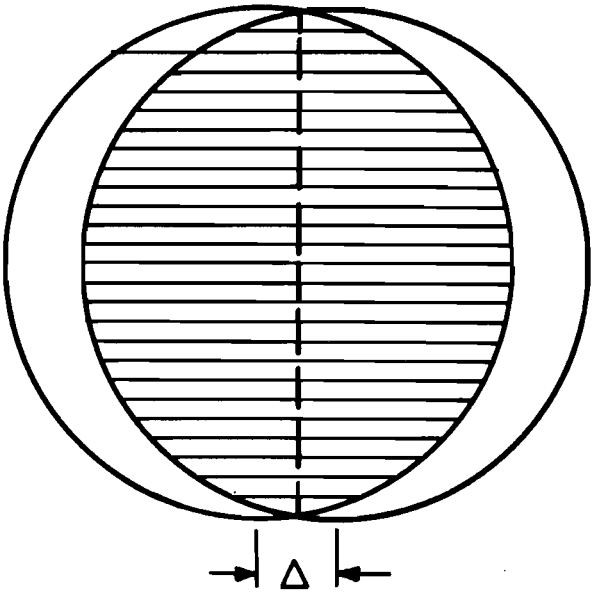

Figure C.1. Shearing Area of a Circular Direct Shear Specimen.

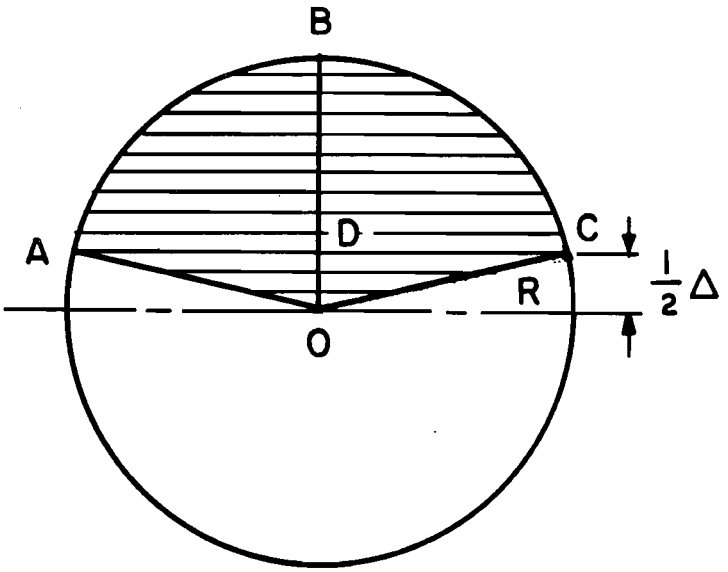

Figure C.2. Nomenclature Used to Calculate Shearing Area of a Circular Direct Shear Specimen.

and substituting Equations C.3 and C.5 into Equation C.4 yields the following equation:

$$A = \frac{1}{90} A_o \cos^{-1} \left(\frac{1}{2} \Delta/R\right) - \Delta R \sin \left[\cos^{-1} \left(\frac{1}{2} \Delta/R\right)\right] \qquad (C.6)$$

For a circular specimen with a diameter of 2.5 inches, as used in these tests, Equation C.6 may be simplified further to the form:

$$A = 0.0545 \cos^{-1} (\Delta/2.5) - 1.25 \Delta \sin \left[\cos^{-1} (\Delta/2.5)\right] \qquad (C.7)$$

where the displacement, Δ, is in inches and the shearing area, A, is in inches squared.

APPENDIX D

Appendix D contains the plots of shear stress versus cumumlative deformation not included in the main text for the direct shear tests (Tests DS-1, DS-2, DS-4, DS-5, DS-6, DS-7, DS-8, and DS-9).

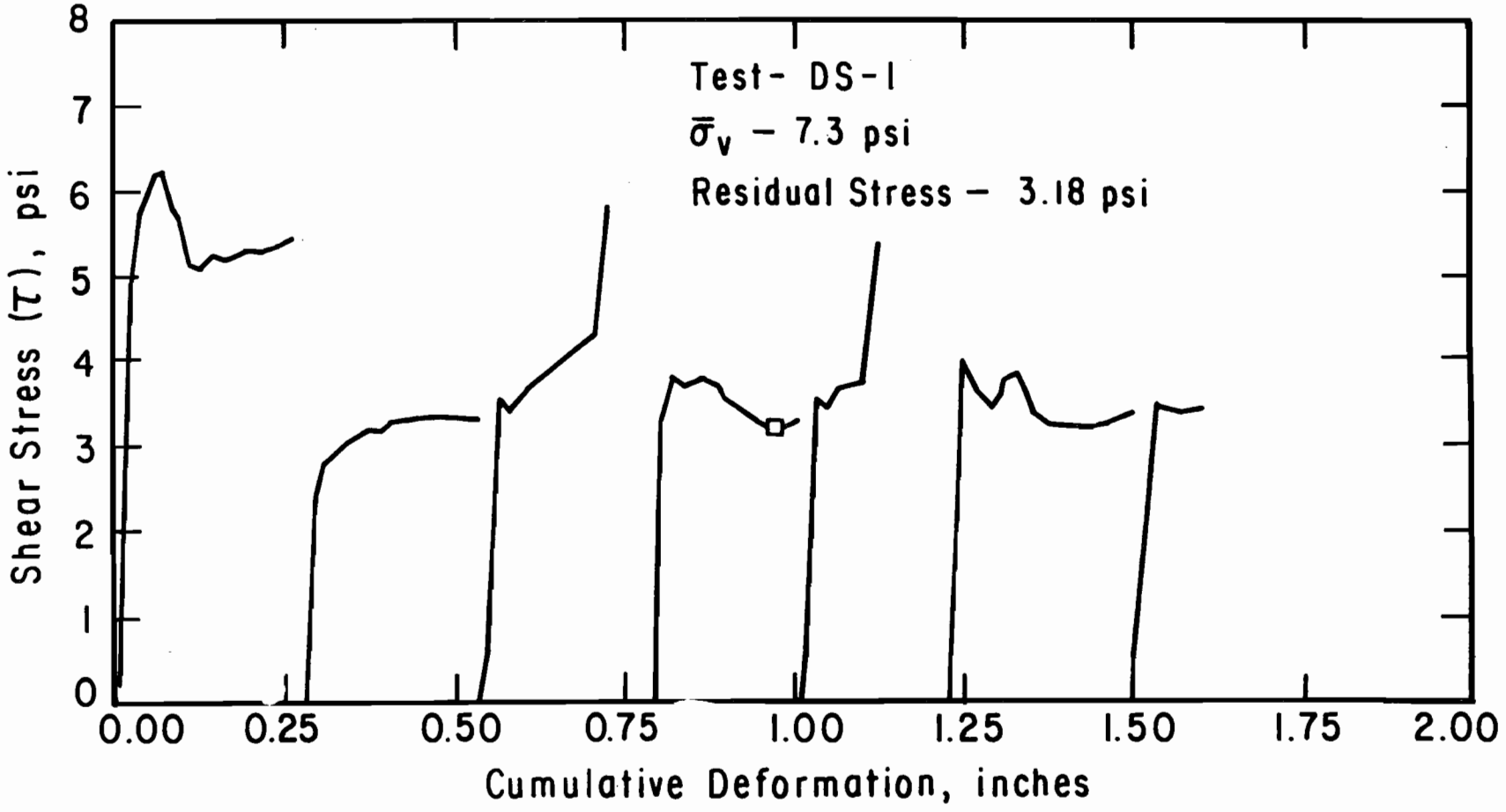

Figure D.1. Horizontal Shear Stress versus Cumulative Deformation for Direct Shear Test DS-1.

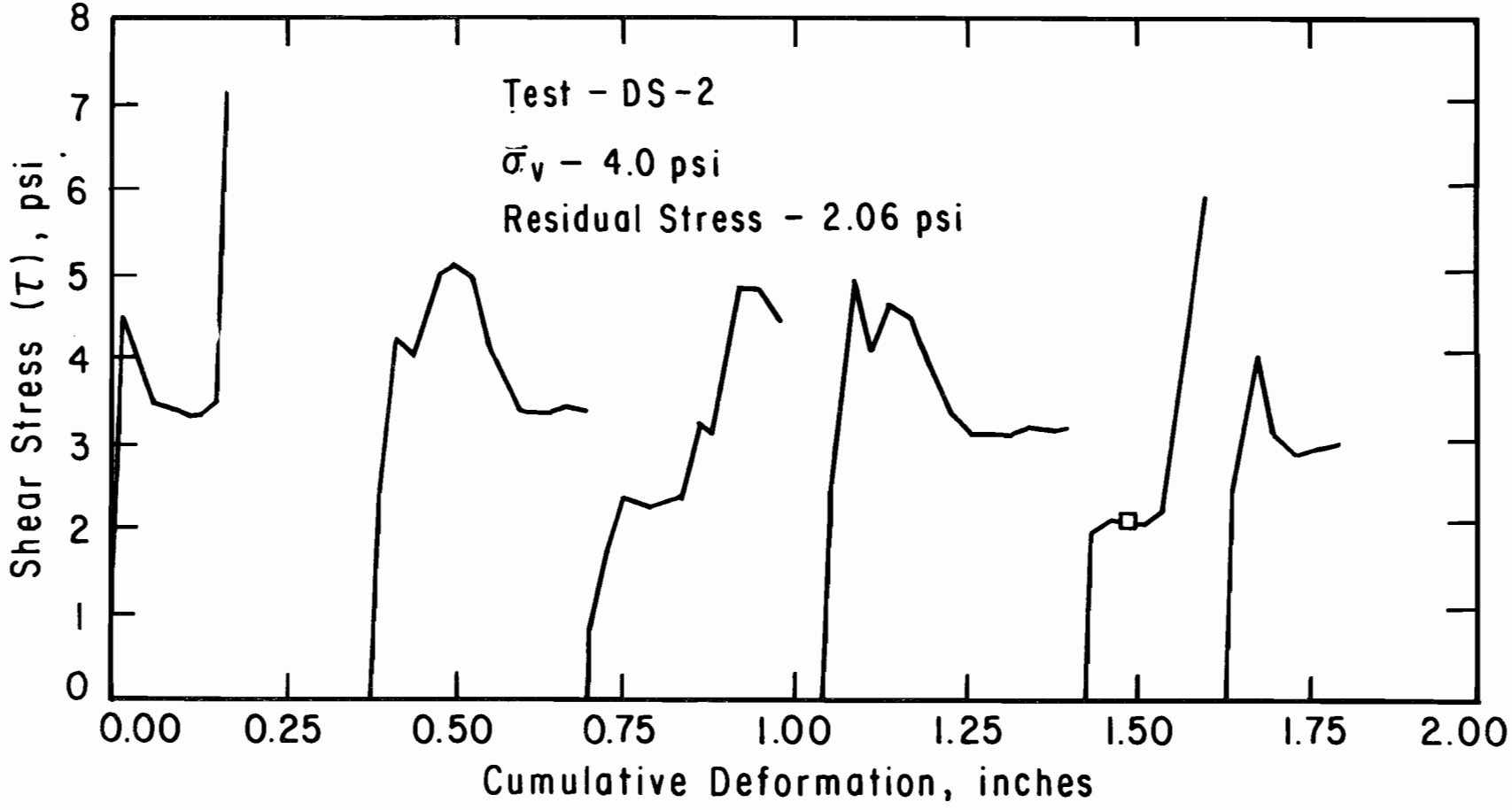

Figure D.2. Horizontal Shear Stress versus Cumulative Deformation for Direct Shear Test DS-2.

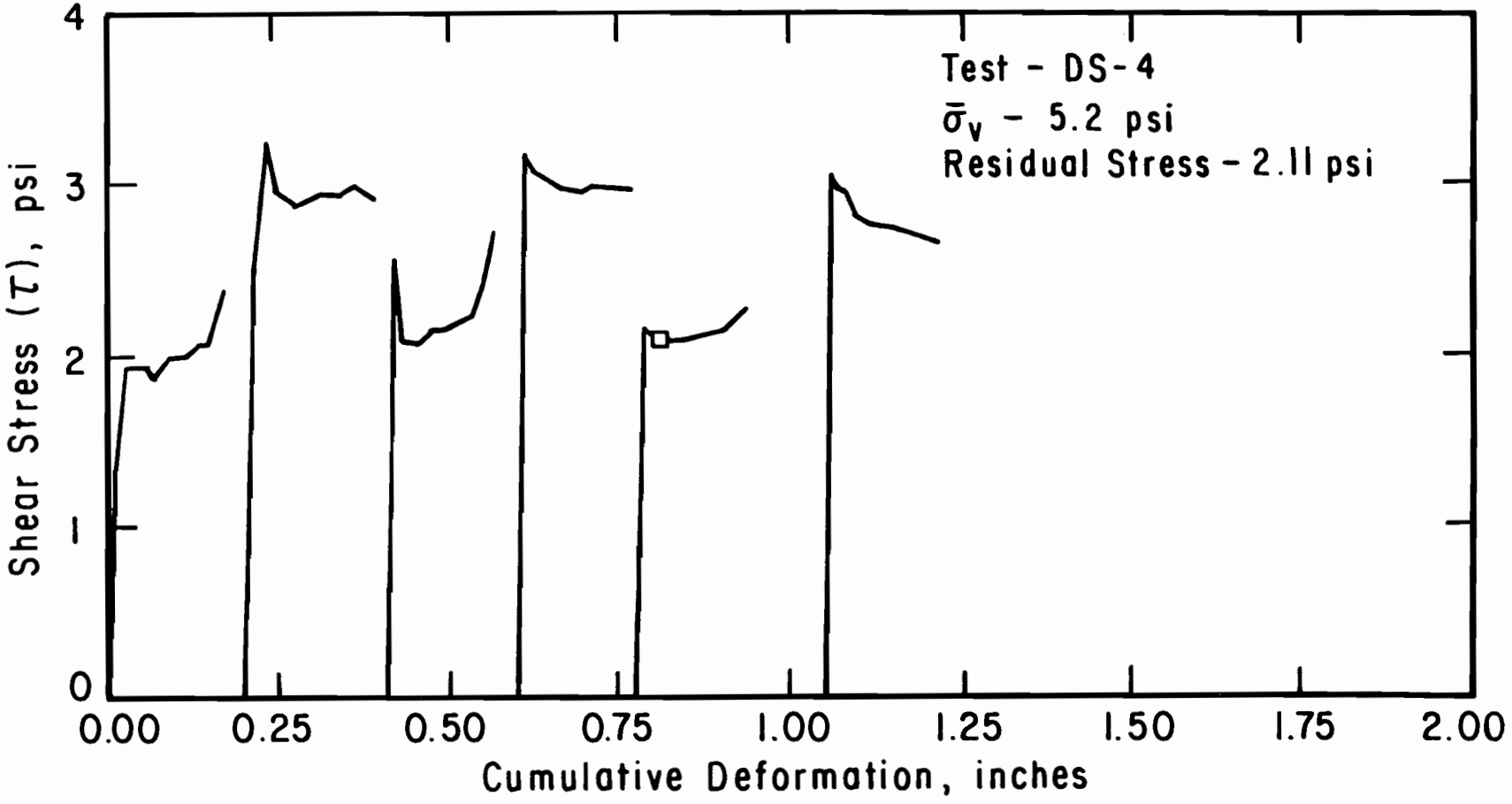

Figure D.3. Horizontal Shear Stress versus Cumulative Deformation for Direct Shear Test DS-4.

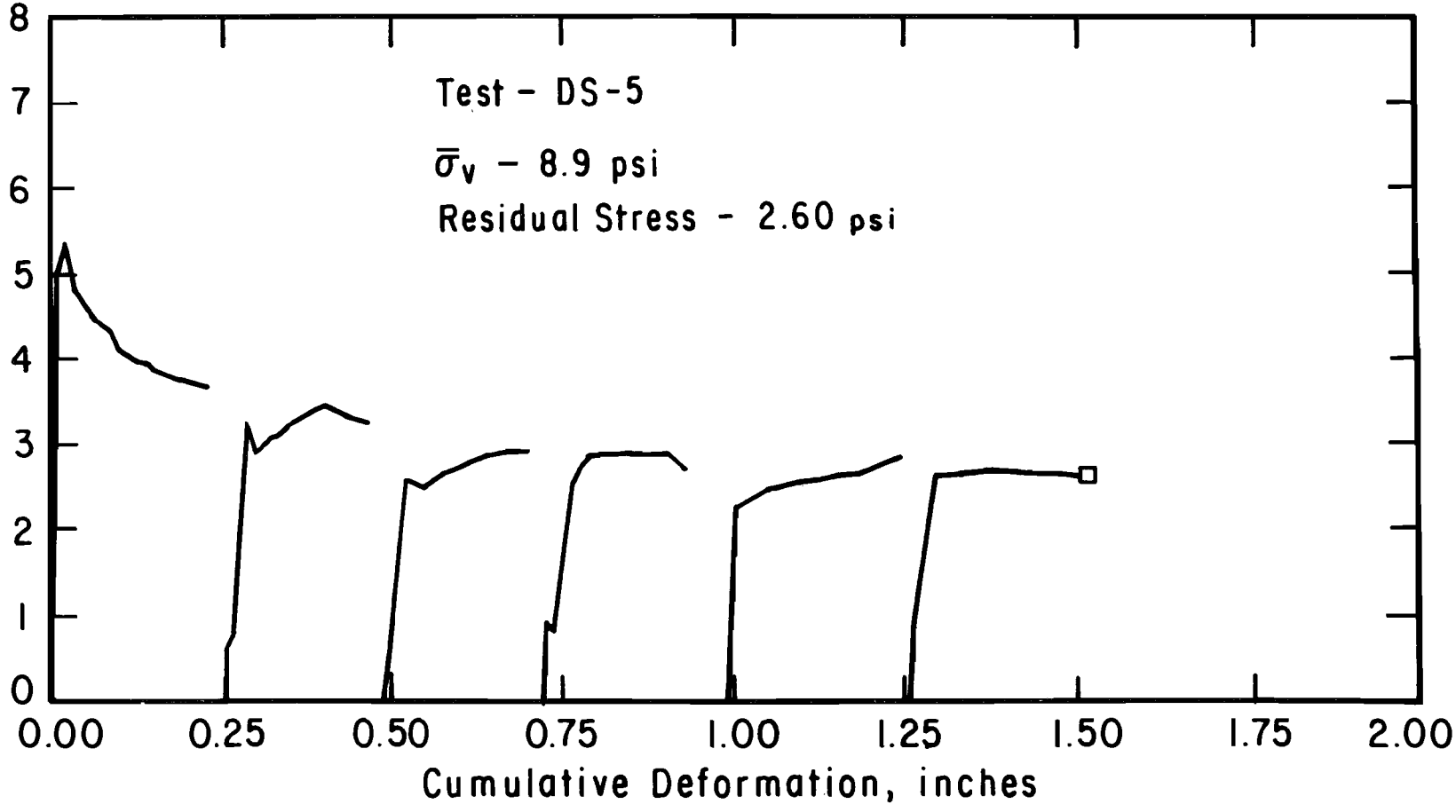

Figure D.4. Horizontal Shear Stress versus Cumulative Deformation for Direct Shear Test DS-5.

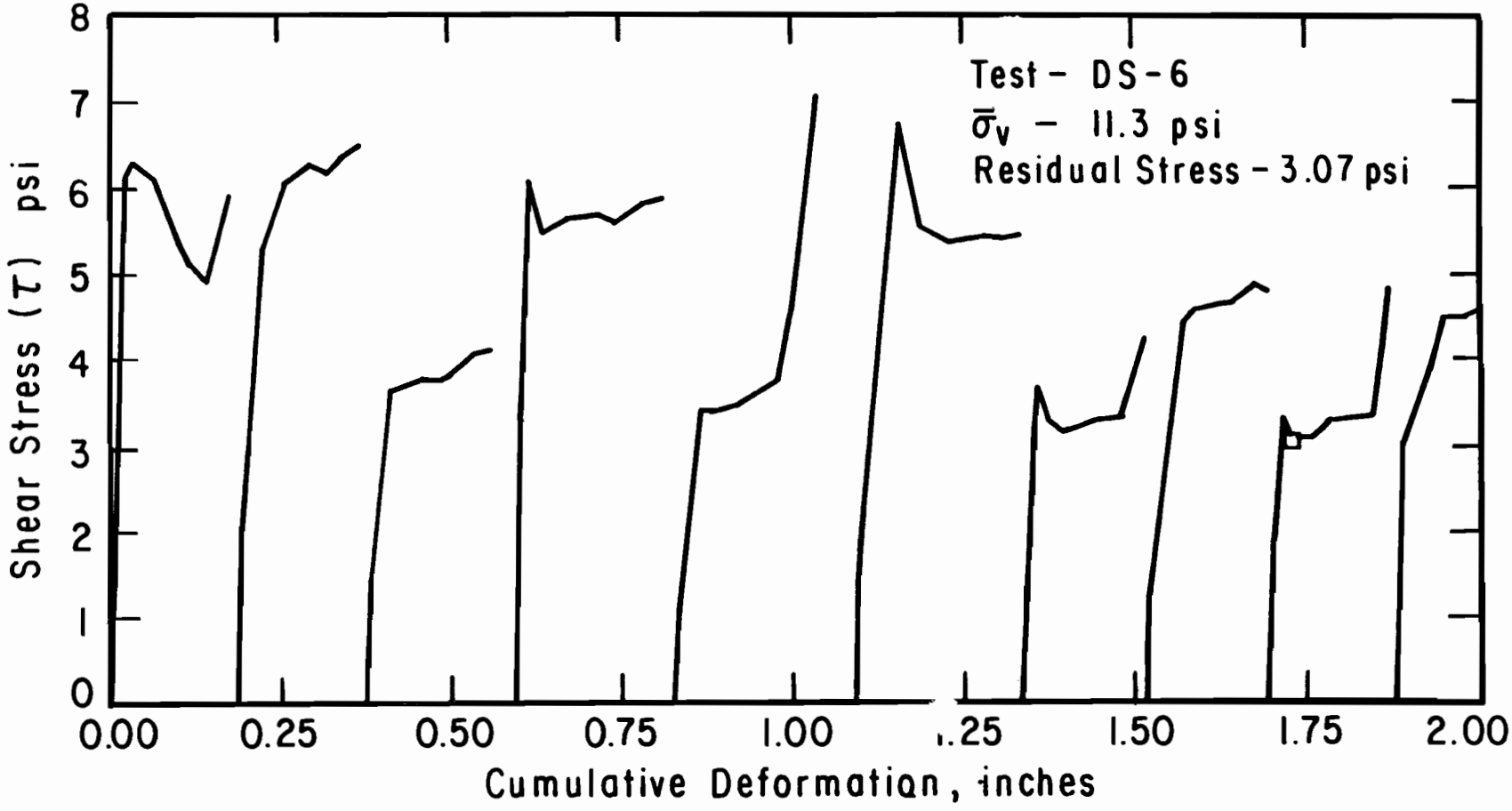

Figure D.5. Horizontal Shear Stress versus Cumulative Deformation for Direct Shear Test DS-6.

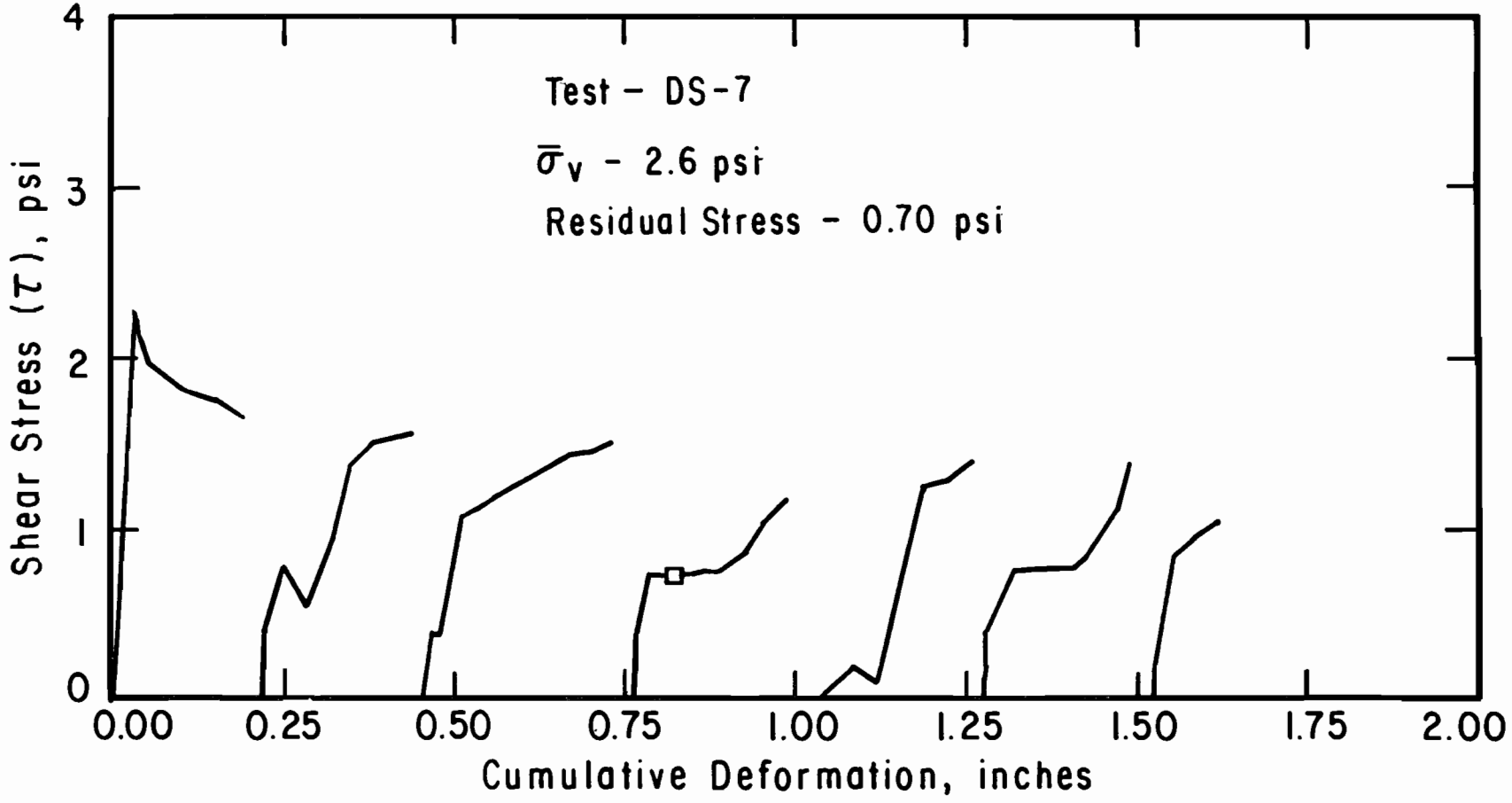

Figure D.6. Horizontal Shear Stress versus Cumulative Deformation for Direct Shear Test DS-7.

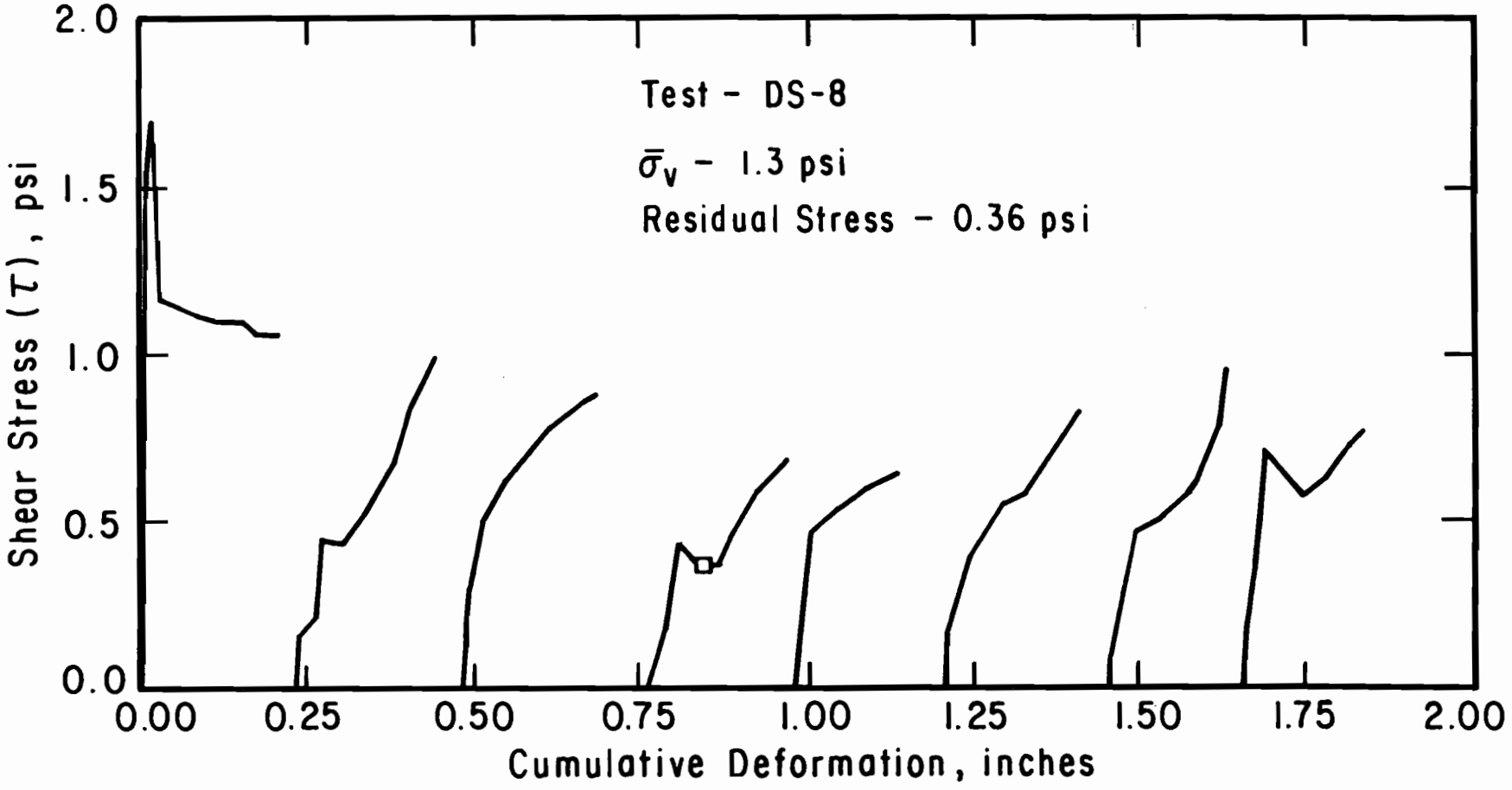

Figure D.7. Horizontal Shear Stress versus Cumulative Deformation for Direct Shear Test DS-8.

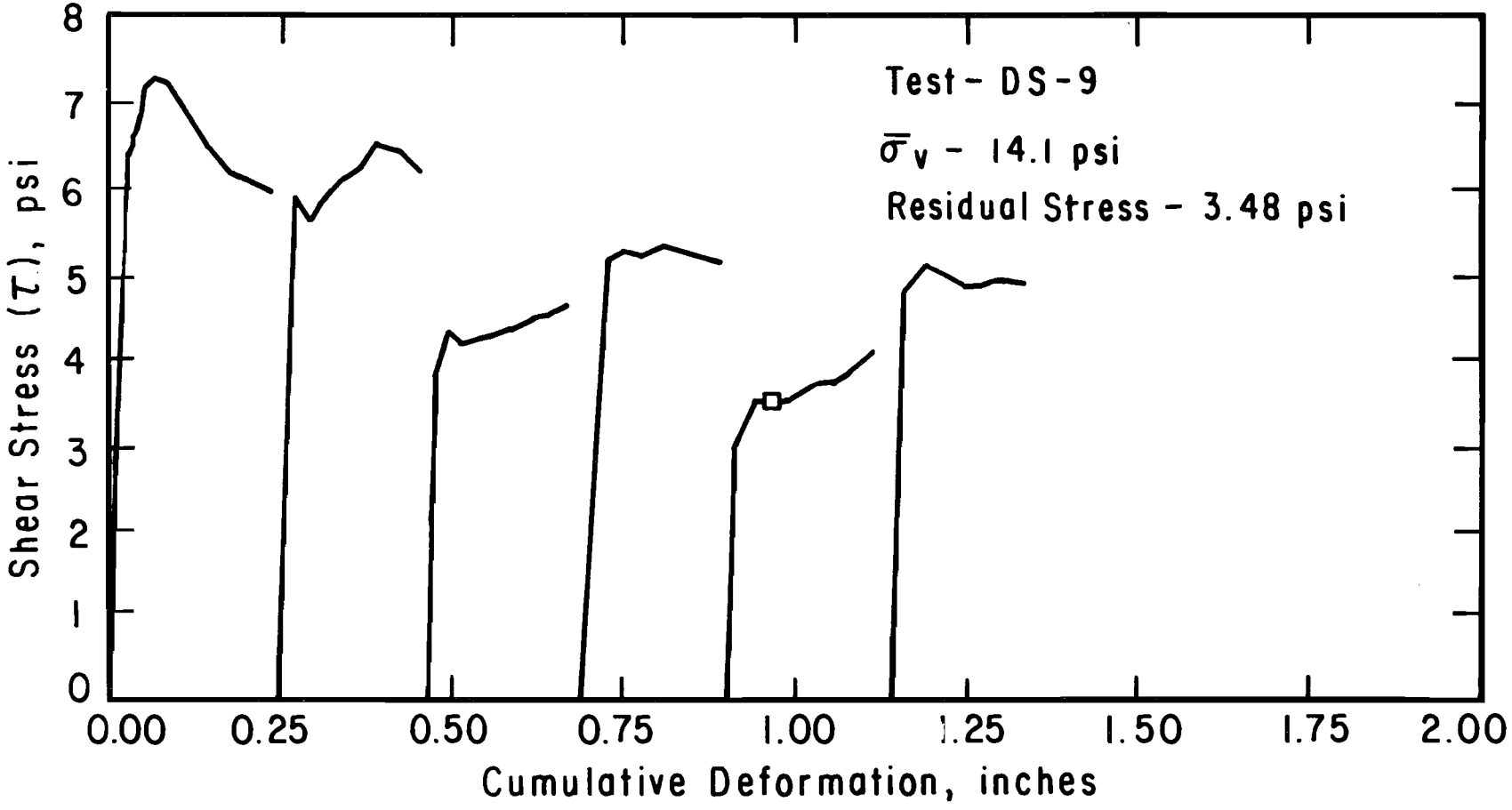

Figure D.8. Horizontal Shear Stress versus Cumulative Deformation for Direct Shear Test DS-9.

APPENDIX E

Appendix E contains the soil profiles found from borings in the I. H. 610 and Scott Street intesection, along with plots of water content and dry density versus depth. The borings included are BH#2 through BH#10.

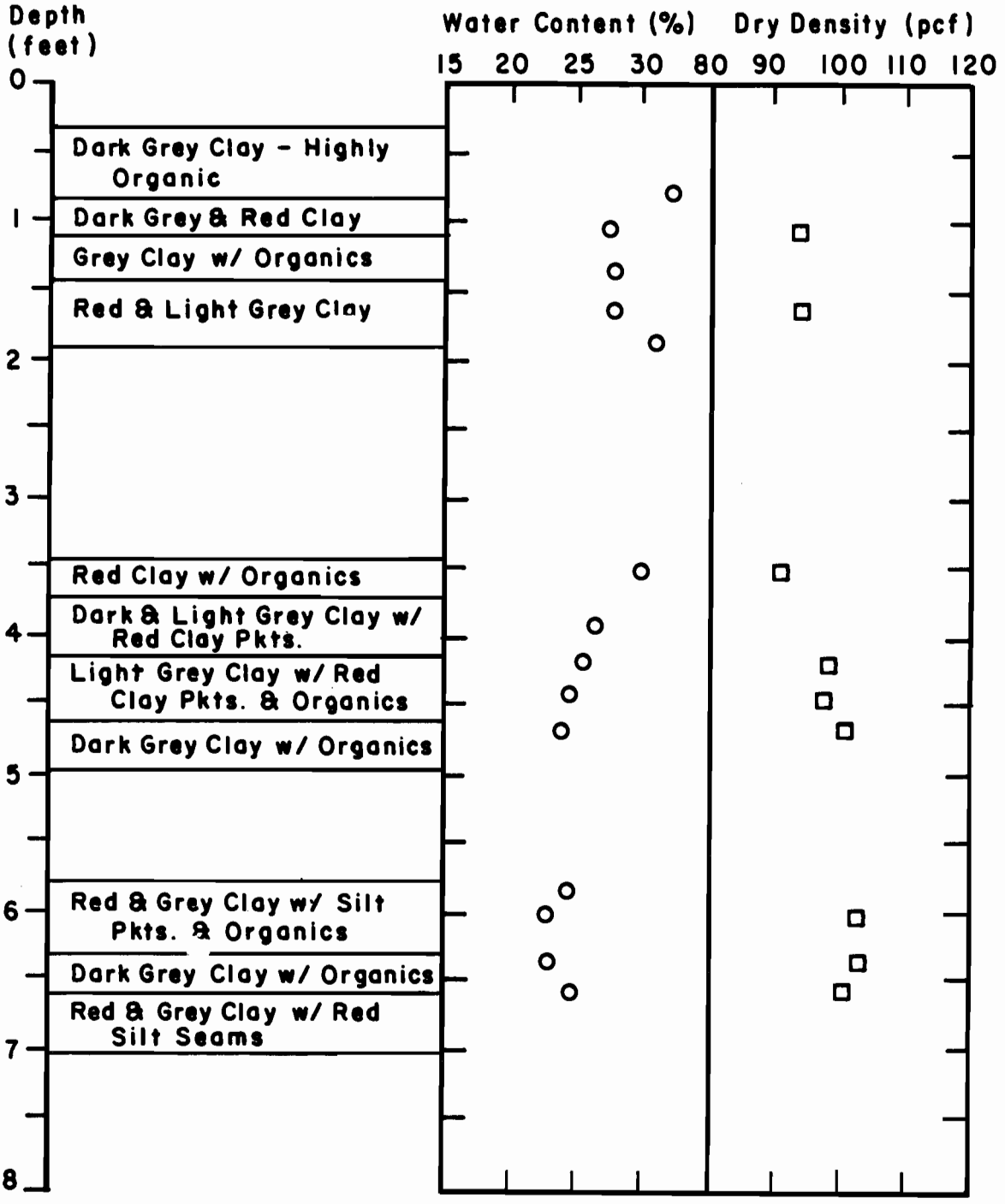

Figure E.1. Soil Profile for Boring BH#2 at I. H. 610 and Scott Street.

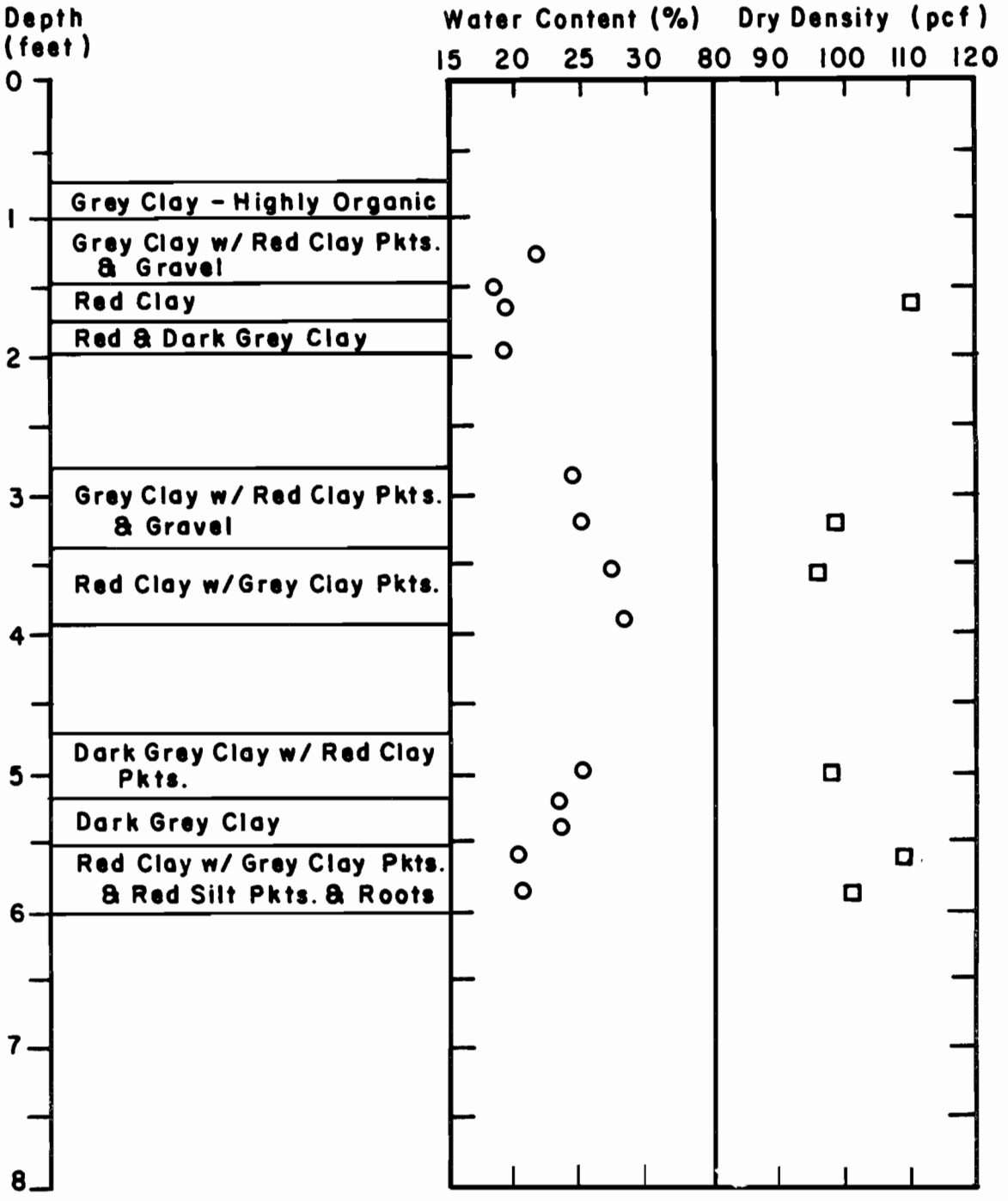

Figure E.2. Soil Profile for Boring BH#3 at I. H. 610 and Scott Street.

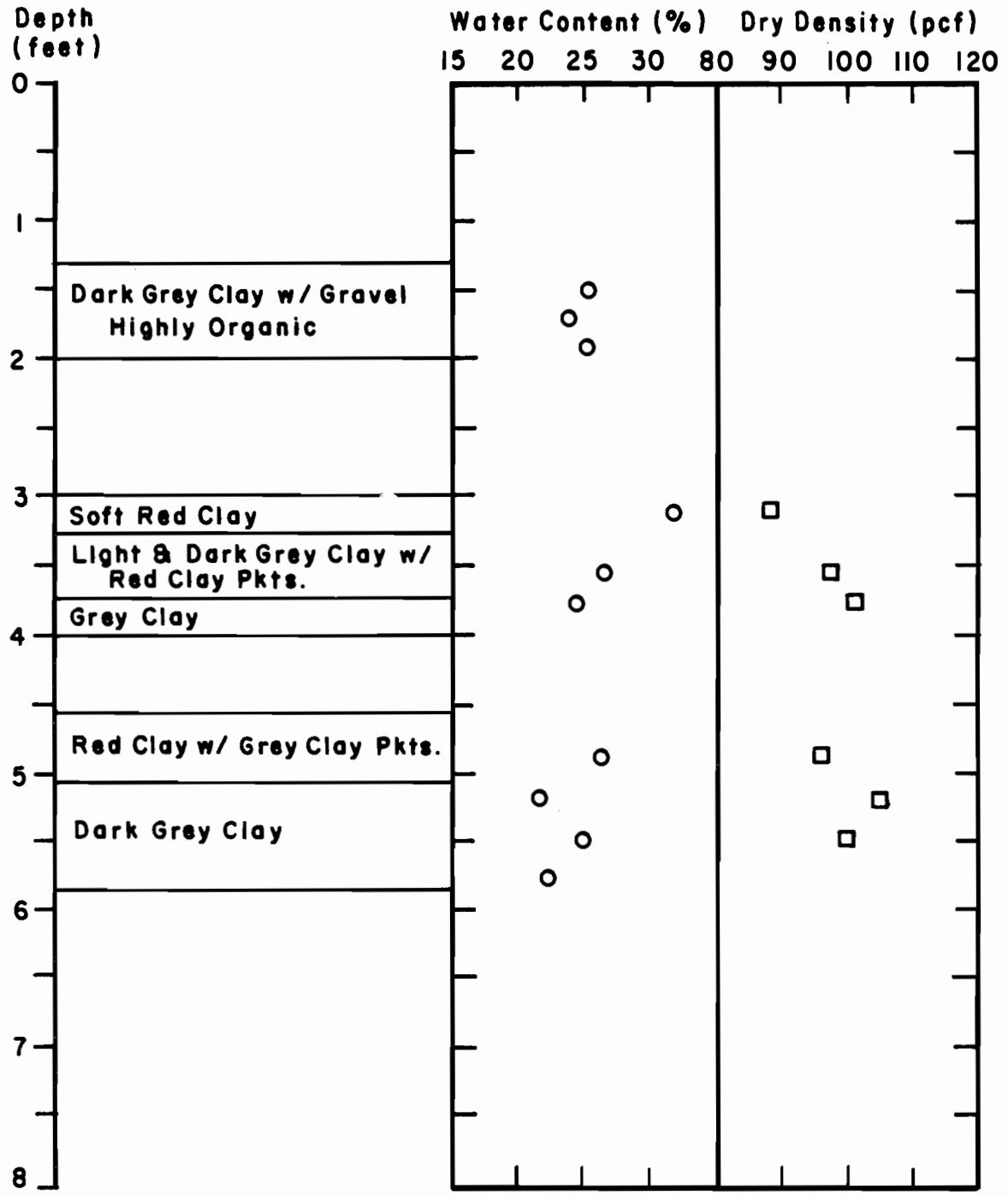

Figure E.3. Soil Profile for Boring BH#4 at I. H. 610 and Scott Street.

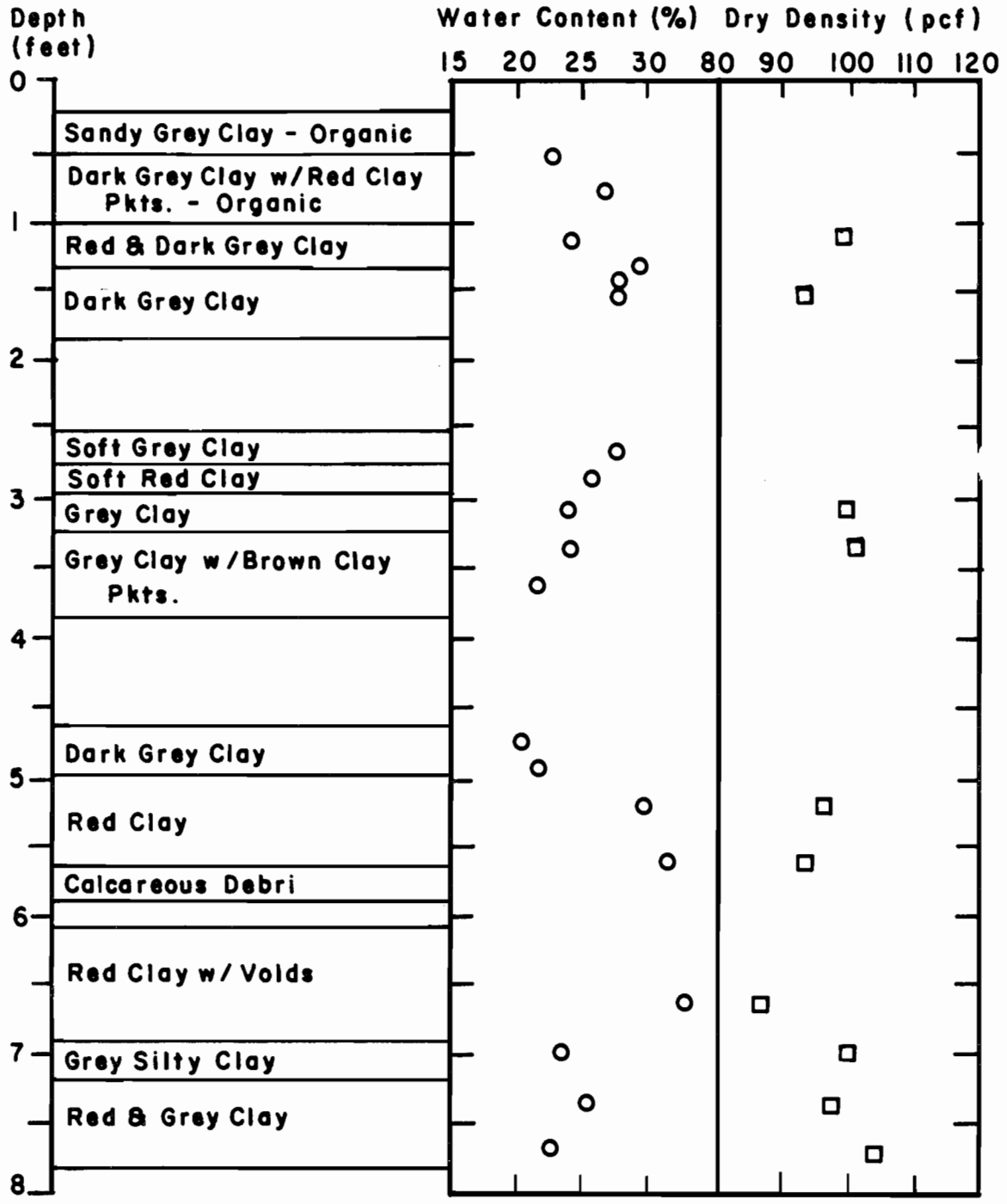

Figure E.4. Soil Profile for Boring BH#5 at I. H. 610 and Scott Street.

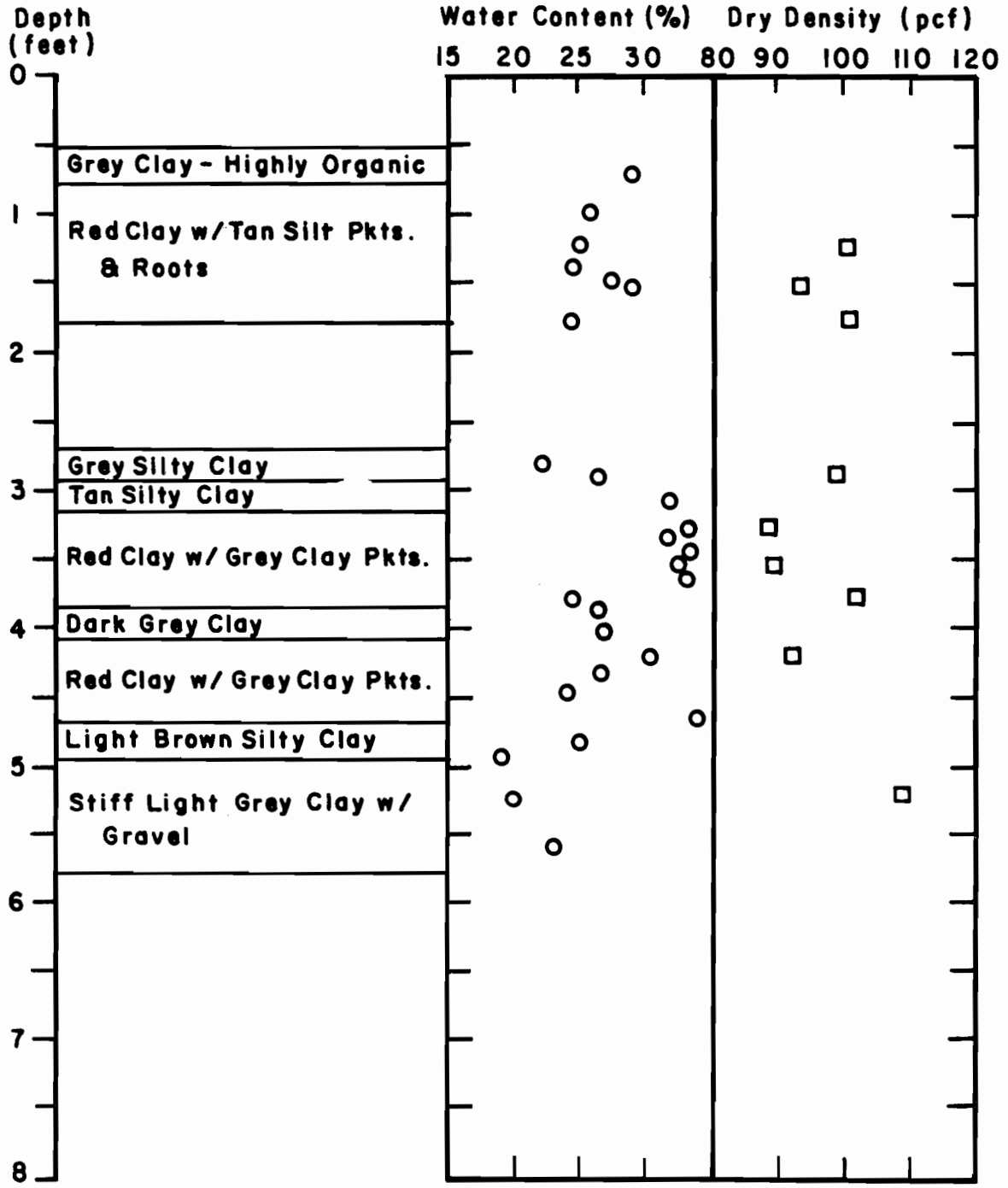

Figure E.5. Soil Profile for Boring BH#6 at I. H. 610 and Scott Street.

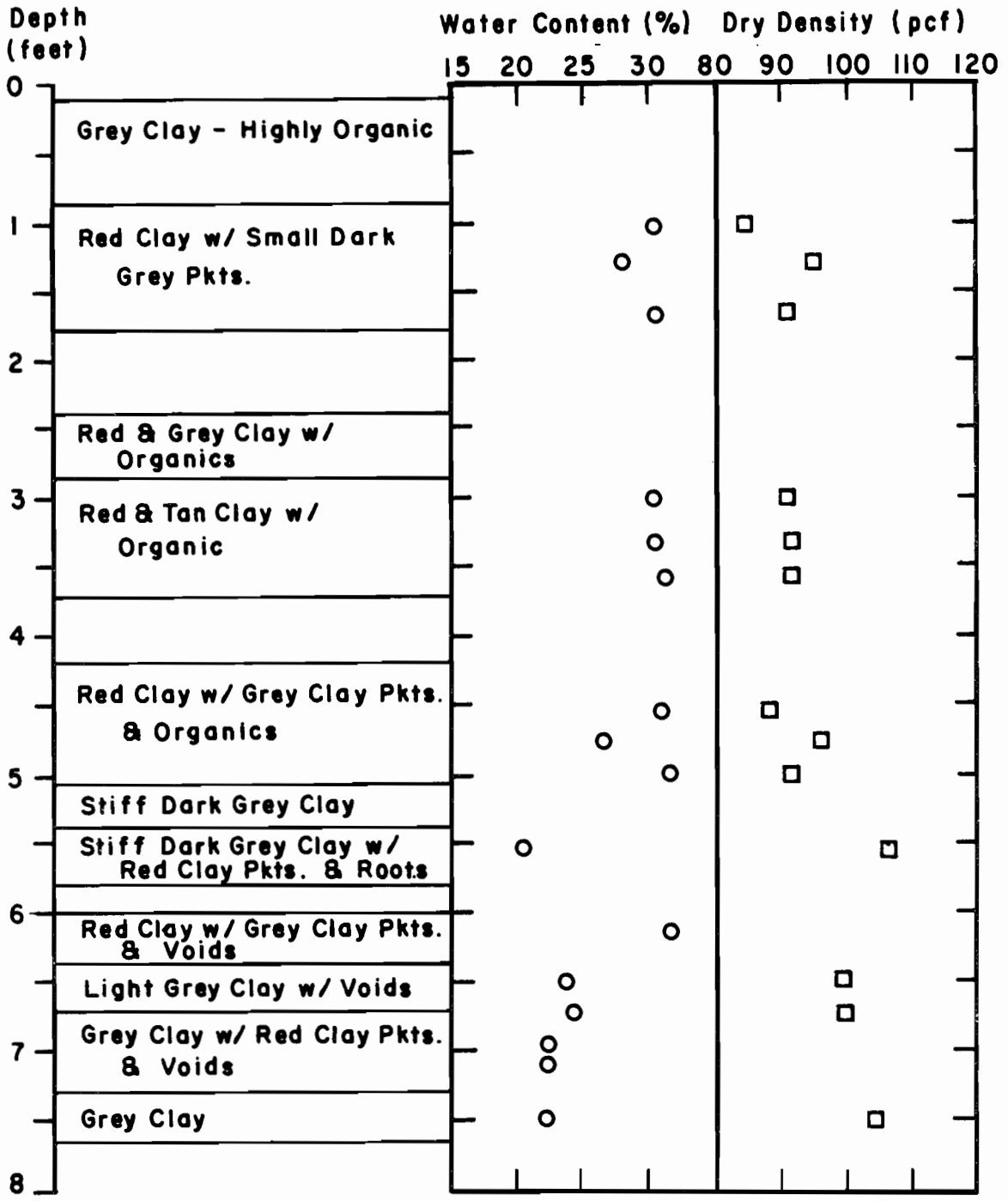

Figure E.6. Soil Profile for Boring BH#7 at I. H. 610 and Scott Street.

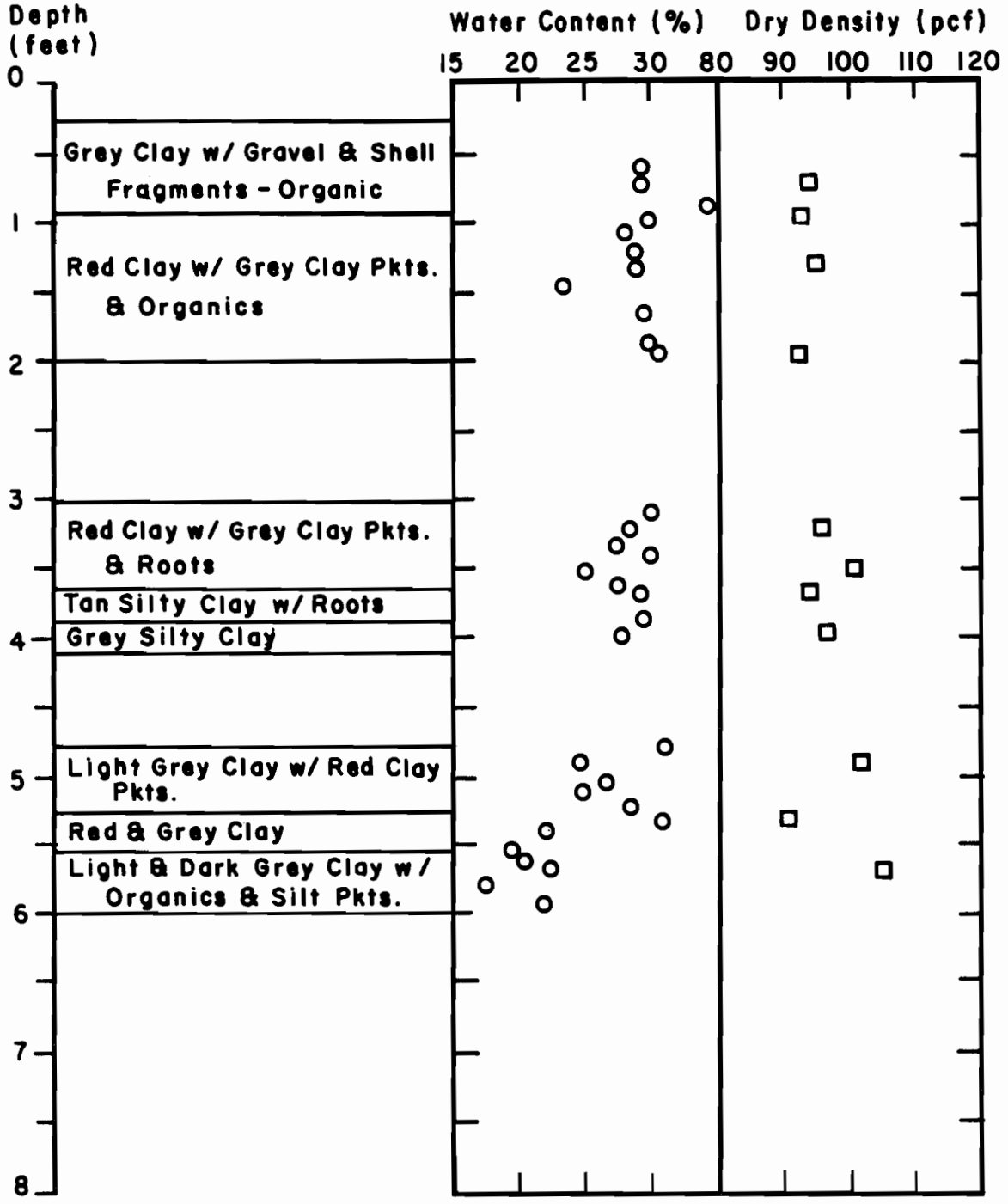

Figure E.7. Soil Profile for Boring BH#8 at I. H. 610 and Scott Street.

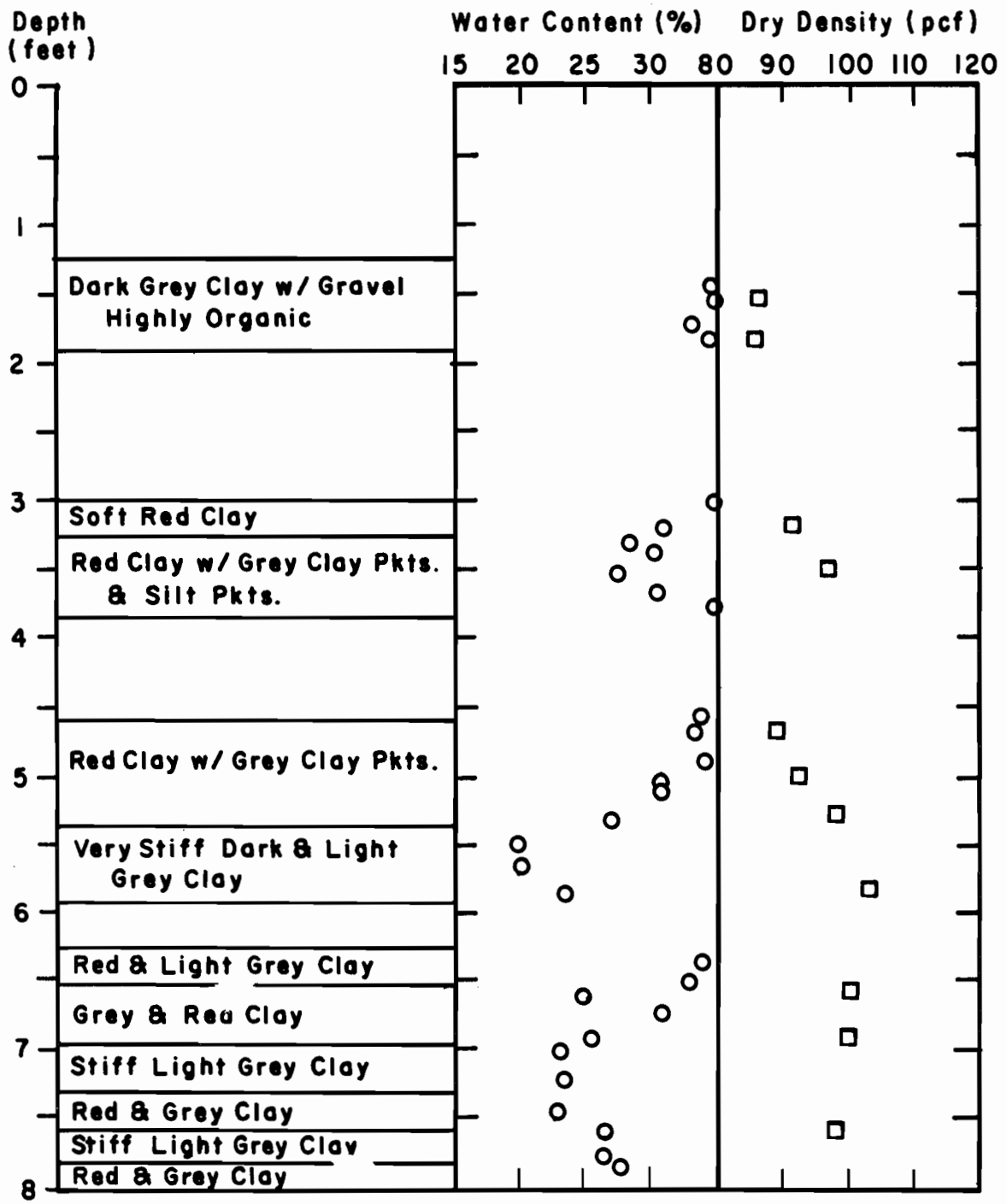

Figure E.8. Soil Profile for Boring BH#9 at I. H. 610 and Scott Street.

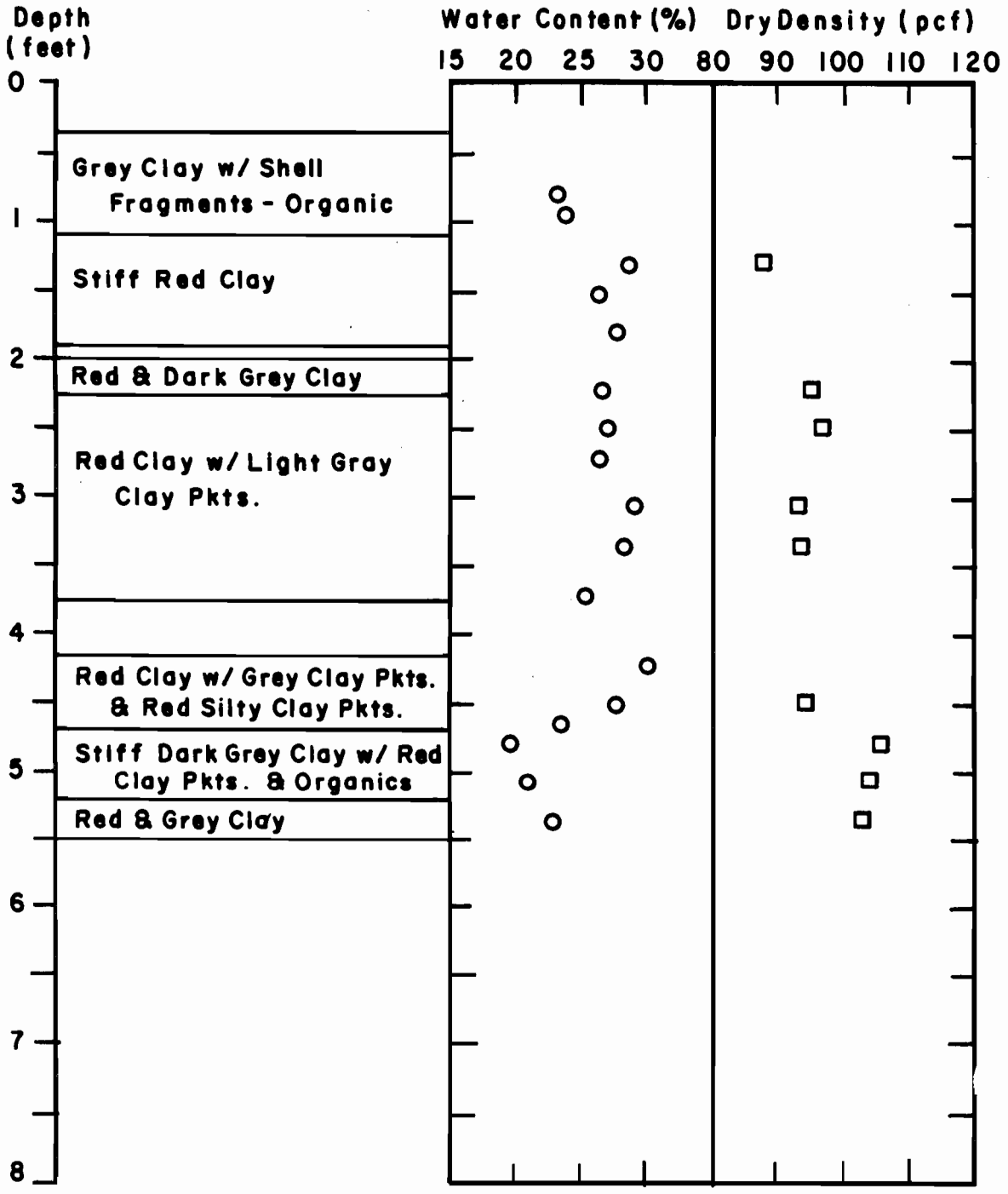

Figure E.9. Soil Profile for Boring BH#10 at I. H. 610 and Scott Street.